A DESCRIPTIVE STUDY OF THE ULTRASTRUCTURE OF THE EQUINE SUPERFICIAL DIGITAL FLEXOR TENDON

Thesis submitted in accordance with the requirements of the University of Liverpool for the degree of Doctor in Philosophy

By

Othman Jalal Ali

July 2016

ABSTRACT

The aim of this study was to describe three-dimensional (3D) anatomy and the histological features of equine superficial digital flexor tendon (SDFT), specifically to determine the organisation of the individual sub-units (fascicles) and how this may vary between individuals and in tendinopathy. For macroscopic 3D study, 17 frozen SDFT (n=13) were sectioned transversely (2-3mm), photographed and processed for 3D reconstruction. In microscopic 3D reconstruction, SDFT from foetal, one-year-old and 9-years-old were fixed in 4% paraformaldehyde solution, paraffin blocked, cut into series sections (5µm), H&E stained and processed for 3D reconstruction. Histologically a novel scoring method was devised using ImageJ to describe the cellular morphology and extracellular matrix (ECM) organisation and quantification (n=24). Tertiary fascicles were defined as being delineated by a well-defined inter-fascicular septum (IFM) (30.45µm ±9.78 SD) with a range of 4.09µm–174.11µm, which is further subdivided into secondary fascicles with a thinner IFM (9.78µm ±2.64 SD) with a range of 2µm–27.43µm in mature horses (n=3). Fascicles were heterogeneous regionally, diverged, converged and inter-connected with each other. Moreover, fascicle showed a twisted configuration when running from the proximal to the distal aspect of the 3D reconstruction. In histological scoring, it was shown that a number of fascicles and the IFM were angulated with a range of 0.2° to 40°. The IFM thickness between the secondary fascicles was significantly decreased during ageing. Intra-fascicular nuclear morphometry (density and lengths) were altered during ageing. Moreover, a number of intra-fascicular chondroid-like bodies were present in elderly horses (17- 20 years), that appeared as an individual or a cluster of large rounded cells, which stained positively for GAG and proteoglycans. In injured SDFT, 3D reconstruction displayed how the disrupted ECM extends in different planes and there was up-regulation of all histological scoring parameters.

We conclude that the secondary and tertiary fascicles display a complex 3D organisation not reflected in current models of the hierarchical organisation of equine tendon. Understanding the 3D anatomy of the tendon will facilitate understanding of tendon structure-function relationships and injury predisposition. Histological parameters including IFM and nucleus morphology were altered with ageing. In particular in aged animal chondroid-like cells were present which may be indicative of chondroid metaplasia in tendon.

TABLE OF CONTENTS

LIST OF FIGURES

LIST OF TABLES

LIST OF ABBREVIATIONS

ANOVA	Analysis of variance
CDET	Common digital extensor tendon
CS	Chondroitin sulphate
C-4-S	Chondroitin-4-sulphate
C-6-S	Chondroitin-6-sulphate
CSA	Cross sectional area
D	Distal
DS	Dermatan sulphate
ECM	Extracellular matrix
EVG	Elastin Van Gieson
rER	Rough endoplasmic reticulum
GAG	Glycosaminoglycan
H&E	Haematoxylin and Eosin
H	Heparin
HS	Heparin sulphate
HA	Hyaluronic acid
IFM	Inter-fascicular matrix
ICB	Intra-fascicular chondroid-like body
KS	Keratan sulphate
L	Left
mg	Milligram,
ml	Millilitre
P	Proximal
RNA	Ribonucleic acid
SLRPs	Small leucine rich proteoglycans
SD	Standard deviation
SDFT	Superficial digital flexor tendon
TBST	Tris-buffered saline-Tween
TEM	Transmission electron microscopy
PBS	Phosphate buffer saline
PG	Proteoglycan
M	Mid-metacarpal
mm	Millimeter
µm	Micrometre
MTJ	Musculotendinous junction
OTJ	Osteotendinous junction
R	Right
3D	Three-dimension

AKNOWLEDGEMENT

Initially I would like to say my deep thanks to my primary supervisor, Professor Peter D Clegg, for his continued guidance, invaluable support and for giving me opportunity to advance my research career. Likewise I would like to thank my secondary supervisors, Professor Eithne Comerford and Dr. Elizabeth Canty-Laird for their help, profound knowledge and scientific support.

I would like to thanks the Higher Committee for Education Development in Iraq (HCED) for their insightful support and organising my PhD scholarship.

I am very grateful to Valerie Tilston and Adam Bertram for their help and introduce me into all steps of histology from the beginning till the preparation of slides as well as Marion Pope for processing my sample for transmission electron microscopy.

I would like to take this opportunity to acknowledge and express my gratitude to everyone in the Comparative Musculoskeletal Science Research Group, Department of Musculoskeletal Biology particularly my laboratory colleagues Yalda, Sumaya, Ben, Alan, Rhiannon, Danae, Jade, Kate, Katie, Louise, Eleri, Kirsty, Luke and Fai for their friendship and encouragement throughout my lab work.

I should express my gratitude to Mandy Peffer for her guidance into next generation sequencing, Thomas Maddox for his statistical support and Diane Ashton for her on English writing skill.

Finally, I must express my very profound gratitude to my parents and to my beloved spouse Sazan for her patience, continuous encouragement throughout my PhD study and paying attention to our gorgeous kids, without them this accomplishment would not have been achieved.

CHAPTER ONE

INTRODUCTION AND REVIEW OF THE LITERATURE

1.1 INTRODUCTION

Tendon is a tough fibrous connective tissue band that connects the end of the muscle, or musculotendinous junction (MTJ) to the skeletal system at the osteotendinous junction (OTJ) (Kastelic et al., 1978, Kannus, 2000, Benjamin et al., 2008). The word tendon is derived from the Latin word, *tendere* which means stretching, referring to its high resistance to force (Ker et al., 1988). Tendon shapes vary according to their location from round (such as the Achilles tendon) to flattened sheets such as the aponeuroses of the abdominal transversus muscle (Getty, 1975, O'Brien, 2005). The main function of the tendon is to transfer muscular force to bone, which subsequently leads to skeletal locomotion. Additionally some tendons have the ability to store energy through their elastic properties, provided by the inter-fascicular matrix (IFM), and the presence of intra-fascicular microscopic helical structures that act as a spring during retraction (Kannus, 2000, Thorpe et al., 2012, Thorpe et al., 2013b).

A specific example of an energy-storing tendon is the equine superficial digital flexor tendon (SDFT), which is much more prone to injury than positional tendons such as the common digital extensor tendon (CDET) (Thorpe et al., 2010a). In a three years surveillance study conducted from 1996 to 1998 by Williams and colleagues, it was reported that 81% of all injuries in Thoroughbred horses in the National Hunt and Flat races in the UK were musculoskeletal injuries. From this the forelimb SDFT and the suspensory ligament injury accounted for about 46% of these injuries with ligament and tendon re-injury rates as high as 56% (Williams et al., 2001). In a prospective cohort study conducted from January 2000 to December 2001 of race starts on six UK race courses there were in total 83 cases of suspensory ligament and digital flexor tendon injuries from a total 2879 (2.88%) race starts (Pinchbeck et al., 2004). Further, a study by Ely and colleagues suggested that the training intensity and management methods in horses significantly affect the rate of injury to the musculoskeletal system (Ely et al., 2004). Other studies also indicate that damage to SDFT and DDFT is a common causes of horse retirement and wastage both in racehorses and in sport horses (Dyson, 2004, Thorpe et al., 2010a).

Due a number of factors, some of which are still unclear, the healing process in tendon is often prolonged (Ross and Dyson, 2010). While healing in tendinopathy

follows the standard stages of wound healing including acute inflammatory, proliferative and maturation phases followed by remodelling (Ross and Dyson, 2010) this takes longer than the standard period of wound healing in soft tissues and in the horse requires 9-12 month (Schultz, 2004). In a sheep Achilles healing model it was found that that the maximum tissue strength (81.18%) was reached after 12 months (Bruns et al., 2000). Further it has been recorded in an experimentally induced injury model, at the ultra-structural level in terms of collagen fibril diameter distribution and crimp formation, that healing was not complete even at fourteen months post injury (Williams et al., 1985). Therefore the mechanical strength even after complete healing of a tendon is inferior to that of normal tendon and there is a higher likelihood of re-injury (Williams et al., 1985, Ross and Dyson, 2010).

1.2 MACROSCOPIC STRUCTURES OF TENDON

The SDFT is a long tendon of the superficial digital flexor muscle that originates from the medial epicondyle of the humerus and inserts onto the proximal eminence of the middle phalanx, collateral ligaments and the distal part of the proximal phalanx. At the level of the distal radius/proximal carpus the SDFT combines with an accessory ligament (the superior check ligament). Then it continues to run distally through the carpal canal to the metacarpus. At the level of the carpal joint the SDFT is surrounded by a synovial structure called the carpal sheath but along the metacarpal length the SDFT is extra-synovial and is surrounded by another layer called the paratenon. The paratenon acts as an elastic sleeve, facilitating free movement of the tendon through the surrounding tissues. At the upper level of the metacarpophalangeal joint the SDFT forms a manica flexoria, a flat fibrous band, which encircles the deep digital flexor tendon (DDFT) (Pasquini et al., 2003, Ross and Dyson, 2010, Baxter, 2011).

At the level of the metacarpophalangeal joint, there is a tendon sheath which assists in lubrication as the tendons pass over the flexor aspect of this joint. The tendon sheath consists of three layers; the first is the external fibrous layer or retinacula, which is a canal through which the tendon passes. The second is the reflection pulley, located at those points where the tendon bends and acts as an anatomic re-enforcement to the tendon sheath. The third layer is the inner synovial layer, composed of the parietal and visceral layers, secreting synovial fluid, and

aiding lubrication of the tendon surface (epitenon), reducing the rate of friction and allowing the tendon to glide freely through the canal (Jozsa and Kannus, 1997, Kannus, 2000). The tendon sheath plays an important role in the reduction of friction when the tendon undergoes heavy compressive loads (Kannus, 2000, Benjamin et al., 2008).

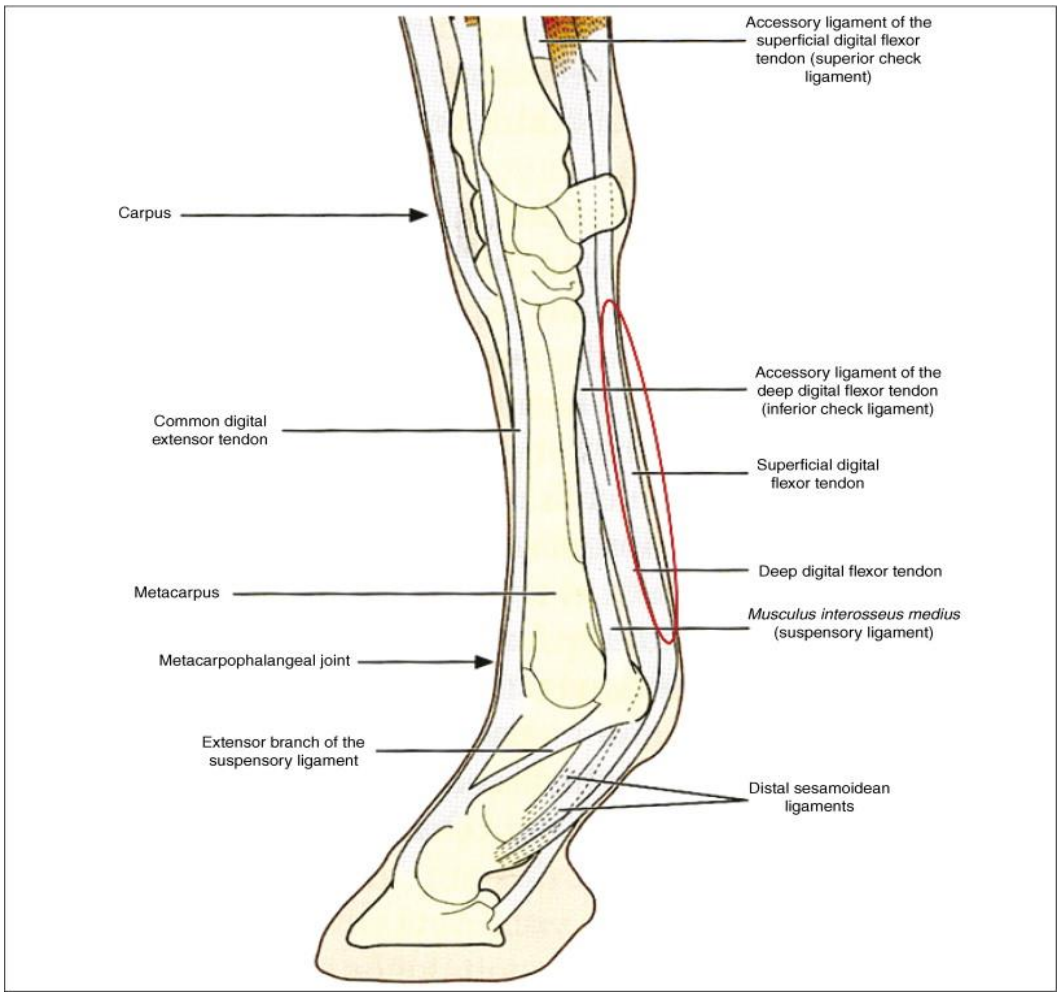

Figure 1.1: Illustration of the anatomy of the horse forelimb, lateral aspect, adapted from (Richardson et al., 2007).

The epitenon is a thin smooth layer lying under the paratenon and covering the tendon surface. It consists of a dense fibrillar network of collagen fibrils, elastic fibres and non-collagenous proteins (Yang et al., 2012). The epitenon covers the tendon entirely, tightly attached to the underlying tendon matrix. It sends connective

tissue septa deeply to form a reticular network called inter-fascicular matrix (IFM) or endotenon, which defines the hierarchical organisation of the tendon (O'Brien, 1992, Kannus, 2000).

1.3 BLOOD SUPPLY

Long tendons usually have a triple blood supply; from the musculotendinous junction (MTJ), the tendon body length and the osteotendinous junction (OTJ) (Edwards, 1946, O'Brien, 1997). At the MTJ, the muscle fibres are surrounded by an isolated capillary network that is fed from larger perimysium vessels. Where the muscle fibres cease, branches of the perimysium vessels continue and penetrate into the tendon through the IFM while some perimysium vessels continue as peritendinous vessels (Edwards, 1946). Therefore there is not a direct capillary network circulation between the muscles and the tendon at the MTJ. Similarly the SDFT proximally has a direct connection with the blood supply of the superficial digital flexor muscles from branches of the median artery extending through the carpal canal (Smith, 1965, Kraus-Hansen et al., 1992).

The body of the tendon is vascularised from the surrounding paratenon or mesotenon. At regular intervals small vessels course through the paratenon and cross into the body of the tendon and then branch several times parallel to the longitudinal axis of the tendon (Edwards, 1946, Ochiai et al., 1979). The body of the SDFT is mainly supplied by the intra-tendinous and the paratenon sheath vessels (Kraus-Hansen et al., 1992). The intra-tendinous vessel courses between the fascicles mostly through the IFM. These longitudinal vessels are of arteriolar sizes with a definitive tunica media and a regular lumen; they arise from the surface vessels, run transversely through the tendon body and connect to the longitudinal vessels to form a plexus (Edwards, 1946, Lundborg et al., 1977).

At the OTJ the vessels in the IFM do not increase in size but simply continue and rarely anastomose with the periosteal vessels. In a few areas small branches might be seen to penetrate the cortical layers. Meanwhile, the collagen fibres continue to join the bone and concomitantly the IFM carries blood vessels toward the periosteum. However, this region is poorly vascularised in contrast to the other parts of the tendon (Kraus-Hansen et al., 1992, Schultz, 2004, Durham and Dyson, 2011).

1.4 MICROSCOPIC STRUCTURES OF TENDON

The body of the tendon is compartmentalised into different sized fascicles by the IFM that arises from the epitenon (Kastelic et al., 1978, Kannus, 2000). Larger units are called tertiary fascicles and include a number of smaller secondary fascicles and in turn primary collagen fibril bundles. The primary bundles contain bunches of collagen fibrils (Figure 1.2), arranged helically along the longitudinal axis of the tendon (Aparecida de Aro et al., 2012). The number of the secondary fascicles vary within a tertiary fascicle, ranging from 10 to 12 sub-fascicles (Kastelic et al., 1978), however Kannus (2000) stated that each tertiary fascicle usually contains only 3-4 sub-fascicles.

No specific criteria have been adopted to specify and quantify the anatomical hierarchical subunits of the tendon. However, Kastelic (1978) and Kannus (2000) adopted the following nomenclature subunits; a number of collagen fibres form a primary bundle, subsequently a number of primary fascicles form bigger secondary fascicles, and few secondary fascicles join to form tertiary fascicles and then the tendon. The IFM outlining the fascicles carries nerve fibres, lymphatic and blood vessel into deep tendon structures and enables the fascicles to glide over each other (Elliott, 1965, Jozsa et al., 1991, Kannus, 2000).

The size of the primary bundles, secondary and tertiary fascicles vary according to the species and region (Edwards, 1946). Their diameters range between 15-400 micrometre (µm), 150µm-1000µm and 1000µm-3000µm respectively in human tendon (Kannus, 2000) and 10µm-20µm, 20µm-200µm and 100µm-300µm in rat tendon (Kastelic et al., 1978, Wang, 2006).

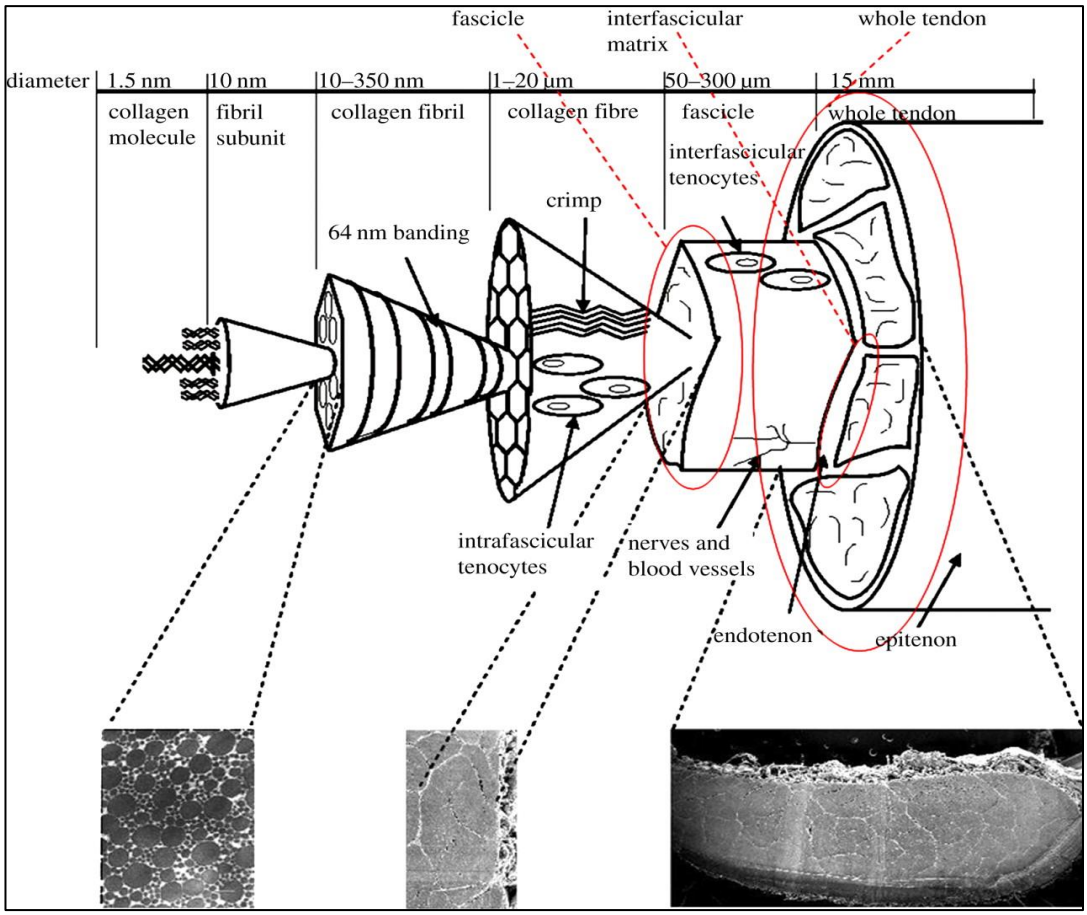

Figure 1.2: Illustration of the microscopic anatomy of the horse SDFT adapted from (Thorpe et al., 2012).

1.5 COMPOSITION OF TENDON

1.5.1 Water

Tendon is composed mainly of water (60-80%), that binds to hydrophilic molecules such as PGs and GAG, which provide the viscoelastic properties to the tissue matrix and improve the biomechanical elasticity of the tendon (O'Brien, 1997, Kannus, 2000). In horse the SDFT has a water content of 63% ±2 (Batson et al., 2003, Lin et al., 2005b, Birch, 2007) and recently a range of 64-70% has been recorded among three different breeds (Warm bloods, Friesians and Thoroughbreds) (Hazeleger, 2013). However it has been recorded that the water content is not significantly altered by low and high intensity exercise (Birch et al., 2008).

1.5.2 Collagen fibres

The collagen fibre is considered to be the basic functional unit of the tendon responsible for force transmission and many of the mechanical properties of the tissue (Parry and Craig, 1984, Pins et al., 1997, Silver et al., 2003, Magnusson et al., 2003b). Tendon is mainly composed of collagen that makes up to 30% of the wet weight of tendon, with the remainder being predominantly water and tenocytes (68%) and elastic fibres (2%). Collagen make up 65-80% of the dry weight; in which up to 95% is type I collagen and the remainder are type II, III, IV, V and VI collagens (Hanson and Bentley, 1983, Benjamin et al., 1991, Riley et al., 1994, Birch et al., 1999a). The elastic fibres are dispersed between the collagen fibres and in the IFM and are thought to give elasticity to the extracellular matrix (Kannus, 2000, Thorpe et al., 2012). The pattern of the collagen fibres is not complex, most fibres run parallel to the longitudinal axis of the tendon, while a few of them cross each other forming a spiral plait and up-tying with the adjacent parallel fibres (Jozsa et al., 1991, Kannus, 2000). The rate of interwoven, branched or fused collagen fibres is greatest in foetal tendons (Provenzano and Vanderby, 2006). However in mature animals most of the fibrils run parallel to each other but there are still some disorganised fibrils running in various directions (Provenzano and Vanderby, 2006). This organisation of the collagen fibrils forms a super-twisted cord, which affects the biomechanical properties of the tendon (Feitosa et al., 2006, Aparecida de Aro et al., 2012).

In their longitudinal axis, collagen fibres have a crimp (corrugate) pattern, which appears as a zig-zag or undulating form, but with the degree of angulation declining during ageing (Gathercole and Keller, 1978, Gathercole and Keller, 1991, Franchi et al., 2007a). In human tendon a wide range of crimp angles is present, ranging from 0º- 60º (Rowe, 1985, Jozsa and Kannus, 1997). Whereas, in horse SDFT the crimp angle and crimp length decline from 19-20˚and 17μm -19μm in the mid-metacarpal region in young horses to 12-17˚ and 11μm -15μm in adults (Wilmink et al., 1992). This anatomical configuration partly leads to the tendon's ability to conserve elastic energy by recoiling the fibres after mechanically induced extension (Kastelic et al., 1980, Kirkendall and Garrett, 1997, Shearer, 2015a)

The number and diameter of collagen fibrils are not constant between regions and vary from tendon to tendon (Elliott, 1965, Birk et al., 1996). In equine SDFT the mean collagen fibril diameter varied regionally from the MTJ to the OTJ and even in different areas of the same region; they varied from 41nm to 100nm. Fibril diameters are smallest close to the MTJ but steadily increase toward the OTJ in both the peripheral and central areas of the tendon. It has been found that in equine SDFT the collagen fibrils diameters are approximately 40nm, 48nm and 68nm in the in the central area of the proximal mid-metacarpal and distal region of the tendon. However, the average fibril diameter in the periphery of the tendon was larger than in the central areas and were 44nm, 60nm and 99nm respectively from proximal to the distal region. This might reflect the role of different regions in carrying different loads (Watanabe et al., 2005, Sese et al., 2007).

1.5.2.1 Structures of collagen

The structural unit of collagen is tropocollagen, which is a long thin straight protein approximately 280nm long by 1.5nm wide. Basically, the collagen-I molecule consists of three aligned helical polypeptides (three alpha-chains); two alpha-1 (α1) and one α2 chains, in which each alpha chain is comprises 100 amino acids. Two-thirds of the amino acids consist of three specific amino acids: glycine, proline and hydroxyproline (1:2 ratio). The amino acid sequence consists of a repeating Gly-X-Y triplet, where X and Y can be any amino acid. Glycine is therefore found in every third residue of the alpha chain. One-third of the X positions are proline, and a similar number (one-third) of the Y positions are hydroxyproline. These three molecules (glycine, proline and hydroxyproline) are important to stabilize the triple collagen helix through the hydrogen bonds created within the right-handed super-helical trimer (Silver and Birk, 1984, Shoulders and Raines, 2009). Two main types of hydrogen bond are involved in these interactions; the first is between the hydroxyproline hydroxyl of one tropocollagen and a glycine carbonyl in the adjacent tropocollagen and the second between two hydroxyproline hydroxyl groups, where a water molecule form a bridge between two adjacent tropocollagens (Piez, 1984, Streeter, 2011).

The procollagen molecules are produced intra-cellularly inside the fibroblast (tenoblast) and then transferred to the extracellular space, where they are cleaved and

deposited as collagen fibrils (Piez, 1984). Fibrils reach up to one millimeter in length with a wide range of 12nm-500nm, which varied from different tissues and stage of development (Canty and Kadler, 2005, Kadler et al., 2007). The three polypeptides α1 or α2 chains combine together to form either a hetero or homotrimer. It has been found that collagen type I is a heterotrimeric collagen, which consists of two α1 chains and one α2 chain (Kadler et al., 2007). Synthesis and degradation of collagen fibrils is mediated by a complex cellular pathway and is illustrated in (Figure 1.3).

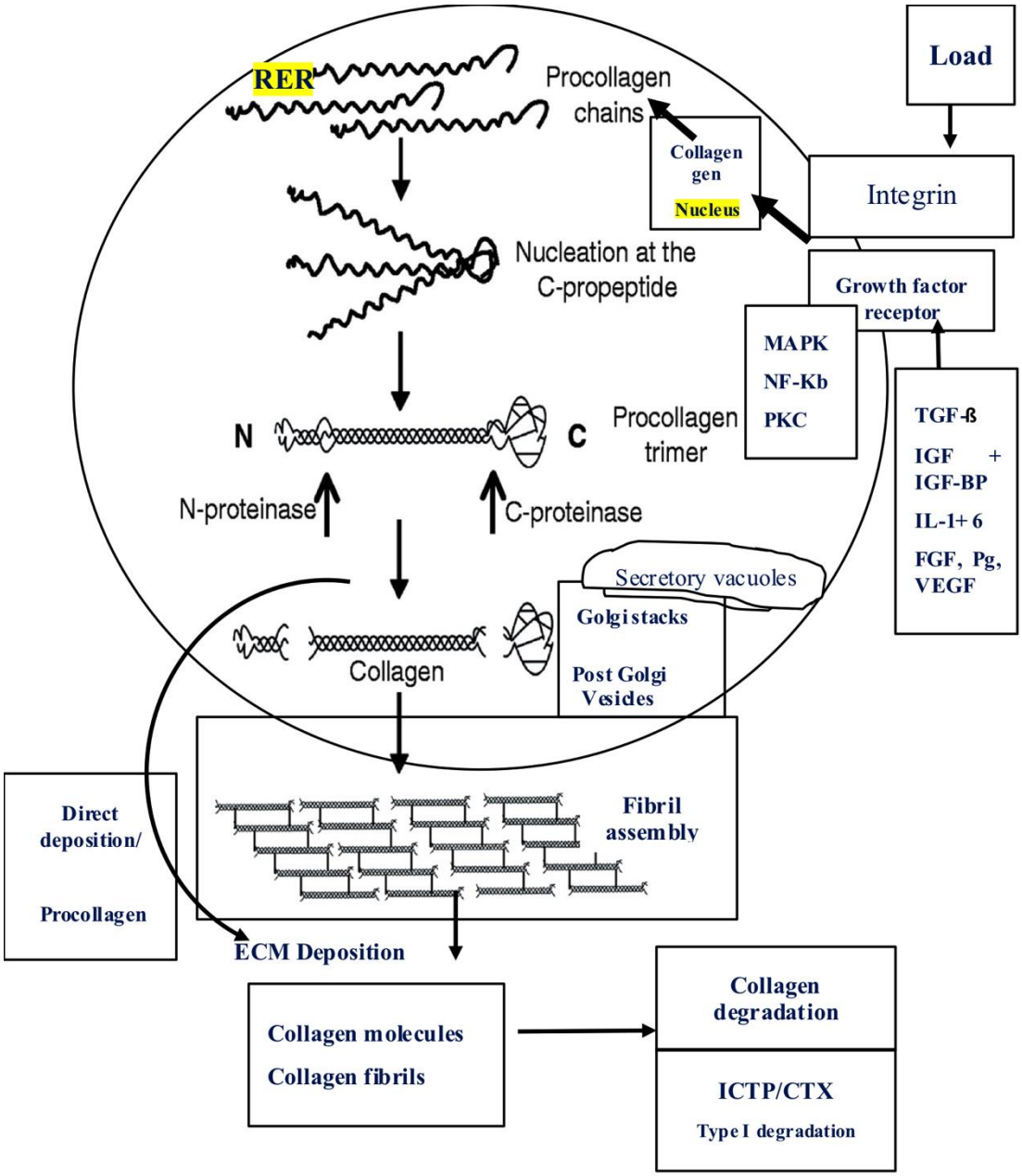

Figure 1.3: Schematic pathway involved in the synthesis, deposition and degradation of type I collagen. Growth factor function is an important regulator of gene activation and includes transforming growth factor beta (TGF-ß), insulin-like growth factor and its binding proteins (IGF/IGFBP), IL (interleukin), fibroblast growth factor (FGF), prostaglandin (Pg) and vascular endothelial growth factor (VEGF). Mitogen-activated protein kinase (MAPK) plays an important regulatory role for initiation of gene signals. Procollagen molecules are initially synthesised in the rough endoplasmic reticulum (RER). The matrix metalloproteinase (MMP) are major regulators of collagen degradation in relation to mechanical loading. Procollagen 1 C-terminal peptide (PICP), Procollagen type I N-terminal propeptide (PINP), type I collagen cross-linked carboxy or C-terminal telopeptide (ICTP/CTX), adapted from (Kjaer, 2004, Canty and Kadler, 2005).

1.5.3 Proteoglycan

Other tendon ECM constituents comprise important proteins of which one group is proteoglycans (PG). PGs are composed of a central protein core, which is covalently bonded to at least one glycosaminoglycan (GAG) molecule (Iozzo and Murdoch, 1996, Yoon and Halper, 2005). According to their sizes, PG can be categorised into two groups:

1-The first group comprises small leucine rich PGs (SLRP), which include decorin (abundant), biglycan, fibromodulin, lumican and keratocan. They are characterised by the presence of a Leucine-rich protein (LRP), which is composed of a series of approximately 20-30 extended amino acid repeats containing conserved leucine residues. Moreover, this group is also characterised by having a small central core protein (approximately 40 Kilo Dalton (kDa)), to which a number of GAG are attached (1-2 chondroitin sulphate (CS) or dermatan sulphate (DS) or several keratin sulphate (KS)). SLRPs bind to collagen fibrils, playing a major role in fibrillogenesis and the production of collagen fibres (Table 1.1) (Samiric et al., 2004, Yoon and Halper, 2005, Wight and Mecham, 2013, Thorpe et al., 2016a).

2-The second group comprises large or modular PGs, including aggrecan (220 kDa) and versican (265-370 kDa), which are rich in CS and DS (Yoon and Halper, 2005). These PGs enable collagen fibres to resist high compressive and tensional forces (Evanko and Vogel, 1990, Rees et al., 2009). On the other hand, the presence of the considerable amount of DS will reduce the diameter of collagen fibrils by preventing the lateral aggregation and assembly of collagen fibrils (Table 1.1) (Vogel and Trotter, 1987).

Table 1.1: Common types of proteoglycan properties, distribution and functions in tendons. (Proteoglycan (PG), Small Leucin-Rich Proteoglycan (SLRP), Glycosaminoglycan (GAG), Kilo Dalton (kDa), Chondroitin sulphate (CS), Dermatan sulphate (DS), Keratan sulphate (KS), Transform growth factor-β (TGFβ), Epidermal growth factor (EGF).

PGs	Protein (kDa)	GAG chains	Distribution	Function
Decorin (SLRP)	36	1 CS/DS and/or + 1 KS	Binds to collagen fibrils, TGFβ and EGF. Is the most abundant (80%).	Regulates fibrillogenesis, responsible for fibre alignment and connect fibrils by an inter-fibrillar bridge. Affects cell proliferation and enhances immune responses (Iozzo, 1999, Samiric et al., 2004, Vesentini et al., 2005)
Biglycan (SLRP)	38	1-2 CS/DS	Binds to collagen fibrils and TGFβ. More abundant in fibro-cartilaginous areas	Enhances cell proliferation, help to produce large mature collagen fibrils and compensates for the function of decorin in decorin deficient instances (Robbins and Vogel, 1994, Iozzo, 1999, Yoon and Halper, 2005)
Fibromodulin (SLRP)	42	4 KS	Binds to type I, II collagen fibrils and TGF-ß	Enhance the formation of mature collagen fibrils, regulates TGF-ß activities and fusion of fibrils, and confers tendon strength (Hedbom and Heinegard, 1989, Waggett et al., 1998, Yoon and Halper, 2005)
Lumican (SLRP)	38	2- 3 KS	Binds to type I collagen fibrils	Regulate fibrillogensis, cross sectional growth (determining the actual fibril size) and fibril fusion (Hedbom and Heinegard, 1989, Iozzo, 1999, Yoon and Halper, 2005)
Aggrecan Modular (lectican)	220	~ 100 CS + ~60 KS	Cartilage-specific PG, present in fibrocartilaginous areas of tendon, bind to hyaluronan.	Resists compressive forces and facilitates sliding of collagen fibre bundles over each other, provides cell to cell and matrix interaction through hyaluronan (Vogel et al., 1994, Rees et al., 2000, Vogel and Peters, 2005, Rees et al., 2007)
Versican Modular (lectican)	265-370	10-30 CS	Present in the tensional region of tendon, the endotenon, around blood vessels and in pericellular spaces. Binds to hyaluronan	Interacts with elastic fibres and provide viscoelasticity, enhances cell migration, proliferation and adhesion. Involved in ECM morphogenesis, homeostasis and angiogenesis (Corps et al., 2004, Samiric et al., 2004, Yoon and Halper, 2005)

1.5.4 Glycosaminoglycan (GAG)

Glycosaminoglycans are composed of long linear polysaccharide polymers, which contain repeated disaccharide units. The disaccharide units contain two modified sugars, hexosamine (*N*-acetylgalactosamine (GalNAc) or *N*-acetylglucosamine (GlcNAc) and one hexuronic acid (Glucuronate (GlcA) or iduronate). Along the hexosamine chain either a carboxylate or sulphate group are attached to one or both monomers of the disaccharide units. They are covalently bonded to the protein core of the PG by a specific tri-saccharide linker (two Galactose and one Xylose residues) to Serine and Threonine residue inside the core of PG (Hileman et al., 1998, Yoon and Halper, 2005, Esko JD, 2009).

GAGs are located on the cell surface or distributed through the ECM, and are occasionally present inside the secretory vesicles of some cells. Inside the ECM GAGs have a role in cell-to-cell or cell-to-protein interactions. GAGs are sulphated (except hyaluronic acid) and this sulphation gives the PG a strong negative charge, which attracts water molecules and so imparts tissue viscosity. Further, the acidic GAGs that are located in the ECM play a role in modulating cellular proliferation and differentiation by interacting with cytokines and fibroblast growth factors (Hileman et al., 1998, Yoon and Halper, 2005, Esko JD, 2009, Franchi et al., 2010).

Different types of GAG have been found in the equine SDFT including chondroitin sulphate (CS), dermatan sulphate (DS), keratan sulphate (KS), heparin (H), heparin sulphate (HS) and hyaluronic acid (HA). They are hydrophilic molecules localised within and between the collagen fibres, which bind collagen molecules and act as a bridge between fibrils. GAG molecules attract and bind water and form a viscous gel, which has important implications for tendon function (Silbert, 1982, Vogel and Heinegard, 1985, Hileman et al., 1998, Yoon and Halper, 2005). Generally GAG are classified into six classes as shown in (table 1.2):

Table 1.2: Types of GAG and a brief overview of some specific properties. N-acetylgalactosamine (GalNAc), glucuronate (GlcA), Fibroblast Growth Factor (FGF), Vascular Endothelial Growth Factor (VEGF), Hepatocytes Growth Factor (HGF), Kilo Dalton (kDa), Glycosaminoglycan (GAG), Chondroitin sulphate (CS), Dermatan sulphate (DS), Keratan sulphate (KS), Hyaluronic acid (HA), Heparan sulphate (HS), Heparin (H).

GAG	Structure	Chain	Size (kDa)	Distribution	Function
CS	Consist of highly sulphated GalNAc and GlcA, and the disaccharide units called CS A or C that have 4 and 6 sulphation fractions respectively.	20-100	5-50	Cartilage, bone, heart valve aorta, ligament and compressed area of the tendon. It is the most abundant GAG in brain.	Provides tissue strength, bind to water, forms hydrated matrices and provides lubrication. Play a role in regulation of ECM and fibrillogenesis (Vogel and Heinegard, 1985, Rees et al., 2000, Martinez et al., 2015)
DS	Consists of repeated disaccharide units of iduronic acid and GalNAc. Binds to PGs such as decorin and a numbers of proteins and growth factors	2-8	15-40	Skin, blood vessels, heart valves, and lung, ligaments and throughout the tendon Linked to heparin cofactor-II, thrombin, activated protein C and fibroblast growth factor family members (FGF-2 and FGF-7).	Plays a role in coagulation, wound repair, fibrosis and cell proliferation. Binds water and form hydrated matrices. Plays a role in the regulation of ECM and fibrillogenesis (Franchi et al., 2010, Biancalana et al., 2012)
KS	Composed of highly sulphated poly-*N*-acetyllactosamine chains. Associated with SLRPs such as lumican, keratocan, fibromodulin, osteoadherin and aggrecan.	2-3	4-20	Cornea (KSI), bone, cartilage, compressed area of tendon. Present with chondroitin sulphates (KSII) and brain (KSIII).	Dynamic buffering of corneal hydration and preservation of the regular spacing of collagen fibres. Involved in tissue distribution and load bearing capacity of aggrecan (Fu et al., 2007, Franchi et al., 2010, Kiani et al., 2002)
HA	Large polymer chain, not sulphated, produced and localised on the cell surface by three hyaluronan synthases: HAS1, HAS2, and HAS3. Composed of alternating residues of β-D-(1→3) (GlcA) and β-D-(1→4)- (GlcNAc)	10000	4000-8000	Synovial fluid, articular cartilage, skin, vitreous humor, scar tissue and ECM of loose connective tissue and tendon	Play roles in tissue organization, viscosity and healing. Involved in cell signalling, adhesion and proliferation. Capacity to absorb high compressive load by desorption and resorption of water (Yoon and Halper, 2005, Franchi et al., 2010)
HS	Linear sulphated polysaccharide composed mainly of glucuronic acid (GlcA) linked to N-acetylglucosamine (Glc NAc)	4-6	10-70	Basement membrane, cell surfaces, muscles and the myotendinous junction.	Present as Heparan Sulphate PG (HSPG). Binds to the FGFs, VEGF, HGF and chylomicron remnants of hepatocytes. Associate with the tissue development and pathology (Vogel and Heinegard, 1985, Esko JD, 2009, Yoon and Halper, 2005)
H	Modified form of HS but is more sulphated.	1-4	3-30	Mast cells intracellular granules, endothelial lining of lung, liver and skin arteries	Anticoagulant (Silva and Dietrich, 1975, Yoon and Halper, 2005)

1.5.5 Cartilage oligomeric matrix protein (COMP)

The non-collagenous glycoprotein COMP forms up to 1% of the tendon dry weight. It is a member of the thrombospondin family, composed of five identical coiled-coil molecules (Pentamer) joined together in the N-terminal domain. Each arm has a binding site for collagen type -I or -II. It is located in the spaces between the collagen fibrils and it acts as a catalyst for fibrillogenesis. It has been used as a serum biomarker for diagnosis of subclinical tendinopathic injury (Smith et al., 1997, Muller et al., 1998, Sodersten et al., 2013).

1.5.6 Matrix metalloproteinase MMP

MMPs play a role in the enzymatic degradation of matrix and non-matrix proteins by a number of mechanisms. MMP1, MMP2, MMP8, MMP13, MMP14 all act as collagenases in the process of collagen degradation and remodelling and can be inhibited by tissue metalloproteinase inhibitors (TIMPs) (Nagase et al., 2006); they also play role in the ECM homeostasis. MMPs are classified into four groups according to their primary substrates, collagenases, gelatinases, membrane-bound MMPs, and stromelysins (Nagase and Woessner, 1999).

1.5.7 Cells

Tendon is less cellular when compared to many other tissues but contains tenocytes distributed both inside the fascicles (intra-fascicular) and on the periphery (inter-fascicular) of the fascicles. The intra-fascicular tenocytes are distributed regularly in a uniaxial direction between the collagen fibres and their morphology varies from round, elliptical and cigarette-shaped to a longitudinal fusiform shape. More cells are localised within the IFM, which are characterised by having an irregular shape and morphology (Clegg et al., 2007, Benjamin et al., 2008). Tenocytes form approximately 90-95% the cellular element of the tendon. The other 5-10% are predominantly chondrocyte- like cells, present in the compressed regions such as the region passing over the metacarpophalangeal joint and at the bony enthesis(Kannus, 2000, O'Brien, 1992). Tenocytes are responsible for deposition and maintenance of the extracellular matrix, and are key in the process of tissue turnover. Moreover, tenocytes adapt themselves to the surrounding environment, undergoing regional modification of their morphology and activity (Feitosa et al., 2006, Hosaka

et al., 2010). They respond to mechanical load, leading to an increase in the rate of collagen synthesis (Kjaer et al., 2006), a process regulated by the hormones and growth factors, including IGF-1, TGF-beta and IL-6 (Langberg et al., 2002, Heinemeier et al., 2003). A number of differences have been observed in tenocyte morphology and proliferation in different regions (MTJ, Mid-metacarpal and OTJ). For example, collagen synthetic ability has been found to be significantly lower in cells from the mid-metacarpal region, particularly when cells were treated with TNF-α, but the level of proMMP-9 produced was substantially lower in cells toward the OTJ (Hosaka et al., 2010).

1.6 HISTOLOGY OF TENDON

Normal tendon architecture comprises dense regularly organised longitudinal collagen fibres. The fibres are organised in aligned uniform different-sized bundles that are outlined by various amount of IFM (Rowe, 1985, Kannus, 2000, Benjamin et al., 2008). The collagen fibres (type I) of the fascicles are dense and crimped on their longitudinal axis (Kastelic et al., 1980, Patterson-Kane et al., 1998). Other collagen fibres that have been found in tendon are collagen type II that is found in the cartilaginous zone, type III in the reticular fibres of the blood vessels wall, types IV and IX in the capillaries basement membranes, type V in the vessels wall and type X in the mineralized zone in the enthesis adjacent to bone surfaces (Jozsa and Kannus, 1997, Fukuta et al., 1998, Aparecida de Aro et al., 2012). The elastic fibres are dispersed between the collagen fibres and extend longitudinally parallel with the collagen fibres. A larger proportion of the elastic fibres are localised within the IFM, where they arranged in various directions (Grant et al., 2013, Thorpe et al., 2016a). The intra-fascicular tenocytes are characterised by having different sized nuclei, which are inversely proportional with their cytoplasm. They are regularly distributed in a uniaxial direction between the collagen fibres. Their shapes range from a round to an elliptical form in young animals and to round, elliptical, cigarette-shaped or longitudinal fusiform in adult animals (O'Brien, 1992, Kirkendall and Garrett, 1997).

IFM is composed of an irregular loose fibrous connective tissue network containing various structures such as vessels, nerve fibres, cells and both collagenous and non-collagenous extracellular proteins (Yang et al., 2012). Furthermore, it contains elastic fibres, collagen type III, VI, lubricin, decorin, versican, and various

GAGs (Korol et al., 2007, Kim et al., 2010, Sodersten et al., 2013, Thorpe et al., 2013a, Thorpe et al., 2016a). The IFM is more cellular and contains more abundant proteins than the fascicles (Thorpe et al., 2016b). The IFM assists the fascicles to glide freely over each other and also provides tissue elasticity, which plays a role in the mechanobiology of the tendon (Thorpe et al., 2012). However little information is available on the IFM structure's composition and organisation, and how it may alter with age and tendinopathy (Figure 1.4) (Thorpe et al., 2015b).

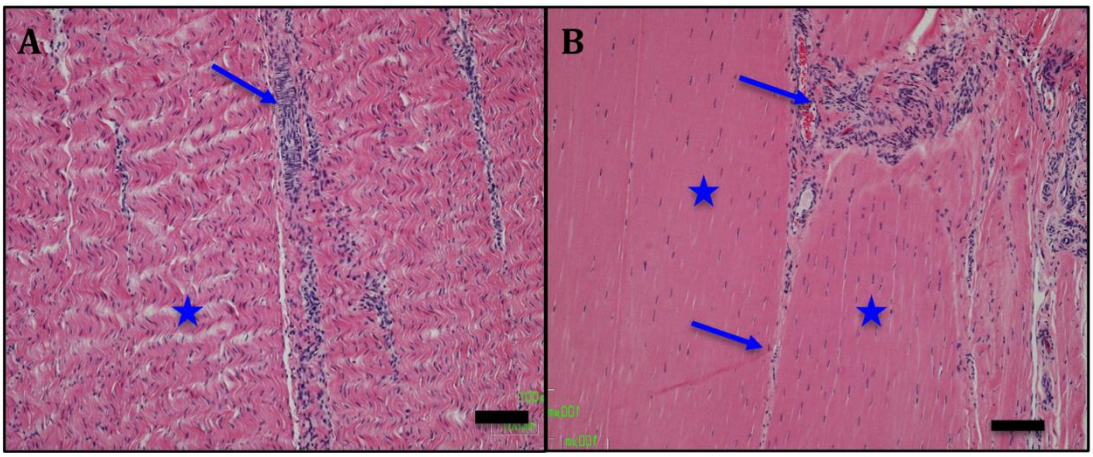

Figure 1.4: Normal histology of a longitudinal section of foetus (A) and fourteen years old (B) SDFT, H&E stain. Note the longitudinal arrangement of collagen fibres within fascicles (Asterisks). The crimp pattern is obvious in foetal tendon. The IFM outline the fascicles (arrows) and contain blood vessels and a larger number of cells (Scale bar=100μm), (Unpublished).

1.6.1 Appropriate staining of the tendon

To explore the tendon architectures different stains can be used to define both the general and the specific components of the tendon. Examples of these stains are:

1.6.1.1 Haematoxylin and Eosin stain (H&E)

H&E is the simplest and most frequently used stain, composed of the acidic (eosin) and basic (haematoxylin) dyes that react with the acidic and basic

components of the tissue respectively. H&E stains the tendon background (collagen fibres) pink, erythrocytes cherry red colour and the nuclei blue to purple (Luna, 1968).

1.6.1.2 Alcian blue and periodic acid Schiff (Alcian blue-PAS)

This stain can be used separately or in combination, the combination of these two stains is used to demonstrate the full complement of connective tissue PGs. The results show a blue colour reaction with the acidic mucopolysaccharides and magenta with the presence of neutral polysaccharides. Further it gives varying shades of purple to deep blue in the presence of GAGs, and stains the nucleus pale blue (Yamabayashi, 1987, Wulff et al., 2004).

1.6.1.2 Safranin-O

Safranin-O is cationic dye and reacts with the PGs and GAGs, it can be used to identify mucins, cartilaginous tissues and mast cells in tendinopathies where chondroid metaplasia is a feature (Schmitz et al., 2010).

1.6.1.3 Toluidine blue

Toluidine blue is a basic thiazine metachromatic stain, which reacts strongly with the acidic component of the tissue such as GAG. The results demonstrate components such as mast cell granules and GAG, which stain pinkish purple and the nuclei, which stain light blue. The cytoplasm and other tissue elements have various shades of light blue (Schmitz et al., 2010).

1.6.1.4 Elastic Van Gieson's stain (EVG)

EVG is used to stain elastic fibres and differentiate them from the rest of the tissue. Elastic fibres are stained with Millers stain and then counter-stained with Van Giesons stain. The elastic fibres are stained deep blue to black colour, collagen fibres red and other component yellow colour (Wulff et al., 2004).

1.6.1.5 Masson's trichrome

Masson's trichrome is applied selectively to stain muscles, collagen fibres and erythrocytes. Different staining protocols are available that are used to stain and

identify the collagen fibres. The tissue components such as nuclei stain dark brown, collagen fibres green or blue, whilst the cytoplasm, erythrocytes and muscle fibres stain red (O'Connor and Valle, 1982, Wulff et al., 2004).

1.6.1.5 Other stains

Russel-Movat Pentachrome stain is used to demonstrate muscle, elastic fibres, collagen, reticular fibres and the ground substance. Von Kossa stain is used to demonstrate deposition of calcium and osteoid metaplasia (Wulff et al., 2004).

1.7 MECHANICAL CONCEPT OF TENDON

The main function of the tendon is to transmit mechanical force from the muscle to the bone, which subsequently leads to skeletal locomotion (Kannus, 2000). The equine SDFT is a long elastic tendon, exposed to a heavy mechanical load particularly during racing and galloping exercise (Birch et al., 1998, Meghoufel et al., 2010). Internal transmission of the mechanical force is carried out through multiple tendon subunits (fascicles). The force is transmitted mainly within the individual fascicle and the fascicle is made up from tendon features that contribute to force transmission such as collagen fibrils, crimp flattening and inter-fibrillar communication (Franchi et al., 2007b, Fessel et al., 2012). Ultimately, the force is directly transferred through these collagen fibrils, which form the basic functional units of the fascicles (Kastelic et al., 1978, Wang, 2006). They are inter-connected with each other by many inter-fibrillar bonds (for instance, PG bridges), however, it has been shown that in human Achilles tendon these do not play a role in the transmission of mechanical forces (Provenzano and Vanderby, 2006). The mechanical properties of the fascicles have been found not to be homogenous within human tendons and between genders. Fascicles from the Patellar and Achilles tendons are functionally independent structures in force transmission whilst one study showed that the IFM does not play role in force transmission (Haraldsson et al., 2008), in the equine SDFT it has been shown that the IFM contributes to the mechanobiology, of the tendon (Thorpe et al., 2012).

The SDFT like other tendons comprises different sized and shaped fascicles, extending longitudinally and parallel to the long axis, and are optimised to transfer mechanical forces (Riemersma and Schamhardt, 1985, Meghoufel et al., 2010).

Different studies in mature animals such as chicken and mouse have shown that the main fascicular structures, the collagen fibrils, are mainly parallel to each other. However, at some regions disorganised fibrils could be seen, which contain interwoven, branched and converging fibrils (Birk et al., 1996, Birk et al., 1997, Vanderby Jr and Provenzano, 2003).

In equine SDFT electron microscopy and mechanical data have demonstrated that fascicles are rotated around their longitudinal axis. This rotation indicates that the fascicles have a twisted or helical configuration when running along the longitudinal axis of the tendon (Thorpe et al., 2013b, Thorpe et al., 2015d). At the microscopic scale a number of helical configuration models of fascicles have also been documented and demonstrated in different tendons such as the human patellar, rat-tail tendons and bovine Achilles tendon (de Campos Vidal, 2003, Reese and Weiss, 2013). These models have demonstrated that the crimped and un-crimped collagen fibrils are either aligned and run parallel with the longitudinal axis of the fascicles, or are helically arranged on their longitudinal axis or around the longitudinal axis of the fascicles (Grytz and Meschke, 2009, Shearer, 2015b, Shearer, 2015a). The presence of this helical configuration in certain tendons and particularly in the equine SDFT results in fascicles being capable of acting as springs and storing a greater amount of energy (Shadwick, 1990, Thorpe et al., 2014b). In a study of quasi-static loading of fascicles from the SDFT and CDET, it was found that fascicles from SDFT recorded greater fatigue resistance than those from CDET; a cyclic load of 16,825 and 2017 before failure was recorded in SDFT and CDET respectively. Post-experimental strain assessment of the fascicular structure reported that the microstructures became damaged and disorganised and that there was decreased rotation and recovery after loading. Thus fascicles from equine SDFT are shaped to enable greater tendon capacity to recoil and store energy than those from the positional CDET (Thorpe et al., 2014b, Thorpe et al., 2014a).

The equine SDFT can therefore be categorised as a tendon with recoiling capacity, which can store a large amount of energy and give a greater extensibility than the other tendons. Furthermore, there is evidence of regional strain differences in equine SDFT that make the tendon mechanically anisotropic (Crevier et al., 1996). It has been found that the SDFT in the metacarpal region is stiffer, has a higher

modulus, higher yield stress, lower yield strain and lower yield load than the distal (sesamoid-digital) region. Together with the higher stiffness and smaller cross sectional area of the metacarpal region it has been hypothesised that the mid-metacarpal region is relatively weak, which could lead to the higher incidence of injuries (Crevier et al., 1996, Crevier-Denoix and Pourcelot, 1997). A study did identify that the SDFT cross sectional area is significantly greater in trained horses than the non-trained horses (Gillis et al., 1995a); in contrast, an experimental study, found that both short and long term exercise did not lead to hypertrophy of SDFT in young horses (Birch et al., 1999b).

An in vitro mechanical study of the equine SDFT has recorded a maximum failure strain and stress of 17.7± 1.2% and 64.9± 2.9 Mpa respectively (Dowling et al., 2002), whilst a failure strain of 16% has been recorded *in vivo* (Stephens et al., 1989). In other studies different average ultimate strains (failure load) of 12.13% (Riemersma and Schamhardt, 1985) and 12.5% (Crevier et al., 1996) were recorded. In foals the mean failure strain is less than that of the mature horses and a strain of 11-12% has been identified. Thus the mechanical properties of the elastic storing SDFT depend on age, collagen fibre assembly, collagen cross-links, IFM and the arrangement of the fibrils in a form of a helical substructure (Dowling and Dart, 2005).

1.8 TENDON DURING AGEING

Tendon, like the other connective tissues, undergoes morphological, mechanical, pathological and biochemical alteration during ageing; these involve both the cellular and ECM components. Age related alteration reduces the tendon's ability to resist environmental stress and results in decreased tissue homeostasis, which can be observed on both the macro and microscopic levels (Tuite et al., 1997, Russo et al., 2015).

1.8.1 Structural development

Within the tendon, collagen fibres are among the units most vulnerable to alteration during ageing and this subsequently affects the mechanical properties of the tendon (Moore and De Beaux, 1987). Like other tissue tendon develops and grows concomitantly with the skeletal system (Gillis et al., 1995b, Gillis et al., 1995c,

Patterson-Kane et al., 1997a). The SDFTs reach their maximal size when the horse becomes sexually mature at around two years old (Gillis et al., 1995b). It has been recorded that the SDFT cross sectional area increases rapidly from age 5 to 8 months, and then continues to increase slowly until reach the age of 12 to 18 months, beyond which it is not increased significantly and even with an increasing body weight (Moffat et al., 2008). Meanwhile, growth of the cannon bone in length completely stops and the growth plates disappear around 1½ year old, but maximum bone mineral content (BMC) is not achieved until the horse reaches six years old, therefore the SDFT CSA reach maximum size before skeletal maturity (Bennet, 2008, Lawrence, 2008). It seems that from the foetal period until maturity, the SDFT undergo conformational change and biochemical accretion on both the vertical and horizontal dimensions and it appears that the SDFT undergo further biochemical and mechanical alteration after maturity (Gillis et al., 1995c, Patterson-Kane et al., 1997a). It has been demonstrated that the mechanical properties of developing skeletal tissues could be specified by the presence of a cross-link network of collagen fibrils specifically in foetal tissue, as well as the viscous sliding action of collagen fibrils, which plays a vital response during movement before birth (Birk et al., 1996, Silver et al., 2002). Then after birth, at the start of locomotion, mechanical stability results essentially from the elastic deformation of the flexible portion of collagen molecules within the cross-linked fibrils (Patterson-Kane et al., 1997b). Concomitantly the inter-fibrillar viscosity declines and this results in a reduction in sliding between the fibrils and then the fascicles (Silver et al., 2003). Beyond maturity tendon is still subjected to mechanical, biochemical and cellular alteration, as manifested by a decline in the ability to tolerate environmental stress and a decrease in tissue homeostasis during ageing (Tuite et al., 1997, Russo et al., 2015). Moreover in rat tail tendon it has been recorded that the collagen volume fraction increases steadily and the numbers of tenoblasts rapidly decline from new born to 12 weeks of age (Moore and De Beaux, 1987).

1.8.2 Gross configuration during ageing

The SDFT colour alters in aged horses; specifically on a transverse section it became darker from the pearly-white in foal to a yellow-brown in aged horses (Figure 1.5). Moreover, multiple white or yellow spots can be seen at the distal region at the level of the proximal sesamoid bones in older samples (Webbon, 1977).

Tendons from mature rat are stiffer, stronger and more rebound resilient than tendons from older animals (Nakagawa et al., 1996) and it has been recorded that the cross sectional area of the human Achilles tendon is increased by approximately 22% at older ages (Magnusson et al., 2003a). In the equine SDFT the cross sectional area showed no significant increase after 18 months of age (Moffat et al., 2008). The increase in tendon cross sectional area has been stated to be related to the amount of stress to which the tendon is subjected (Ker et al., 1988). This is accompanied by an increased collagen content that increases the tensile strength of the tendon. It has also been recorded that tendons with a cross-sectional area of 1 cm^2 have the ability to sustain weights of 500 to 1000 Kg (Shadwick, 1990).

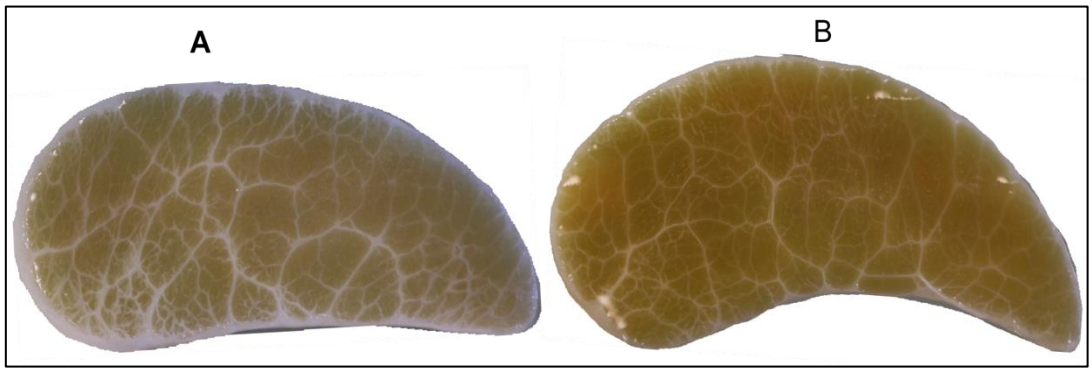

Figure 1.5: Transverse sections of the SDFT approximately at the mid-metacarpal region of 4-years-old (A) and 12-years-old (B) horses. Note the aged SDFT is darker in colour (yellow-brown) than the young (lighter) (Unpublished).

1.8.3 Ageing and Mechanobiology

It has been shown that ageing results in a reduction in the fascicular sub-helical configuration, corresponding to a decrease in fatigue resistance in aged horses which is likely to make the aged equine SDFT more prone to mechanical injury (Thorpe et al., 2013b). In a study of rat-tail tendon, it was found that the ultimate strength, elastic modulus and ultimate strain increased in aged rats and the total collagen content decreased in aged rat compared to mature animals leading to a moderate decline in the tendon's hysteresis (Vogel, 1980). These alterations lead to a decrease in the rate of force transmission in aged compared with young tendons (Narici and

Maganaris, 2006). Similarly in a study of Achilles tendon in women it was shown that the older Achilles tendons were approximately 15% stiffer than younger tendons and this occurred as a result of alterations of the tendon structure during ageing (Magnusson et al., 2003a).

In equine SDFT it has been shown that fascicles from aged horses were less resistant to cyclical load failure and failed at a lower cycle than in younger horses (16825 ±6104 in young horses; 4062 ±927 in old horses) (Thorpe et al., 2014b). In addition to the fascicles, the IFM also contributes to the mechanical properties of the SDFT, in which the IFM withstands the cyclic loading and is more extensible than in the positional CDET tendon (Thorpe et al., 2012). The IFM is also altered during ageing and it becomes stiffer and less able to withstand the cyclical load in aged horses (Thorpe et al., 2013c, Thorpe et al., 2015b). Moreover, it has been recorded that intermolecular cross-linking of the collagen fibres significantly correlates with the mechanical features of the tendon (Thorpe et al., 2010b, Fessel et al., 2012). It was shown that there was a significant correlation between the pyrrole cross-link level and the values of ultimate-stress, yield-stress and the elastic-modulus in the equine SDFT. However there was no positive mechanical correlation with either hydroxylysyl or lysyl-pyridinoline levels (Birch et al., 2008, Thorpe et al., 2010b). In aged tendon the amount of the non-reducible collagen crosslinks is increased, which subsequently decreases the biochemical and mechanical properties of the tendon (Eyre et al., 2008). When the amount of the non-reducible collagen crosslink increases, it makes the collagen fibre become less soluble, more resistant to thermal denaturation and resistant to degradative enzymatic digestion (Menard and Stanish, 1989, Shadwick, 1990, McLatchie and Lennox, 1993). In a study of porcine tendon ageing, it was found that the tendon was stiffer and stronger in the older animal than in the foetus or young animals. In young pigs, the flexor tendons has higher mechanical hysteresis and extensibility but a lower elastic modulus, tensile strength and energy storage capability than the mature tendon (Shadwick, 1990).

1.8.4 Cellular morphometry and ageing

An assessment of the cellular activity in the equine SDFT at various ages (3-30 years old) by measuring specific mRNA and protein levels, found no decline in cellular density or specific mRNA or protein levels with age. It was hypothesised

that the mechanism of age related tendon degeneration is not due to reduced cellular density or cellular synthetic activity but an alternative mechanism should be investigated (Thorpe et al., 2015c). It has also been shown that the rate of tendon oxygen uptake is 7.5% lower than in the muscles, and in aged animals the metabolic activity of tendon and ligaments are shifted from aerobic to a slightly anaerobic pathway as a result in a decline in capillary blood flow (Vailas et al., 1978, Astrom, 2000).

Studies on rat tendon stem cells (TSC) using quartz thickness shear mode (TSM) resonators showed that the storage modulus is ten times greater in aged than in young TSC. Further, on phase contrast and SEM, these cells showed an enlarged flattened and heterogeneous appearance during ageing in contrast to the immature cells which they had a homogenous elongated form (Wu et al., 2015). At the cellular level, there is also up-regulation of miR-135a, which targets ROCK1 genes in young TSPCs. The authors expressed the view that it suppressed the process of ageing, enhancing cell proliferation, migration and differentiation, while down- regulation of miR-135a in aged TSPCs reversed this situation (Chen et al., 2015). Meanwhile in an in vivo study on mouse TSCs has found that ageing results in the deposition of various materials including fat, PG and calcium and that moderate treadmill running enhances tendon cell regeneration capacity and decreases degeneration in aged tendon (Zhang and Wang, 2015). Long-term microscopic degeneration of the ECM develops focal areas of chondroid metaplasia that stimulate tenocytes to produce specific ECM components such as PGs and GAG (Lui et al., 2009, Tamam et al., 2011). Recently, in vitro induction of the tendon stem/progenitor cells (TSPC) populations of equine SDFT with osteogenic and chondrogenic media, found that the TSPCs when plated with a medium pre-coated with fibronectin promote both osteogenic and chondrogenic differentiation (Williamson et al., 2015). However, chondroid metaplasia normally occurs in bird tendon (Berge and Storer, 1995, Landis and Silver, 2002, Organ and Adams, 2005)

During ageing human tendon cells undergo morphological alteration from an ovoid and small spindle shape to an elongated form (Russo et al., 2015). The cell to matrix ratio progressively declines during ageing and the tenoblasts become mature with an increase in size from 20μm-70μm to 80μm-300μm. The tendon cell

processes become more elongated (2-10μm), the nuclear ratio to cytoplasm is also increased and their nuclear chromatin is condensed (Jozsa and Kannus, 1997, Kannus, 2000). Similarly it has been shown in ageing rat-tail tendon that the cellular density decreased in proportion to the ECM contents and that the plasma volume fraction and tenoblast density also significantly decreased with age (Greenlee and Ross, 1967, Squier and Magnes, 1983, Moore and De Beaux, 1987). In a study measuring the DNA content in both the SDFT and the DDFT, it was found that the DNA content was significantly decreased only in the DDFT during ageing (Birch et al., 1999a). In contrast, another study found that the DNA content decreased with age only in the SDFT (Batson et al., 2003).

1.8.5 Cartilage oligomeric matrix protein (COMP)

The level of COMP rapidly increases in the SDFT after birth and through development. It reaches its highest level (~ 10mg/g wet weight) during the first and second years of age and then decreases during ageing throughout the whole SDFT particularly at the mid-metacarpal region (Smith et al., 1997). Others reported that COMP mRNA was not detected in the foetal SDFT and that it reaches the highest level at about three years old, which was positively correlated with the smallest fibril diameter (<60nm) (Sodersten et al., 2005).

1.8.6 Biochemical Properties during ageing

1.8.6.1 Collagen

In a study using racemization of aspartic acid and indirect measurements of the level of a type I collagen degradation marker, in order to calculate the half life of aging for collagenous components in equine SDFT and CDET, it was found that the average half-life of collagen was approximately 197.53 (±18.23) years in SDFT and 34.03 (±3.39) years in CDET and these values increased significantly with aging (Thorpe et al., 2010c). In a study on the rabbit Achilles tendon, it was shown that the amount of collagen increased to approximately 21% dry weight and the water content decreased to approximately 15% as the animals aged (Ippolito et al., 1980). In the equine SDFT the average mass diameter of the collagen fibres were did not change during ageing (Patterson-Kane et al., 1997a). In a study of self-assembly of collagen fibres, it was found that tensional loading increased the ultimate tensile

strength, packing and fibril orientation. Furthermore, decorin also increased the tensile strength of uncross-linked collagen fibres by facilitating the amount of inter-fibrillar slippage (Pins et al., 1997). It has been shown that tissue turnover and the production of the collagen molecules declines during ageing; metabolically it is thought to be related to the density of the tenocytes between the collagen fibres, which is concomitantly decreased during ageing. Therefore, reduction in the cellular density will result in a decline in tenocytes ability to re-generate new collagen fibres and to replace damaged fibrils resulting from an accumulation of a long term micro-damage during exercise or galloping (Batson et al., 2003).

The mass-average diameter of the collagen fibrils in the central core of SDFT is approximately 60.9nm (±3.1) in the foetus. It is significantly increased to 127.8nm (±6.6) in young horses (3- 4 year-old) and reaches the highest level of 143.5nm (±4.1) in middle-aged animals (5- 7 years old). Then during ageing diameters decline to 133.9nm (±12.9) nm in aged horses (10-15 year-old) where there is no significant difference between the central and peripheral regions. Further, the crimp angle of the collagen fibrils also declines progressively in the SDFT central region and with age. The crimp angel are 26.7°, 14.6°, 13.1° and 10.5° in the foetal, young, middle-aged and old horses respectively (Parry et al., 1978, Patterson-Kane et al., 1997a).

1.8.4.2 Biochemical cross-link

A study has indicated that the replacement of the immature collagen crosslink and complete maturation takes place within the first two years of life. So the concentration of the immature crosslink (dihydroxylysinonorleucine (DHLNL) and hydroxylysinonorleucin (HLNL)) decreases rapidly after birth. The DHLNL crosslink continues to decrease till it reaches an undetectable amount by the two years of age but HLNL declines to zero during the first few months of life. However, as tendon matures the collagen crosslink hydroxylysylpyridinoline (HP) increases rapidly and reaches its highest level at three years old and not altered with age, but lysylpyridinoline (LP) increased significantly with ages (Patterson-Kane et al., 1997b, Thorpe et al., 2010c).

Lin and others recorded that SDFT composition varied between regions (Lin et al., 2005). Most of the biochemical parameters do not alter during ageing except that

the pentosidine crosslink is markedly increased in the compressive site during ageing. Regionally the cellular, water and both degraded and the total collagen content are significantly higher in the mid-metacarpal region, but the GAG, hyaluronic acid (HA) and lysylpyridinoline-cross link is only half as high in the compressive region (Lin et al., 2005). Meanwhile, in porcine SDFT it has been recorded that higher levels of GAG (CS) are found in the compressive regions, near the metacarpophalangeal joint (Feitosa et al., 2006). Nevertheless, collagen fibrils contain a considerable amount of water, which is distributed throughout the fibrils and substantially affects their mechanical properties (Vogel, 1980, Thorpe et al., 2010b). By using dynamic mechanical spectroscopy five types of water molecules have been identified, these include the water molecules that form a paired hydrogen bond peptide carbonyl inside the tropocollagen molecules (Pro-Gly-Pro) (Ramachandran and Chandrasekharan, 1968) and the specific water molecule associated with a number of specific sites such as the hydroxyl group of hydroxyproline. The third type is located inside the micro-fibrils and is associated with the polar and ionic sides groups in the form of hydration spheres. When the tissues cool below zero a cubic form water molecule formed between the collage micro-fibrils (fourth type). This type is strongly associated with the tendon structures and dispersed between the micro-fibrils. Finally, the fibrils are embedded in the gelatinous hydrated extracellular matrix (Morawetz, 1958, Yonath and Traub, 1969, Baer et al., 1976).

1.8.4.3 Molecular studies

In a transcriptomic analysis on the human Achilles tendon, it was shown that gene expression of protein-coding and non-coding transcripts (small non-coding RNAs, pseudo-genes, long non-coding RNAs and a single microRNA) were altered in a total of 325 genes between young and old tendons (Peffers et al., 2015). Where, 191 genes showed increased expression in older ages and the remainder were decreased. The study found that RNA alters at various genomic levels during ageing, demonstrating that reduced matrix protein turnover is not the only factor altered during tendon ageing, but that alteration in the regulation of transcriptional networks plays a key role (Peffers et al., 2015). In other studies, it was shown that gap junction intercellular communication (GJIC) proteins including connexins 43 and 32 played an important role in the production of collagen during strain, but GJIC expression

significantly declined during SDFT maturation (Stanley et al., 2007, Young et al., 2009).

1.9 INJURIES OF TENDON

1.9.1 Injury predisposition with ageing

Injuries to the SDFT are common in all racing disciplines but risk of injury is increased in aged horses (Perkins et al., 2005, Avella et al., 2009). Different studies have recorded that age is considered as an important factor of musculoskeletal injury, where the distal part of the forelimb is injured particularly in steeplechase races (Williams et al., 2001, Perkins et al., 2005). During ageing horses are exposed to cumulative exercise regimens and this possibly leads to an accumulation of the micro-damage. However the steeplechase uses older horses (median=8 years old) than hurdles (median=6 years old) (Lam et al., 2007b, Reardon, 2013). The entire SDFT is prone to injury but commonly the mid-metacarpal region is most frequently injured (Perkins et al., 2005, Thorpe et al., 2010a). In an ultrasonographic study of SDFT tendinitis in the proximal metacarpal region it was shown that the severity of injury varied regionally, with 50-100% of the SDFT CSA involved. Such injuries were accompanied by clinical lameness, which affected the horses' performance and a poor prognosis in aged horses (Chesen et al., 2009). In another retrospective study to determine the prevalence of overstrain injury in Japan in 1999 on a population of 10,262 Thoroughbred racehorses, it was found that the prevalence of SDFT tendinopathy was 11.16%. Interestingly injuries commonly affected the fore limb and their incidence was increased with age: at 2, 3, 4, and 5 years of age the rate of injury was 6.05%, 12.54%, 14.16% and 16.32% respectively (Kasashima et al., 2004). Similarly, in a study of National Hunt racehorses in two different seasons, it was recorded that the prevalence of SDFT pathology was 24% and that this increased with ageing (Avella et al., 2009). Additionally, it has been shown that other surrounding structures are also prone to injury during ageing, for instance lateral condylar fractures occur 2.6 times more frequently in horses that started racing at at 3 or 4 years old than in horses that first raced as 2 years olds (Parkin et al., 2005). Tendon components such as mucopolysaccharide, collagen crimp angles and collagen turnover are decreased during ageing (Nakagawa et al., 1994, Tuite et al., 1997, Kjaer, 2004). Furthermore, the rate of oxygen consumption also decreases

during ageing, which leads to a decreased metabolic activity and slower rate of healing (Vailas et al., 1978). It has been shown in human tendon that repetitive and continuous micro-structural damage occurs even within physiological limits as a result of non-uniform and different frictional forces between the collagen fibrils, that leads to an accumulative micro-trauma (Arndt et al., 1998). These structural alteration affect the mechanical and tensile performance of the tendon in addition to the continuous cyclical loading, which results in a tendon more prone to injury during ageing (Jozsa and Kannus, 1997). In a three year prospective study on human athletes, it was shown that tendon injury occurred during endurance sports and the rate of injury was 29% higher in older people (Kannus et al., 1989). The equine SDFT is exposed to a continuous heavy mechanical loading particularly during racing, which particularly makes the tendon prone to injury (Kalisiak, 2012, Thorpe et al., 2013c)

Injuries of the SDFT are common causes of equine wastage and it has been recorded that the rate of injury is increased with ageing. The incidence of injury is higher in horses racing over hard surfaces than on softer surfaces (Williams et al., 2001). Moreover, it has been shown that injury primarily involves SDFT and the forelimb is affected most commonly (95% of injuries affect the forelimbs). Tendon injury is more common in heavy stallions that raced and were exposed to courses requiring jumping (Kalisiak, 2012, Reardon et al., 2012, Reardon et al., 2013).

1.9.2 Clinical features

Tendinitis is an acute inflammatory reaction to sudden injury or infection but tendinosis is a chronic degenerative change of the tissues without notable inflammatory reactions (Paavola et al., 2002). Tendinosis is thought to be a sequel of micro-traumas that occurs as a result of continuous degeneration of the tendon in response to overuse (Sharma and Maffulli, 2005, Bass, 2012). The injured SDFT is manifested by swelling, heat, lameness and pain on palpation. On gross section, the localised lesion manifests a dark red discolouration, haemorrhage and oedematous swelling of the tendon parenchyma, epitenon and paratenon sheath (Watkins et al., 1985, Webbon, 1977, Birch et al., 1998, Cadby et al., 2013). On evaluation of the clinically injured SDFT using ultrasound B-scan image simulation, it was observed that the size of the injured SDFT increased as a result of bleeding and diffusion of

lesions through the ECM. In addition the number of fascicles bundles was decreased by approximately 20% (50 ±11 decreased to 40 ± 7) due to disruption of the thinnest IFM (Meghoufel et al., 2010, Cadby et al., 2013). Different tools can be used for diagnosis of equine tendinopathy but one study has shown that using MRI for diagnosis of clinical tendinitis in cases where there is a chronic scar formation in the core of the tissue is much more accurate than Ultrasonography (Kasashima et al., 2002).

Microscopically, with injury there is a granulomatous inflammation with an increased number of tenocytes and infiltration of inflammatory cells (leucocytes), fibrils are disorganised and there is evidence of neo-vascularisation (Kobayashi et al., 1999). The cells become larger and more rounded with an increase in the amount of GAG particularly in an older patient (Maffulli et al., 2000). In experimentally induced injuries of the equine SDFT, it has been demonstrated that the injured SDFT is softer, discoloured and is accompanied by the presence of a red tinged fibrous lesion. Histologically, there was an alteration to collagen fibres alignment, an increased number of both intra-fascicular and inter-fascicular cells, cell morphology was altered and there was a positive staining for PG and GAG (Cadby et al., 2013, Jacobsen et al., 2015). Similarly in experimentally induced chronic tendinopathy of sheep (infraspinatus tendon), it has been shown that in both overstressed and stress-deprived conditions the injured tendon develops areas of chondroid metaplasia, accompanied by an increase in the amount of PG and GAG (Smith et al., 2009).

In human tendinopathy, the injured tendon manifests similar clinical, gross and histological alteration but occasionally in chronic cases it is accompanied by mineralisation; specifically the tendon develops areas of hyalinisation that is followed by intra-tendinous ossification (Aksoy and Surat, 1998, Richards et al., 2008, Tamam et al., 2011). Typically, it has been observed that in chronic rotator shoulder tendinosis, calcium (hydroxyapatite crystals) are deposited within the tendon ECM resulting in calcific tendinitis, which is preceded by degenerative dystrophic calcification lesions, where there is initial differentiation into a fibrocartilaginous mass with subsequent calcium deposition (Uhthoff et al., 1976, Weintraub, 2003). Intra-tendinous ossification is considered as a pathological tendonitis in mammals but it is normal in certain birds and dinosaurs (Berge and

Storer, 1995, Landis and Silver, 2002, Organ and Adams, 2005, Regnault et al., 2014).

1.9.3 Gen expression during injury

It has been observed that several genes show increased expression in different stages during injury of the SDFT. These include the MMP-1 during the acute phase and MMP-13, Collagen-II, -IX, -X, -XI, aggrecan, biglycan gene subsequent to injury (Clegg et al., 2007). In human rotator cuff injury it has been demonstrated that the amount of MMP-1 and MMP-9 is significantly increased in contrast to MMP-3 that is significantly decreased (Lakemeier et al., 2011). Moreover, in acute injury of the SDFT the mass average diameter of the collagen fibrils is decreased from 69 nm (±54.4) to 61.7nm (±36.5), and DS is up regulated but HA and CS are down regulated (Kobayashi et al., 1999). The DS regulation could play an important role in fibrosis. It has been shown that the levels of DS increase during chronic inflammation and DS regulates the organisation of collagen fibres and fibrillinogenesis (Mori, 1991). Decorin-DS binds to the surface of collagen fibres, regulates collagen fibre assembly and enhances lateral and the longitudinal growth of the collagen fibres (Birk et al., 1995, Silver et al., 2003). Further, it has been found that four cytokines (IL1-α, IL1-β, TNFα and IFNγ) are elevated variously in injured equine SDFT and act to enhance wound healing (Hosaka et al., 2002, Dakin et al., 2012). Meanwhile, an in vitro mechanical study on SDFT fascicles exposed to cyclic overloading, found that tissue overloading results in ECM micro-damage. Moreover, cells became more rounded and the inflammatory markers cyclooxygenase-2 and interleukin-6 were increased, as well as matrix metalloproteinase-13 and the collagen degradation marker C1, 2C (Thorpe et al., 2015a).

1.10 HEALING

Injured tendon progresses through the normal stages of healing including inflammation, repair organisation and remodelling phases. The healing process takes place through intrinsic and extrinsic tissue responses (Gigante et al., 1996, Reddy et al., 1999). The inflammatory phase extends up to one week after injury and during this period the cells migrate from the surrounding tissues toward the injured area. This is then followed by tissue exudation and formation of granulation tissues

(Maeda et al., 2013). In the repair phase, large numbers of fibroblasts, mainly of intrinsic origin, begin to produce collagen fibres. Migrating fibroblasts continue to increase in the injury site over a period of five weeks (Sharma and Maffulli, 2005). They are fundamental cells in the healing process by enabling the production and degradation of the collagen molecules, and this requires a period of approximately two months. The final, remodelling, phase is characterised by stability, organisation of the collagen fibres into normal axial directions, increases of the collagen cross-links and increased tissue strength (Parry et al., 1978). However, it has been noticed that with intensive remodelling over a few months complete regeneration and normal mechanical properties were not achieved (Maffulli et al., 2002).

Researchers found that during the healing and the remodelling period the crimp periodicity sharply declined and did not regain a normal value in the following 14 months after injury. Moreover, the mechanical properties of the repaired tendon remained abnormal compared to that of the normal tendon for at least 14 months after injury (Williams et al., 1985). Cells obtained from an injured SDFT have dissimilar phenotypic properties compared to that of normal tendon (Clegg et al., 2007, Yuan et al., 2003). Injured cells display higher collagen gel contraction, reduced adhesion topepsin-digested collagen and decreased migration capacity over ECM proteins. These features indicate that the cells of injured SDFT may be of inferior quality to heal and regenerate the injured tissue (Kihara et al., 2011). In experimentally induced injury of the SDFT using collagenase, it has been observed that there was a marked expression of collagen type I and III genes (Dahlgren et al., 2005) then after 24 hours the collagen fibril diameter altered from a bimodal distribution (35nm–220nm) to an intermediate uni-modal size (73.1nm ±10.7). The uni-modal form remained for up to 14 months until the normal diameter, distribution and mechanical properties were re-established (reach the maximum strength) (Williams et al., 1985). In a study on rabbit patellar tendon, researchers found that ageing negatively suppressed the rate of both healing and remodelling on the experimentally resected central third of the patellar tendon (Maeda et al., 2013). It has been found that COMP and type III collagen are potentially involved in SDFT healing, as they have been localised in injured SDFT, and may represent a prompt healing response of the tissue after injury (Sodersten et al., 2013).

1.11 HYPOTHESIS AND AIM OF THIS STUDY

This study will address the hypothesis that in equine SDFT there is a variable anatomical arrangement to tendon fascicles longitudinally and fascicles split, merge or intermittently inter-connect with each other and not always continuous through the length of the equine SDFT. Moreover, the cellular and ECM organisation of these structural subunits vary regionally and are altered in tendinopathy. Thus characterising the equine SDFT ultrastructure, its organisation and alteration during health and pathology will facilitate our understanding of the tendon structure-functional relationship and injury predisposition. The aim of this thesis is to:

Describe the gross three-dimensional (3D) anatomy of equine SDFT: specifically to document the organisation of the individual sub-units (fascicles) and how this may vary regionally.

1- Identify the 3D anatomy of the SDFT from histological sections with a view to understanding the tendon ultra-structural hierarchy and how this varies regionally.
2- Complete histological scoring of the SDFT and document how the tendon's histological structures vary regionally and during ageing.
3- Document in detail the presence of chondroid metaplasia in elderly horses.
4- Study the 3D, gross and histological alteration of equine SDFT following injury.

CHAPTER TWO

THREE-DIMENSIONAL ANATOMY OF THE EQUINE SUPERFICIAL DIGITAL FLEXOR TENDON (SDFT)

2.1 INTRODUCTION

Tendon extracellular matrix (ECM) is made from tough fibrous connective tissue components, predominantly collagen fibres. Tendons have a low cellularity and connect muscle to the bone via the musculotendinous and osteotendinous junctions (MTJ and OTJ) respectively (Kastelic et al., 1978, O'Brien, 1997, Kannus, 2000). The main function of a tendon is to transfer muscular forces to the bone and facilitate skeletal locomotion. Additionally, some tendons, such as the equine superficial digital flexor tendon (SDFT) have the ability to store energy force through their elastic properties, thereby acting as a spring during stretching (Thorpe et al., 2013b, Tresoldi et al., 2013). Grossly tendon appears brilliant white and portions of it may be surrounded by a synovial sheath, which secretes synovial fluid to lubricate the tendon surface (epitenon) and allows the tendon to glide freely by decreasing surface friction (Kannus, 2000, Pont et al., 2004). The epitenon is a dense irregular network of collagen fibrils, which also contains other ECM components such as elastic fibres and non-collagenous proteins (Yang et al., 2012).

The epitenon surrounds the tendon and sends connective tissue septa into the tendon to form a reticular network known as the endotenon or inter-fascicular matrix (IFM) (Kastelic et al., 1978, Kannus, 2000). IFM organises the tendon architecture into many different sections termed fascicles. Moreover, the IFM contains nerve fibres, lymphatic vessels, blood vessels and different amounts of proteoglycans (PG) that facilitates the smooth gliding of fascicles during tendon extension (Jozsa et al., 1991, Thorpe et al., 2012). When the body of the tendon is compartmentalised into separate fascicles by the IFM; larger fascicular units are called tertiary fibre bundles (tertiary fascicles), which encompass a number of smaller secondary fibre bundles (secondary fascicles). The secondary fascicle comprises a number of primary fibre bundles called sub-fascicles. Their numbers, sizes and shapes differ from tendon to tendon and are not constant throughout the tendon (Baer et al., 1976, Kastelic et al., 1978, Kannus, 2000). Furthermore, the size of the primary, secondary and tertiary fascicle varies between the species, tendons, and regions, ranging between 15µm-400µm (micrometre), 20µm-1000µm and 1000µm-3000 respectively (Figure 2.1). Meanwhile, the collagen fibre is the basic units of the fascicles and is considered to be the basic functional unit of tendon, being responsible of force transmission and many of the mechanical properties of the tendon (Kastelic et al., 1978, Wang, 2006).

To date, in equine SDFT no criteria have been adopted to describe different types of fascicles. Although, most recently, gross and B-scanning ultrasound imaging has been used to describe the fascicles and IFM organisation of the equine SDFT (Meghoufel et al., 2010). However, their organisations throughout the SDFT have not been identified properly. Therefore, further work is needed to characterise and describe the anatomy of the fascicles at different levels, including their length, shape and orientation within the tendon (Parry and Craig, 1984, Magnusson et al., 2003b). My hypotheses are:

- There is a variable anatomical arrangement to tendon fascicles longitudinally through the tendon
- That fascicles are not always continuous through the length of the equine SDFT
- The fascicles may split, merge or intermittently inter-connect with each other

To address the hypothesis, the aim was to define tendon fascicles macroscopically and then to outline and reconstruct specific fascicles throughout serial tendon sections using ImageJ and IMOD programmes, in order to describe the three dimensional (3D) anatomy of these structures. I wished to describe how fascicular shape, continuity and inter-connection are altered within tendons and further to document how these parameters vary between different legs (front/hind).

2.2 MATERIALS AND METHODS

2.2.1 SAMPLES

SDFT samples were taken from Thoroughbred and Thoroughbred cross horses of different ages euthanized for reasons other than orthopaedic disease or injury. Samples were obtained either from a commercial abattoir (Potters, Taunton or Wooton Bassett) or from horses euthanased at the University of Liverpool Equine Hospital with the owner's informed consent. The study was assessed and approved by the University of Liverpool, Veterinary School Research Ethics Committee (VREC, study 214). Seventeen SDFT from 13 horses of different ages (Table 2.1) were prepared for this study. SDFT were dissected from surrounding tissues, wrapping in foil and storing at -20ºC. The dissected SDFT represented the whole metacarpal or metatarsal length, extending from the carpometacarpal to the metacarpophalangeal joints.

The SDFT samples were designed and divided for three descriptive studies;

First study: SDFT from three similar aged (8-years-old) were used to measure the cross sectional areas (CSA) of the tendon in the proximal, mid-metacarpal and the distal regions and further to define fascicles, using ImageJ.

Second study: three paired legs (4, 6 and 18 years-old) were used to demonstrate the pattern of the fascicles and IFM in transverse sections.

Third study: thirteen SDFT were used for 3D reconstruction of the SDFT with their fascicles using IMOD (Table 2.1).

2.2.2 DISSECTION TECHNIQUE

The frozen SDFT samples were sectioned transversely in a palmar-dorsal or plantar-dorsal direction over a dissecting wooden cutting board. Starting from the most proximal aspect at the level of carpometacarpal joint, tendons were sectioned using a post-mortem knife by a regular sawing motion method while applying gentle pressure onto the knife in order to cut in a regular harmonic way; the thickness of the sections varied between 2-3mm (Figure 2.1 A). The numbers of sections per SDFT was not constant, due to the differing sizes and breeds of the horses from which the tendons were collected. The number of SDFT sections was higher in the hind limb

(ranging from 61-65) than the forelimb, which ranged from 43-55, reflecting the greater length of the metatarsus than the metacarpus (Table 2.1).

Table 2.1: SDFT samples collected from limbs of different aged horses with the number of sections of 2-3 mm thick, obtained from each tendon shown, (LF= left forelimb, RF= right forelimb, LH=left hind limb, RH=right hind limb).

<table>
<tr><th colspan="6">SDFT</th></tr>
<tr><th>No</th><th>Side</th><th>Age/ year</th><th>Paired or not</th><th>Number of sections/ SDFT</th><th colspan="2">Selected SDFT for different descriptive studies</th></tr>
<tr><td>1</td><td>LF</td><td>8</td><td>-</td><td>50</td><td rowspan="3">Selected 3 SDFT (No 1-3) for the first descriptive study</td><td></td></tr>
<tr><td>2</td><td>LF</td><td>8</td><td>-</td><td>43</td><td rowspan="16">Selected SDFT (No 3, 4, 5, 6, 7, 8, 9, 10, 12, 13, 14, 16, 17) for the third descriptive study (3D modelling)</td></tr>
<tr><td>3</td><td>RF</td><td>8</td><td>-</td><td>45</td></tr>
<tr><td></td><td colspan="5"></td></tr>
<tr><td>4</td><td>LF</td><td>4</td><td rowspan="2">Paired</td><td>46</td><td rowspan="6">Selected 3 paired SDFT (No 4-9) for the second descriptive study</td></tr>
<tr><td>5</td><td>RF</td><td>4</td><td>47</td></tr>
<tr><td>6</td><td>LF</td><td>6</td><td rowspan="2">Paired</td><td>52</td></tr>
<tr><td>7</td><td>RF</td><td>6</td><td>55</td></tr>
<tr><td>8</td><td>RH</td><td>18</td><td rowspan="2">Paired</td><td>65</td></tr>
<tr><td>9</td><td>LH</td><td>18</td><td>60</td></tr>
<tr><td></td><td colspan="5"></td></tr>
<tr><td>10</td><td>LF</td><td>7</td><td>-</td><td>48</td><td rowspan="8"></td></tr>
<tr><td>11</td><td>RF</td><td>5</td><td>-</td><td>55</td></tr>
<tr><td>12</td><td>RF</td><td>11</td><td>-</td><td>47</td></tr>
<tr><td>13</td><td>LF</td><td>12</td><td>-</td><td>49</td></tr>
<tr><td>14</td><td>LF</td><td>17</td><td>-</td><td>46</td></tr>
<tr><td>15</td><td>RH</td><td>20</td><td>-</td><td>61</td></tr>
<tr><td>16</td><td>LF</td><td>21</td><td rowspan="2">Paired</td><td>43</td></tr>
<tr><td>17</td><td>RF</td><td>21</td><td>44</td></tr>
</table>

2.2.3 TISSUE HYDRATION

All SDFT sections were placed on a wet tissue paper, with their proximal aspect facing upward. This process required 10-15 minutes. The absorbed water appears to be distributed throughout the tissue, probably due to the presence of negatively charged glycosaminoglycan, which attract water molecules (Yoon and Halper, 2005). With hydration the IFM bulged and protruded above the level of the cut surfaces and

appeared clearly between the fascicles as white outlined structures, which could easily be observed between the fascicles (Figures 2.1B and 2.2).

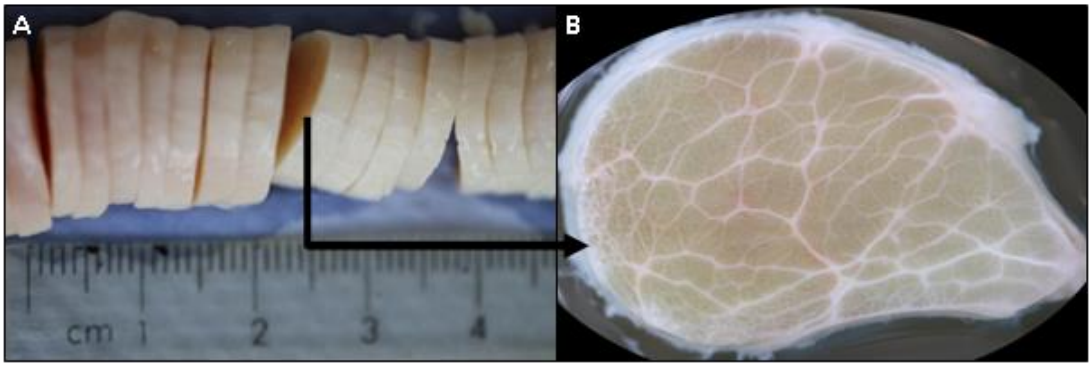

Figure 2.1: A: A series of transverse sections (2-3mm thick) of SDFT from the proximal to the distal part of the metacarpal portion. B: Surface view of a transverse section after hydration, demonstrates obvious IFM tissue between the fascicles as irregularly distributed white lines.

2.2.4 PHOTOGRAPHY OF THE SECTIONS

These sections were transferred individually onto a transparent flat glass plate adjacent to a calibrated ruler and photographed sequentially using a Canon camera (Canon EOS 5D Mark III, 1000 IOS-speed, 100mm focal length) at a distance of 20 cm and without using the flash (Figure 2.1B). All sections were photographed serially as JPEG images, cropped and converted to greyscale images using Paint Shop Pro X4 Ultimate by selecting channel mixer (- 40% red, - 40% green, - 40% blue and 110-120% contrast) followed by a subsequent fade correction (50) to enhance the image clarity. A specific crop contour size was applied to all sections equally and all cropped photos saved as TIFF images for compatibility with IMOD (Figure 2.2).

Figure 2.2: A series of 45 transverse sections of forelimb SDFT (6-years-old) from proximal to distal, following hydration. Sections 1-45 represent SDFT sections sequentially from the level of the carpometacarpal to the metacarpophalangeal joint respectively. The shape and the size of the tendon sections progressively altered from proximal to the distal. Different sized and shaped fascicles are discriminated from each other by the IFM.

2.2.5 IMAGE PROCESSING

Both ImageJ and IMOD programmes were used in order to define, outline and reconstruct the three dimensional anatomy of the SDFT and fascicles from proximal to the distal end longitudinally through the tendon.

2.2.5.1 First descriptive study: ImageJ methods to measure SDFT CSA and define fascicle

The average CSA of the entire SDFT in the proximal, mid-metacarpal and distal region of three individual horses (8-years-old) were measured using ImageJ freehand selection toolbar.

To define fascicles in transverse SDFT sections a new method was developed by using ImageJ to outline different fascicles and measure specific parameters as follow:

1- Surface interactive view of the 2D images

After importing the 2D image of each section into ImageJ (Version 1.49) (Schneider et al., 2012), the proposed section surface was selected with the freehand selecting toolbar. Then through the plugins toolbar the interactive 3D surface plot was opened to show 3D plot view of the section. The surface plot was adjusted by selecting the following parameters; filled, original colours, selecting z-ratio = XY-Ratio with an invert option, 1.40-1.70 scale, 4.00-4.10 z-scale, 65-75% Max, 0% Min, 512 Grid size and 0.1 perspective. The optimum value is mainly dependant on the Max and Min ratio, which is needed to optimize the degree of fascicular discrimination from each other (Figure 2.3). After adjustment of these parameters the surface of the tendon section appeared with clear boundaries around the fascicles. The larger tertiary fascicles were easily defined due to the abundant IFM surrounding them; however the secondary fascicles were difficult to accurately define due to the thinner, less distinct IFM. However, in places the IFM surrounding tertiary fascicles also became narrower and poorly defined. During the interactive 3D surface plot visualisation the tertiary fascicles were outlined and their morphology identified by continuing the image optimisation until the fascicles were totally discriminated from each other. Further, secondary fascicles were also visualised by zooming the image in order to see the detailed arrangement of the IFM and its thickness compared to the IFM that surrounds the tertiary fascicles.

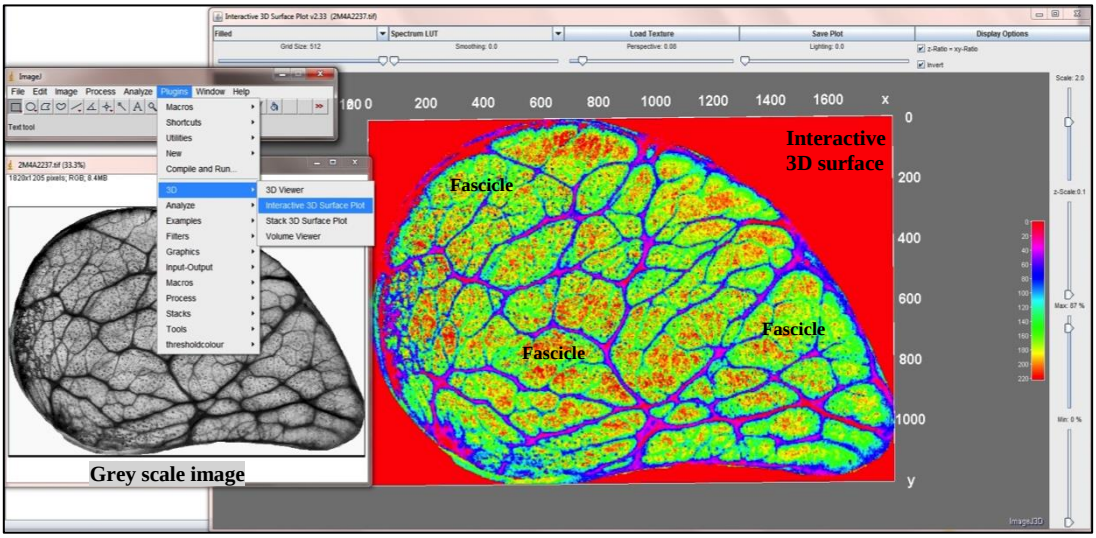

Figure 2.3: Snapshot of using ImageJ, how the interactive 3D surface plot view is created from a greyscale image. Initially the greyscale image loaded into ImageJ and through the plugin toolbar the image turned into interactive 3D surface plot in order to outline fascicles. Note the tertiary fascicles are well delineated by a clear IFM while the secondary fascicles not detached from each other.

2- Diameter of the tertiary and secondary fascicles

After optimisation of the image, when the tertiary fascicles outlined and separated from each other and from the secondary fascicles, the estimated area and the diameters of both the tertiary and secondary fascicles were measured in the proximal, mid-metacarpal and distal region in three horses (8-years-old) by using ImageJ. Fascicles measurements were performed using the freehand selection tool and outlining each individual fascicle. By selecting the measuring tool the outlined area of each fascicle was determined. Subsequently the diameter of each fascicle was calculated from the formula below:

$A = \pi r^2$

(A= area, π= 3.14 and r= radius)

3- The IFM thickness

In order to measure the IFM thickness in the SDFT, tendons were analysed from forelimb of three horses (8-years-old). Photographs of the SDFT were analysed using ImageJ and the IFM thickness was measured between both tertiary and secondary fascicles. Measurements were done on the greyscale images in order to identify the well-defined IFM found between fascicles. Different points around the tertiary and secondary fascicles were measured, starting from the periphery of the sections toward the centre. For each tendon 300 points between the tertiary fascicles and 300 points between the secondary fascicles were measured, which were taken from three different regions (proximal, mid-metacarpal and distal). Therefore, for each region 100 points of IFM were selected for each fascicle category (Figure 2.4).

The measurement was performed on the ruler-calibrated images using ImageJ. Initially, when the image was opened the straight-line selection tool was used to drag a line across the calibrated ruler on the image in order to specify the distance (e. g. 1000µm). Then, using the Analyze tool, the set scale window was opened show the length of the dragged line in pixels, which could then be converted to micrometres (µm). To allow maximum accuracy the line was drawn parallel to the pixel lines to avoid angulations in the measured line tool. Then by selecting the measure tool the length of the dragged lines was displayed in a new window. This process was repeated to measure all the selected points across the tendon sections. Cross-junction areas of the IFM were excluded as they form an irregular outlined stellate structure having different orientations (Figure 2.4).

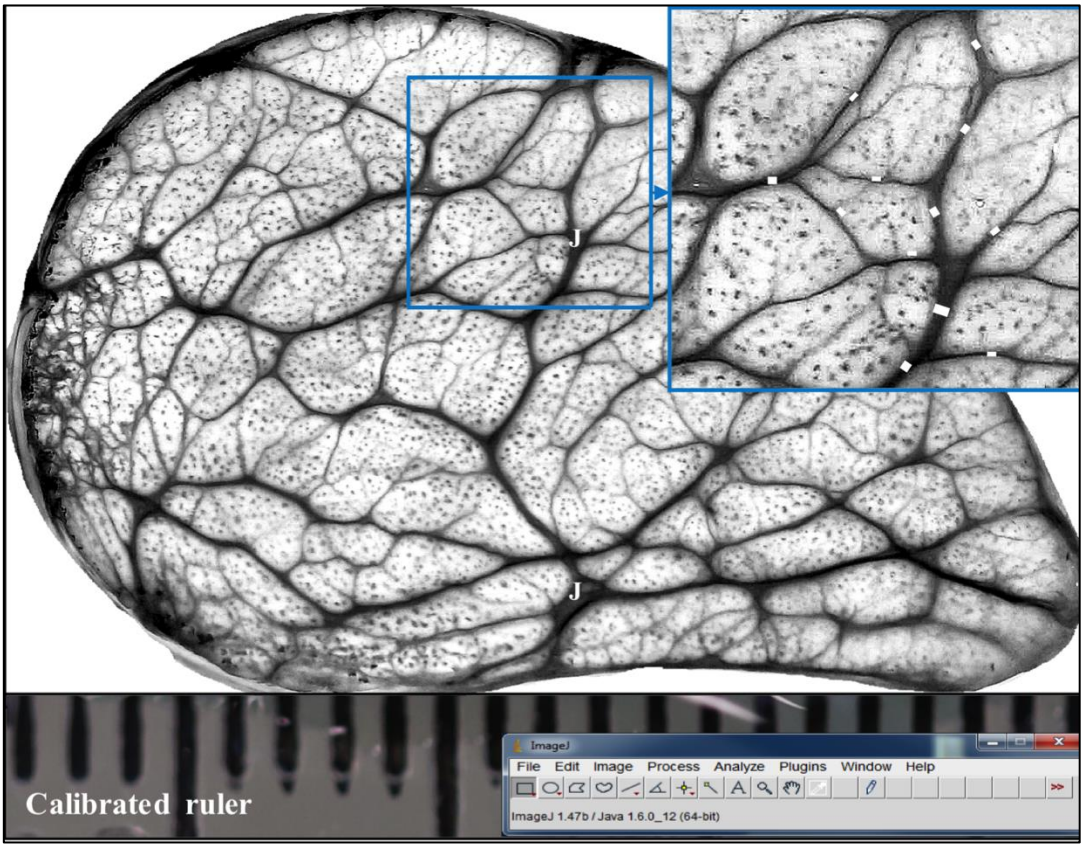

Figure 2.4: Illustration of the steps required for IFM measurement in ImageJ. The IFM widths were measured over the entire section, taking 100 points around each group of secondary and tertiary fascicles. A magnified area (inset box) shows well-defined IFM areas and the transverse small white bars between the fascicles indicate measured lines of IFM thickness. The letter (J) on the main image indicates a junction area of IFM that excluded from the analysis.

2.2.5.1.2 Second descriptive study: Pattern of fascicles and IFM in different legs

In order to demonstrate the pattern of the fascicles and their IFM on the SDFT transverse image sections in the right and left of the front and hind limbs were processed separately for both categories as follows:

1- Pattern of fascicles

Initially tertiary and secondary fascicles were identified according to their ImageJ optimizations. The tertiary fascicles were clearly outlined by a thick IFM, and the secondary fascicles were localised within the tertiary fascicles and outlined by a

thinner IFM. From the interactive 3D surface plot, the pattern of the fascicles were viewed in different legs by increasing the amount of perspective and Min up to 0.25 and 10% respectively and the image manipulated to achieve optimal visualisation (Figure 2.4). This optimisation allowed enhanced visualisation of the intact fascicles on the cut surface, as they appeared to protrude individually from the outlined IFM. The fascicular morphology was compared regionally between different paired limbs at a range of ages (4, 6 and 18 years-old).

Further, on the basis of the above ImageJ criteria, tertiary and secondary fascicles were defined and counted in the proximal, mid-metacarpal and distal regions in different legs. The average numbers of the tertiary fascicles calculated were compared regionally. Secondary fascicles were also visualised by zooming the image in order to see the detailed arrangement of the IFM and its thickness. The total numbers of the secondary fascicles within each tertiary fascicle and in different regions were recorded.

2- Pattern of IFM

To highlight the IFM pattern the SDFT images were enhanced in order to visualise the IFM clearly by using Paint Shop Pro X4 through the following steps: loading images into Paint Shop Pro X4 Ultimate, selecting the channel mixer (Red -40%, Green -40%, Blue -40% and contrast of 110%) followed by a fade correction of 50. Then using the Enhance Photo toolbar, Local Tone Mapping (Strength of 100 and Block size of 50) was selected followed by High Pass Sharpen and then fade correction (50). The final outcome of this optimisation was the production of images with an obvious and distinct IFM that appear as a shiny white line between the fascicles (Figure 2.5).

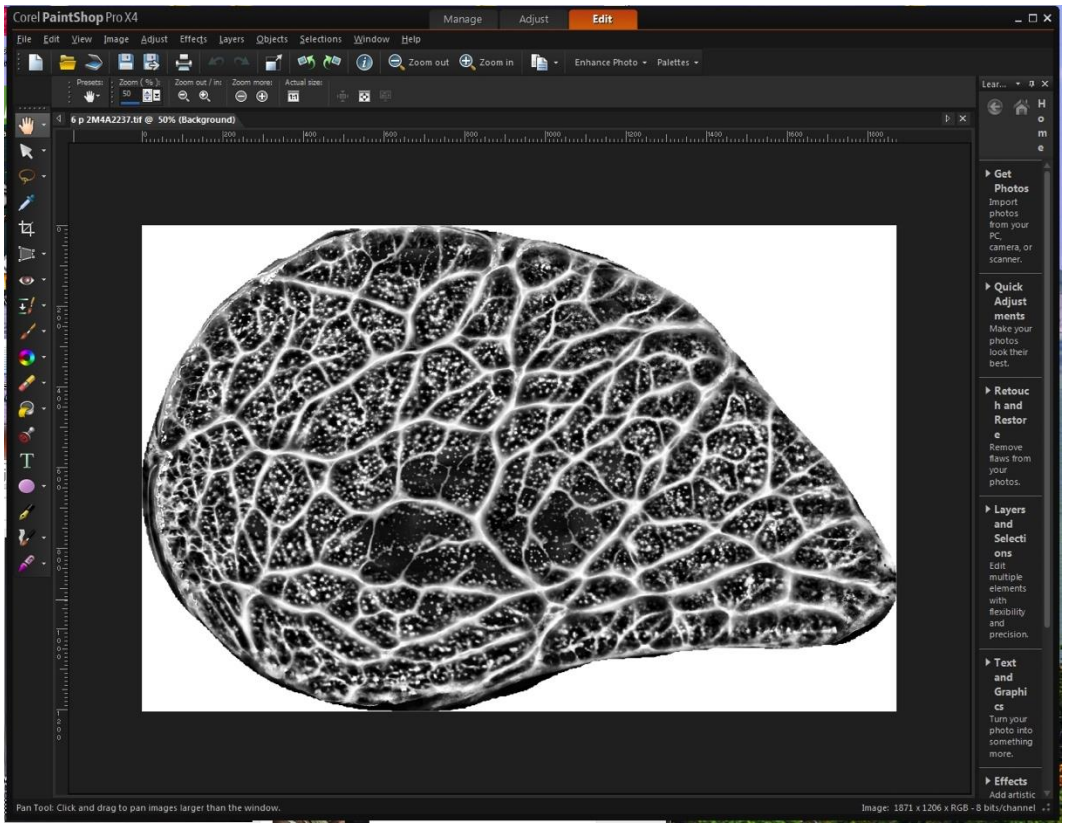

Figure 2.5: Snapshot of the use of Paint Shop Pro X4 Ultimate to enhance and visualise the IFM between the fascicles. Note the white lines mesh indicate the IFM between the fascicles.

2.2.5.2 Third descriptive study: IMOD three-dimensional (3D) modelling

IMOD is a free software (Version 4.7) used to process a series or a set of TIFF images, perform modelling and display tomographic reconstructions and 3D volumes. It has tools used to assemble and align a series of images within for multiple Z-stack types and sizes and to view them in a three dimensional (3D) form (Kremer J.R., 1996).

2.2.5.2.1 Three-dimensional reconstructions with drawing tool

IMOD was used to create a 3D reconstruction of the SDFT from the series of transverse sections, allowing definition of the longitudinal fascicular anatomy. A number of SDFT from different ages and legs were processed for 3D reconstruction. Four SDFT and the mid-metacarpal regions (~6.5cm) of 13 SDFT were reconstructed and from each SDFT one fascicles was outlined and traced in order to

monitor the degree of fascicular alteration. Moreover, all fascicles of the mid-metacarpal region (~ 6.5cm) of one SDFT were completely reconstructed.

IMOD works with mrc image files, which can either be a stack or individual TIFF images. Initially, all images were loaded into the Cygwin home directory at window /home/username/file name. To create a Z-stack from this file of TIFF images they are loaded into IMOD programmes by typing (LS) followed by typing the file name in order to open the directory file. When the file directory or subdirectory is opened, then by typing (tif2mrc *.tif newfilename.mrc) in the program, images are automatically converted into an mrc file (Z-stack). These files can then be manually aligned using the midas programme by typing (midas filename.mrc) which is followed by a manual alignment and then saved to a home directory as an mrc Z-stack (Figure 2.6A).

The mrc image file was opened in the IMOD programme by typing 3DMOD and selecting the mrc file in the directory or subdirectory file. Then by using the drawing tool, fascicles of interest were outlined sequentially in order to re-construct the fascicular anatomy of the SDFT. From the first section one fascicle was outlined and subsequently in the following sections various fascicles were outlined. Different colours were used to delineate different fascicles. Outlined fascicles were then converted to 3D models by selecting the model view option where it opens a new window and shows all contours in a 3D form (Figure 2.6 B-I). The contours were then meshed to create a complete 3D reconstruction of the entire tendon and the selected fascicle. To rectify minor degrees of contour wrinkle or small irregularities, specific options such as the surface and low-resolution mesh in the meshing tool bar were used in order to obtain optimal contour adjustment.

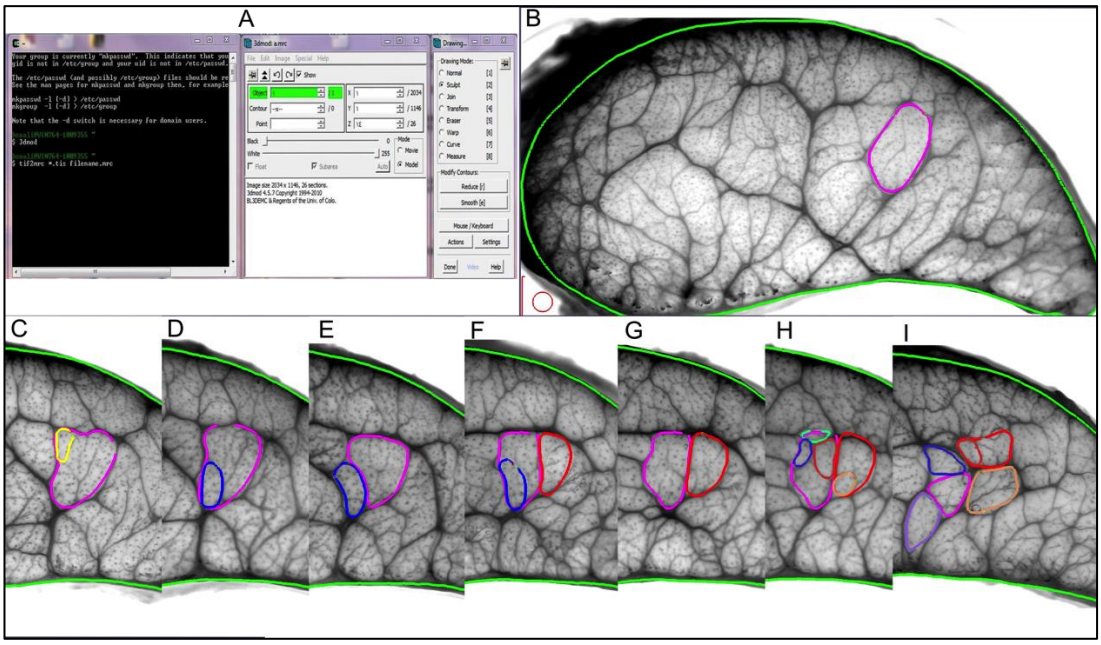

Figure 2.6: A: IMOD window with the drawing tool bar used to outline the tendon and specific fascicles. B -I: Demonstration of the steps of outlining one fascicle (B) in the proximal aspect of the tendon and then going throughout the series images (Z-stack) toward the distal (I), determining any modification of this fascicle by using different colour. Note how the fascicle outline modified from proximal to distal (B-I), it undergoes regional modification such as divergence, convergence and inter-relation to the neighbouring fascicles.

2.2.5.2.2 The XYZ plane's view of the Z-stack

Initially, the IFM were enhanced as described in section 2.2.5.1.2 (Pattern of IFM). Then a series of images were processed into a (mrc file) Z-stack. The X, Y and Z planes were explored by selecting the Image option in the 3D window to show a three-planes view of the image stack. Then by manipulating the X and Y planes fascicles could be observed in three different planes. In this view, it is possible to view the fascicle's outline longitudinally (in the Z-stack) from proximal to distal through the XY planes (Figure 2.7). Specific alterations in a fascicle's anatomy such as fascicle divergence, convergence, inter-relation and re-splitting of the selected fascicle could then be determined.

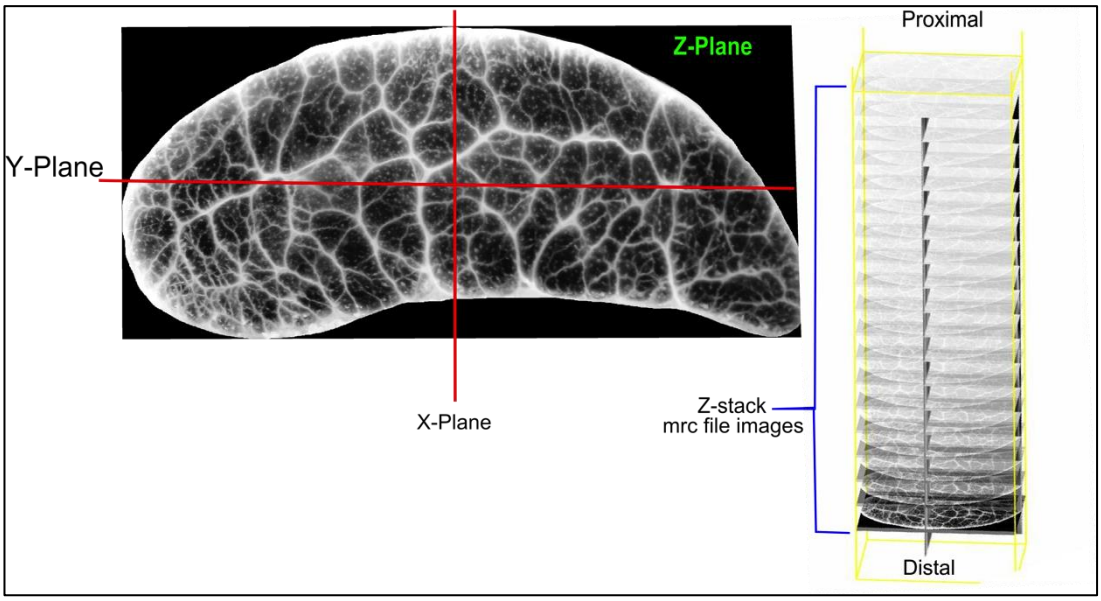

Figure 2.7: View of the X, Y and Z planes of the SDFT Z-stack of an mrc file in the mid-metacarpal region (~ 6.5 cm long). The tendon and the fascicles could be viewed from X, Y and Z-planes and this helps to demonstrate how the fascicles are arranged within the tendon from the proximal to the distal end.

2.2.5.2.2 Isosurface of the IFM over a specific area within the Z-stack (IFM 3D reconstruction)

The isosurface method allows visualisation and isolation of a certain colour of the image by setting a threshold for the pixel intensity values over or under which they appear in the model. By using the bounding box option an area of approximately 8×6 mm^2 over the image was determined. Meanwhile, the XY outer limit tools were used to manipulate the size and position of the proposed area. Then the proposed area over the first image was thresholded in order to find the optimal contrast for the IFM. When the optimal contrast was achieved multiple thread like lines were present over the IFM of the first section (Figure 2.8). Then the image was enhanced by selecting options such as smoothing and deleting of small pieces (which removes extraneous noise). Later the IFM was reconstructed over the proposed area running down through the whole Z-stack in a proximal to distal direction. Finally, by meshing the outlined images all the parallel thread like colour of all sections were connected to each other in both the vertical and the horizontal planes and reconstructed a 3D form of the IFM through the whole Z-stack.

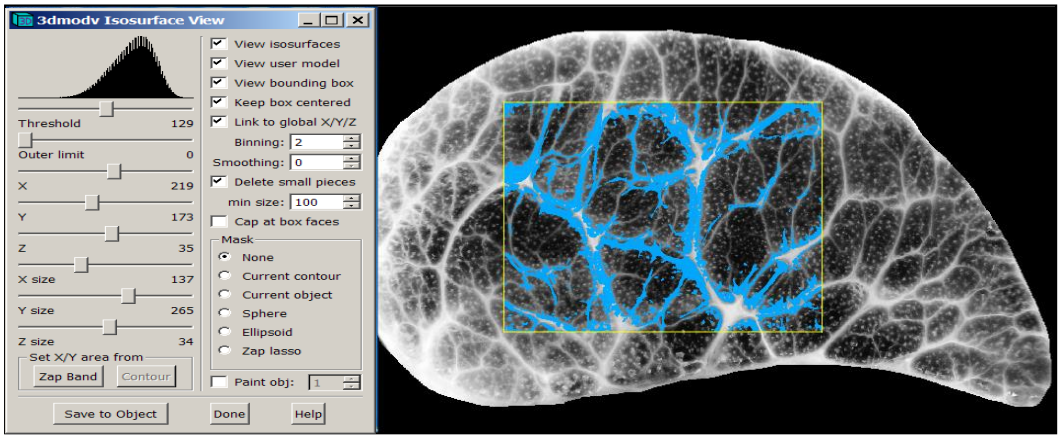

Figure 2.8: Illustrate isosurface 3D modelling of the IFM through the series image (Z-stack) with the toolbar on the left side. An area of (8×6 mm^2) over the first transverse section in the proximal region was selected and the IFM was isosurfaced (3D reconstruction) by thresholding of the image from proximal to distal. In this example blue thread-like lines represent the IFM. The blue IFM isosurface runs down through the Z-stack with a similar intensity to create an automated reconstruction of the IFM.

2.2.5.2.3 Creating a 3D video output in IMOD

The degree of rotation, orientation and speed of the 3D movie was specified using the control option from the edit toolbar in the 3dmod model view window. The snap direction was selected in the file tool in the same window and the snap file specified in the Cygwin directory (see the IMOD website for more detail) (Kremer J.R., 1996). When opening the model view, the Movie/Montage tool was selected from the file toolbar and the required snapshot number typed into a gap in front of the **# of movie frames**, such as 10000 snap shots. Then Movie action, Tiff images and Write files were selected before clicking on 'make'. All snapped images were converted to a movie by uploading them into the Video Mach-Audio/Video Converter and Builder programme (http://videomach.en.softonic.com) (File version 5.9.13.0).

2.2.6 STATISTICAL ANALYSIS

Statistical analysis was carried out using Graph Pad Prism version 6 (California-USA). Initially the data were checked for normality using D'Agostino & Pearson omnibus normality test and if required were normalised using normalise option tool. Data were analysed using non-parametric one-way ANOVA (Kruskal-Wallis and

Tukey's multiple comparism tests) and paired T-tests (Mann-Whitney test). Significance was set at p value of < 0.05.

2.3 RESULTS

2.3.1 FIRST DESCRIPTIVE STUDY

2.3.1.1 Cross sectional area and shapes of tendon

The average CSA of the entire SDFT in the proximal, mid-metacarpal and distal region of three individual horses (8-years-old) was 141.1mm^2 (±18.31 SD), 130.6mm^2 (±12.17 SD) and 135.5mm^2 (±13.41 SD) respectively. Thus the CSA varied between individuals and apparently decreased in the mid-metacarpal region by 7.4%, however, this was not significant statistically (Figure 2.9).

The shapes of the tendon cross-section also altered gradually from proximal to distal. The SDFT transverse section at the proximal region was more elliptical (Figures 2.13, A and B). It then progressively became compressed dorso-palmarly to become tear-shaped at the mid metacarpal region (Figures 2.13, C and D) and was then completely flattened dorso-palmarly in the distal region (Figures 2.14, E and F).

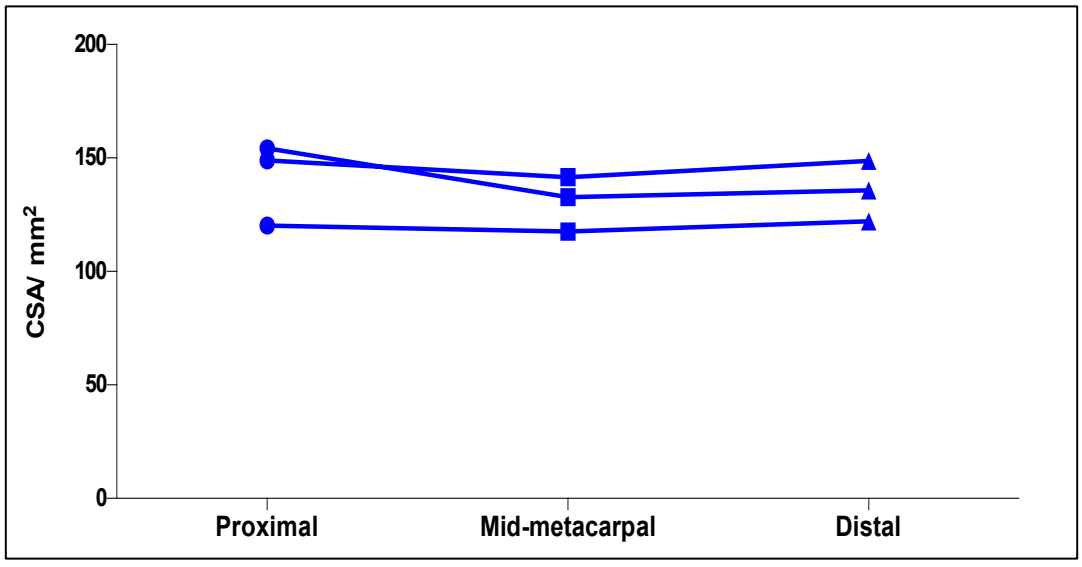

Figure 2.9: Variation of the SDFT cross sectional area (CSA) (mm^2) from the proximal to the distal region in three 8-years-old horses, using ImageJ, this was not significant statistically (P value > 0.05).

2.3.1.2 Identification of fascicles in the transverse SDFT sections

2.3.1.2.1 Image optimisation and outlining the fascicles

The interactive 3D surface plot was used to show the 3D plot of the greyscale images, in which the fascicles were heterogeneous and irregular structures were outlined by the IFM. Due to image enhancement, the appearance of the IFM was accentuated, making it appear wider and more easily discernible. Tertiary fascicles considered to be outlined by a well-defined and/or thick IFM. During thresholding tertiary fascicles were completely separated from each other. The IFM thickness was not homogenous around the tertiary fascicles and varied around the circumference. Tertiary fascicles were composed of a number of smaller secondary fascicles. The secondary fascicles were closely packed and outlined by a thinner endotenon, and the fascicles could not always be separated from each other during image optimisation (Figures 2.13 and 2.15). Primary fascicular bundles could not be defined using this photographic methodology.

2.3.1.2.2 Size of the tertiary and secondary fascicles

A wide range of fascicular size of both the tertiary and secondary fascicles was recorded. The average cross sectional area (CSA) of the tertiary fascicles was 1757μm^2 (±1489 SD) with a range of 22μm^2 - 9424μm^2 while the average CSA of the secondary fascicles was 248.7μm^2 (±232 SD) with a range of 2μm^2 - 1503μm^2. The average diameter of the tertiary fascicles was 1372µm (±596.9 SD) with a range of 167-3464µm. The average diameter of the secondary fascicles was 509.6µm (±238.8 SD) with a range of 50µm-1383µm when measured in the SDFTs of three 8-years-old horses. Generally there was a proportional relationship between the size and the diameter of the fascicles (Figure 2.10 A, B). There was a significant difference in the size between tertiary and secondary fascicles, with the average area and diameter of the tertiary fascicles being greater ($p < 0.001$) than that of secondary fascicles (Figure 2.10 C, D). However, there was an overlap in the dimensions of secondary and tertiary fascicles when these structures were defined using our criteria. Thus it was not possible to define the secondary/tertiary fascicles on the basis of size alone.

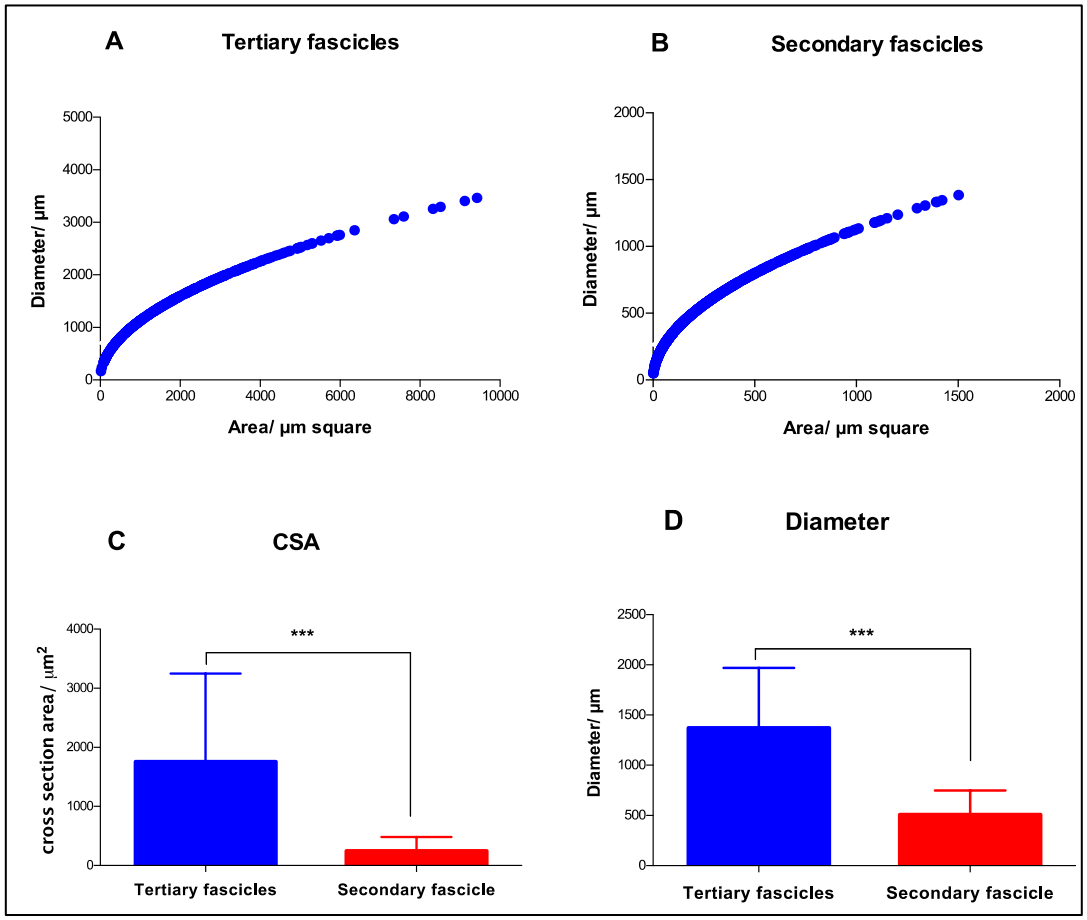

Figure 2.10: Positive correlation between the CSA (μm^2) and diameters of the tertiary and secondary fascicles (A, B). Average CSA (μm^2) and the diameter of the tertiary and secondary fascicles are significant when measured in the proximal, mid-metacarpal and distal region (C, D) in mature horses (8-years-old) (n=3), error bars represent the standard deviation, unpaired t-test (P< 0.001).

2.3.1.2.3 IFM thickness

Measurements of the IFM thickness between the tertiary and secondary fascicles showed a wide variation. IFM thickness was measured in the forelimbs of 8-years-old-horses (n=3) at the proximal, mid-metacarpal and distal regions. The mean IFM thickness between tertiary fascicles was 30.45µm (±9.78 SD) with a range of 4.09µm-174.1µm whilst the mean IFM thickness between secondary fascicles was 9.78µm (± 2.64 SD) with a range of 2µm –27.43µm. There was a statistically significant difference in the IFM thickness between the tertiary and secondary fascicles when using a paired t-test with a P-value of (p <0.001) (Figure 2.11). The IFM thickness between horses was very similar with no significant differences

identified between individuals. For example, the mean IFM thickness between tertiary fascicles in each horse was 30.96µm, 28.82µm and 31.59µm and for the secondary fascicles was 9.26µm, 9.93µm and 10.14µm. Therefore, there is no significant variation in IFM thickness between individual SDFTs but clearly a marked difference in IFM thickness was observed between the tertiary and secondary fascicles. However, once again there was an overlap in the IFM thickness between tertiary and secondary fascicles and it was not possible to accurately discriminate between the tertiary and secondary fascicles based on the thickness of the surrounding IFM.

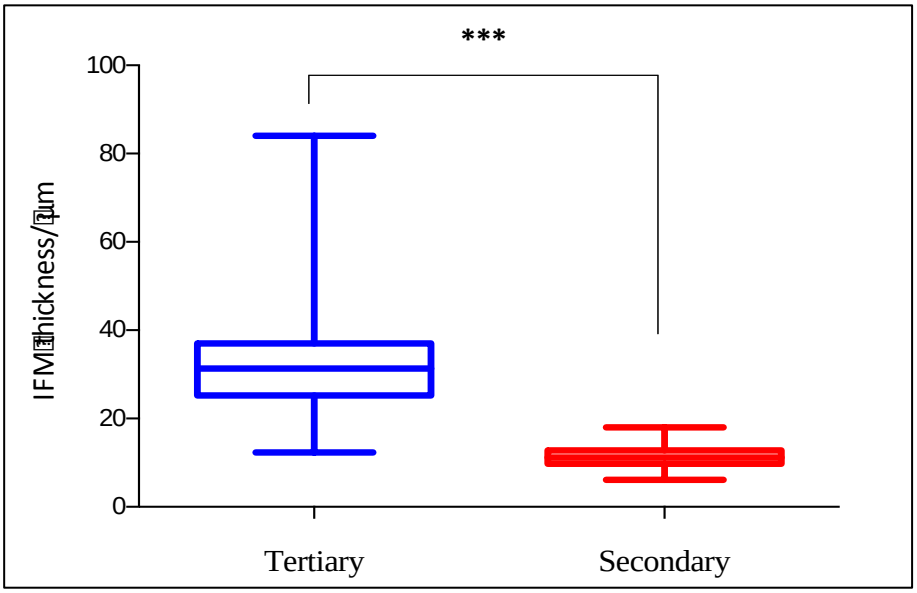

Figure 2.11: Average thickness (µm) of the IFM between the tertiary and secondary fascicles in 8-years-old horses (n=3). For each tendon 300 points between the tertiary fascicles and 300 points between the secondary fascicles were measured distributed over the proximal, mid-metacarpal and distal region equally. The difference was statistically significant (Mann-Whitney test, P value < 0.001).

The IFM thickness did not vary significantly longitudinally through the tendon when measured in the three specified anatomical regions. The mean thickness of the IFM in the proximal, mid-metacarpal and distal region was 35.05µm (±4.03 SD), 28.72µm (±3.47 SD) and 27.59µm (±2.68 SD) respectively (n=3). The average IFM thickness between the secondary fascicles in the proximal, mid-metacarpal and distal

regions also showed no significant difference, with its thickness being 10.74µm (±0.29 SD), 9.35µm (±1.66 SD) and 9.23µm (±0.10 SD) in the proximal, mid-metacarpal and distal region respectively ($P > 0.05$).

Secondary and tertiary fascicles were defined according to our ImageJ criteria on the basis of IFM clarity, thickness and sizes (as described in ImageJ optimisation) and counted in three regions (proximal, mid-metacarpal and distal) in the SDFT. The number of tertiary fascicles was counted in seventeen SDFTs (n=13). The average numbers of tertiary fascicles in the proximal, mid-metacarpal and distal region of the tendon were 36.06 (±4.06 SD), 49.4 (±3.6SD) and 58.53 (±2.96 SD). There was a significant increase in the number of tertiary fascicles in the distal region in comparison to the proximal and mid-metacarpal region ($p < 0.001$) (Figure 2.12 A).

The numbers of secondary fascicles also varied at different anatomical levels. Overall, a range of 1-12 secondary fascicles was observed to make up individual tertiary fascicles. These numbers also varied between different areas within the same region. Secondary fascicles appear closer to each other as they are outlined by a thinner IFM. Frequently the IFM surrounding the secondary fascicles did not completely delineate fascicles from each other. Discrimination of the secondary and tertiary fascicles was often not simple because of them both having similar IFM thickness at certain points; for instance at the junction areas between the secondary and tertiary fascicles or when fascicles start to diverge. We also demonstrated that the number of secondary fascicles progressively increased from the proximal to the distal region in all samples. The average numbers of all secondary fascicles in the proximal, mid-metacarpal and distal region were 91.59 (±16.13 SD), 121.3 (±19.96 SD), and 136 (±21.9 SD). There was a significant increase in the total number of secondary fascicles between the proximal, mid-metacarpal ($P< 0.05$) and the distal region ($P< 0.001$) of the tendon (Figure 2.12 B).

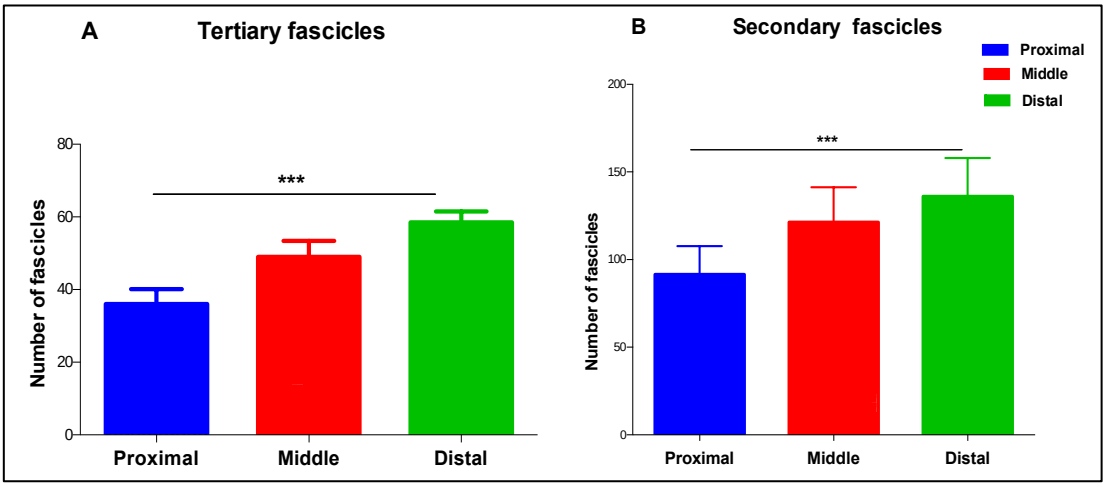

Figure 2.12: Average number of the tertiary and the secondary fascicles are progressively increased from the proximal to the distal region (n=13). The bars represent the SD, one-way ANOVA (Tukey's multiple comparison tests), (P< 0.001).

Overall, our data identified that in the normal SDFT (8-years-old) fascicles can be defined as a tendon longitudinal subunit of variable size and shape that is outlined by the IFM. The largest units, called tertiary fascicles were outlined, by a well-defined IFM. Tertiary fascicles are further subdivided into smaller subunits, called secondary fascicles that are outlined by a thinner IFM. The fascicular subunit undergoes regional modification as it runs longitudinally through the tendon. There are more fascicles in the distal compared with the proximal aspect of the tendon.

2.3.2 SECOND DESCRIPTIVE STUDY

2.3.2.1 Pattern of fascicles and IFM in different legs

In 2.3.2 we demonstrated that the morphology of fascicles varied from the proximal to the distal region in the SDFT. We then wished to discover how this fascicle arrangement varied between right and left limbs within an individual as well as between fore and hind limb.

Two pairs of forelimbs (4 and 6 years-old) and one pair of hind limbs (18 years-old) were selected and processed to determine similarity between the right and left limbs and to document variation between individuals. When matching the fascicular organisation between them at the three different transverse anatomical levels

(proximal, mid-metacarpal and distal), heterogeneous and asymmetric fascicular patterns were observed. Fascicles in the forelimbs of 4-years-old manifested different shapes and sizes in different regions and between the right and left limbs (Figure 2.13).

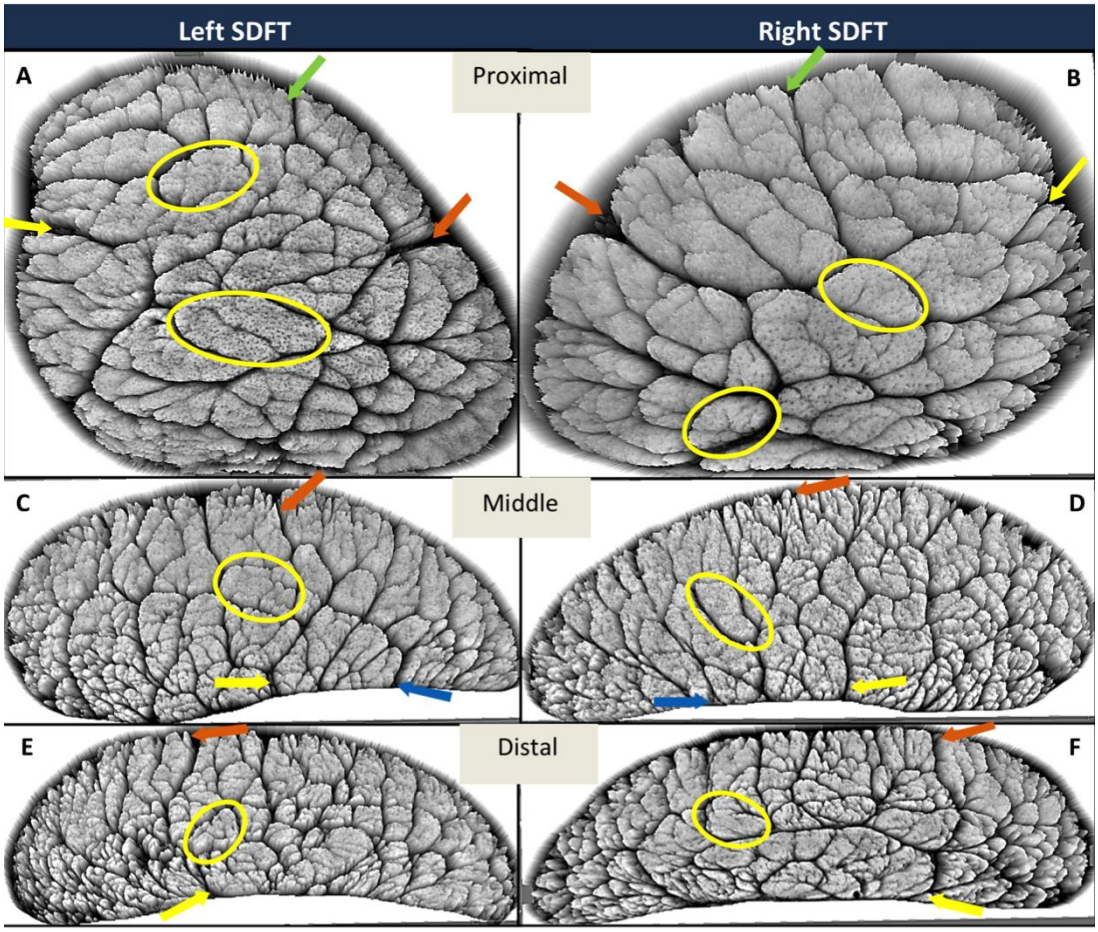

Figure 2.13: The ImageJ interactive 3D surface plot of a paired forelimb in three different regions (proximal, mid-metacarpal and distal) of 4-years-old horse. (A, B), (C, D) and (E, F) represent the proximal, mid-metacarpal and distal regions respectively. Tertiary fascicles are outlined by a well-defined IFM (yellow circle) and have different sizes and shapes, whereas secondary fascicles are delineated by a thinner IFM. However, some of the tertiary and secondary fascicles have a relatively equal IFM thickness. Note that the IFM joined with the epitenon at the same points on both the right and left limbs (coloured arrows).

The IFM appears as a reticular meshwork running in different orientations throughout the entire cross section of the tendon. Where the IFM joins the epitenon it is normally relatively thick. At points where the IFMs join together (so called

junction regions) the IFM is often thickened and irregular in shape. As in the fascicle pattern, there were regional alterations in the organisation of the IFM from proximal to distal and in each region, the IFM showed specific conformational patterns. In the young sample (4-years-old) the IFM was clear, with distinct outlines between both the tertiary and secondary fascicles (Figure 2.14). The clarity of the IFM between right and the left limbs and in different regions was similar. Therfore the IFM appears as an inter-connected network extending in all directions. The IFM organised the tendon architecture into many compartments (fascicles). However, discrimination of these different fascicular units was not feasible because the IFM thickness was not constant around the fascicles and continued to undergo regional alteration.

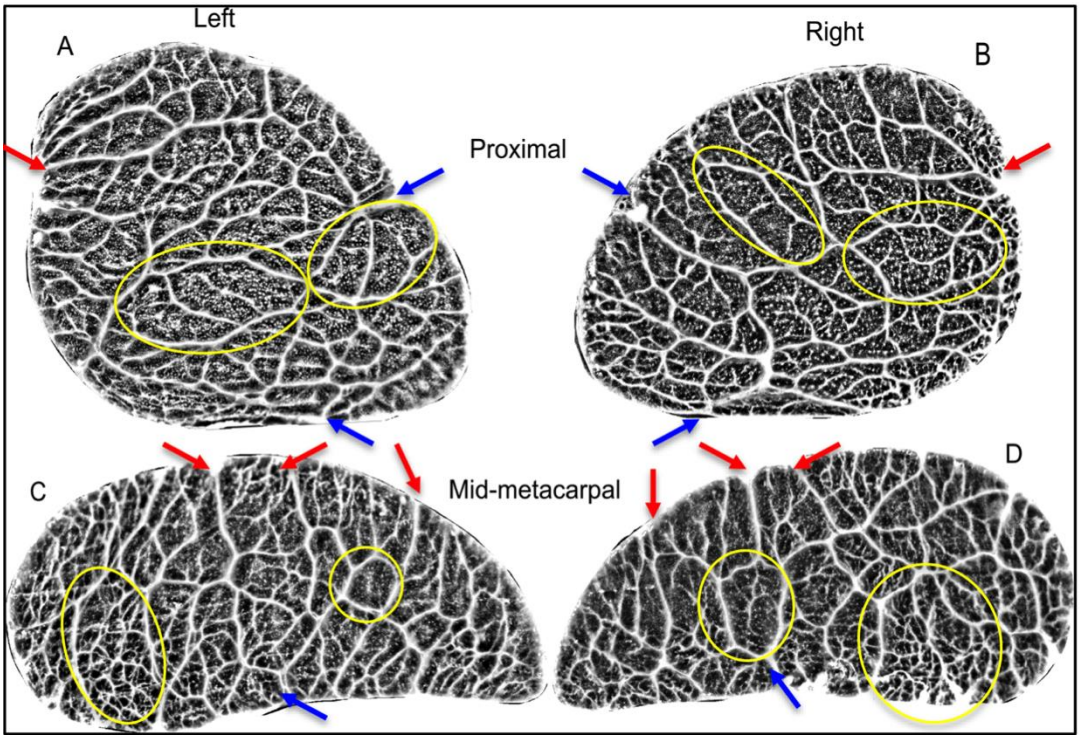

Figure 2.14: The reticular pattern of the IFM between fascicles (yellow circles) in paired forelimbs (4-years-old horse), processed in Paint Shop Pro X4. The right and left sides (A and B) of the proximal region show different IFM arrangements and they are dissimilar to the mid-metacarpal regions (C and D). The peripheral communication of the IFM and the epitenon are similar (red and blue arrows).

In the 6-years-old samples, fascicles were again clearly outlined and manifested different patterns between regions and, between the left and right limbs (Figure 2.15).

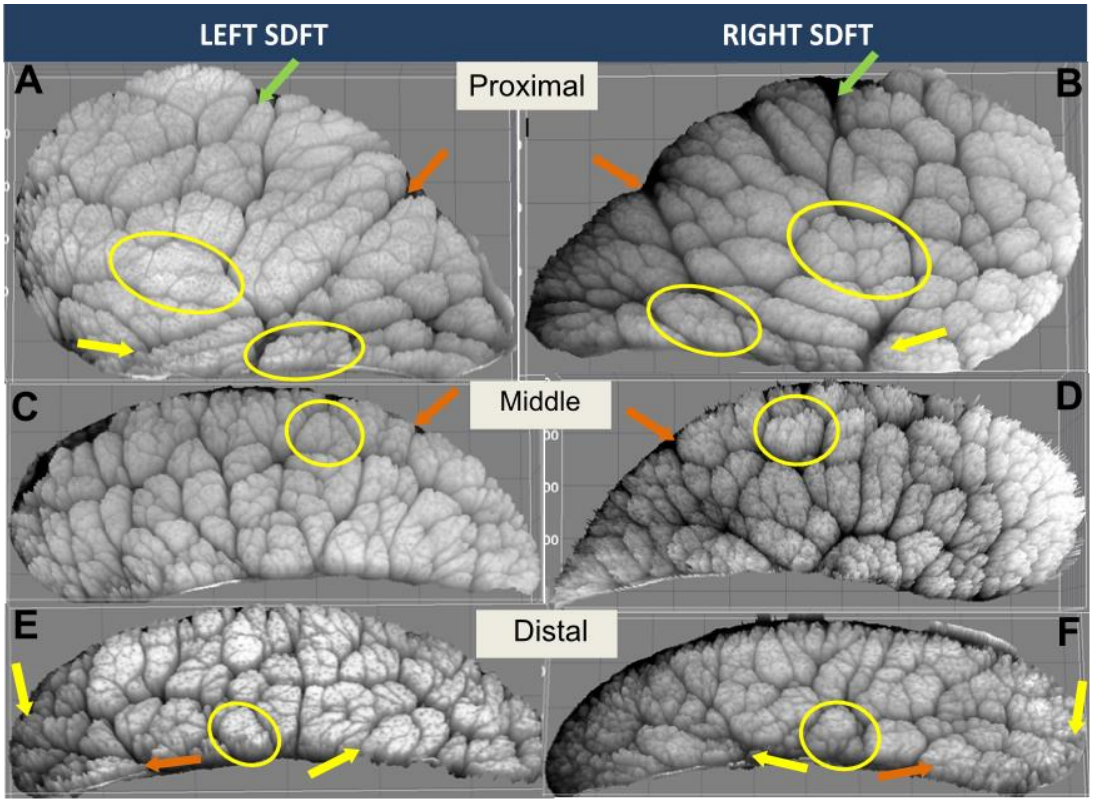

Figure 2.15: The imageJ interactive 3D surface plot of paired forelimbs in three different regions (proximal, mid-metacarpal and distal) of 6-years-old horse. (A, B), (C, D) and (E, F) represent the proximal, mid-metacarpal and distal regions respectively. The tertiary fascicles are outlined by a well-defined IFM (yellow circle) and have different sizes and shapes whereas secondary fascicles are delineated by a thinner IFM. However some of the tertiary and secondary fascicles have relatively equal IFM thickness. Note the IFM joined with the epitenon at the same points on both the right and left limbs (coloured arrows).

As in the 4-years-old samples, the IFM was clearly visible between the tertiary fascicles and secondary in the 6-years-old tendon (Figure 2.16).

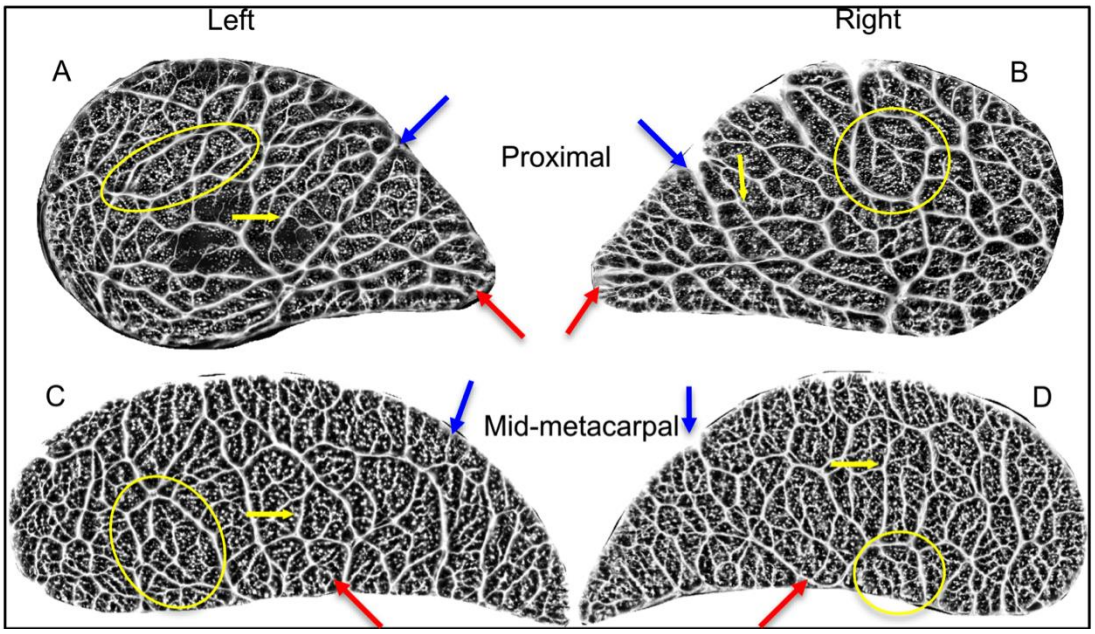

Figure 2.16: The reticular pattern of the IFM between fascicles (yellow circles) in paired forelimbs (6-years-old horse), processed in Paint Shop Pro X4. The right and left sides (A and B) of the proximal region show different IFM arrangements and they are dissimilar to the mid-metacarpal regions (C and D). The IFM thickness at certain points is similar for both tertiary and secondary fascicles (yellow arrows). The peripheral communication of the IFM and the epitenon are similar (red and blue arrows).

In close observation of the SDFT sections, both IFM and the fascicles were clearly identified. In some areas, discrimination between the tertiary and the secondary fascicles were not feasible. Where the IFM between the tertiary and secondary fascicles is of relatively similar thickness, this indicating secondary and tertiary fascicles cannot be discriminated on the basis of IFM thickness (Figure 2.17).

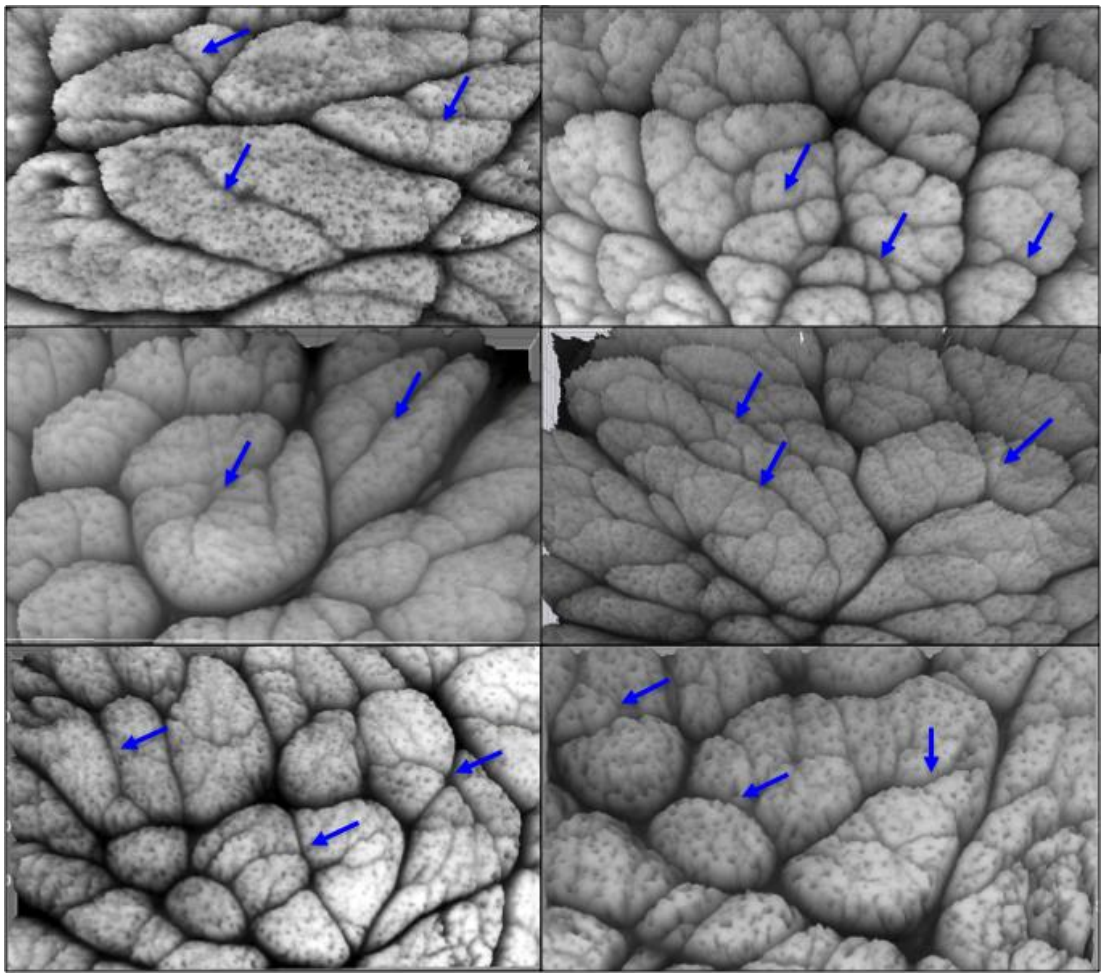

Figure 2.17: Higher magnification of some selected areas where the IFM between the tertiary and secondary fascicles is of relatively similar thickness (arrows) indicating secondary and tertiary fascicles cannot be discriminated on the basis of IFM thickness alone.

Previously I have shown that the fascicular pattern differs longitudinally through the tendon. The fascicular morphology also varied between the fore and hind limbs at different levels of the tendon. In the hind limbs fascicles were more or less elongated elliptical shapes with their long axis orientated in a dorso-plantar direction especially in the mid-metatarsal and the distal regions (Figure 2.18). Similarly, in the hind limb the shapes of fascicles were not similar from proximal to the distal regions. Further, patterns of the fascicles between right and left limbs were apparently asymmetric.

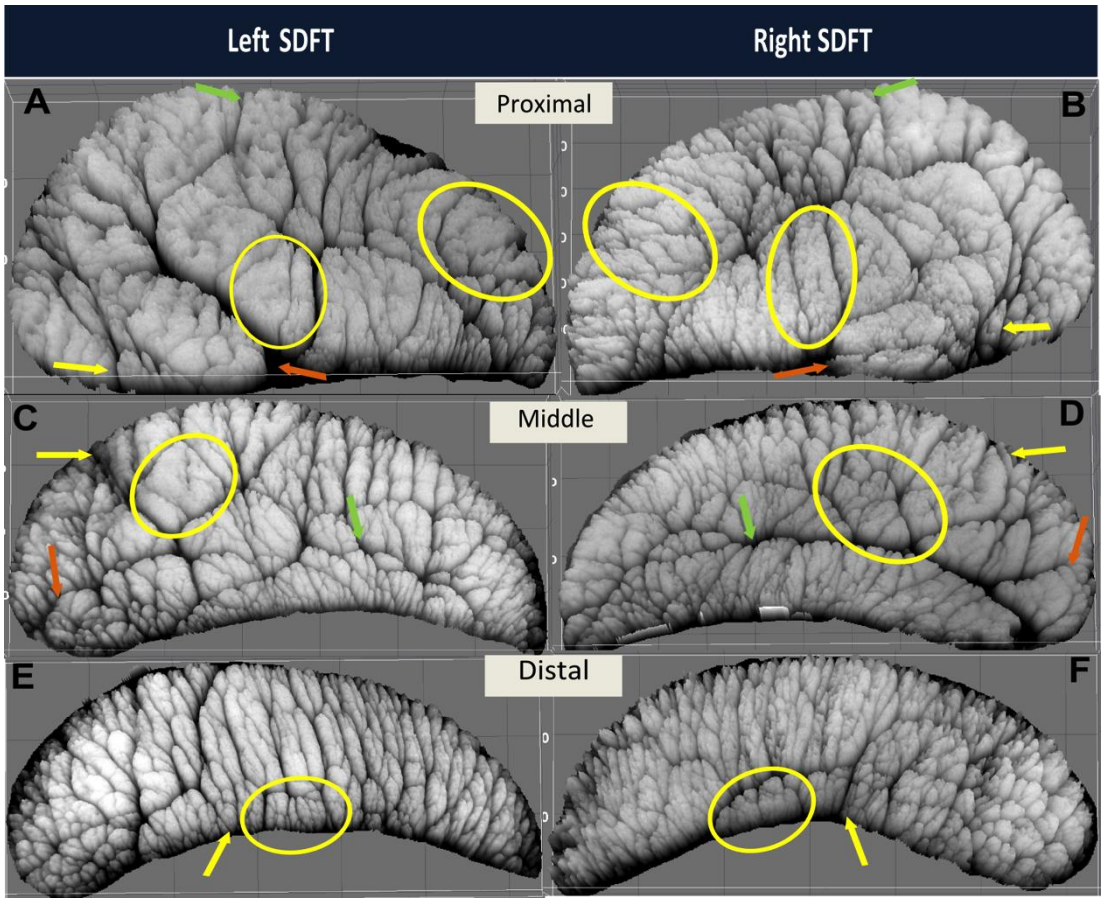

Figure 2.18: The ImageJ interactive 3D surface plot of paired hind limbs in three different regions (proximal, mid-metacarpal and distal) of an 18-years-old horse. (A, B), (C, D) and (E, F) represent the proximal, mid- and distal metatarsal regions respectively. Tertiary fascicles are outlined by a well-defined IFM (yellow circles), having different sizes and shapes whereas secondary fascicles are delineated by a thinner IFM. Note the shapes of the fascicles are generally elliptical on the dorso-plantar direction. Note the IFM joined with the epitenon at the same points on both the right and left limbs (arrows)

Interestingly the pattern of the IFM in the hind limb was not exactly similar to the forelimb. Regionally, the IFM pattern as well as the outlines of the tendon in cross section were also not similar. However, the ability to delineate the IFM was approximately similar between the right and the left limb and in different regions. Again, as for the fascicles, the IFM of the right and left hind limb also adopted different patterns. Therefore, the IFM is not a consitent homgenous structure and is different in different regions of the tendon. At some points the the IFM surrounding secondary fascicles becomes indistinct, leading to IFM which does not fully outline

the secondary fascicles, with the IFM here causing an apparent split in the fascicle (Figure 2.19).

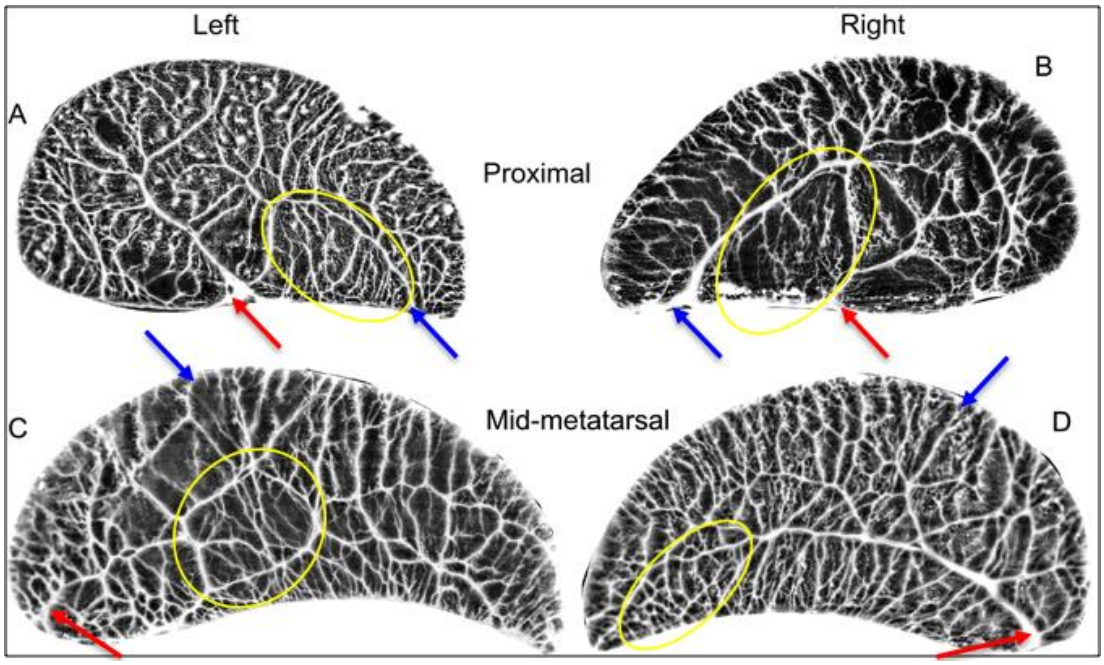

Figure 2.19: The reticular pattern of the IFM between fascicles from the SDFT in paired hind limbs of an 18-year-old horse, processed in Paint Shop Pro X4. The right and left sides (A and B) of the proximal region show different IFM arrangements and they are dissimilar to the mid-metacarpal regions (C and D) (yellow circle). The peripheral communication of the IFM and the epitenon are similar (arrows).

The SDFT cross sectional shape between paired limbs were similar but the pattern of the fascicles between the right and left in both the fore and hind limbs showed various conformational morphologies and was heterogeneous. The connection points (where the IFM joins/connects with the epitenon) between the IFM and the epitenon were similar in both SDFTs from different horses and in the paired contralateral limbs, although paired legs always had differences in the IFM cross-sectional pattern other than where the IFM joined the epitenon.

2.3.4 THIRD DESCRIPTIVE STUDY

2.3.4.1 IMOD three-dimensional reconstructions

Using IMOD I developed a 3-dimensional (3D) model of the fascicular anatomy. In particular we traced how fascicles altered as they ran longitudinally from proximal to distal in the SDFT. We identified a number of novel anatomical features (Figure 2.23):

1-Fascicle divergence: this is where fascicles divided into two or more separate branches, which then course through the tendon.

2- Fascicle convergence: this is where two (or more) fascicles merge together into a single fascicle

3- Fascicle inter-connection: where parts of two adjacent fascicles join and split apart intermittently over a short distance.

4- Fascicle Re-splitting: fascicles re-split or re-diverge after initial convergence or inter-connection.

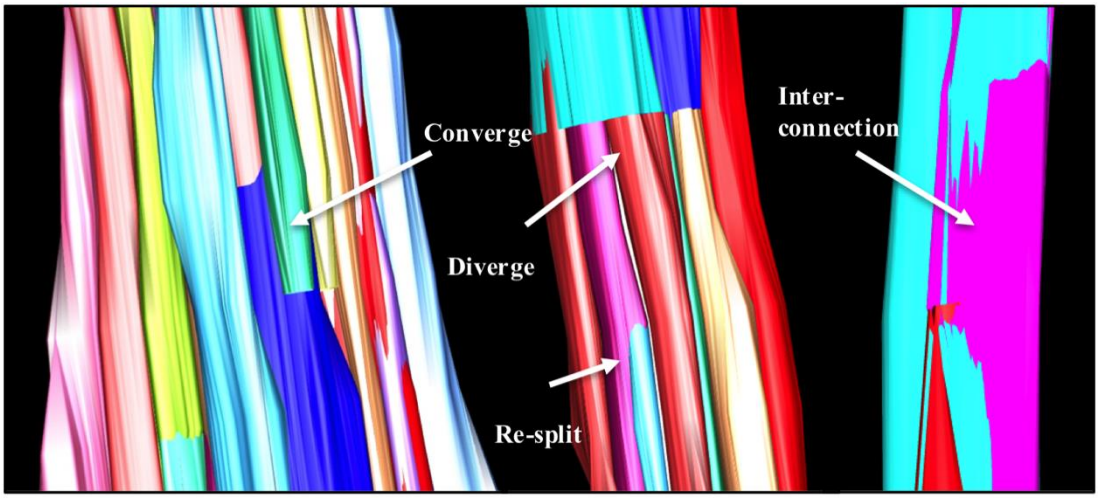

Figure 2.23: 3D reconstruction of the SDFT fascicles, demonstrating the novel anatomical features of the fascicles in relation to each other.

At different levels the outlined fascicle either diverged (splitting) into new fascicles or communicated or converged with adjacent fascicles. This configuration results in an extremely complex tendon structure. Each individual fascicle does not have a constant morphology throughout the tendon. We identified that fascicles inter-connect at different levels through the tendon or join with adjacent fascicles demonstrated by disappearance of the IFM between them (Figures 2.24 and 2.25). Individual fascicles could diverge or converge with neighbouring fascicles and then, more distally, either re-split or converge to become part of a larger fascicle.

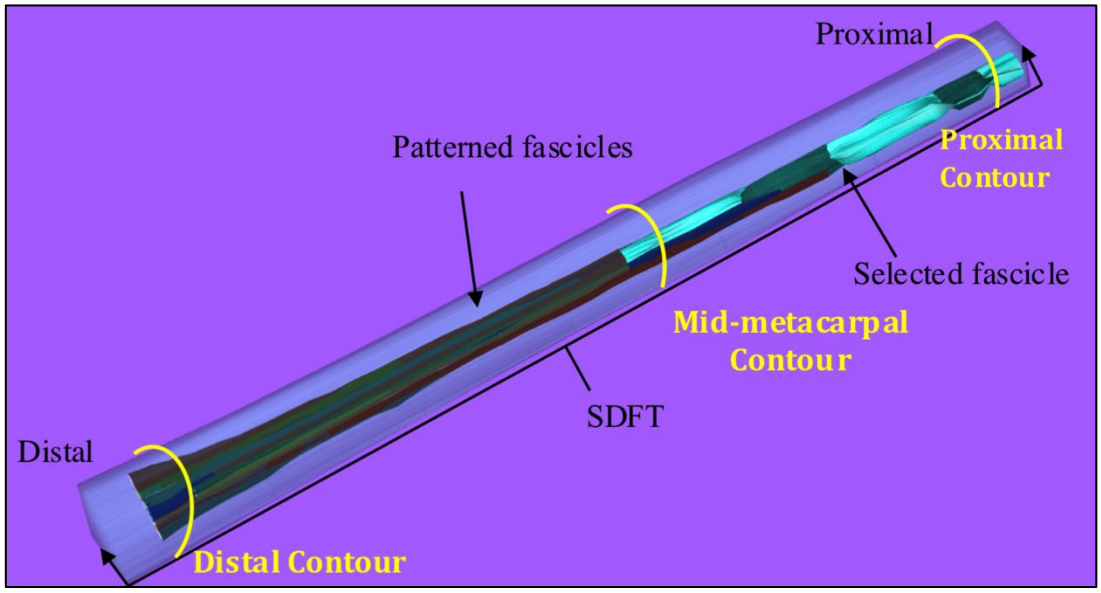

Figure 2.24: 3D view of SDFT through the metacarpal bone length, from a 12-years-old horse. The tendon contour outline is progressively altered toward the distal region. The selected fascicle when running down from proximal to distal undergoes regional alteration. It diverges and is inter-connected with other fascicles at different levels. Different colours inside the tendon contour represent different fascicles, which diverge or are inter-connected with each other. Supplementary videos (2.1, 2.2) of the reconstruction (6 and 12-years-old) can be accessed from the links below:

PhD thesis- Othman, Ali- Three-dimensional supplementary videos/2.1.wmv

PhD thesis- Othman, Ali- Three-dimensional supplementary videos/2.2.wmv

Table 2.2 shows a number of alterations of a selected fascicle at different levels in the mid-metacarpal and metatarsal regions (~ 6.5 cm length). Frequently, fascicles

intermittently inter-connected with each other and at some points parts of fascicles could have short sections of IFM that were apparent at the point they had re-split. These alterations were observed through the length of the tendon in all selected SDFT samples (Table 2.2). I did not identify any discontinuous fascicles with all fascicles apparently extending longitudinally through the whole length of the SDFT. In one 12-years-old SDFT, the whole mid-metacarpal region (~ 6.5 cm long) was reconstructed. Over a distance longitudinally of 3-6mm, I would identify a number of the features described above; specifically diverging, converging, inter-connection and re-splitting. At some sites the outlined fascicles would completely alter and would either split or join with an adjacent fascicle. From a total number of 47 reconstructed fascicles I found that 11 fascicles (23%) were extended and maintained their configuration throughout the metacarpal region (~6.5cm long) without splitting or converging. However, some fascicles inter-connected with the adjacent fascicles, before detaching more distally and continue to course distally as individual fascicles (Figure 2.25 and associated videos 2.3, 2.4, 2.5).

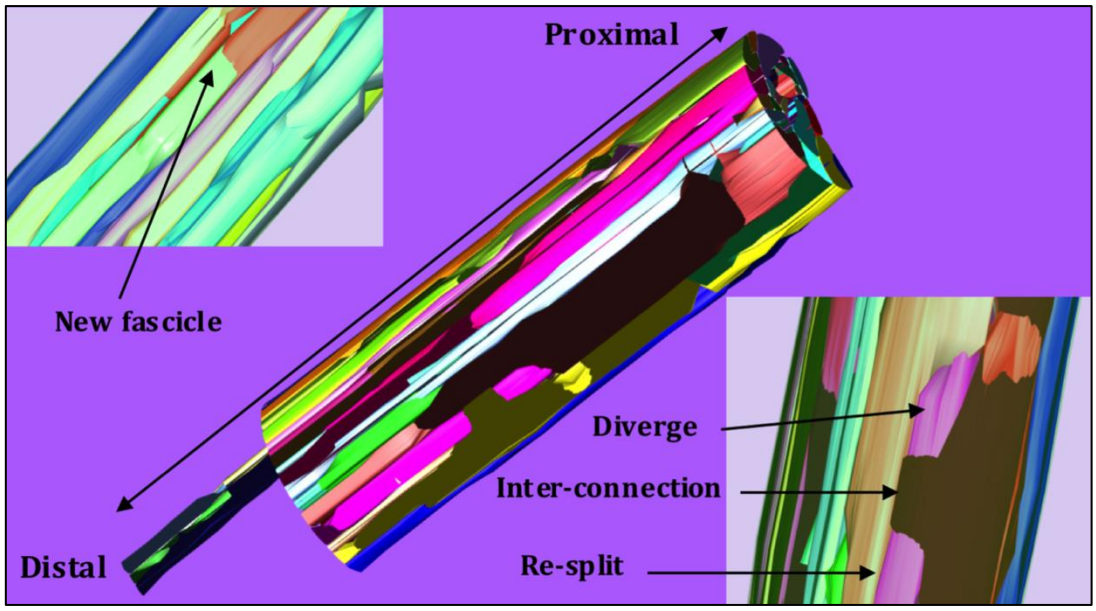

Figure 2.25: 3D view of the SDFT mid-metacarpal region (~ 6.5 cm long) of a 12-years-old horse, showing how all the tendon fascicles run parallel with each other from the proximal to the distal region through the tendon. The fascicles have a strong interrelationship with each other and at points diverged, inter-connected and re-split (arrows). The links below contain 3D views of reconstructions from three different ages (4, 12 and 21-years-old) (videos 2.3, 2.4, 2.5);

PhD thesis- Othman, Ali- Three-dimensional supplementary videos/2.3.wmv

PhD thesis- Othman, Ali- Three-dimensional supplementary videos/2.4.wmv

PhD thesis- Othman, Ali- Three-dimensional supplementary videos/2.5.wmv

For each individual SDFT (n=13) and their reconstructed fascicles through the length of mid-metacarpal region (~6.5 cm) we found that all of the fascicles were undergoing regional alteration when they ran through the tendon. The numbers of alterations were not constant from region to region and could occur through the entire length of the fascicles. The average number of inter-connection of fascicles was higher (36%) than the other alterations. The percentages of divergence, convergence and re-splitting were 18%, 24.2% and 21.7 respectively. Therefore fascicles clearly underwent regional alteration the largest proportions were inter-connected with each other, as compared to other alterations (Figure 2.26).

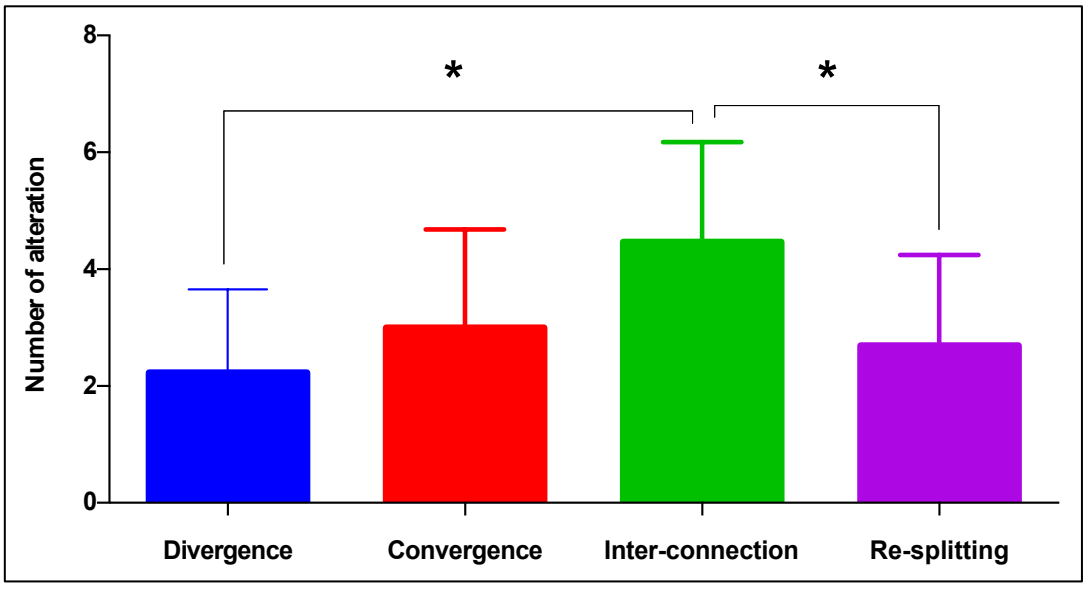

Figure 2.26: The average number of regional alterations of reconstructed fascicles through the length of the mid-metacarpal region (~ 6.5 cm). Note a larger number of fascicles undergo regional inter-connection and a smaller number divergence, one way ANOVA, Kruskal-Wallis test (P value < 0.05), (Error bar = standard deviation) (n=13).

Table 2.2: Different values including the SDFT CSA, the number of fascicles in three different regions and the pattern of the outlined fascicles through the mid-metacarpal and mid-metatarsal regions (~ 6.5 cm long) from different ages (F=Forelimb, H= Hind limb, R=Right L=Left, P=proximal, M=mid-metacarpal and D=distal regions).

		Number of tertiary fascicles/ ImageJ			**Number of secondary fascicles**			**3D reconstruction/IMOD** **Degree of fascicular alteration through the tendon (~6.5 cm long) (one tracked fascicle in each tendon)**			
Legs	**Age/ year**	**P**	**M**	**D**	**P**	**M**	**D**	**Diverge**	**Converge**	**Inter-connect**	**Re-splitting**
LF	4	30	44	60	91	102	120	1	1	5	1
RF	**Paired**	40	50	56	90	110	123	1	1	5	1
RF	5	37	53	57	84	103	116	3	5	8	4
LF	6	43	57	63	108	118	115	2	3	4	3
RF	**Paired**	44	56	64	100	117	120	0	2	2	2
LF	7	35	54	60	107	144	157	2	4	5	3
LF	8	35	52	60	83	136	170	5	3	4	2
LF	8	34	47	54	113	128	143	-	-	-	-
RF	8	33	45	55	120	123	132	-	-	-	-
RF	11	40	48	55	99	126	129	-	-	-	-
LF	12	32	43	56	100	129	165	3	2	3	3
LF	17	37	52	62	101	138	130	1	5	5	4
RH	18	35	44	60	70	146	135	3	1	3	0
LH	**Paired**	40	50	59	67	158	183	4	6	6	6
RH	20	32	45	60	75	108	150	-	-	-	-
LF	21	33	47	58	70	85	114	1	4	6	3
RF	**Paired**	33	46	56	79	91	110	3	2	2	3
Mean	**11.15**	**36.05**	**49**	**58.52**	**91.59**	**121.3**	**136**	**2.23**	**3**	**4.46**	**2.69**
Median	**8**	**35**	**48**	**59**	**91**	**123**	**130**	**2**	**3**	**5**	**3**
Maximum	**21**	**44**	**57**	**64**	**120**	**158**	**183**	**5**	**6**	**8**	**6**
Minimum	**4**	**30**	**43**	**54**	**67**	**85**	**110**	**0**	**1**	**2**	**0**
SD	**5.91**	**4.06**	**4.40**	**2.96**	**16.13**	**19.96**	**21.9**	**1.42**	**1.68**	**1.713**	**1.54**

2.3.4.2 XYZ planes

When viewing the Z-stack on different planes (X, Y and Z), fascicles (black colour) were seen to extend parallel to each other and along the longitudinal axis of the tendon. These fascicles were separated from each other by variable amounts of IFM (white colour) (Figure 2.27). The IFM in the Z-plane was orientated irregularly in different directions and outlined tertiary and secondary fascicles. In the X and Y planes fascicles were outlined by a regularly arranged IFM. Further, the size and thickness of both the fascicles and the IFM were altered in the longitudinal direction (XY planes). At some points, the ends of the fascicles became tapered (Figure 2.27 D) and appeared to partly cease, while a few of them ran for a short distance and then interpolated between other fascicles (Figure 2.27 T). Therefore, both fascicles and IFM extended longitudinally and altered regionally in their morphology.

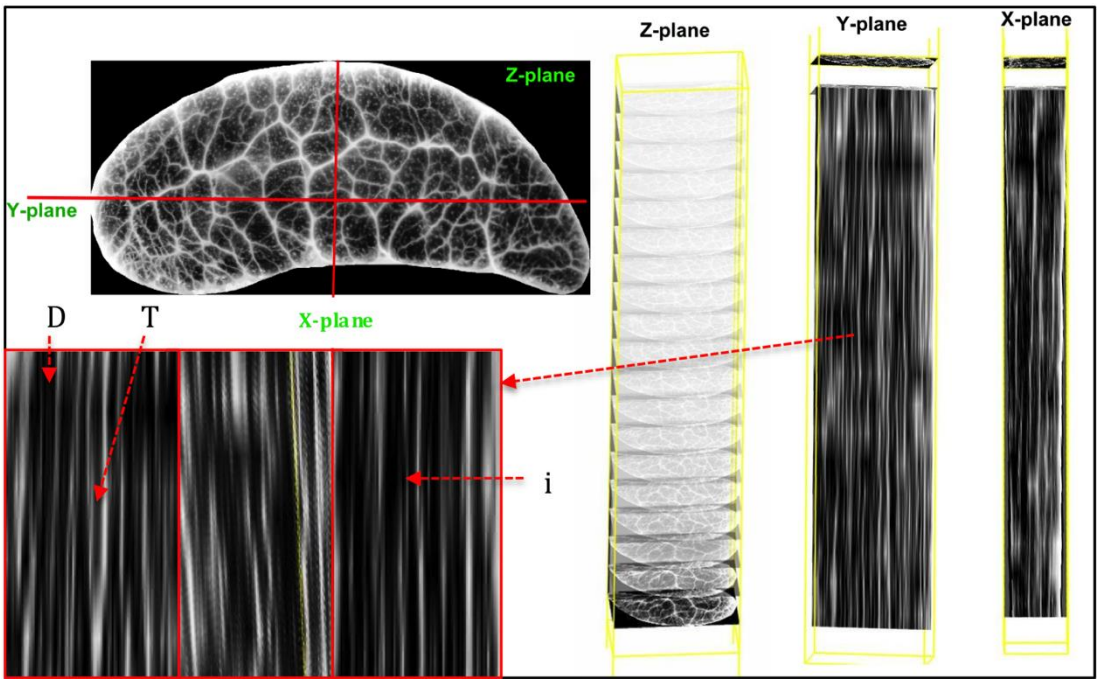

Figure 2.27: The 3D views of the whole Z-stack the mid-metacarpal region of the SDFT, 12-years-old, (~ 6.5 cm long) with the X, Y and Z planes. The continuation of the fascicles throughout the tendon vertically can be seen and are outlined by the IFM. Anatomical features such as divergence (D), tapered fascicular ends/ or interpolation (T) and inter-connection (i) are observed on a close observation.

Interestingly, by moving the XY planes across the tendon frequent fascicular communication was demonstrated. However, at some points a fascicle would course distally as an isolated fascicle before ultimately communicating with adjacent fascicles (Figure 2.27 i). The IFM seemed to alter more frequently than the fascicular anatomy. The IFM was less often continuous and would often become thinner or discontinuous, allowing fascicles to merge. This finding supports the previous 3D reconstruction and fascicle tracking data in which the fascicles are parallel to each other on their longitudinal axis and undergo regional modification (Figure 2.27).

2.3.4.3 Isosurface of a specific area throughout the Z-stack

An isosurface-based 3D reconstruction of the IFM was used to determine the IFM pattern throughout a specific region of the tendon. The degree of IFM isosurface varied at different points in both the horizontal and vertical direction throughout the tendon. Horizontally, the IFMs ran in all directions with a variable degree of density as a result of different thicknesses of the IFM between fascicles. Longitudinally, it extended from the proximal to the distal region and also it has a different degree of isosurface (Figure 2.28 A). At some points the IFM discontinued or disappeared for a short distance, forming a gap, which meant the fascicles had to connect/inter-connect at that point (Figure 2.28 A and associated video 2.6). Interestingly, when the Z-stack was viewed from the proximal aspect down to the distal the IFM appeared as multiple layers of overlapped meshes (Figure 2.28 B). Nevertheless, these overlapped layers were not entirely identical at different levels of the tendon and they appeared as an irregular outlined structure. Further, when viewed from proximal to distal, a number of vertical longitudinal spaces could be identified which coursed through the entire tendon length indicating continuous fascicles. The IFM formed reticular structures of various widths around the fascicles and extended on both the horizontal and vertical directions with various morphologies at different levels and regions (Figure 2.28 B and associated video 2.6).

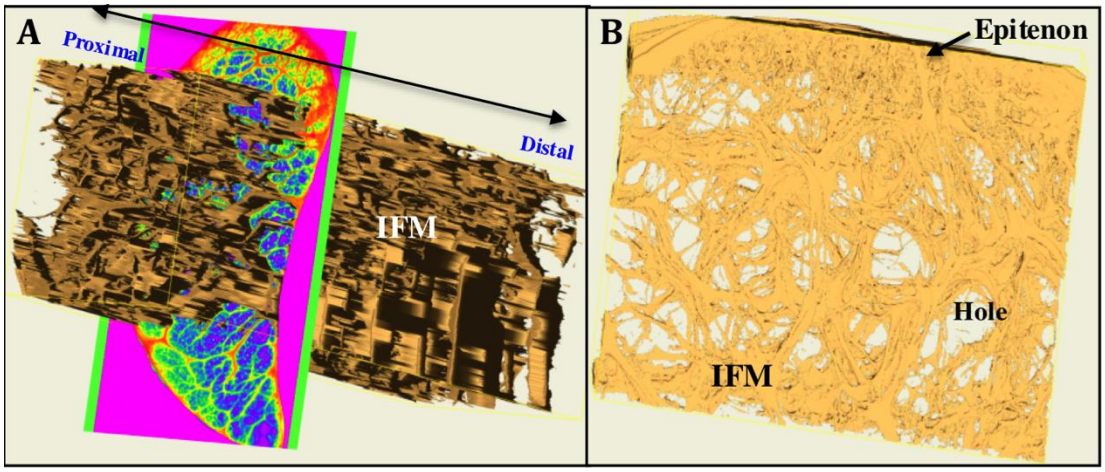

Figure 2.28: Isosurface of the SDFT Z-stack, metacarpal region (~ 6.5 cm) of 6-years-old horse, manifesting the continuation of the IFM throughout the tendon sections (A). The network view of the vertical axis shows the IFM pattern in different directions with overlaps at different points (B). Detail is in the video (2.6) from the link below:

PhD thesis- Othman, Ali- Three-dimensional supplementary videos/2.6.wmv

2.4 DISCUSSION

2.4.1 THE SDFT CROSS-SECTIONAL MORPHOMETRY

In this study we observed that the cross sectional shape of the SDFT was progressively altered from the proximal to the distal metacarpal region. At the most proximal region the cross sectional shape was almost circular and as it progressed to the mid-metacarpal region, it became flattened dorsopalmerly into a semi-circular form, and then became more progressively flattened in the distal metacarpal region. The progressive regional alteration (Figure 2.2) could be used as an anatomical reference in order to identify regional deformity or an increase in tendon size such as in case of tendonitis and more objectively to assess any internal disruption of the tendon architectures (Smith et al., 1994, Vilar et al., 2011).

Whilst the SDFT CSA appeared to decrease in the mid-metacarpal region and then apparently increase again more distally, these alterations were not statistically significant. Regional alteration in tendon CSA have been shown by others using ultrasonography. Previous studies divided the metacarpal region into seven levels from the proximal to distal end. They demonstrated that the SDFT CSA decreased by 5.33% in the mid-metacarpal region (Smith et al., 1994, Agut et al., 2009) in comparison to the SDFT in the proximal metacarpal region. Research has also demonstrated the relationship between different anatomical regions of the SDFT and its mechanobiology, in that the elasticity modulus was homogeneous but there appeared to be a slight increase in the mid-metacarpal region (Crevier et al., 1996) but it is not representative of tissue strength (Riemersma and Debruyn, 1986).

It has been shown in the canine rotator cuff tendon that regional alteration is also accompanied by alterations to the tendon ultrastructure, with the amount of collagen fibrils being higher in the enthesis (15.7%) than in the tendon proper (Fan et al., 1997). Similarly, in the equine SDFT the size of collagen fibrils were also altered and increased toward the distal region; their diameters were 40nm, 48nm and 68nm in the upper, mid-metacarpal and distal regions respectively (Sese et al., 2007, Watanabe et al., 2007). Other researchers have demonstrated that the number and diameter of collagen fibrils was not constant between tendons and ranged from 5μm-30μm in rat tail tendon, and reached at least 300μm in human tendons (Elliott, 1965, Franchi et al., 2007b). Alteration of these parameters (number and diameter of

fibrils) makes the SDFT non-homogeneous in terms of gross and microscopic morphology from the origin to the insertion point. Alterations to the structural organisation of tendons, for instance the fibre diameter, makes the collagen fibres of the fascicles stiffer in the distal region and potentially capable of sustaining a heavy mechanical load (Rigozzi et al., 2010). These studies confirm structural alterations longitudinally through the tendon.

2.4.2 FASCICLES AND IFM QUANTIFICATION

In this study the number and pattern of the tendon fascicles was described in the SDFT regionally and between paired legs. From our work, it is possible to make qualitative statements on the SDFT fascicular structure. Previous researchers defined different fascicles according to their sizes (Kastelic et al., 1978, O'Brien, 1997, Kannus, 2000). Fascicles are the largest basic conformational unit of the tendon hierarchical organization, and can be defined as a bundle of collagen fibres, outlined by the IFM, which vary in morphology at different levels of the tendon.

2.4.2.1 Fascicles

On the basis of ImageJ optimisation, diameters and the IFM thickness, the size and number of fascicles were quantified. As to be expected, secondary fascicles are smaller than tertiary fascicles. Previous studies have classified the basic units of the tendon hierarchical structures according to their sizes (Kastelic et al., 1978, Kannus, 2000). A wide range of fascicular diameter was recorded ranged from 50µm-3463µm. From this wide range different ranges for both the secondary and tertiary fascicles were also determined (50µm-1383µm and 167µm-3463µm respectively). Other studies have also recorded different diameter measurements for both the secondary and tertiary fascicles were 150µm-1000µm and 1000µm-3000µm in human Achilles tendon (Jozsa and Kannus, 1997, Silver et al., 2003), and 20µm-200µm and 100µm-300µm in rat tendon respectively (Kastelic et al., 1978, Wang, 2006). Whilst secondary fascicles are obviously generally smaller than tertiary fascicles, there is overlap and variability between these groups meaning it is not possible to simply classify them on the basis of size alone. Similarly the CSA of the fascicles varies from region to region and we found a different CSA of fascicles, which were 22µm^2-9424µm^2 and 2µm^2-1503µm^2 for the tertiary and the secondary

fascicles respectively. A study using flexor and extensor tendons of cow, calf, human, dog and guinea pig observed that the CSA of fascicles varies between tendons and species but lies within the range 124μm^2-375μm^2 (Edwards, 1946).

In this study, we determined that the numbers of the fascicles were not constant longitudinally through the tendon. Their average numbers increased toward the distal region of the tendon, which also coincided with an apparent statistically insignificant increase in the CSA of the tendon (Smith et al., 1994). This increase in the number of fascicles could occur due to either diverging/splitting of fascicles or the starting of new fascicles. The numbers of secondary fascicles were also not constant longitudinally through the tendon. We found the number of secondary fascicles within a tertiary fascicle varied from 1-12. Our findings are supported by previous research which also found that up to 10-12 secondary fascicles were present in each tertiary fascicles in rat tail tendon (Kastelic et al., 1978). However, (Kannus, 2000) suggested that the number ranged between 3-4 secondary fascicles and varied from tendon to tendon and, at times, within the same tendon. There would appear to be considerable variation of the tendon subunits between different individuals and species, which has yet to be comprehensively defined.

2.4.2.2 IFM

The IFM that surrounds the tertiary fascicles was thicker than that between the secondary fascicles. These differences have also been mentioned by previous studies in rat tail tendon (Kastelic et al., 1978), human tendon (Kannus, 2000, Fallon et al., 2002) and equine SDFT (Meghoufel et al., 2010) respectively. In a study of B-scanning ultrasonography of equine SDFT, demonstrated a wide range of IFM thickness (from 54μm to 378μm). They also observed that the IFM that surrounds the tertiary fascicles was thicker than that between secondary fascicles. This study did not define tertiary and secondary fascicles on the basis of their IFM measurements. Similarly, our data suggested a wide range of IFM thickness (2μm - 174.11μm), which varied between different fascicles in different regions. This variation in IFM thickness between the tertiary and secondary fascicles was quantified using our ImageJ measurement protocol. Great variation in the mean IFM thickness between the tertiary and secondary fascicles was recorded, even though the IFM of the cross-junction areas were excluded from the measurements due to their

irregularity. A wide range of IFM thickness between both the tertiary and the secondary fascicles were recorded indicating that the IFM thickness was not constant around the fascicles and levels and regions of the tendon (Meghoufel et al., 2010). Our ImageJ quantification method demonstrated a quantitative difference in IFM thickness between the tertiary and secondary fascicles with an average of 30.45µm and 9.78µm in a mature SDFT respectively. It was not possible to discriminate tertiary from the secondary fascicles, as there was overlap between their measurements. This findings could however be used as a complementary criteria to classify fascicles along with the fascicle size and thresholding methods.

The IFM width and size of fascicles were not constant longitudinally through the tendon and they both underwent regional alteration in term of dimensions and shape. However, to understand this regional configuration and how the hierarchical organisation varies between tendon subunits more advanced work is needed such as the use of micro CT or more accurately 3D reconstruction from a histological Z-stack in order to completely understand the conformational pattern of the fascicles, which could help to specifically define fascicle organisation at different levels of the tendon (Screen, 2009).

The IFM as an organising and a binding structure has an important role in transferring energy forces between the fascicles especially at those points where the fascicles cease and new ones start. Similarly the IFM which binds two or more fascicles on their lateral aspect also plays an important role in the mechanobiology of the SDFT by facilitating fascicular sliding and elastic recoil (Thorpe et al., 2012). It has been shown that the mechanical properties of fascicles in force transmission are homogeneous throughout the tendon (Meghoufel et al., 2011) and the IFM is crucial in equalising and specifying transmitted force between the fascicles (Thorpe et al., 2012).

2.4.2.3 Patterns of the fascicles on different transverse levels of the tendon

My results show that the fascicular pattern was not similar between the right and left limbs; however the communication points between the IFM and the epitenon were identical around the tendon periphery (Figures 2.13-2.19). This peripheral configuration of the IFM clarifies that the IFM is symmetrically distributed on the

peripheral aspects between the right and left SDFT. However, more centrally the IFM did not show a symmetrical pattern in paired limbs. This variation in the IFM and the tendon units (fascicles) between different SDFTs was consistently identified, although the possibility of technical error has to be considered as the sectioning levels may not have been exactly similar. Interestingly a marked variation was observed between the forelimbs and hind limbs, which might be due to tendon length, metatarsal conformation and the mechanical action of the hind limb in contrast to the forelimb (Kannus, 2000). In the hind limb the fascicular and IFM patterns were more consistently orientated in one direction and were dissimilar to the pattern seen in the forelimb. The fascicles in the hind limb were elliptical and oriented in a dorso-plantar direction rather than being semi-circular as seen in the forelimb.

2.4.3 3D RECONSTRUCTION AND FASCICULAR TRACKING

We showed that the conformational pattern of the fascicles and the IFM were not constant transversely at different longitudinal levels through the SDFT. Previously how fascicles relate to each other and how they alter, as they run through the tendon has not been entirely clear (Kannus, 2000, Franchi et al., 2007b). From our 3D reconstructions, the outlined fascicle appeared to run longitudinally through the length of the tendon and underwent regional alterations. We found that fascicles diverged into more than one branches or converged with the adjacent fascicles or inter-connected and further underwent alteration when coursing longitudinally through the tendon. It is obvious that converging of the fascicles occurs as the IFM thins and disappears between two fascicles. Whereas, in divergence the IFM inside fascicles created branches such that the fascicles divide into two or more smaller fascicles (Figure 2.24 and 2.25, video links). In a study of 3D reconstruction of different collagen bundles of chick embryo tendon, from electron microscopic transverse serial section, has shown divergence, convergence and inter-connection between the fascicles (Birk et al., 1989). In other tendons such as human supraspinatus tendons, it was found that an average of 18% of the supraspinatus tendon fascicles converged into larger fascicles from the proximal to the distal end. This finding indicates that joining of fascicles can occur at different levels and from proximal to distal (Fallon et al., 2002, Meghoufel et al., 2010). At a different hierarchical level, in a study of human tendon using Transmission Election

Microscopy (TEM), it was shown that the collagen fibres were oriented in various directions. Whilst most of the individual fibril and fibril bundles were longitudinally oriented and ran parallel to the longitudinal axis of the tendon, some bundles crossed each other and formed a spiral plait. The ratio of fibril orientation from longitudinal to transverse and horizontal was 10:1 and 26:1 respectively (Jozsa et al., 1991).

Other studies in human tendons and animal species such as rat, bovine and feline tendons have demonstrated that the core of the tendon contains mainly longitudinal fibres although some fibres were distributed in horizontal and transverse planes, bifurcating, fusing and at times interweaved with each other (Jozsa et al., 1991, Provenzano and Vanderby, 2006). These studies partly support our finding that fascicles run longitudinally whilst having sites where they inter-connect with each other (Figure 2.25 and 2.26). At a different hierarchical level, a study by Starborg and others used 3D EM to view the collagen fibrils in mouse embryo tail tendon. They demonstrated that the Y-shape branching of the collagen fibrils occurred at a rate of 1:20000 D-periods but the mechanism of branching was not obvious. It might be through fusion of fibril-tip to the shaft (lateral fusion) or by growing of a new fibril from the tip or lateral surface of the existing fibrils. Bipolar fibrils have two N-tips, which are important for binding with C-tips of unipolar fibrils in tip-to-tip fusion. However, it was unclear whether this promotes tip to shaft fusion. Thus, branching in tendon might reflect an adaptation of tendon units to their size or functional demand (Starborg et al., 2009). Conceptually, diverging and fusion of the collagen fibrils could be relevant when observing different shaped and sized fibrils throughout the tendon at both the macroscopic and micro-scale levels. This could indicate that in regions where the tendon becomes thicker, collagen fibrils arrange themselves by increasing their diameter or branching to increase fibril numbers per cross sectional area. Further it may be due to an increase in the number of collagen fibrils toward the distal end of the tendon, which is concomitant with an increasing number of fascicles (Sese, Ueda et al. 2007). These findings suggest that tendon is a much more complex and sophisticated structure than previously demonstrated by current anatomical models (Kastelic et al., 1978, Kannus, 2000). Whilst we did not look at enough aged samples to have a statistically relevant dataset in order to demonstrate any obvious alteration with age.

2.4.4 PLANES AND ISOSURFACE VIEWS

When the Z-stack images were viewed in either the X or Y planes it was apparent that all the fascicles continued throughout the Z-stack with considerable variation in their shapes and inter-connection (Figure 2.27). However, at certain points the end of the fascicle became tapered which might indicate that the fascicle partly terminated. In an anatomical study of the human Achilles tendon it was shown that fascicles were not homogenous and continued through the length of the entire tendon (Szaro et al., 2009). From our isosurface-based 3D reconstruction of the IFM through the Z-stack, we found that the IFM also continued longitudinally between the fascicles and outlined the fascicles throughout the tendon. In the core of the tendon, the IFM formed multiple longitudinal holes where the fascicles ran longitudinally from the proximal to the distal region (Jozsa et al., 1991). In the peripheral regions the IFM was more intertwined which may indicate considerable fascicular alteration and heterogeneity as compared to the core of the tendon. This variation could relate to the tendon mechanobiology in terms of tensional force transfer and the preferential risk of injury in this central site. It has been recorded that following injury lesions are frequently localised in the central core of the tendon (Patterson-Kane et al., 1997a). This central localisation occur due to direct disruption of the normal matrix components as a result of repetitive loading cycles or tensional forces (Birch et al., 1998). In one study it was found that following injury the thinnest parts of the IFM are disrupted and this results in a reduction in the number of fascicles due to an abnormal fusion of a number of injured fascicles (Meghoufel et al., 2010). The IFM between the fascicles runs in various orientations and plays a vital role in load transfer between fascicles and in resisting shear forces when the fascicles slide over each other during stretching (Thorpe et al., 2012) .

2.5 CONCLUSION

We conclude that the secondary and tertiary fascicles display a complex 3D organisation that is not reflected in current models of the hierarchical organisation of mammalian tendon. Additionally, this data indicates that the number of both secondary and tertiary fascicles may vary in different regions of equine SDFT. In particular we demonstrated that fascicles are continuous through the length of the tendon and undergo regional morphometric variation. This morphometric variation

results from the fascicles' heterogeneity in terms of diverging, converging and inter-connection throughout the tendon. Understanding the 3D anatomy of the tendon subunits could facilitate understanding of tendon structure-function relationships, age-related changes and injury predisposition.

2.6 FUTURE WORK

Further investigation is needed to define and understand the fascicular organisation, either by microscopy (histology) or by using another advanced technique such as computed tomography (Micro CT) scanning. In addition, exploration of the structural properties of the IFM will aid understanding of its role in tendon hierarchy and mechanobiology.

This methodology described in this study could also be used to describe the anatomical structure of other tendons and possibly also that of ligaments and in additional samples of the same type for detailed quantitative analysis.

CHAPTER THREE

THREE-DIMENSIONAL HISTOMORPHOLOGY OF EQUINE SUPERFICIAL DIGITAL FLEXOR TENDON (SDFT) FASCICLES

3.1 INTRODUCTION

The hierarchical architecture of tendon comprises various sized fascicles, which run down vertically through longitudinal axis of the tendon (Kastelic et al., 1978, O'Brien, 1997, Kannus, 2000, Benjamin et al., 2008). Different hierarchical sub-units of tendon may all have roles in the mechanical function of the tendon at the fibril, fibre (fibril bundle/primary fascicle) and fascicle level (Yahia and Drouin, 1989, Jozsa et al., 1991, Yang et al., 2012). The force is transmitted mainly within the individual fascicle and the fascicle is made up from tendon features that contribute to force transmission such as collagen fibrils, crimp flattening and inter-fibrillar communication (Franchi et al., 2007b, Fessel et al., 2012).

In a study at the electron microscopic scale followed by a 3D reconstruction of a series images of chick embryo tendon, have demonstrated the presence of specific features such as divergence, convergence and inter-connection between the collagen (Birk et al., 1989). Fascicles can be inter-connected and it has been shown in the human supraspinatus tendon that adjacent fascicles converged but not are inter-digitated (Fallon et al., 2002). Mechanical force transfer is likely through inter-connected fascicles and this has implications for tendon function and loading (Thorpe et al., 2012).

Equine SDFT is a long tendon and contain different sized and shape fascicles that extend longitudinally throughout the tendon from the proximal to the distal regions (Meghoufel et al., 2010). Studies at the electron microscopy scale, have demonstrated the presence of sub-helical structures that are rotated around their longitudinal axis (Thorpe et al., 2013b, Thorpe et al., 2015d). A helical sub-structure within the fascicles of the equine SDFT is likely to contribute to tissue elasticity, whilst the IFM has also been shown to provide elasticity, by assisting sliding and reducing shear forces between fascicles (Thorpe et al., 2013b, Thorpe et al., 2014b, Shearer, 2015a). Similarly the helical configuration models of collagen fibre bundles have also been documented and demonstrated in different tendons such as the human patellar, rat-tail tendons and bovine Achilles tendon (de Campos Vidal, 2003, Reese and Weiss, 2013). Apparently, from the foetal period until full maturity the SDFT undergoes conformational changes and biochemical accretion in both the vertical and horizontal dimensions (Tuite et al., 1997, Russo et al., 2015). Currently, there are no

data on the organisation of SDFT fascicles, particularly in relation to fascicle continuity, fascicular inter-connections, convergence and fascicle splitting/ divergence. This chapter aims to describe the three-dimensional (3D) ultra-structural fascicular anatomy of the SDFT and to document whether:

1- Fascicle morphology would differ between the proximal, mid-metacarpal and distal regions of the tendon.

2- Fascicles would inter-connect and either divide into smaller fascicles or converge along the longitudinal axis of the tendon.

3- Fascicles may adopt a spiral or twisted conformation.

3.2 MATERIALS AND METHODS

3.2.1 SAMPLES

SDFT samples were obtained from Thoroughbred and Thoroughbred Cross horses either from a commercial abattoir (Potters, Taunton or Wooton Bassett) or from horse's euthanased at the University of Liverpool Equine Hospital with the owner's informed consent. The study was assessed and approved by the University of Liverpool's, Veterinary School Research Ethics Committee (VREC, study 214). Four SDFT samples were collected from the forelimb and designed for this study as follow:

1- Foetal SDFT (6 months of gestation): portions (1cm length) were taken from proximal (carpo-metacarpal level), mid-metacarpal and the distal metacarpal (metacarpo-phalangeal level) regions (Figure 3.1 A). Fixed in 4% paraformaldehyde for 24 hours and paraffin embedded in dorso-palmar orientation. The tissues were initially trimmed (Microtome) by taking 100µm sections, in order to reach the entire SDFT surface. A series of twenty (5µm thick) longitudinal sections were collected on polylysine slides and stained with Haematoxylin & Eosin (H&E) (Figure 3.1 B) (See chapter four, section 4.2.5.1 for H&E staining procedure).

2- One-year-old SDFT: treated similarly as in foetal SDFT. Moreover, for the mid-metacarpal region 65 sections were collected.

3- Nine-years-old SDFT: portions (1cm length) were taken from proximal (carpo-metacarpal level), mid-metacarpal and the distal metacarpal (metacarpo-phalangeal level) regions (Figure 3.1 A). Sample was split sagittally and only one half of an approximately 1cm long block was Fixed in 4% paraformaldehyde for 24 hours and paraffin embedded in sagitto-lateral orientation. The tissues were initially trimmed (Microtome) by taking 100µm sections, in order to reach the entire SDFT surface. A series of twenty (5µm thick) longitudinal sections were collected on polylysine slides and stained with Haematoxylin & Eosin (H&E) (Figure 3.1 B).

4- One-year-old SDFT: portions (1cm length) were taken from the mid-metacarpal region (Figure 3.1). Fixed in 4% paraformaldehyde for 24 hours and paraffin embedded in dorso-palmar orientation. The whole depth of the tissue block

remaining after trimming was sectioned into 500 sections and every other section were collected on to polylysine slides and stained with haematoxylin and eosin (H&E) (Figure 3.1 B).

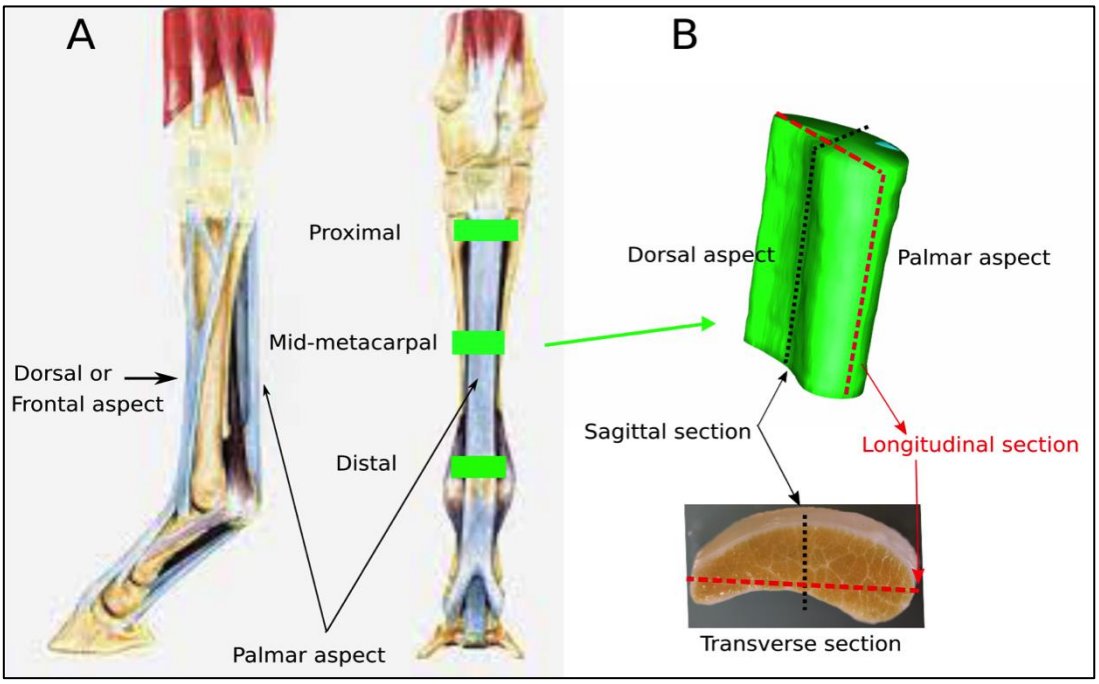

Figure 3.1: A. Normal anatomy of the SDFT from (Ferraro et al., 2009), indicating points of specimen collection from the proximal, mid-metacarpal and distal regions (green lines). B. Orientation of longitudinal (red dotted line) and sagittal (black dotted line) sections in relation to a 3D representation (top) and whole tissue slice (bottom) of the SDFT.

3.2.2 CAPTURING OF THE ENTIRE H&E STAINED SECTION

Each section was imaged using a Nikon Eclipse 80i microscope fitted with a digital camera. Several images were taken using the 4X objective so that the entire surface was captured for all sections.

3.2.3 PHOTO COLLAGE

All captured photos were collated and converted to one image using either Inkscape and saved as png image format (Figure 3.2) (www.inkscape.org). Then all

collated images were cropped (Crop Tool) using Paint Shop Pro x4 Ultimate and converted to TIFF. Then the collated sections were named according to the sectioning series (dorso-palmar) from number 01 to 20 for 20 series sections or 01-500 for the whole mid-metacarpal thickness (sample number 4) to be compatible for IMOD 3D reconstruction

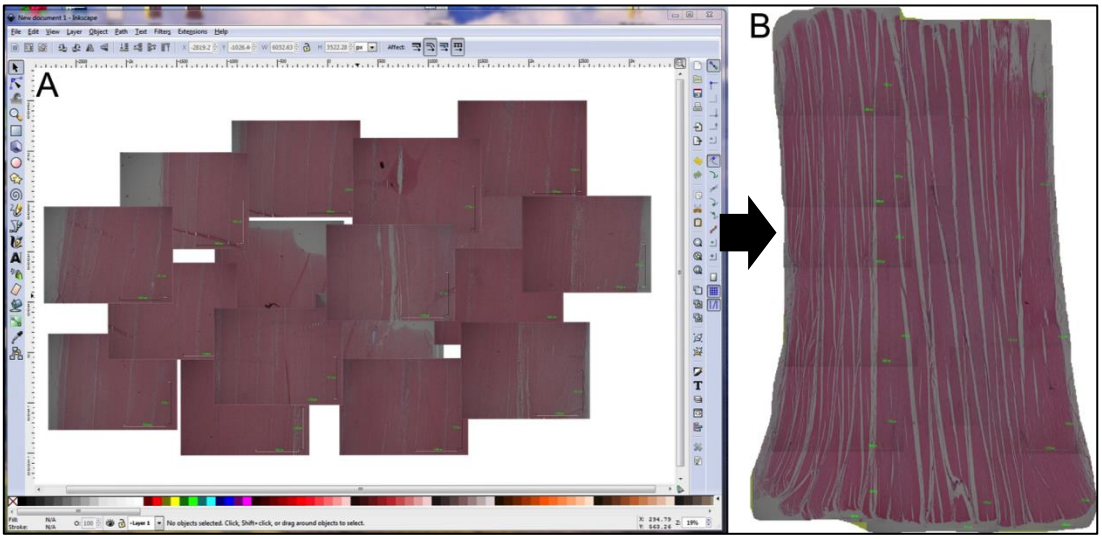

Figure 3.2: Screenshots demonstrating how several images (A) were manually rearranged to create a collage of the entire section (B) using Inkscape software.

3.2.4 PRINCIPLE APPLIED DURING 3D RECONSTRUCTION

3D reconstruction was carried out in order to accurately discriminate between fascicles and inter-fascicular matrix (IFM) at a resolution not currently possible using micro computed tomography or magnetic resonance imaging. The following criteria were used in order obtain good 3D reconstructions of the fascicles from histological sections.

1-The SDFT specimens should be intact and not damaged

2- Sectioning orientation as well as the location of any missing sections should be recorded.

3-All slides should be stained altogether at the same time to obtain the same staining density and contrast.

4-Each entire section should be meticulously captured using the same orientation and magnification power for all images.

5-Image collages should be cropped to include the tissue section alone and then saved as Tiff images.

6-Fascicles are defined as being delineated by the IFM (endotenon) and different colours should be used to discriminate between individual fascicles in the 3D reconstruction.

7-Fascicles should be tracked individually and any alteration to the fascicular outline indicated either by including this information in the reconstruction or by using different colours where fascicles diverge or converge.

3.2.5 THREE-DIMENSIOANL RECONSTRUCTION USING IMOD

Initially, all Tiff images were loaded into the Cygwin home directory from /home/username/file name. To create a Z-stack from the TIFF images they were loaded into IMOD by typing (LS) followed by typing the (CD file name) in order to open the directory file. When the file directory or subdirectory was opened, then by typing (tif2mrc *.tif newfilename.mrc) in the programme, images were automatically converted into .mrc files (Z-stack). These files were automatically aligned using the midas programme by typing (midas filename.mrc) followed by manual alignment and then saved to the home directory as an mrc Z-stack.

The mrc image file was opened in the IMOD programme by typing 3DMOD and selecting the mrc file in the directory or subdirectory file. Then by using the drawing tool, fascicles of interest were outlined sequentially in order to re-construct the fascicular anatomy. Different colours were used to delineate different fascicles (Figure 3.3). Outlined fascicles were then converted to 3D models by selecting the model view option where it opens a new window and shows all contours in a 3D form. The contours were then meshed to create a complete 3D reconstruction. To rectify minor degrees of contour wrinkle or small irregularities, specific options such

as the surface and low-resolution mesh in the meshing tool bar were used in order to obtain optimal contour adjustment.

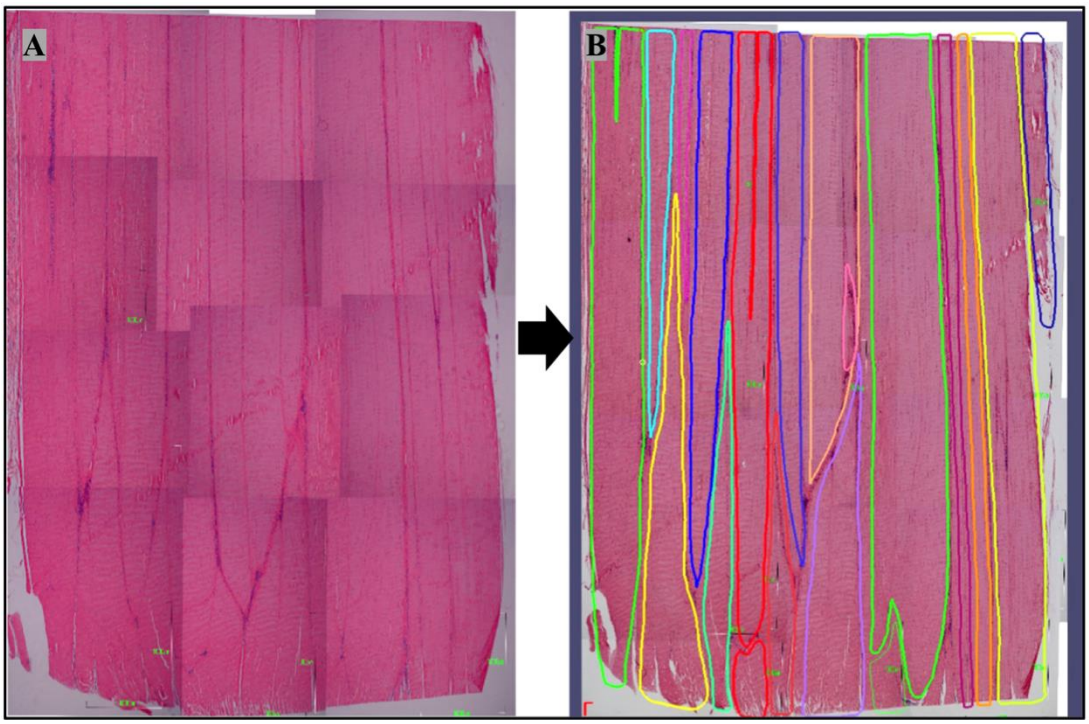

Figure 3.3: A: Image collage obtained using Inkscape from 12 captured photos covering the entire section of the mid-metacarpal region of a one-year-old sample. B: Example of fascicles outlined with different colours using the drawing tools in IMOD.

3.2.6 CREATING A 3D VIDEO OUTPUT

Described in chapter two (section 2.2.5.2.3)

3.2.7 DESCRIPTIVE AND ANALYTICAL MEASURES

During the 3D reconstruction of the proximal, mid-metacarpal and the distal region, the following steps were used in order to describe fascicles regionally and in different horses:

3.2.7.1 Pattern of fascicles

Fascicles were described in a 3D form that created from a series of 20 sections in the proximal, mid-metacarpal and the distal regions in all samples in order to determine regional variation.

3.2.7.2 Measurement of the contour length in all regions (Analysis and summary of contours length)

The contours lengths of all fascicles were measured through the Z-stack using the Drawing Tool of the main 3dmod window. From the Drawing Tool the Action Tool was then selected to open a Perform Action toolbar, which allows a number of different measurements values to be obtained. All contours were first converted from closed to open contours and then the analyze tubes option selected from the Perform Action menu to measure the length of all contours in pixels (Figure 3.4). Fascicular contour lengths for the 1^{st}, 5^{th}, 10^{th}, 15^{th} and 20^{th} sections were selected due to strong similarities between at least 3 adjacent sections. When their lengths were measured some of them had dual contours measure, under the name of one object (fascicle). These two measures indicated that the fascicles were divided at certain level into two parts. The contour length in all regions were collected on an excel spreadsheet in order to demonstrate how the fascicular outlined contour altered through the Z-stack.

3.2.7.3 Measurement of the degree of divergence, convergence and inter-connection

The number of fascicular divergence, convergence and inter-connection were counted through the 1^{st}, 5^{th}, 10^{th}, 15^{th} and 20^{th} histological sections in all regions. These based on the fascicular outlines and the visibility of the IFM between the fascicles. In areas where the IFM disappeared between two fascicles it means that these fascicles tend to converge with each other and vice versa. Points of inter-connection were determined by intermittent disappearance of a small part of IFM between the fascicles or inter-crossing of the collagen fibres between them (Figure 3.4). The data was collected on an excel spreadsheet in order to demonstrate regional difference of the above-mentioned features.

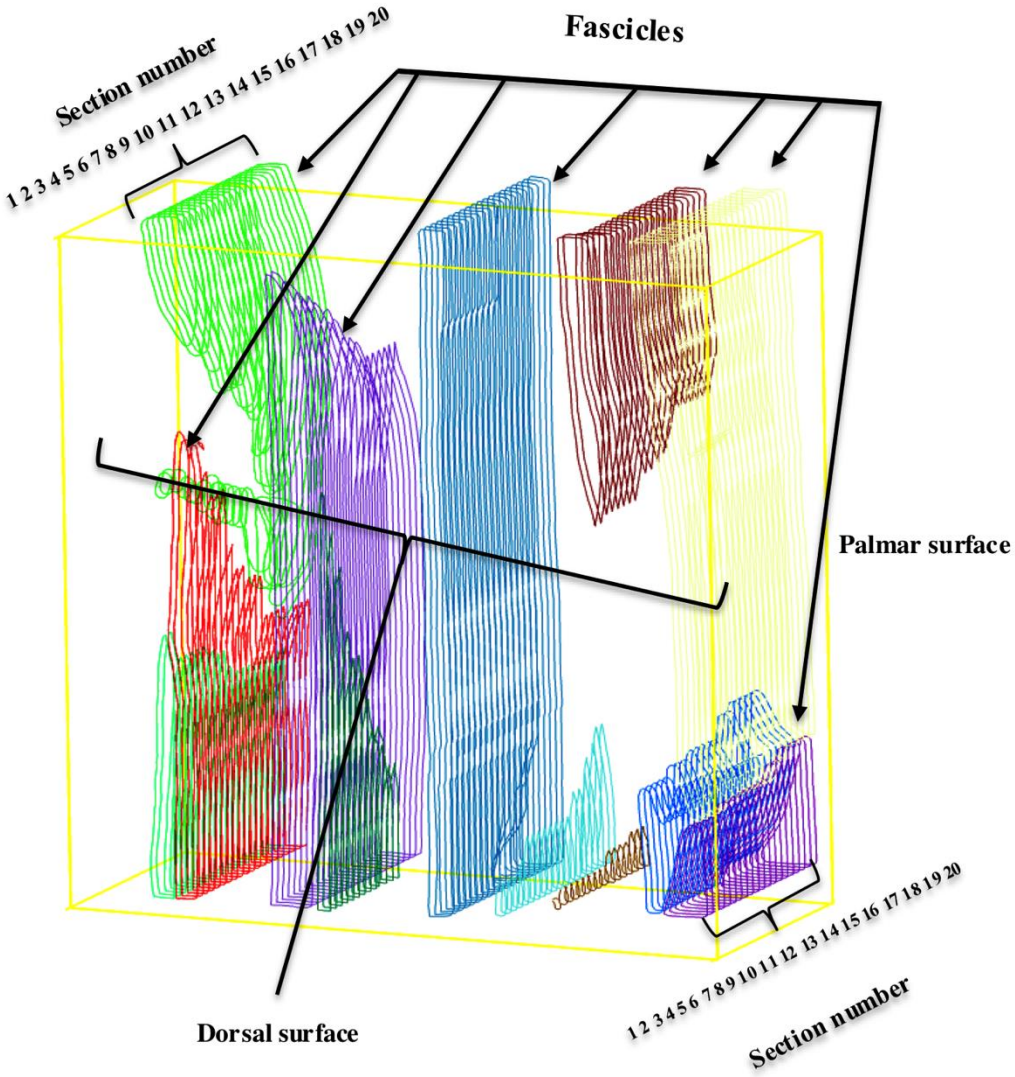

Figure 3.4: The contour outline of some selected fascicles through the Z-stack; each colour represents one fascicle that includes a number of series of histological sections (20 sections). The Drawing Tool was used to draw different coloured lines (contours) around the fascicles through the Z-stack from the dorsal to the palmar aspect of the tendon.

3.2.7.4 Describing the 3D form of the whole mid-metacarpal thickness

For the reconstruction of the whole mid-metacarpal thickness of the additional one-year-old horse, contour lengths were measured for all 250 sections, as only every other 5µm section (of 500 total) was included in the 3D reconstruction in order to

fully explore the shape and orientation of the fascicles as a whole in the mid-metacarpal region. The contour length were entered on an excel spreadsheet in order to demonstrate how the fascicular outline altered through the Z-stack.

3.2.7.5 Histological view of the altered fascicles on a dorso-palmar view

In order to describe the 3D form of the fascicles and how they were modified through the Z-stack, images of first and the last section were selected to show novel features such as discontinuities, inter-connections, fascicle ends, convergence and divergence.

3.3 RESULTS

3.3.1 THREE-DIMENSIONAL RECONSTRUCTION OF DIFFERENT SDFT

Different SDFT were processed in order to determine the tendon fascicular anatomy and how fascicles vary regionally. Three different SDFT were assessed, foetal (6 month of gestation), one-year and nine-years-old. In all three specimens three different regions (proximal, mid and distal metacarpus) were examined. For each sample and in each region, a longitudinal section of approximately 1cm length was analysed. A depth of approximately 100µm was reconstructed for each sample, except for the mid-metacarpal region of the one-year-old sample for which a depth of approximately 325µm was reconstructed. For an additional one-year-old sample a depth of 2500µm of the mid-metacarpal region was reconstructed.

3.3.1.1 Three-dimensional reconstructions of the foetal SDFT

3.3.1.1.1 Three-dimensional reconstruction of the foetal proximal-metacarpal region

3D reconstruction of the foetal proximal-metacarpal region demonstrated that almost all fascicles ran parallel to the longitudinal axis of the tendon. Fascicle shape ranged from wedge-shaped to small irregular structures. Most fascicles coursed longitudinally through the entire region however a few fascicles showed some discontinuity with the presence of a complete or partial discontinuity in their structure and some fascicles had tapered ends that overlapped with adjacent or preceding fascicles (Figure 3.5). Where transverse discontinuities occurred within a fascicle the profile of the proximal portion of the fascicle was morphologically similar to the distal portion beyond the points of discontinuation. Points of partial or complete discontinuities were filled with IFM that was joined to the longitudinally oriented IFM present between the fascicles. A number of small isolated IFM were occasionally present inside some large fascicles. These isolated intra-fascicular IFM may indicate that these large fascicles were underwent their initial differentiation and they were responsible either for divergence or convergence of the fascicles. The 3D profile of the reconstructed fascicles progressively altered from the dorsal to the palmar aspect over the 100µm reconstruction depth and almost all fascicles underwent some progressive morphological alteration. Fascicles decreased or

increased in size, diverged or converged and inter-connected with each other. Moreover, fascicles on the upper side level (top) of the Z-stack were not similar to the lower side level (bottom); these include their number, sizes and shapes (Figure 3.5 and the associated video 3.1).

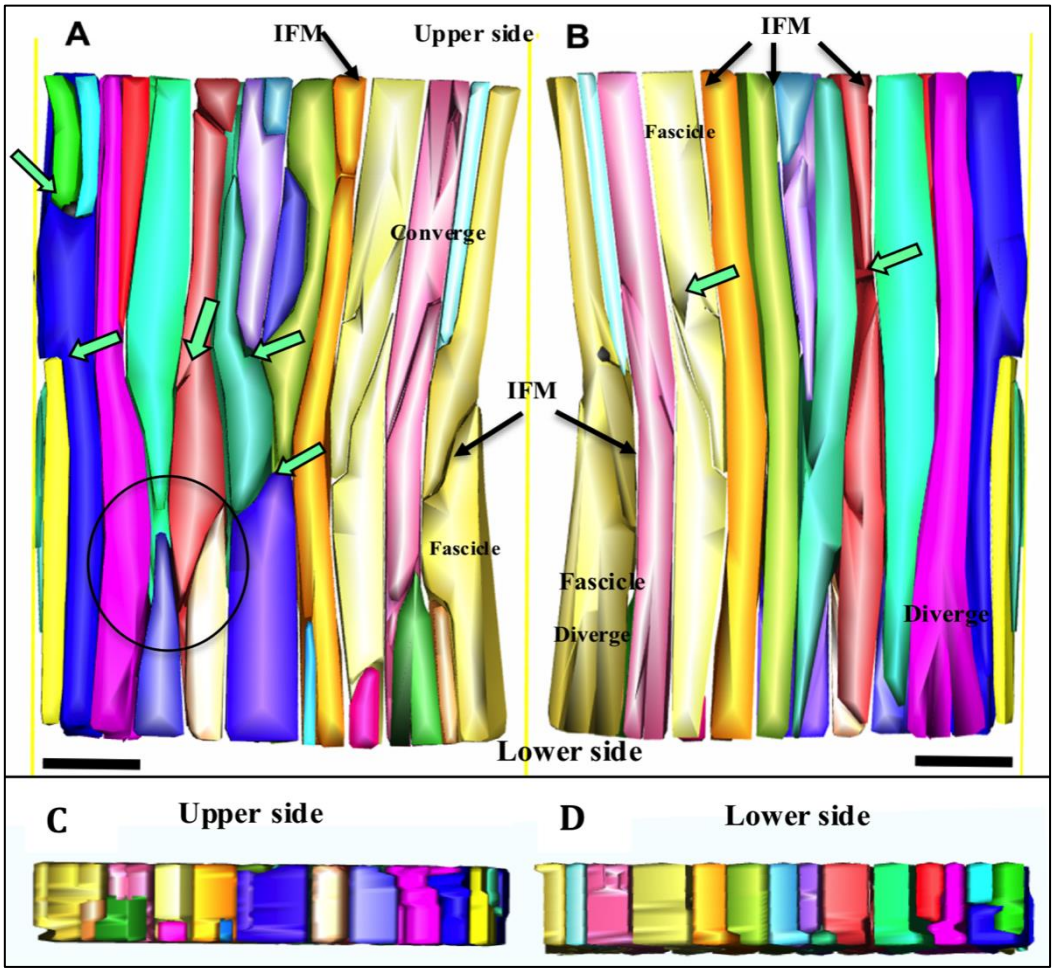

Figure 3.5: Three-dimensional reconstruction of the proximal-metacarpal region of the foetal SDFT from a Z-stack of 20 slides (100µm thick). Fascicles are approximately parallel to the longitudinal axis of the tissue. Fascicles were heterogeneous in shape and were dissimilar when viewed from the dorsal (A) or palmar (B) aspect and from the upper (C) or lower (D) aspect of the reconstruction. The end of some fascicles overlapped with the adjacent or the preceding fascicles (circle) and appeared to taper end-to-end. Some fascicles converged, diverged and had distinct discontinuities, (green arrows), (Scale bar = 1000µm). A supplementary video (3.1) is provided in the link below:

PhD thesis- Othman, Ali- Three-dimensional supplementary videos/3.1.wmv

3.3.1.1.2 Three-dimensional reconstruction of the foetal mid-metacarpal region

3D reconstruction of the mid-metacarpal region similarly demonstrated that all fascicles were extended parallel to the tendon longitudinal axis. However, a small number of fascicular discontinuities were observed. The fascicular morphology also changed from the dorsal to the palmar aspect of the tendon. Alterations to fascicular morphology included the presence of partial or complete discontinuities, variations in fascicular contour outlines and convergence or divergence of the fascicles. Fascicles at the upper level (top) of the Z-stack were not similar to the lower level (bottom) (Figure 3.6 and the associated video 3.2).

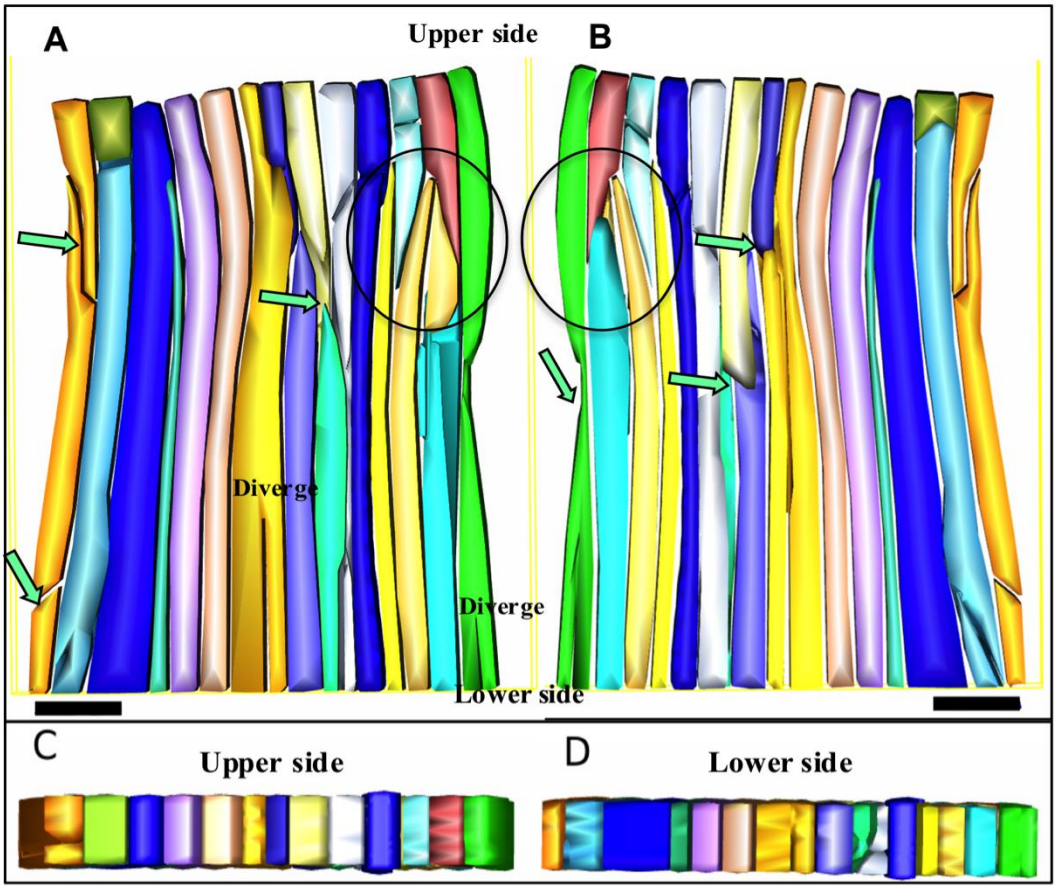

Figure 3.6: Three-dimensional reconstruction of the mid-metacarpal region of the foetal SDFT from a Z-stack of 20 slides (100µm thick). Fascicles are primarily longitudinal and parallel to the long axis of the tendon. Fascicles were heterogeneous in shape and were dissimilar when viewed from the dorsal (A) or palmar (B) aspect and from the upper (C) or lower (D) aspect of the reconstruction. Fascicles were overlapped (circles), diverged or inter-connect (arrows) with each other, (Scale bar= 1000µm). A supplementary video (3.2) is provided in the link below:

PhD thesis- Othman, Ali- Three-dimensional supplementary videos/3.2.wmv

3.3.1.1.3 Three-dimensional reconstruction of foetal distal-metacarpal region

The orientation of the fascicles in the foetal distal-metacarpal region was very similar to that in the proximal and mid-metacarpal regions, with fascicles running parallel to the longitudinal axis of the tendon. As described for the proximal and mid-metacarpal regions the fascicular morphology was altered from the dorsal to the palmar aspect of the tendon. There was variation in the fascicular anatomy from the dorsal to the palmer view. These include fascicle discontinuities, alteration to fascicle shapes in both the vertical and horizontal directions and the presence of smaller sized fascicles. Various amounts of isolated IFMs were interspersed throughout the body of the fascicles. These isolated IFMs altered progressively through different levels of the Z-stack, either disappearing or extending and dividing fascicles into smaller ones (Figure 3.7 and the associated video 3.3).

The presence of larger amount of the isolated IFMs would indicate that fascicles in this region undergo further alteration in term of convergence, divergence and inter-connections. Moreover, on the lateral aspect a few small irregular shaped fascicles were present throughout the whole Z-stack thickness with only minor alterations to their morphology from dorsal to the palmar side (Figure 3.7, circle). Again, fascicles on the upper side level (top) of the Z-stack were not similar to the lower level (bottom) (Figure 3.7 C, D).

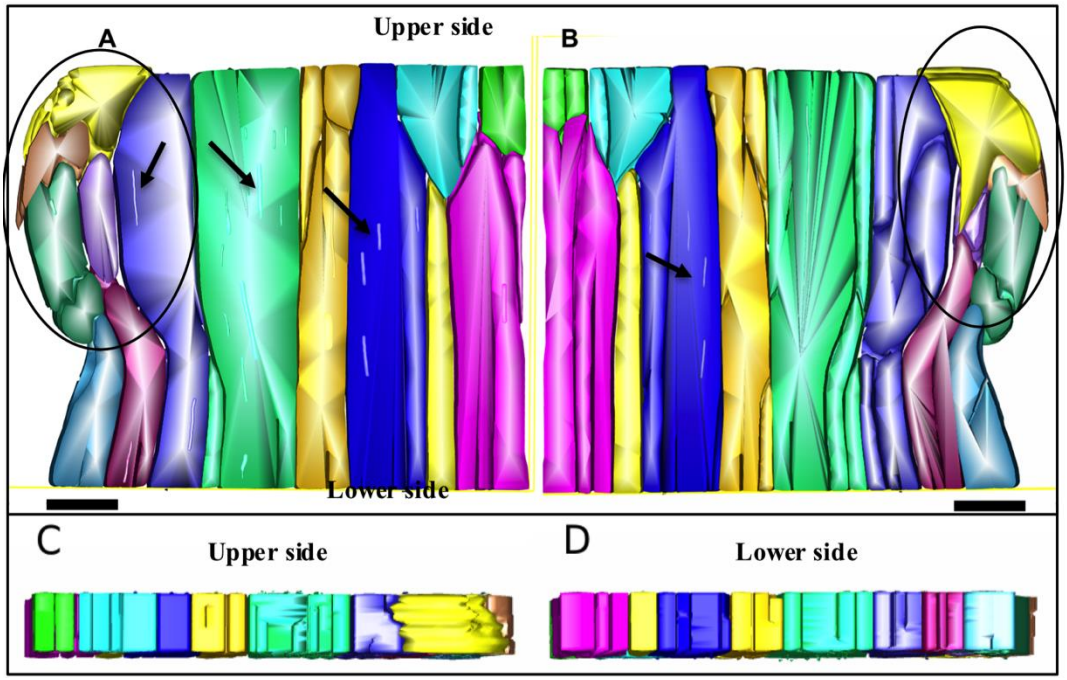

Figure 3.7: Three-dimensional reconstruction of the distal-metacarpal region of the foetal SDFT from a Z-stack of 20 slides (100µm thick). Fascicles were heterogeneous in shape and were dissimilar when viewed from the dorsal (A) or palmar (B) aspect and from the upper (C) or lower (D) aspect of the reconstruction. A few fascicles have irregular shapes (circle) on both the dorsal and palmar aspects. Presence of a various amount of isolated IFMs, were not completely continued longitudinally through the body of the fascicles (arrows), (Scale bar = 1000µm). A supplementary video (3.3) is provided in the link below:

PhD thesis- Othman, Ali- Three-dimensional supplementary videos/3.3.wmv

3.3.1.1.4 Analysis and summary of the three-dimensional structure of the foetal SDFT

The longitudinal contour outline lengths of the reconstructed fascicles throughout the Z-stack in the three different regions (proximal, mid-metacarpal and distal) are shown in Figure 3.8. The longitudinal contour lengths of fascicles were not constant and their sizes tended to either decrease or increase from the dorsal to the palmar aspect of the tendon. However, the lengths of a few fascicle contours remained constant either for a short distance or occasionally throughout the Z-stack.

Eight out of twenty four fascicles (33.33%) in the proximal region underwent further modification such as dividing into more than one fascicle in either the

transverse or longitudinal direction without inter-connection. In the mid-metacarpal region the contour length properties were similar to that of the proximal region but a larger number of fascicles (10 fascicles out of 20) underwent further modification (50%). In the distal region the degree of alteration was even higher with 9 fascicles out of 14 undergoing further modification (64.28%).

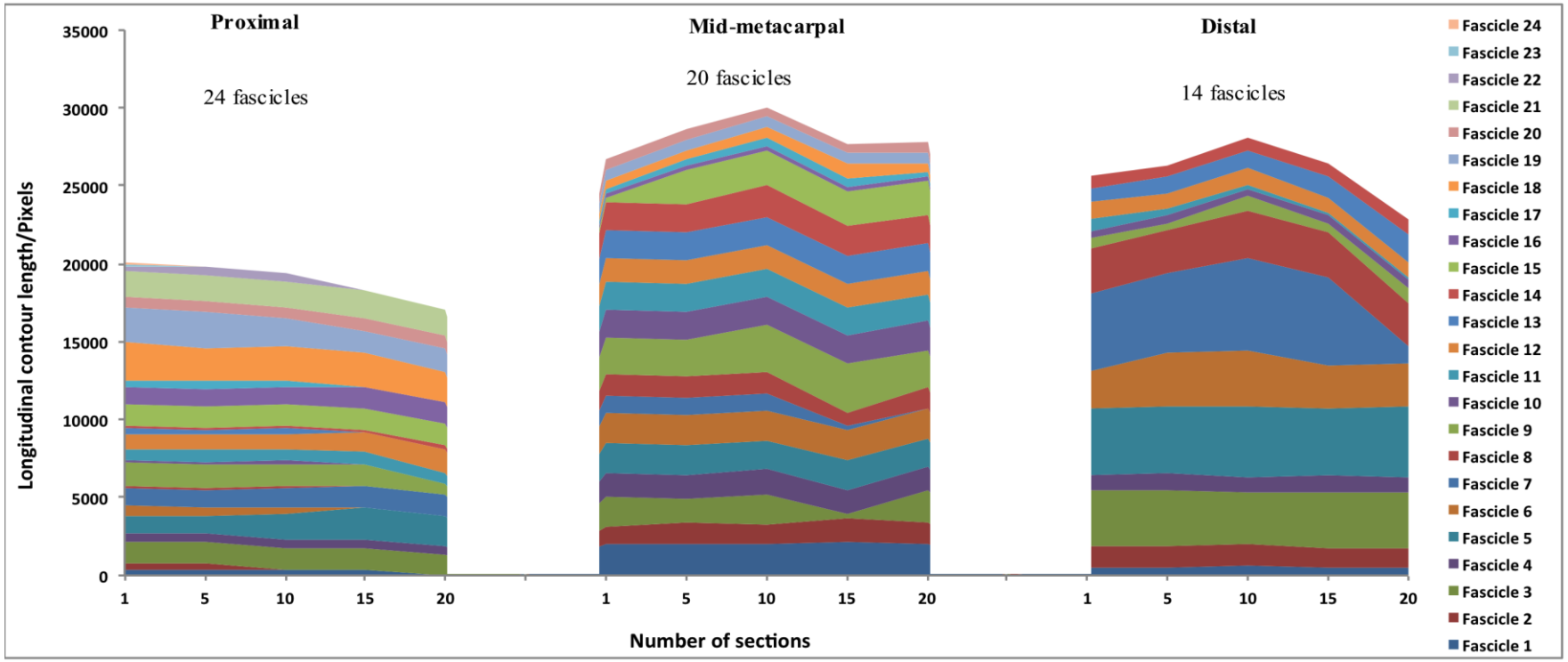

Figure 3.8: Longitudinal contour lengths (pixels) of the outlined fascicles in section numbers 1, 5, 10, 15 and 20 throughout the Z-stack in the proximal, mid-metacarpal and distal regions of the foetal SDFT. Contour lengths were not constant reflecting alterations to fascicles morphology from the dorsal to the palmar side of the Z-stack.

3.3.1.2 Three-dimensional reconstruction of one-year-old SDFT

3.3.1.2.1 Three-dimensional reconstruction of one-year-old proximal-metacarpal region

In the 3D reconstruction of the proximal-metacarpal region, fascicles had a similar orientation along the long axis of the tendon as in the foetal tendon. As previously, fascicle morphology was found to differ between the dorsal and palmar aspects of the tendon. There were fascicles of various sizes, points of inter-connection and fascicular gaps. A new small fascicle appeared on the lateral aspect on section 10 and continued to increase in size. Intra-fascicular IFM was not observed but some IFM was observed in the upper or lower part of a few large fascicles, subdividing them into smaller fascicles. Interestingly, at the distal part of this 3D reconstruction the size of the tendon progressively increased (Figure 3.9 circles). Meanwhile, there was a concomitant alteration in the number and cross-sectional area of the fascicles and some apparent flaring of the fascicles (Figure 3.9 and the associated video 3.4).

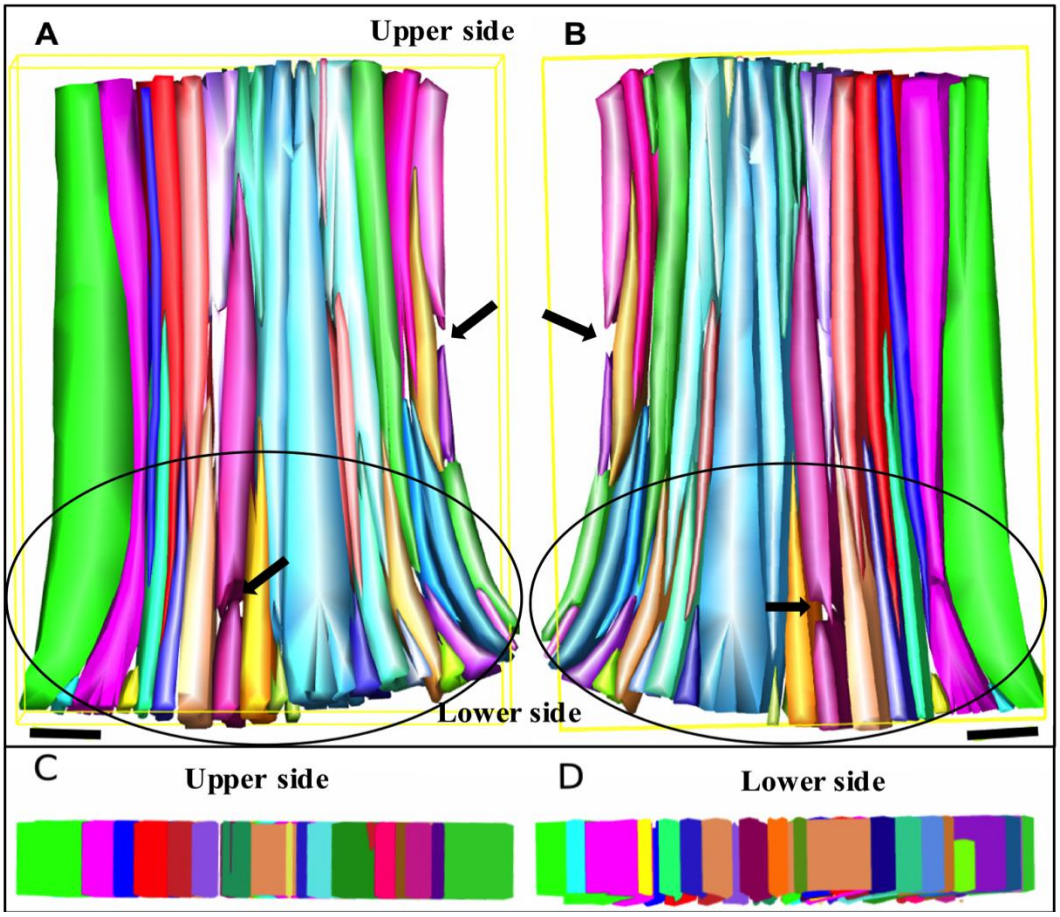

Figure 3.9: Three-dimensional reconstruction of the proximal-metacarpal region of a one-year-old SDFT from a Z-stack of 20 slides (100µm thick). Fascicles were orientated parallel to the longitudinal axis of the tendon. The tendon size increased toward the distal part and where a number of new fascicles started (circles). Fascicles were heterogeneous in shape and were dissimilar when viewed from the dorsal (A) or palmar (B) aspect and from the upper (C) or lower (D) aspect of the reconstruction, few fascicles contained gaps (arrows) and points of inter-connection, (Scale bar= 1000µm). A supplementary video (3.4) is provided in the link below:

PhD thesis- Othman, Ali- Three-dimensional supplementary videos/3.4.wmv

3.3.1.2.2 Three-dimensional reconstructions of one-year-old mid-metacarpal region

In the 3D reconstruction of the mid-metacarpal region, fascicles had a similar orientation along the long axis of the tendon as in the proximal region. Fascicles appeared to be straighter than those in the proximal region. Fewer points of fascicular discontinuation were observed and other features such as inter-connection,

divergence and convergence and interpolation of the ends of fascicles could be seen in this 3D reconstruction (Figure 3.10 and the associated video 3.5).

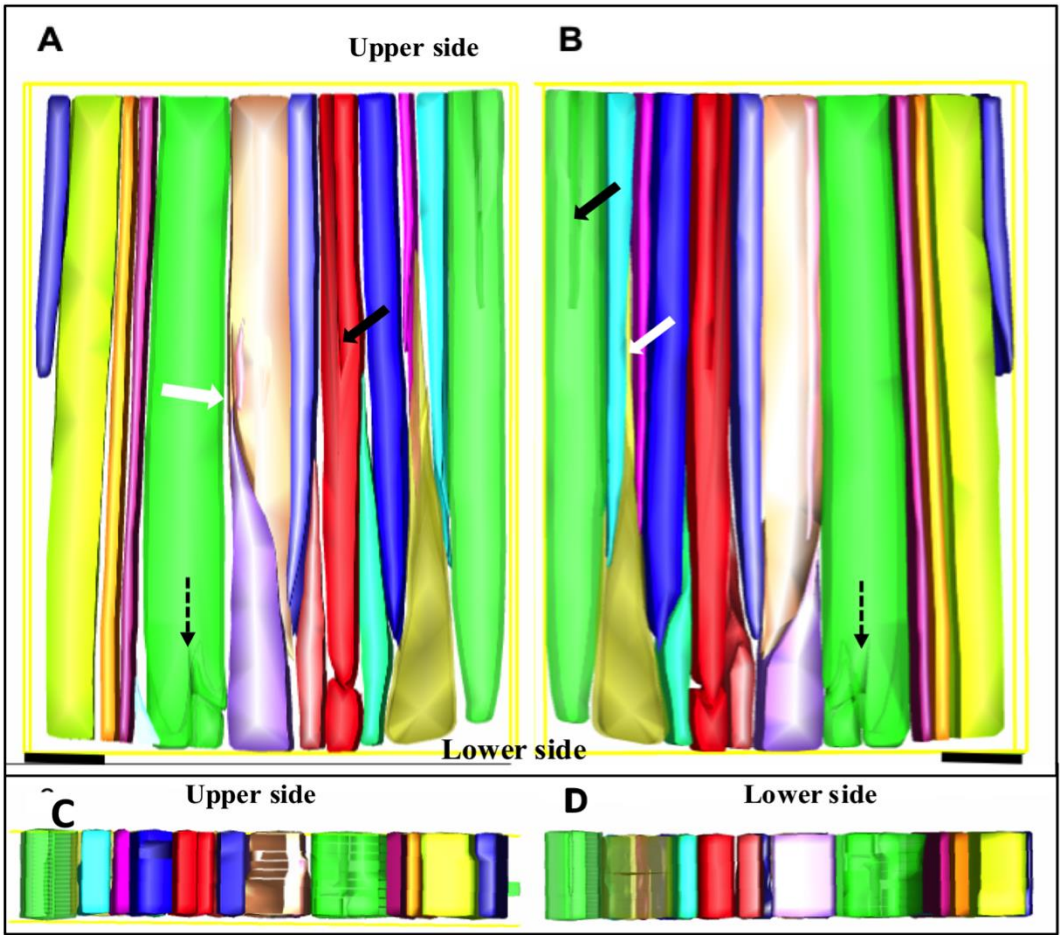

Figure 3.10: Three-dimensional reconstruction of the mid-metacarpal region of a one-year-old SDFT from a Z-stack of 20 slides (100µm thick). Fascicles were heterogeneous in shape and were dissimilar when viewed from the dorsal (A) or palmar (B) aspect and from the upper (C) or lower (D) aspect of the reconstruction. The fascicles were orientated almost longitudinally and parallel to the longitudinal axis of the tendon. Fascicles have different sizes and shapes and were seen to inter-connect, converge (black arrows), diverge (dashed arrows) and have overlapping ends (white arrows), (Scale bar= 1000µm). A supplementary video (3.5) is provided in the link below:

PhD thesis- Othman, Ali- Three-dimensional supplementary videos/3.5.wmv

3.3.1.2.3 Three-dimensional reconstructions of one-year-old distal-metacarpal

Fascicular orientations were approximately similar to those in the proximal and mid-metacarpal regions but were slightly flared at their distal end where the size of

the tendon increased. Fascicles were of various sizes and shapes and fascicular morphology was progressively altered from the dorsal to the palmar aspect of the tendon. Some IFM was found extending longitudinally through the body of the fascicles, which might indicate an early alteration of fascicles prior to divergence or convergence (Figure 3.11 and the associated video 3.6).

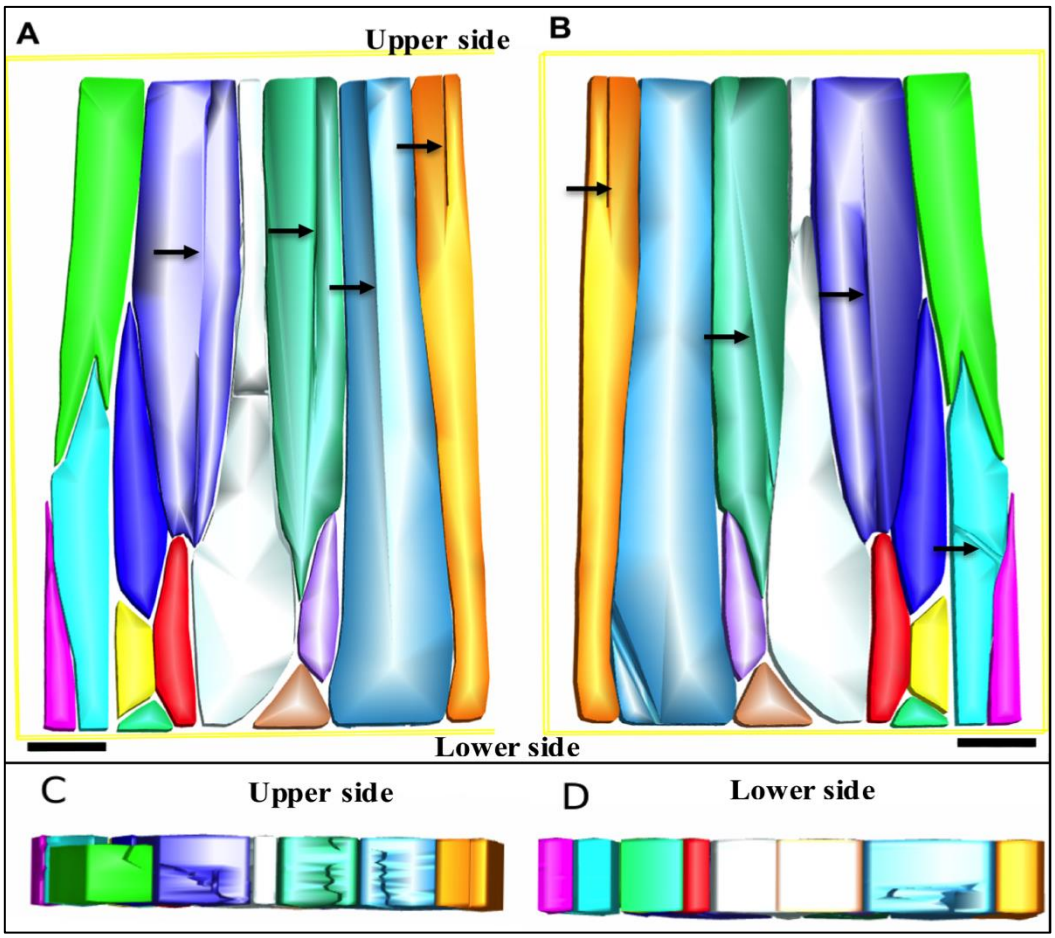

Figure 3.11: Three-dimensional reconstruction of the distal-metacarpal region of a one-year-old SDFT from a Z-stack of 20 slides (100µm thick). The orientations of the fascicles are almost longitudinal and parallel to the longitudinal axis of the tendon. Fascicles were heterogeneous in shape and were dissimilar when viewed from the dorsal (A) or palmar (B) aspect and from the upper (C) or lower (D) aspect of the reconstruction. Fascicles have different sizes and shapes, inter-connecting with each other and inside large fascicles there is incomplete extended IFM (arrows), (Scale bar= 1000µm). A supplementary video (3.6) is provided in the link below:

PhD thesis- Othman, Ali- Three-dimensional supplementary videos/3.6.wmv

3.3.1.2.4 Analysis and summary of the three dimensional structure of the one-year-old SDFT

When the contour length was measured in every fifth section through the Z-stack we found that fascicle profiles were not constant. Fascicles underwent some alteration at different levels and regions of the tendon. In the proximal region the contour length of the fascicles slightly altered throughout the Z-stack from the dorsal to the palmar aspect. Between sections 1-5 the contours length of the fascicles remained constant but then start to alter slightly toward the palmar aspect of the tendon. Fascicles in this region were observed to diverge, converge and inter-connect. A few short fascicles were seen and most continued longitudinally from the proximal to the distal end of the reconstruction. Seven out of thirty four contours underwent further modification (20.58%) (Fascicle divided into more than one fascicle either longitudinally or transversely).

The contour outlines of the fascicles throughout the mid-metacarpal region of the Z-stack were more regular than in the proximal region. Contours were mostly homogeneous from the dorsal to the palmar aspect and only two fascicles out of twenty (10%) underwent further alteration. Fascicle convergence, divergence and inter-connection were also observed. In the distal metacarpal region the contour outlines only slightly altered from the dorsal to the palmar aspect of the tendon. Four out of fourteen fascicles (28.57%) underwent further alteration (Figure 3.12).

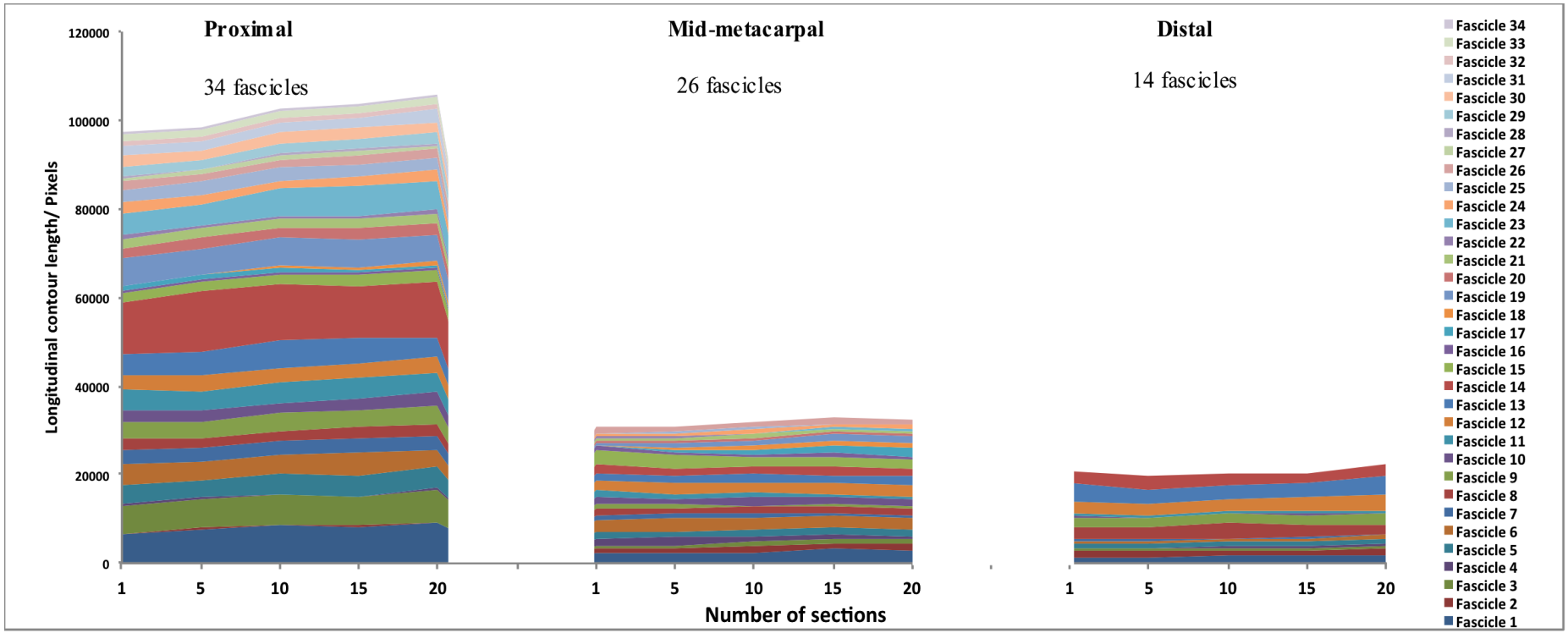

Figure 3.12: Longitudinal contour lengths (pixels) of the outlined fascicles in section numbers 1, 5, 10, 15 and 20 throughout the Z-stack in the proximal, mid-metacarpal and distal regions of the one-year-old SDFT. Contour lengths were similar but not constant reflecting alterations to fascicle morphology from the dorsal to the palmar side of the Z-stack Fascicles were altered in all regions and at different level of the Z-stack but they were less regular in the distal region.

3.3.1.3 Three-dimensional reconstructions of nine-years-old SDFT

3.3.1.3.1 Three-dimensional reconstructions of the nine-years-old proximal-metacarpal region

Fascicles were very similar to those of the foetal and one-year-old SDFT in terms of morphology, orientation and organization. However, they appeared slightly closer together and to have a thinner IFM particularly at those points where the fascicles were connected and apparently the IFM proportionally is more abundant in foetal than in the mature tendons and this also has been shown by other researchers (Russo et al., 2015). Fascicles again tended to diverge or converge and within some fascicles small longitudinally oriented IFMs were dispersed and they were altered at different levels through the Z-stack (Figure 3.13 and the associated video 3.7).

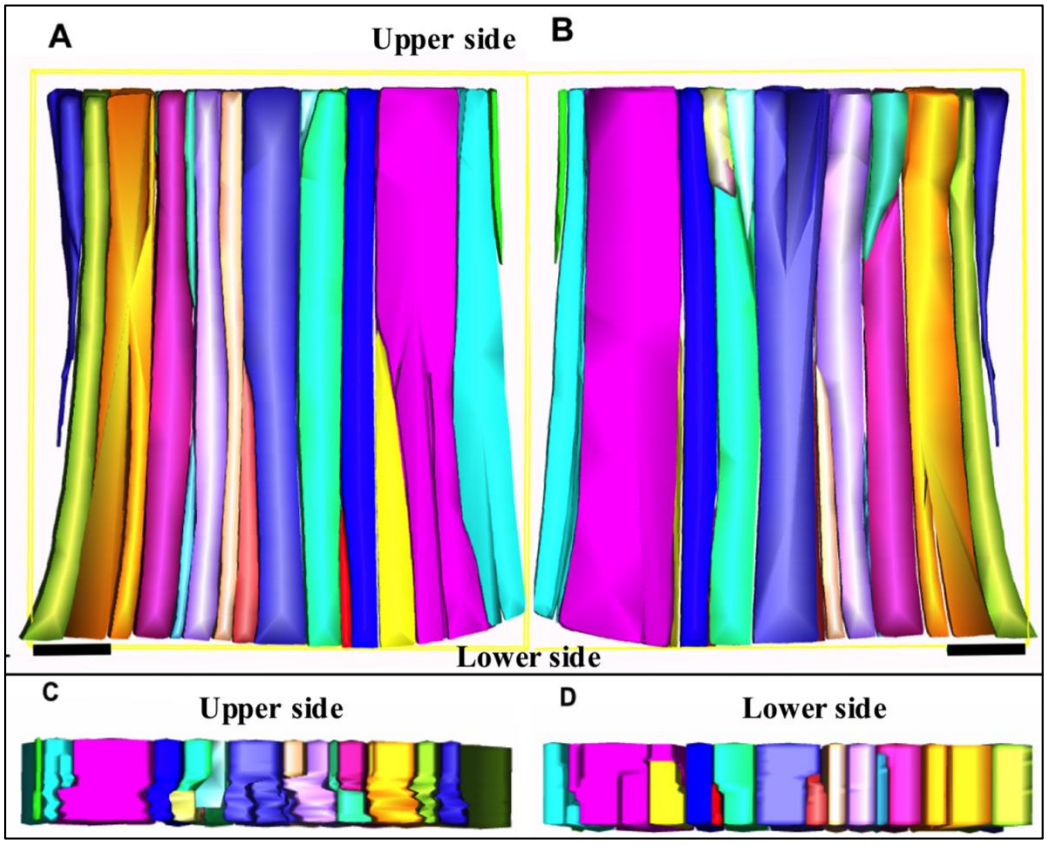

Figure 3.13: Three-dimensional reconstruction of the proximal-metacarpal region of a 9-years-old horse from a Z-stack of 20 slides (100µm thick). The orientations of the fascicles are almost longitudinal and parallel to the longitudinal axis of the tendon. Fascicles were heterogeneous in shape and were dissimilar when viewed from the dorsal (A) or palmar (B) aspect and from the upper (C) or lower (D) aspect of the reconstruction. Fascicles have different sizes and shapes, are inter-connected

and are almost parallel to the longitudinal axis of the tendon, (Scale bar= 1000µm). A supplementary video (3.7) is provided in the link below:

PhD thesis- Othman, Ali- Three-dimensional supplementary videos/3.7.wmv

3.3.1.3.2 Three-dimensional reconstructions of nine-years-old mid-metacarpal region

3D reconstruction of the mid-metacarpal region demonstrated that almost all fascicles ran parallel to the longitudinal axis of the tendon. Fascicles in this region are apparently straighter than in the foetal and the other regions. Interestingly, in this region and on the lateral aspect, part of one fascicle extended obliquely in the palmo-dorsal direction and had a free taped end, which did not connect with the rest of the fascicles. In addition one of the lateral fascicles inserted into the epitenon, where appeared as an irregular obliquely oriented structure. Small amounts of isolated IFM were interspersed throughout the body of the fascicles, were not constant on their amount and continuation at different levels of the Z-stack, where some of them extended through the fascicle bodies and subdivided the fascicles into smaller sub units (Figure 3.14 and the associated video 3.8).

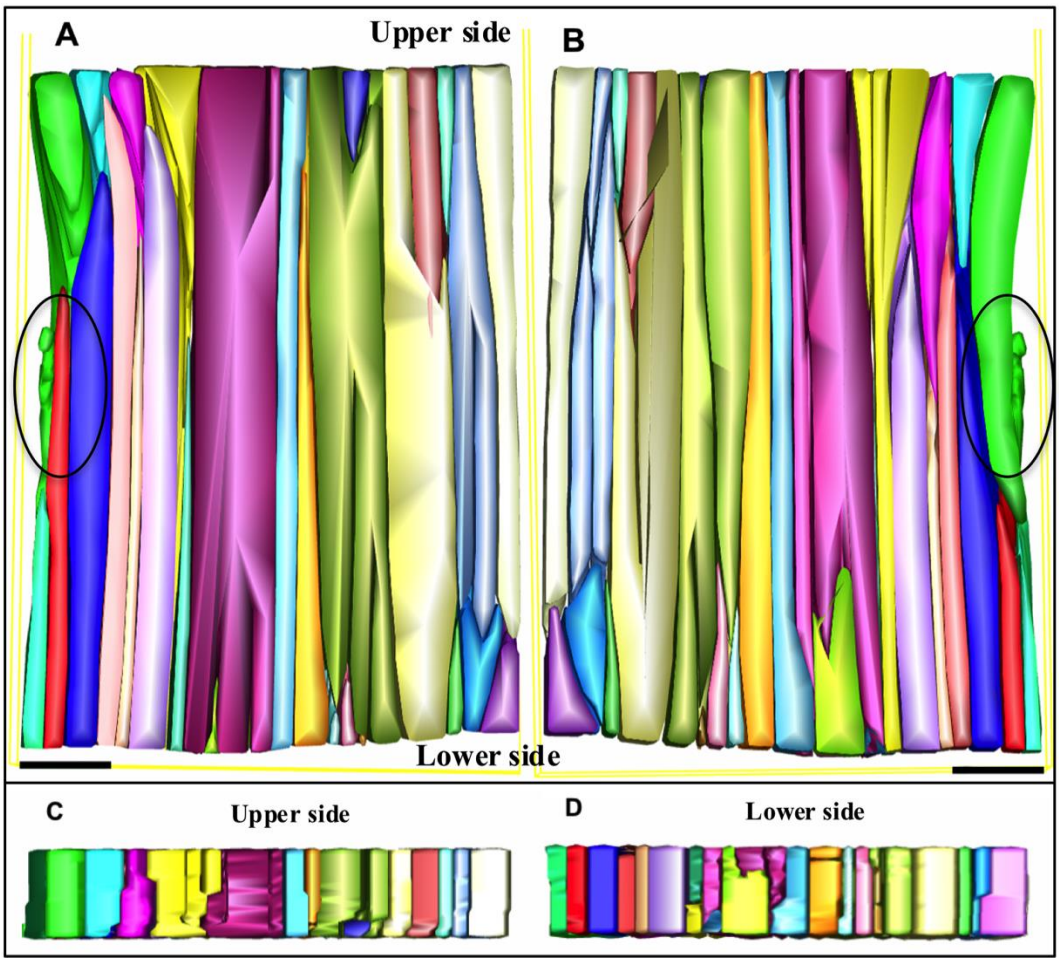

Figure 3.14: Three-dimensional reconstruction of the mid-metacarpal region of a nine-years-old SDFT from a Z-stack of 20 slides (100µm thick). A: The orientations of the fascicles are almost parallel to the longitudinal axis. Fascicles are oriented almost in the upright longitudinal direction and parallel to the longitudinal axis of the tendon. Part of a lateral fascicle obliquely oriented on the palmo-dorsal aspect appeared to insert into the epitenon (circle). Fascicles were heterogeneous in shape and were dissimilar when viewed from the dorsal (A) or palmar (B) aspect and from the upper (C) or lower (D) aspect of the reconstruction, (Scale bar= 1000µm). A supplementary video (3.8) is provided in the link below:

PhD thesis- Othman, Ali- Three-dimensional supplementary videos/3.8.wmv

3.3.1.3.3 Three-dimensional reconstruction of the nine-year-old distal-metacarpal region

In this region the 3D reconstruction demonstrated fascicles ran almost parallel to the longitudinal axis of the tendon. The conformation outlines of the fascicles were not constant on at different levels of the tissue, when going through the Z-stack their

outlines would remain approximately constant or either increased or decreased from dorsal to the palmar aspect. A small isolated intra-fascicular IFM could also be observed in this region. Fascicles tended to converge, diverge and inter-connect with each other. In this reconstruction a large blood vessel was located between fascicles but did not affect their shape (Figure 3.15 and the associated video 3.9).

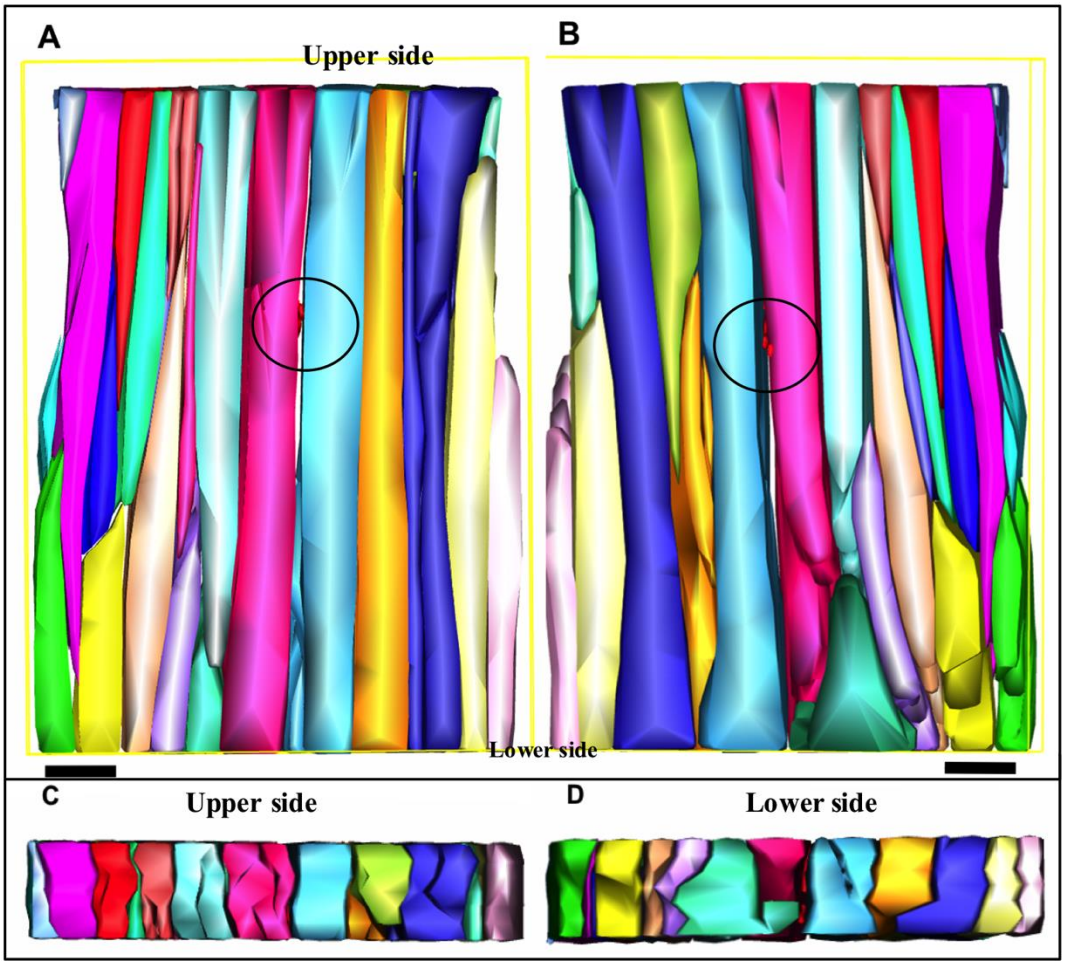

Figure 3.15: Three-dimensional reconstruction of the distal-metacarpal region of a 9-years-old SDFT from a Z-stack of 20 slides (100µm thick). The orientations of the fascicles are almost longitudinal and parallel to the longitudinal axis. Fascicles were heterogeneous in shape and were dissimilar when viewed from the dorsal (A) or palmar (B) aspect and from the upper (C) or lower (D) aspect of the reconstruction. A large obliquely oriented large blood vessel was found between the fascicles (circle), (Scale bar= 1000µm). A supplementary video (3.9) is provided in the link below:

PhD thesis- Othman, Ali- Three-dimensional supplementary videos/3.9.wmv

3.3.1.3.4 Analysis and summary of the three-dimensional structure of nine-years-old SDFT

The longitudinal contour outline lengths of the reconstructed fascicles throughout the Z-stack are shown in Figure 3.16. The longitudinal contour lengths of fascicles were not constant and tended to either decrease or increase from the dorsal to the palmar aspect of the tendon. However, the lengths of a few fascicle contours remained constant either for a short distance or throughout the Z-stack.

In the proximal-metacarpal region, the contour outline lengths were unstable at different levels of the Z-stack. Alteration appeared to be more regular than that of the foetal sample and approximately similar to that of one-year-old. Furthermore two fascicles out of 19 (10.52%) underwent further alteration by completely dividing into two or more than two parts without inter-connection.

The contour configurations in the mid-metacarpal region of the 9-years-old sample were more regular than those in the foetal sample and eight out of 29 fascicles (27.58%) underwent further alteration.

In the distal-metacarpal region, the contour outlines were also irregular. Seven out of twenty contours (35%) underwent further alteration and also had irregular outlines (Figure 3.16). Thus the contour outlines were not regular in all regions and apparently fascicles in both proximal and the distal regions were less regular than those of the mid-metacarpal region. Meanwhile, the number of fascicle underwent further alteration not constant from region to region.

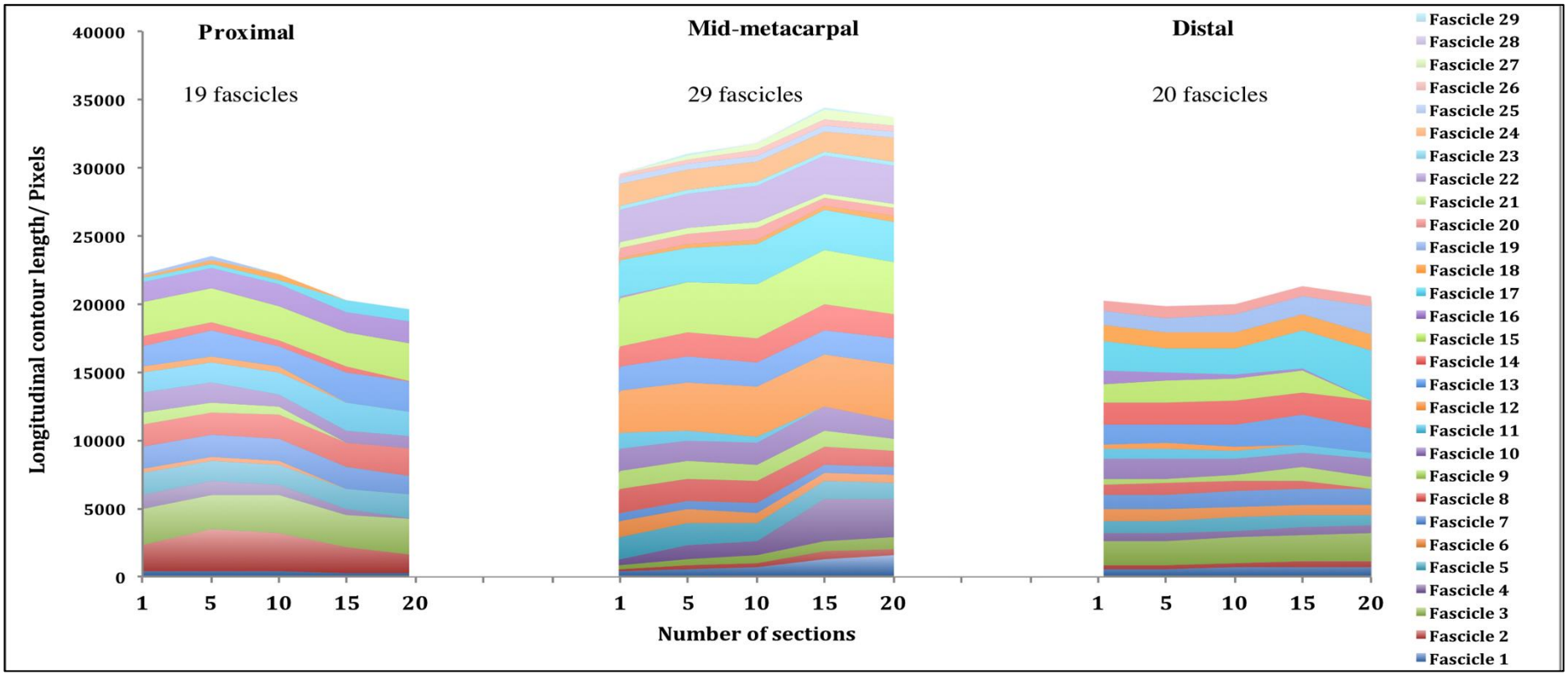

Figure 3.16: Longitudinal contour lengths (pixels) of the outlined fascicles in section numbers 1, 5, 10, 15 and 20 throughout the Z-stack in the proximal, mid-metacarpal and distal regions of a 9-year-old SDFT. Contour lengths were not constant reflecting alterations to fascicle morphology from the dorsal to the palmar side of the Z-stack. Fascicles were altered in all regions and at different level of the Z-stack but they are less regular in the proximal and the distal region.

3.3.1.4 Analysis and summary of the degree convergence, divergence and inter-connection of the fascicles in different regions

The numbers of the reconstructed fascicles were counted in all regions. When their lengths were measured some of them had dual contours measure, under the name of one object (fascicle). Those objects or fascicles that had two measures, which indicated that the fascicles at certain level divided into two smaller fascicles, the division could be in the transverse or longitudinal axis of the fascicles. The summary of this modification was summarised in table 3.1

Table 3.1: Shows summarise number of fascicles were reconstructed in different region with the number of further alteration (Fascicle divided into more than one fascicle in a transverse or longitudinal axis.

	Foetus		**One-year-old**		**Nine-year-old**	
Regions	**Number of fascicles**	**Number of modified fascicle**	**Number of fascicles**	**Number of modified fascicle**	**Number of fascicles**	**Number of modified fascicle**
Proximal	24	8	34	7	19	2
Mid-metacarpal	20	10	20	2	29	8
Distal	14	9	14	4	20	7
Total	**58**	**27**	**68**	**13**	**68**	**17**

Moreover the number of divergence, convergence and inter-connection were also measured through the 1st, 5th, 10th, 15th and 20th sections. The summary of the results shown in table 3.2, it was found that in all regions there were approximately a similar number of divergence, convergence and inter-connection between the fascicles. The average number of these fascicular modification show that a large number of fascicles inter-connected with each other (Table 3.2, Figure 3.17).

Table 3.2: The average number of the fascicular divergence, convergence and inter-connection counted in the 1st, 5th, 10th, 15th and 20th sections, with their standard deviation in the foetal, one-year-old and 9-years-old horses.

	Proximal region			Mid-metacarpal region			Distal region		
	Converge	Diverge	Inter-connection	Converge	Diverge	Inter-connection	Converge	Diverge	Inter-connection
Foetus	**4.6** ±0.89	**6.2** ±1.64	**7.6** ±1.14	**4.6** ±1.51	**5.4** ±1.14	**9.8** ±2.16	**6.8** ±2.04	**5.2** ±0.83	**13.2** ±2.58
One year-old	**3.4** ±1.14	**8** ±1.22	**11.6** ±1.14	**3.6** ±0.54	**5** ±1	**6.2** ±1.64	**3.2** ±0.83	**3.6** ±0.54	**10.2** ±1.64
Nine year-old	**4** ±1.22	**5.8** ±1.3	**7.8** ±0.83	**4.8** ±0.44	**5.8** ±0.44	**7.8** ±1.64	**3** ±1.22	**5.2** ±1.48	**8** ± 1.41

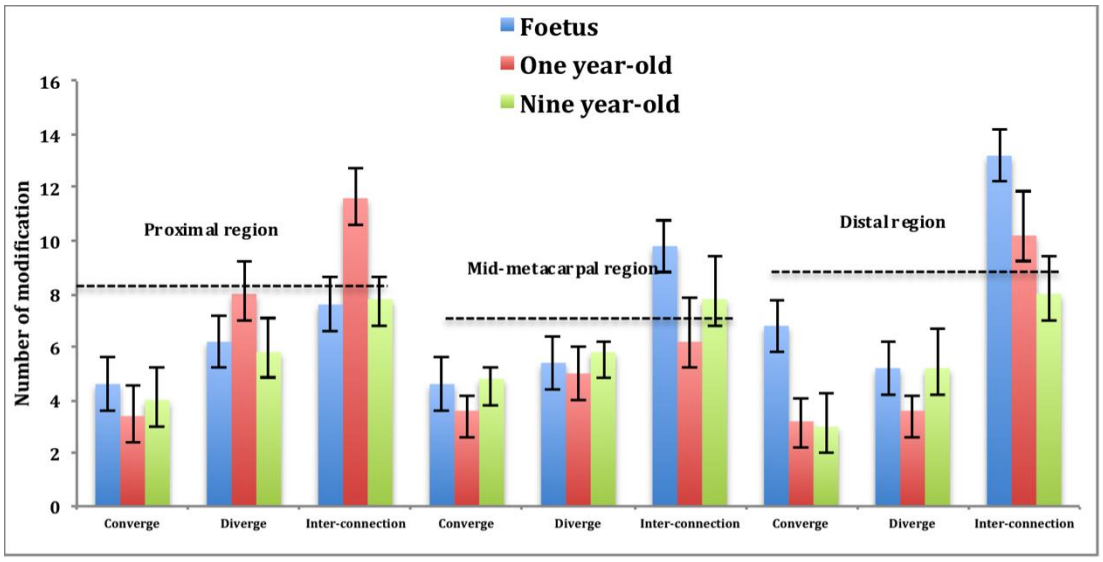

Figure 3.17: The average number of the divergence, convergence and inter-connection of fascicles through the histological Z-stack in the proximal, mid-metacarpal and the distal region of foetal, one-year-old and 9-years-old horses. Note the larger number of fascicular inter-connection occurs in all regions (Scale bar= standard deviation).

3.3.2 THREE-DIMENSIONAL RECONSTRUCTION OF DEEPER LAYERS OF ONE-YEAR-OLD SDFT

3.3.2.1 Three-dimensional reconstruction of a Z-stack of 65 sections of one-year-old SDFT

To explore the pattern of the fascicles more accurately in the dorso-palmar plane, the mid-metacarpal region was sectioned in the frontal plane into 65 longitudinal sections (325µm total thickness). Most fascicles ran throughout the entire reconstruction (approximately 1cm in length) although a few fascicles terminated with a new fascicle starting again nearby. New fascicles interpolated between existing fascicles. Fascicles at the periphery of the tendon tended to be moulded to the shape of the tendon as defined by the epitenon. There were no gaps between the tendon fascicles and the epitenon. A bundle of oblique fibres were observed inside the epitenon, arranged obliquely from the lateral aspect toward the mid-point of the tendon surface (Figure 3.18). Near the mid-point of the palmar surface a large blood vessel was observed to infiltrate the tendon to a depth of 130µm, around which the fascicle formed a semi-circular arc (Figure 3.19 and the associated video 3.10).

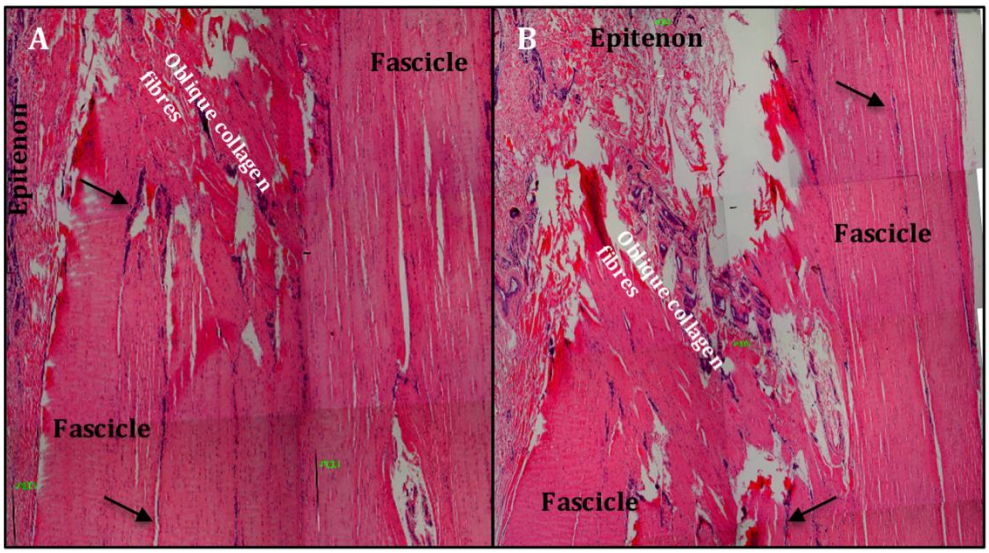

Figure 3.18: Histological appearance of one-year-old SDFT displaying alteration through the Z-stack adjacent to the epitenon, where a number of fascicle separated by IFM (arrows) progressively reduced in size. A; slide number 52 that shows the presence of an obliquely oriented collagen fibres between the epitenon and the fascicles. B; Slide 65 shows the continuation of the obliquely oriented collagen fibres.

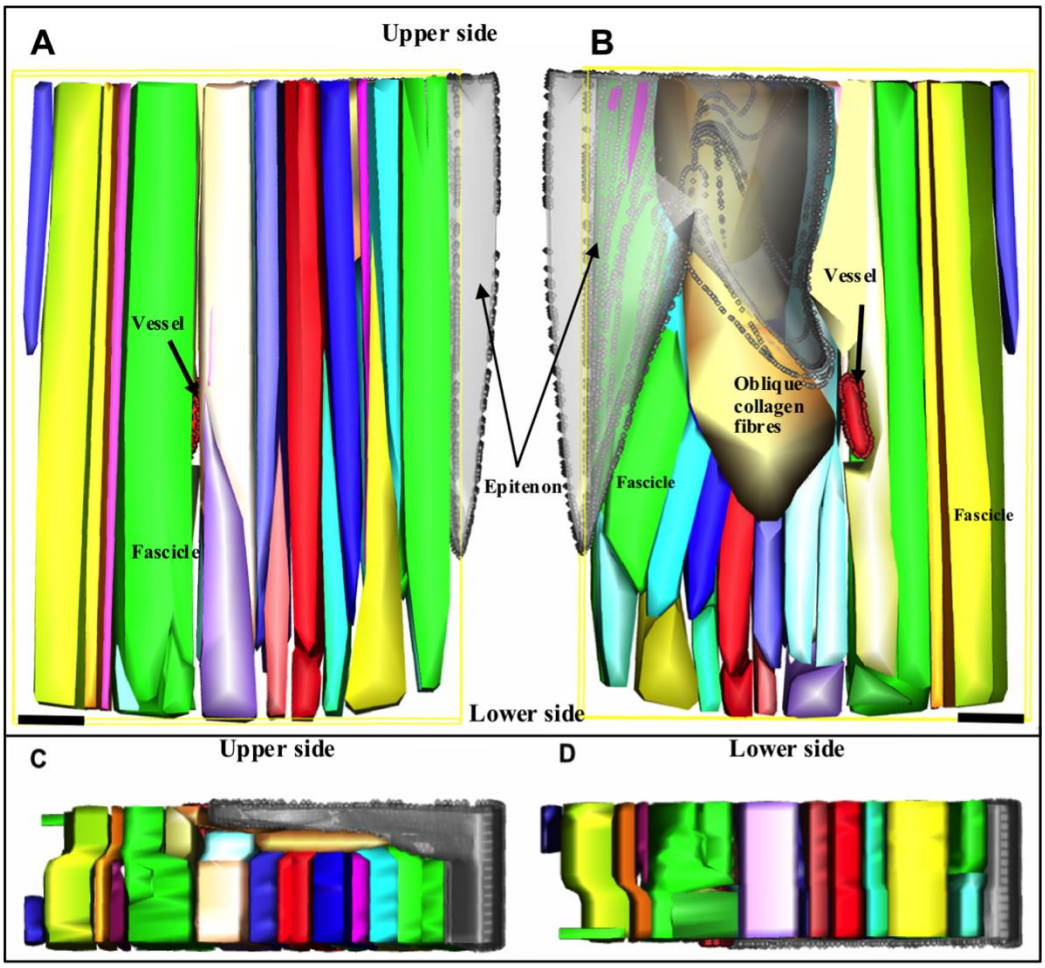

Figure 3.19: Three-dimensional reconstruction of the mid-metacarpal region of one-year-old SDFT from a 65 section Z-stack (325µm thick), sectioned on the dorso-palmer (A-B) aspect. Fascicles were heterogeneous in shape and were dissimilar when viewed from the dorsal (A) or palmar (B) aspect and from the upper (C) or lower (D) aspect of the reconstruction. Adjacent to the epitenon, fascicles were deviated toward the central apex of the tendon. Within the epitenon an oblique bunch of fibres was overlaid on the palmar surface of the fascicles. From the palmar aspect a large blood vessel was seen to pass through the body of the fascicle into the core of the tendon (arrow), (Scale bar= 1000µm). A supplementary video (3.10) is provided in the link below:

PhD thesis- Othman, Ali- Three-dimensional supplementary videos/3.10.wmv

3.3.2.1.1 Analysis and summary of the three-dimensional reconstruction from 65 sections of the one-year-old SDFT

When the mid-metacarpal region was sectioned deeply (65 sections) toward the epitenon of the palmar aspect and reconstructed it was found that most fascicles

continued toward the palmar aspect. Continuous fascicles decreased in their size and tended to deviate toward the central apex of the tendon. The contour lengths of all fascicles throughout the mid-metacarpal region varied from the dorsal to the palmar aspect of the tendon. Fascicles outline lengths altered at different levels and at some points fascicles disappeared and a new one started. Not all fascicles continued throughout the whole Z-stack, as some terminated with a new fascicle starting in the adjacent region, reflecting the depth of the reconstruction that encompassed whole fasicles in cross-section. Some fascicles were also observed to undergo joining, splitting or other inter-connections with adjacent fascicles. The graph shows that the fascicule contours size declined progressively toward the epitenon and eleven fascicles out of 26 fascicles (40%) did not continued through the whole Z-stack thickness. In addition four fascicles underwent further alteration (15.38%), either converging or diverging into smaller fascicles. Thus not all fascicles continued through the whole thickness of the tendon but were inter-connected with other fascicles at different levels of the tendon (Figure 3.20).

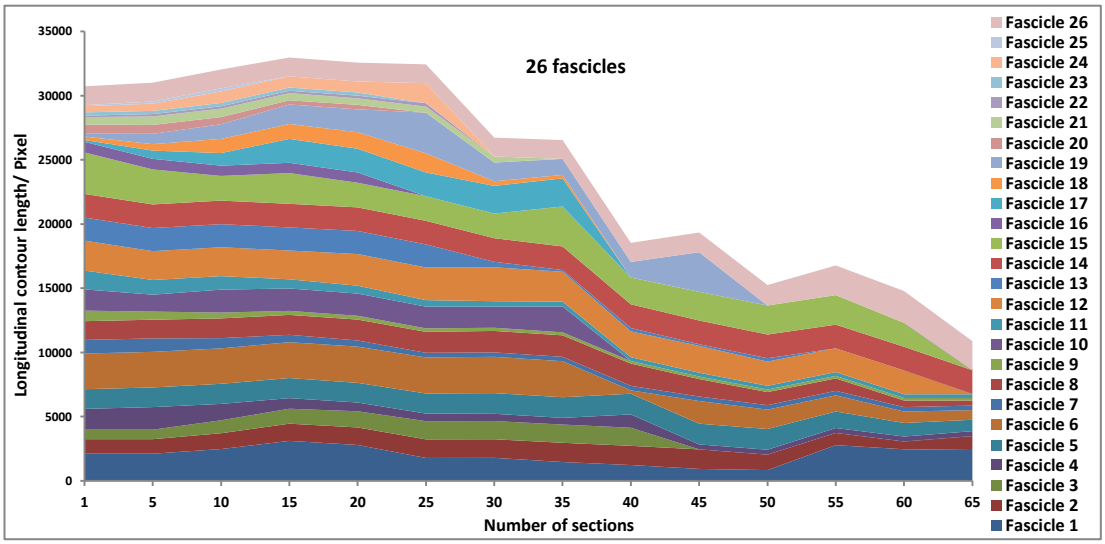

Figure 3.20: Longitudinal contour lengths (pixels) of the outlined fascicles in a Z-stack of 65 sections from the dorsal to the palmar aspect in mid-metacarpal region of one-year-old SDFT. Contour lengths were not constant reflecting alterations of fascicle morphology from the dorsal to the palmar side of the Z-stack. Fascicles had different contour outlines, their sizes progressively decreased toward the epitenon and a few of them underwent further alteration.

3.3.2.2 Three-dimensional-reconstruction of the whole thickness through the mid-metacarpal region of one-year-old

The entire thickness of the mid-metacarpal region (approximately 1cm long) was completely sectioned. Sections were selected in a way that the odd numbers were collected while the even numbers ignored, i.e. each section represents a move through 10µm of tissue. This was possible because adjacent 5µm serial sections were found to be very similar. Therefore 500 sections were cut but 250 sections collected, imaged and processed for 3D reconstruction. The 3D reconstruction highlights various forms of the fascicles and how they are interrelated with each other within a 0.25cm depth and 1cm length of tissue.

All fascicles ran parallel to the longitudinal axis of the tendon and most of them were present throughout the whole reconstruction. However, a few small fascicles were observed interspersed between larger fascicles. These smaller fascicles had proximal and distal ends but were laterally connected to the larger adjacent fascicles. Fascicle shape was heterogeneous and fascicles were inter-connected throughout the tendon length. Occasionally fibres transferred from one fascicle to the next. No fascicles were present as isolated cylindrical structures as all fascicles were connected in some way to other fascicles. Interestingly, the fascicles appeared to be arranged in a slight twisted conformation (Figure 3.21 and the associated videos 3.11, 3.12). From this 3D reconstruction, apparently not all fascicle were continued through the Z-stack (tendon body thickness), those that continued through the Z-stack were displayed inconsistency at different levels of the tendon. Moreover, longitudinal fascicles had straight or a twisted configuration on their longitudinal axis of themselves and the tendon. When fascicles were viewed from upper level down to the distal aspect they were apparently twisted in a lateral-medial direction of the tendon longitudinal axis (clockwise) (Figure 3.21, video 3.12).

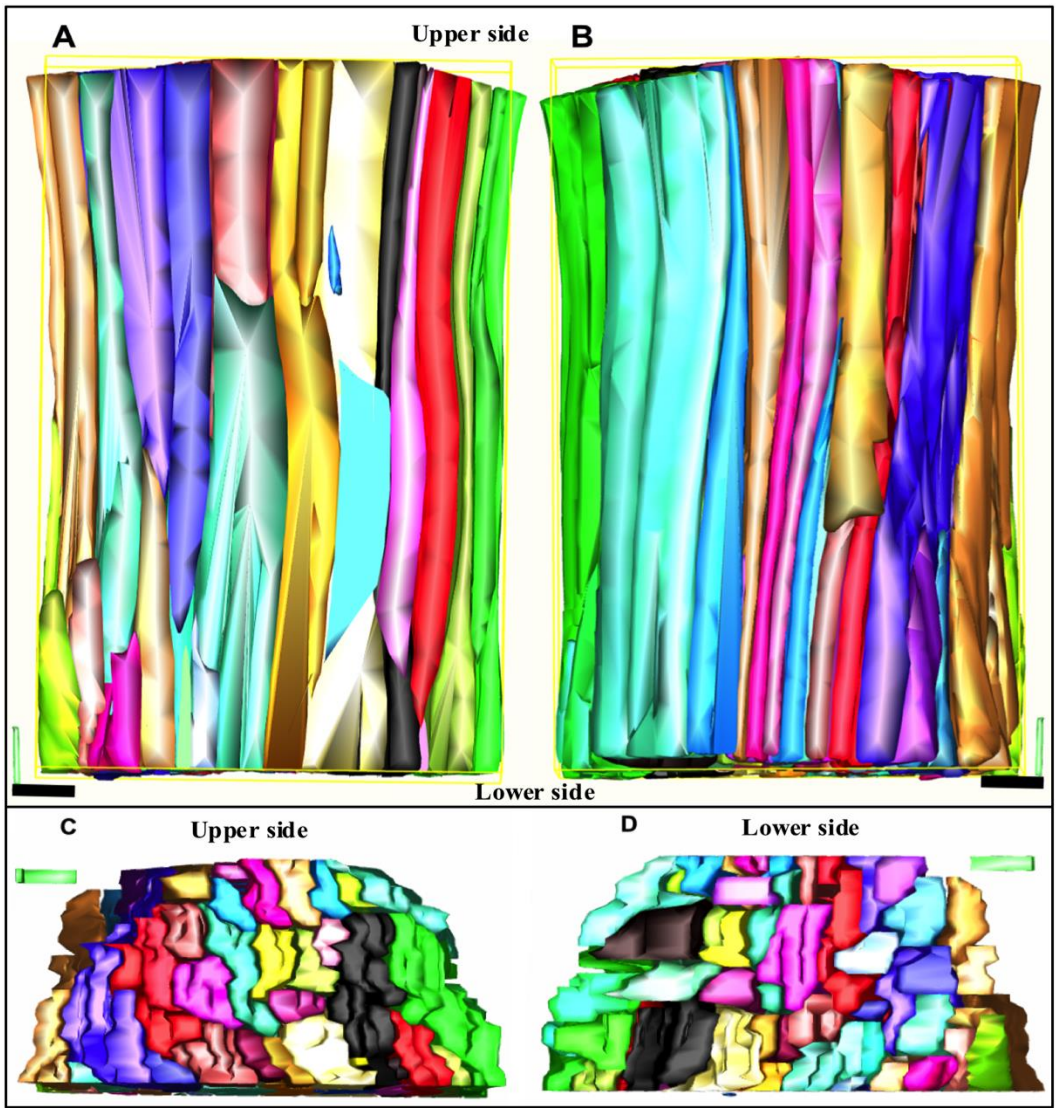

Figure 3.21: Three-dimensional reconstruction of the whole mid-metacarpal thickness of one-year-old from 500 slides Z-stack. The tendon was sectioned on the dorso-palmer (A-B) aspect. The reconstruction covered approximately 2,500µm depth (250 sections were selected by choosing number of odd sections and ignoring the even sections (250 sections). This 3D reconstruction demonstrates that all fascicles within the mid-metacarpal region (1 cm long) were oriented longitudinal and parallel to the longitudinal axis of the tendon. Fascicles were heterogeneous in shape and were dissimilar when viewed from the dorsal (A) or palmar (B) aspect and from the upper (C) or lower (D) aspect of the reconstruction. Fascicles were diverged, converged and inter-connected with each other and had twisted configuration on their longitudinal axis, (Scale bar= 1000µm. A supplementary video (3.11 and 3.12) is provided in the links below:

PhD thesis- Othman, Ali- Three-dimensional supplementary videos/3.11.wmv

PhD thesis- Othman, Ali- Three-dimensional supplementary videos/3.12.wmv

3.3.2.2.1 Analysis and summary of the three-dimensional structure of the whole mid-metacarpal thickness (500 sections) of one-year-old SDFT

The contour lengths of all fascicles were not stable throughout the mid-metacarpal thickness. Fascicles outline lengths altered at different levels and could either increase or decrease. At some points fascicles disappeared and new fascicles started. Fascicles were seen to undergo joining, splitting or inter-connection with adjacent fascicles. The graph demonstrate that the dorsal aspect of the tendon contains a number of fascicles which are altered in number and sizes towards the core of the tendon. The core or mid portion of the tendon contains a larger number of fascicles. When appraching the palmar aspect of the tendon the fascicles substantially decreased both in number and size. Fasicles regressed progressively and became thinner until they joined the epitenon (Figure 3.22). In this 3D reconstruction all fascicle underwent continous alteration and fascicles did not show a constant shape throughout the Z-stack. As previously fascicles were found to split, converged or inter-connected with each other.

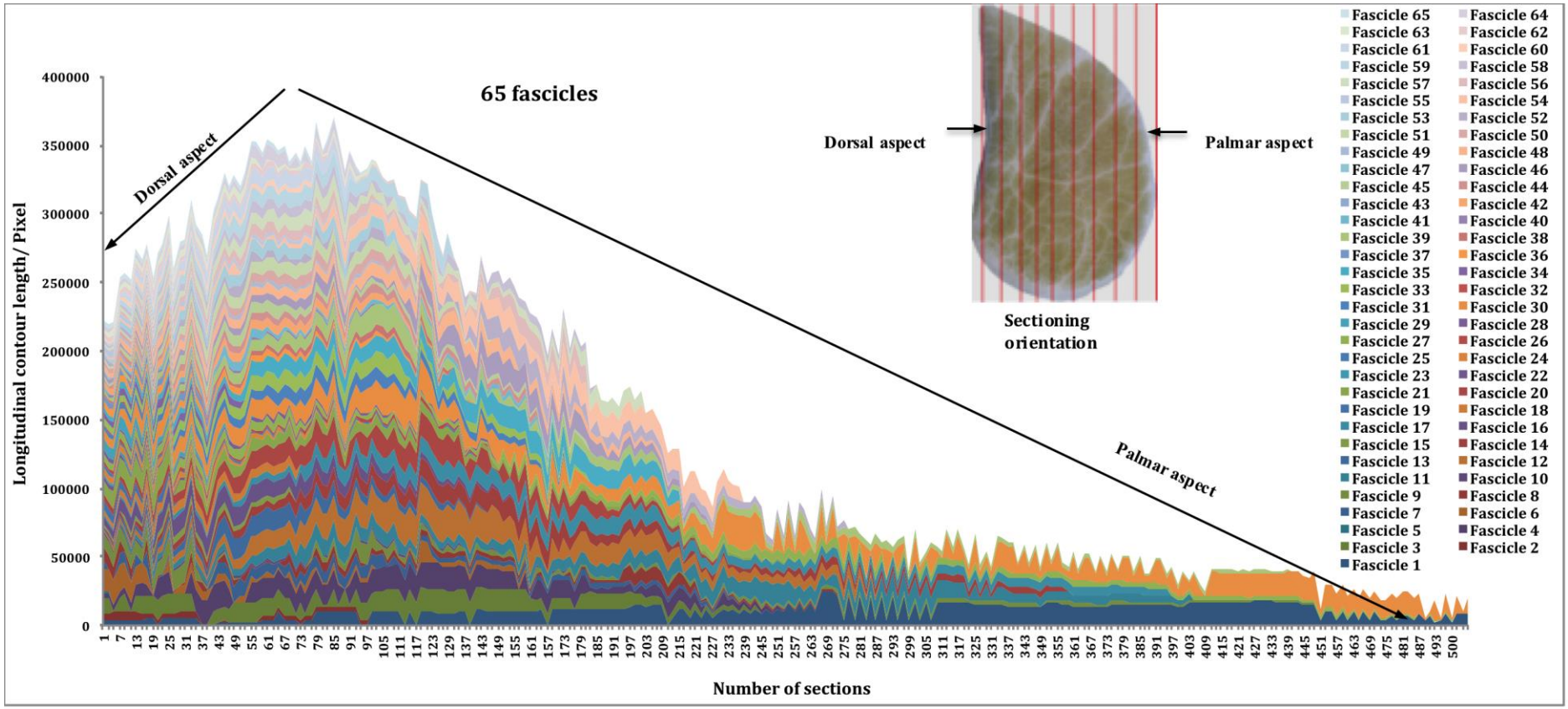

Figure 3.22: Longitudinal contour lengths (pixels) of the outlined fascicles in a Z-stack throughout the whole mid-metacarpal thickness of 500 sections (2500μm thickness) of one-year-old. Fascicles were not constant and were progressively altered on their continuation throughout the Z-stack in both the vertical and horizontal directions. The number and size of the fascicles first increased and then progressively declined toward the palmar aspect of the tendon. Not all fascicles continued through the Z-stack and at different levels they diverged, converged and inter-connected with each other.

3.3.3 GENERAL PROPERTIES OF THE FASCICLE

Fascicles are thought to be the basic mechanobiological units of the tendon and act to transmit forces from muscle to the bone through the longitudinal axis of the tendon. Fascicles were arranged parallel to each other in the longitudinal direction and were outlined by IFM. Fascicular size was not constant in either the horizontal or vertical direction but many fascicles were continuous through the length of the reconstruction. However, a few small fascicles were interspersed between the larger fascicles and were characterised by their heterogeneous size, smaller diameter and shorter length, generally continuing for a few millimetres (approximately 1-3mm) within the reconstruction (Figure 3.21, video 3.11).

Larger fascicles were heterogeneous and their shapes varied through the length of the reconstruction, while some longitudinal fascicles extended throughout the Z-stack with only minor modifications. Fascicles were observed to both diverge and converge. In certain areas part of the diverged fascicle was displaced on its longitudinal axis and inter-digitated with other adjacent fascicles (Figure 3.23).

Fascicle ends ranged from V-shaped tapered ends to flat or an irregular forms that inter-digitated with other fascicle ends. Certain fascicles diverged and continued to run longitudinally while joining with neighbouring fascicles. Occasionally collagen fibres crossed between adjacent fascicles creating points of inter-connection. Other fascicles inter-connected at points where the IFM ceased allowing the fascicles to converge together. The number of inter-connection points varied across the tissue and larger fascicles showed more points of inter-connection than the smaller ones (Figure 3.23).

A twisted conformation of the fascicles was observed within this 3D reconstruction (clockwise). Few fascicles when ran on their longitudinal axis became diverged and then one of the branches were progressively displaced on their axis and merged with the other neighboured fascicles. These properties make the fascicles to have different configuration of their continuation and oblique inter-connection with the adjacent fascicles (Figure 3.21 and the associated video 3.12).

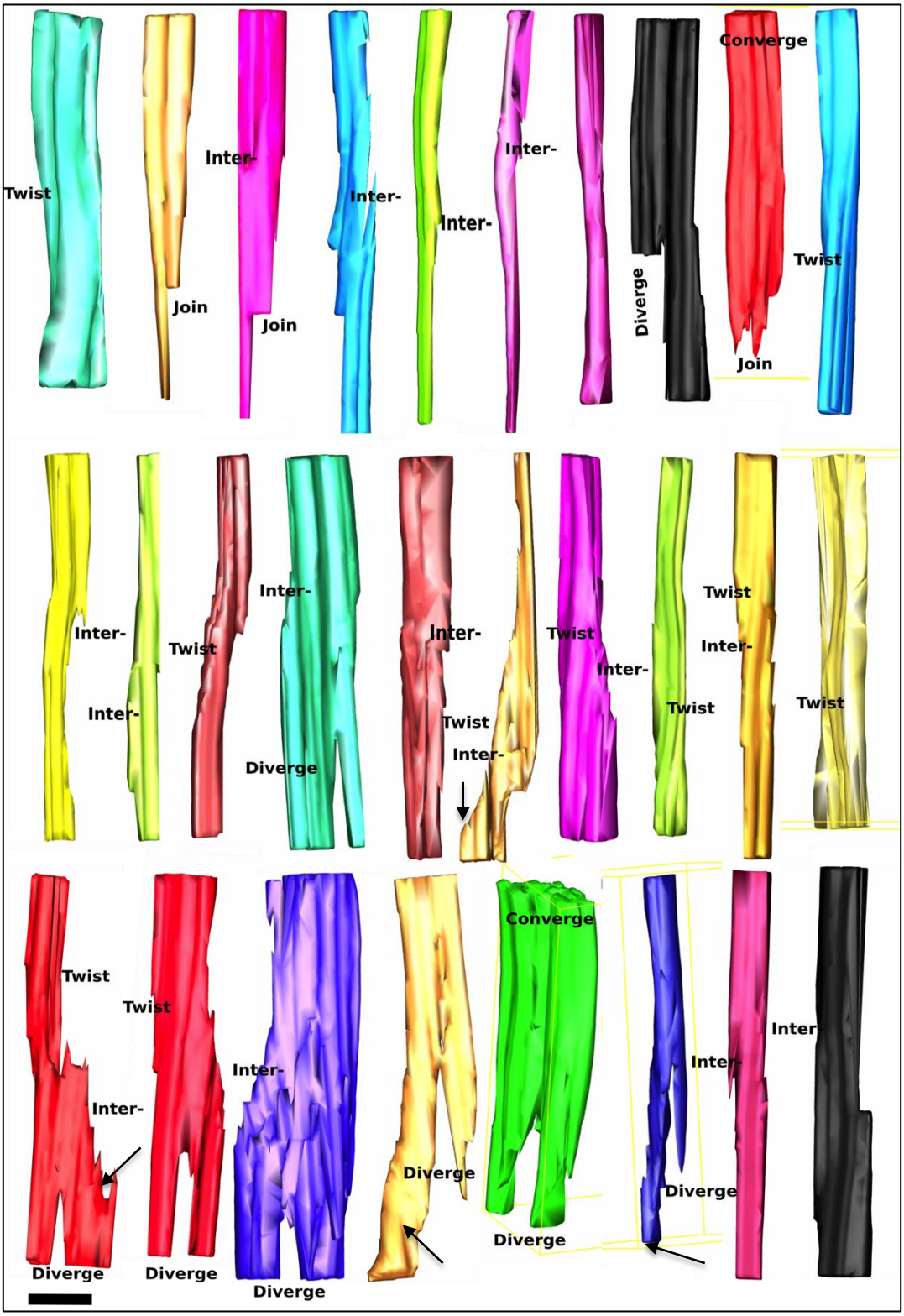

Figure 3.23: Fascicular alterations in various individual fascicles from the 3D reconstruction of the whole mid-metacarpal thickness of one-year-old SDFT. Fascicles run longitudinally through the mid-metacarpal region. These fascicles are arranged from simple straight fascicles to fascicles with a more complex shape (deviated or displaced (arrows) and twisted on their longitudinal axis) and joined to each other at their ends, (Inter= inter-connection), (Scale bar= 1000μm).

These configurations of the fascicle could be simplified into the following pattern as shown in (Figure 3.24). Fascicles could course straight down through the body of the tendon (A) or it becomes part of a larger fascicle (B). Fascicles could be are inter-connected either by merging parts of their bodies together for a short distance or passing fibrils between them (C). Interestingly, fascicles could converge from two or more smaller units to form a wider fascicle (D) or conversely diverge into two or more branches (E). Most fascicles were twisted (F) and occasionally displaced and out of their longitudinal axis.

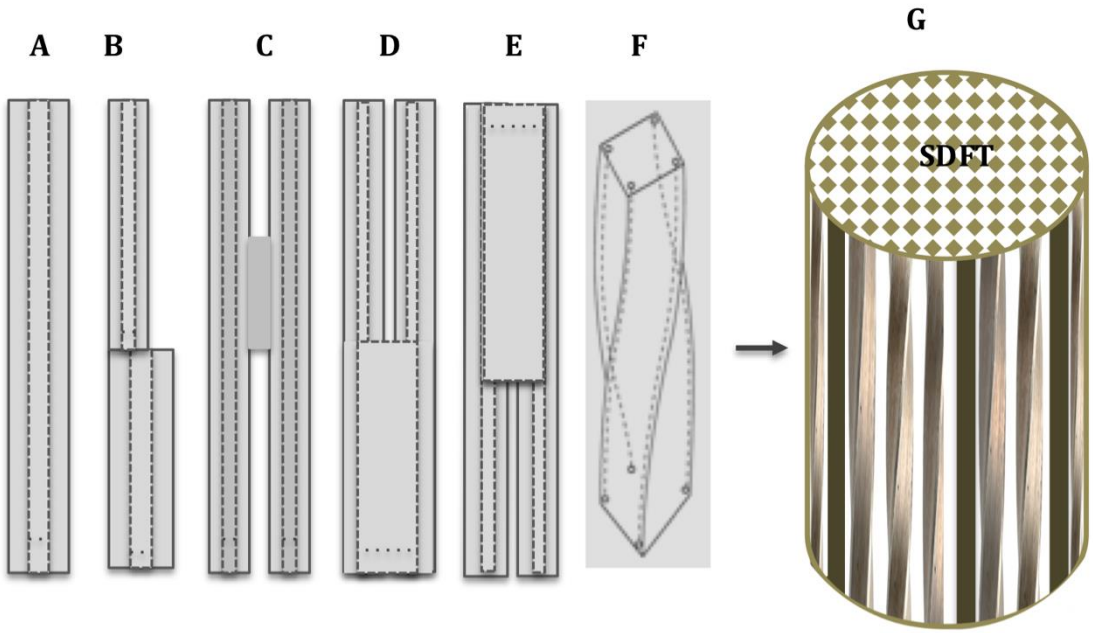

Figure 3.24: Schematic illustration of various outlined fascicles. Fascicles demonstrated different shapes and sizes and when oriented through the tendon, they were straight (A), displayed end to end joining (b), inter-connection (C), converged (D), diverged (E) and/or twisted (F) on their longitudinal axis, that were ran longitudinally through the body of the tendon (G).

3.3.4 HISTOLOGICAL OBSERVATIONS

Images are shown (Figure 3.25) of the histological appearance of fascicular discontinuities, inter-connections, fascicle ends, convergence and divergence as well

as the presence of blood vessels. Images are shown from approximately the first and last slide in order to view the considerable difference between the dorsal and palmar aspect of the tendon.

1- Fascicular discontinuities: This was indicated by the presence of a transverse partial or complete break (discontinuation) in the body of the fascicles. These discontinuation breaks contained different amount of IFM. The sizes of these breaks either increased or decreased through the body of the fascicle when running through the Z-stack. When the breaks make the fascicles to be separated into two portions, here the fascicles underwent further alteration concomitantly the amount of the IFM were also altered with alteration of such discontinuation. (Figure 3.25 A-D).

2- Inter-connection between the fascicles: inter-connections between fascicles were observed as areas of longitudinal tissue continuity maintained where the section had otherwise split between the fascicles or the lack of continuous IFM between adjacent fascicles. (Figure 3.25 B and D, circles).

3- Starting of a new fascicle: a new fascicle started as a small point either on the lateral or the middle part of the tendon and progressively increased in size through the sections. New small fascicles could be in the periphery or central core were progressively increased in size from the first to the last section of the Z-stack (Figure 3.25 E and F).

4- Divergence of the fascicle: IFM divided larger fascicles into smaller fascicles. Smaller fascicles could subsequently further diverge, join or inter-connect to adjacent fascicles (Figure 3.25 G).

5- Convergence of the fascicles: a few fascicles were seen to join to form a larger fascicle. For these fascicles the IFM became thin and then disappeared, such that fascicles joined together to form a larger fascicle (Figure 3.25 H).

6- Blood vessel: blood vessels were usually located within the IFM and in regions where the IFM decreased or disappeared the blood vessels also disappeared. However, (Figure 3.25 I) demonstrates penetration of the superficial aspect of the tendon by a large blood vessel accompanied by a small amount of IFM, which is then

found in the body of the fascicle (130µm depth) forming a tunnel-like passage within it.

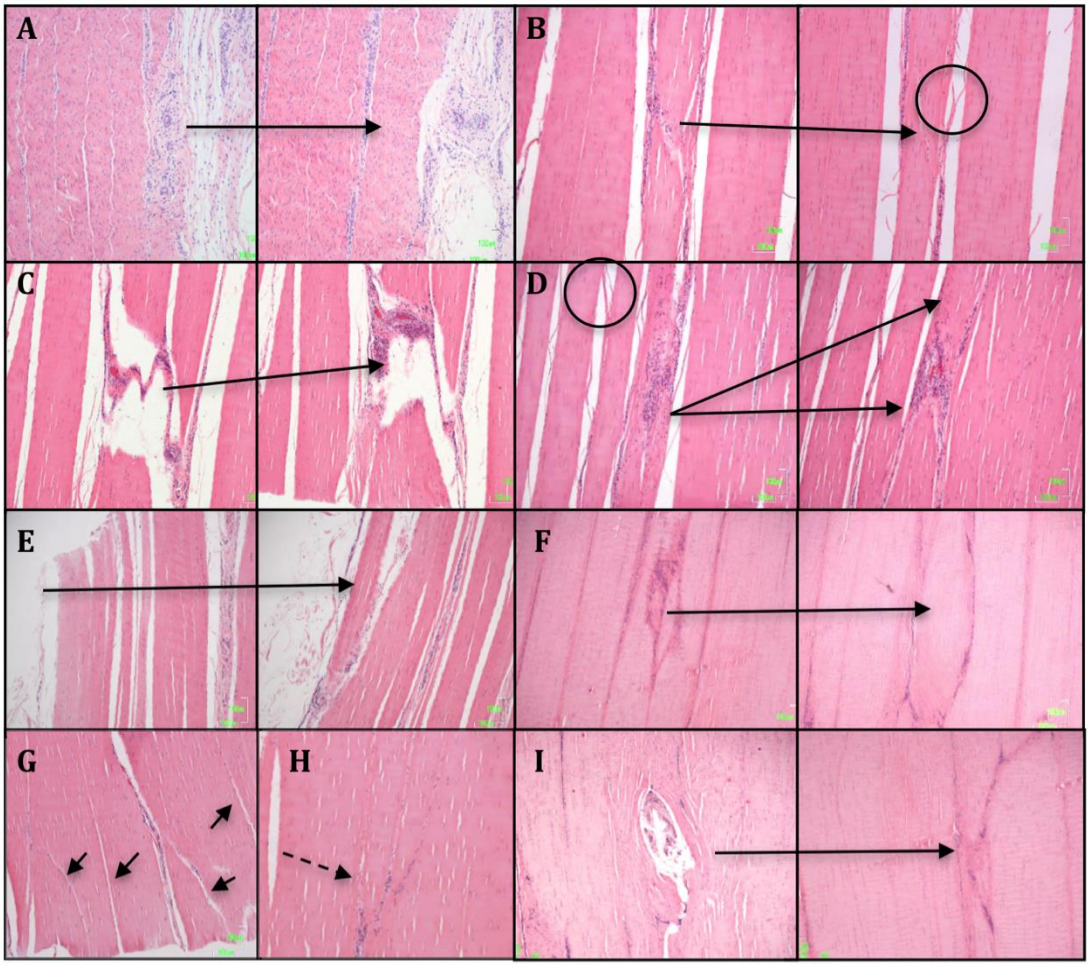

Figure 3.25: Histological appearance of fascicular alterations. Panels A-K include both dorsal (left) and palmar (right) views from different SDFT. A: IFM is replaced by two fascicles that subsequently joined (arrow) in foetal tendon. B: The discontinuation small break and the IFM content tend to decrease in size (arrow), presence of inter-connection (circle) between the fascicles, SDFT from one-year-old horse. C and D: Breaks or discontinuation through the body of the fascicle occupied by IFM progressively increased and were filled by increased amounts of IFM and blood vessels (arrows). Points of inter-connection are indicated (circle). E: Appearance of a new small fascicle on the lateral aspect of the tendon from a one-year-old horse. F: Appearance of a new small fascicle on the central core of the tendon from a one-year-old. G: Divergence of fascicles (arrows) indicates that the IFMs subdivide fascicles. H: Convergence of fascicles (dashed arrow) with joining of IFMs into one line. I: Large blood vessel entering into the tendon through made a tunnel like opening in the body of the fascicle.

3.4 DISCUSSION

3.4.1 THREE-DIMENSIONAL RECONSTRUCTION OF SDFT FASCICLES IN DIFFERENT REGION

Following sectioning on the dorso-palmar aspect the SDFT was found to comprise a number of different sized fascicles. These fascicles were outlined by the IFM (Meghoufel et al., 2010). Fascicles and IFM are enclosed by the epitenon (Kastelic et al., 1978, Yahia and Drouin, 1989, Meghoufel et al., 2010, Meghoufel et al., 2011). Fascicles were found to run longitudinally and parallel to the longitudinal axis of the tendon. In an anatomical study of the human Achilles tendon it was shown that fascicles are heterogeneous and continued through the length of the entire tendon (Szaro et al., 2009). In this study, a similar heterogeneous organisation of SDFT fascicles was found, which were continued longitudinally through each regions.

Fascicles are composed of collagen fibres and are considered the basic mechanical units of the tendon, transferring forces in a uniaxial direction from muscle to bone (Parry and Craig, 1984, Magnusson et al., 2003b). Fascicles have been categorised according to their sizes, to give primary fibril bundles, secondary and tertiary fascicles. Groups of parallel collagen fibrils form a fibre and fibre bundles are then termed fascicles (Kastelic et al., 1978, O'Brien, 1997, Kannus, 2000, Franchi et al., 2007b). The anatomical arrangement of these fascicles throughout the SDFT is still not understandable in term of the hierarchical composition and how long they extend throughout the SDFT (Screen, 2009). This study attempted to accurately outline the fascicles for 3D reconstruction. When these fascicles were reconstructed and viewed from all aspects, we found that fascicles were not completely separated from each other and were connected at several points by collagen fibres. Inter-connections between fascicles have been recorded by other researchers during dissection of rat tail tendon when they passed a cover slip between fascicles and then visualised them using photo-microscopy. It was found that fascicles were did not completely detach from each other and fibrils were observed crossing between fascicles (Kastelic et al., 1978). Together with our findings this indicates that SDFT fascicles cannot be completely separated from one another.

In a study using polarized light microscopy with human tendon, it was found that not all fibres run parallel with each other and for this reason they classified fibre crossing-points into four types; 1) simple crossing of two fibres on their longitudinal axis, 2) crossing of a couple of fibres and one central straight one, 3) plate formation by three differently oriented fibres and finally 4) a fibre wrapped around straight fibres (Józsa et al., 1984, Kannus, 2000). Should these fibre-crossings be present between fascicles in the SDFT they would account for the observed inter-connections between fascicles. The ratio of the longitudinally to transversely and horizontal oriented fibres was previously recorded as 10:1 and 26:1 respectively (Jozsa et al., 1991). These records support the present study and indicate that the transversely oriented fibres inter-connect the longitudinally oriented fibres between the fascicles.

This chapter has described how the morphology of the SDFT fascicles is not constant and is altered when coursing through the tendon. However a few fascicles continued constantly and not modified their shapes for a short distance (few mm), then started to adapt themselves with the surrounding fascicles, where modified their shapes in order to adjust with the surrounding fascicles. As shown in figure (3.23 and 3.24) fascicles were of different shapes, dimensions and almost all of them inter-connected to some extent with adjacent fascicles. Moreover, evidence of converging, diverging and inter-connection of the fascicles was found. Interestingly, fascicles showed a twisted configuration when running from the proximal to the distal aspect of the 3D reconstruction. Similarly, in different studies they suggested various models of fascicular orientation in human patellar and rat-tail and bovine Achilles tendons. These models of both crimped and un-crimped collagen fibrils described how fibrils were aligned and ran parallel with the longitudinal axis of the fascicles or were helically arranged on their longitudinal axis or around the longitudinal axis of the fascicles (Grytz and Meschke, 2009, Shearer, 2015b, Shearer, 2015a). In a 3D reconstruction of a series of tendon section from chick tendon using electron microscopy, has been demonstrated that a collagen bundles bundle rotate approximately 180° on its longitudinal axis over a distance of 10µm -12µm (Birk et al., 1989). In an anatomical study human extensor carpi ulnaris, using plane polarized microscopy, micro CT and 3D reconstruction of the collagen bundles at the level of the carpal joint, it has been shown that fascicles in this region have a clockwise spiral configuration in the right side of the tendon in an average angle of

8° (Kalson et al., 2012). In another mechanical study of equine SDFT, it has shown that the presence of intra-fascicular helical sub-structures provides an efficient mechanism in energy storage tendon (Thorpe et al., 2013b, Thorpe et al., 2015d). In the present a twisted configuration through the body of the SDFT fascicles appeared to be a dual spiral continuation of both individual fascicles (i.e. presumably containing helical fibrils) as well as in their orientation in relation to one another (Figure 3.23). This 3D reconstruction was carried out using tissue from the mid-metacarpal region of the right SDFT. Individual fascicles ranged from straight or slightly twisted to fascicles with a distinct twisted on their longitudinal axis as shown in the video number 3.12 (Figure 3.21). In human Achilles tendon it was shown that fibres were parallel in the proximal region but rotated distally (Szaro et al., 2009), therefore our 3D reconstruction could have captured an intermediate level of fibre and fascicle twisting on their longitudinal axis. When fascicles were viewed from upper level down to the distal level (Figure 3.21, video 3.12), they were apparently twisted from the lateral toward the medial aspect of the tendon (clockwise). This fascicular configuration supports the energy-storing role of the tendon and it has been recorded that the SDFT has a greater recovery and less hysteresis than the CDET (Thorpe et al., 2013b). However in rat's tail and bovine flexor tendon fascicles a spiral configuration has also been observed and is thought to play a role in a large experimentally observed increased in the Poisons ratio which represent a ratio of a transverse strain contraction to a longitudinal extension force in the direction of stretching forces (de Campos Vidal, 2003, Reese and Weiss, 2013). Recently, different staining protocols have been used in order to reach a good contrast to discriminate fascicle from each other, such contrast like using sodium tungstate, phosphotungstic acid and potassium iodine solution. Different results have been shown but still are not possible to detect individual fascicles in the ligaments and tendons (Shearer et al., 2014, Balint et al., 2016).

3.4.2 MECHANICAL NOTION OF THE FASCICLES

The main function of the tendon is to transform force from the muscle to the bone and this action is thought to take place through the tendon subunits (fascicles). Additionally the IFM is plays an important role in equine SDFT mechanobiology and facilitates tendon extensibility (Thorpe et al., 2012). In a study of human Patellar and

Achilles tendons using a stereo microscope it was found that that force transmission mainly took place within individual fascicles and not the IFM (Haraldsson et al., 2008). In this study we found that fascicles have a wide variety of sizes and shapes, which could have implications for force transmission in tendon. Furthermore observations on fascicle splitting, divergence and inter-connections would indicate that force transmission from one end of the tendon to the other is not carried out by multiple parallel fascicles acting in tandem, as might previously have been supposed. At the collagen fibril level it has been shown that in mature tendon, collagen fibrils are relatively long and parallel whilst in foetal tendon fibrils are shorter and discontinuous (Birk et al., 1996, Birk et al., 1997, Vanderby Jr and Provenzano, 2003). Further they described that in regions collagen fibrils can be disorganised and non-axially oriented with interweaving, branching and converging features and concluded that the force within the tendon is directly transferred through collagen fibrils and not through an inter-fibrillar conjunction, such as a proteoglycan bridge (Provenzano and Vanderby, 2006). Therefore collagen fibrils within tendon fascicles could be the primary force-transmitters within tendon. However, discontinuities between fascicles were observed both histologically and in the 3D reconstructions, such that short fascicles were present in between larger inter-connected fascicles (Figures 3.25 A-D). Fascicular discontinuation has also been observed in a chick embryo tendon in a study of 3D reconstruction of different collagen bundles on a transverse serial sections at the electron microscopic scale (Birk et al., 1989). Partial or complete fascicular discontinuities or isolated small fascicles might be expected to might affect the mechanical strength of the individual fascicles (Taylor et al., 1990). Fascicles in the foetal tendon were strongly crimped and clearly outlined by the IFM, due to the presence of a more abundant IFM than in the older samples. These histological features have been previously documented in the ovine foetal calcaneal tendon (Russo et al., 2015). The observation of fascicular to inter-connection, convergence or divergence in these 3D reconstructions would suggest that fascicles are not isolated units.

It was noted (Figure 3.25 I) that a blood vessel penetrated the body of a fascicle rather than coursing primarily through the IFM. Blood vessels usually distributed through the endotendon are thought to arise from three different origins of

myotendinous, mesotenon and osteotendinous junctions (Smith, 1965, Ochiai et al., 1979) but the origin of this blood vessel is unknown.

2.5 CONCLUSION

Following 3D reconstruction it can be concluded that SDFT fascicles are altered morphologically at different points and regions. They are heterogeneous regionally, diverged, converged and inter-connected with each other as the fascicles progresses distally. 3D reconstruction of the whole mid-metacarpal thickness indicated that fascicles had heterogeneous shapes and were twisted on their longitudinal axis. Understanding the 3D structure of tendon fascicles could facilitate understanding of tendon structure-function relationships and predisposition to injury.

2.6 RECOMMENDATION AND FUTURE WORK

Different histological stains could be used to investigate important structures such as elastic fibres of the equine SDFT. It is also important to compare this method with the other techniques such as micro-computed tomography (micro CT) scanning and then evaluate the degree of agreement between them. Analysis of other equine tendons such as the DDFT and CDET as well as human tendons such as the Achilles and Patellar tendons could be used to confirm if the observation of an inter-connected fascicular network is specific to the equine SDFT or is the case across species and tendon types.

2.7 LIMITATIONS

Image stacks (mrc files) reached up to 11 GB and could not be readily manipulated on a standard desktop or laptop computer. Due to the time-intensive and painstaking nature of 3D reconstruction it was only possible to reconstruct one sample (in three different regions) for each of the three SDFTs. Furthermore, the depth of the 3D reconstruction was limited, except for one large 3D reconstruction encompassing half of the tendon cross-section. The histological image quality and 3D reconstruction software used were not amenable to automated quantification of fascicular architecture such as inter-connections between fascicles, fascicular divergence and convergence.

CHAPTER FOUR

HISTOLOGICAL DESCRIPTION AND SCORING OF THE EQUINE SUPERFICIAL DIGITAL FLEXOR TENDON DURING AGEING

4.1 INTRODUCTION

Normal tendon architecture is composed of dense regularly organised longitudinal collagen fibres, connecting muscle to bone. Collagen fibres run parallel to the longitudinal axis of the tendon (Kastelic et al., 1978, Kannus, 2000, O'Brien, 2005). They are corrugated (crimped) along their longitudinal axis to an extent that varies regionally and with age (Gathercole and Keller, 1991, Franchi et al., 2007a). Studies in different tendons including SDFT have found that the longitudinally oriented collagen fibres angulate and pass over each other and form a spiral configuration (Yahia and Drouin, 1989, Vidal, 2003, Kalson et al., 2012, Thorpe et al., 2013b). However, one study has also described a tendon organisation with collagen fibres not arranged parallel to the longitudinal axis of the tendon, but being arranged horizontally between two adjacent fascicles (Jozsa et al., 1991).

The fascicular matrix is mainly composed of collagen fibrils (60-85% of the dry weight). From this dry weight, 60% are type I collagen and the remainder are type II, III, IV, V and VI collagen fibres. In addition a small amount of elastic fibres (1-2%) are scattered between the collagen fibres and the inter-fascicular matrix (IFM) or endotenon (Kannus, 2000, Hayem, 2001). Collagen fibres and fascicles are outlined and kept separated from each other by the IFM. The IFM consists of an irregular loose fibrous connective tissue network containing various structures, such as blood and lymphatic vessels, nerve fibres, cells and both collagenous and non-collagenous extracellular matrix, such as proteoglycans (PGs) and glycosaminoglycans (GAGs) (Benjamin et al., 2008). Different types of PGs and GAGs have been described throughout the tendon. These include small leucine-rich PGs (SLRP) such as decorin, biglycan, fibromodulin, lumican, keratocan and decorin, while large or modular PG which are versican and aggrecan (Vogel and Trotter, 1987, Vogel et al., 1994, Yoon and Halper, 2005, Yang et al., 2012, Thorpe et al., 2016a).

Tendon is less cellular than many tissues, with cells (tenocytes) distributed both within (intra-fascicular) and between (inter-fascicular) the fascicles (Jozsa and Kannus, 1997, O'Brien, 2005). The intra-fascicular tenocytes are distributed regularly in a uniaxial direction between the collagen fibres and their morphology varies between round, elliptical and cigarette-shaped to a longitudinal fusiform shape. The majority of cells in the IFM are characterised by having an irregular

shape and pattern (Kannus, 2000, Clegg et al., 2007, de Mos, 2009). Together these cells form approximately 90-95% of the cellular element of the tendon, which forms up to 1% of equine SDFT tissue matrices. The other 5-10% are chondrocyte-like cells, present in the compressed regions such as the region passing over the metacarpophalangeal joint and at the bony enthesis (O'Brien, 1997, Kannus, 2000, Benjamin et al., 2008). Recently it has been shown that the molecular profile of cells undergoes profound periodical alteration from foetal to the adult in the sheep calcaneal tendon (Russo et al., 2015). Similarly in other animals such as horses, mice and rabbits it was demonstrated that the cellular morphometry undergoes age-related alteration, which could subsequently affect tissue homeostasis (ECM deposition and turnover) (Floridi et al., 1981, Batson et al., 2003, Legerlotz et al., 2014).

The aim of this study was to describe the histological structures of equine SDFT and to document how they vary regionally and during ageing. For this purpose a new scoring method was developed to score the histological components of the tendon regionally and at different stages of life in addition to their histological description, however there is not enough information on the regional differences (Lin et al., 2005a, Feitosa et al., 2006). It was hypothesised that;

1- ECM organisation of the equine SDFT differs regionally and during ageing.

2-The IFM between the tertiary and the secondary fascicles alters regionally and during ageing.

3-The intra-fascicular nuclear morphometry alters regionally and during ageing.

4-SDFT is well vascularised and this vascularity is altered either regionally or during ageing.

5-No inflammatory cells should be present in the normal tendon.

4.2 MATERIALS AND METHODS

4.2.1 SAMPLE COLLECTION

SDFT samples were collected from forelimb of Thoroughbred and Thoroughbred cross horses of different ages, killed for non-orthopaedic reasons. They were obtained either from a commercial abattoir (Potters, Taunton or Wootton Bassett) or from horses euthanased at the University of Liverpool Equine Hospital with the owners' informed consent. The study was assessed and approved by the University of Liverpool Veterinary School Research Ethics Committee (VREC, study 214).

4.2.2 SAMPLE PREPARTION

Samples were taken from three different regions (proximal, mid- and distal metacarpal). The proximal region represents SDFT level at the carpometacarpal joint while the mid- region was exactly at the mid-metacarpal level and the distal region was directly on the upper transverse line of the metacarpo-phalangeal joint. From each region a sample approximately 1cm in length was selected from the central area of the tendon. All the samples were oriented in a similar direction, across the middle the tendon including both the anterior and posterior boundary (epitenon) (Figure 4.1). The specimens were fixed in 4% phosphate-buffered formaldehyde solution, pH 7.4 at room temperature.

SDFT samples were dehydrated overnight through a graded concentration of ethanol (70%, 85%, 96% and 100%) and 24 hours later were embedded in paraffin wax on their longitudinal axis. The tissue blocks were then cut into 5-μm-thick sections, collected on polylysine slides and stained with Haematoxylin & Eosin (H&E), (Section 4.2.5.1)

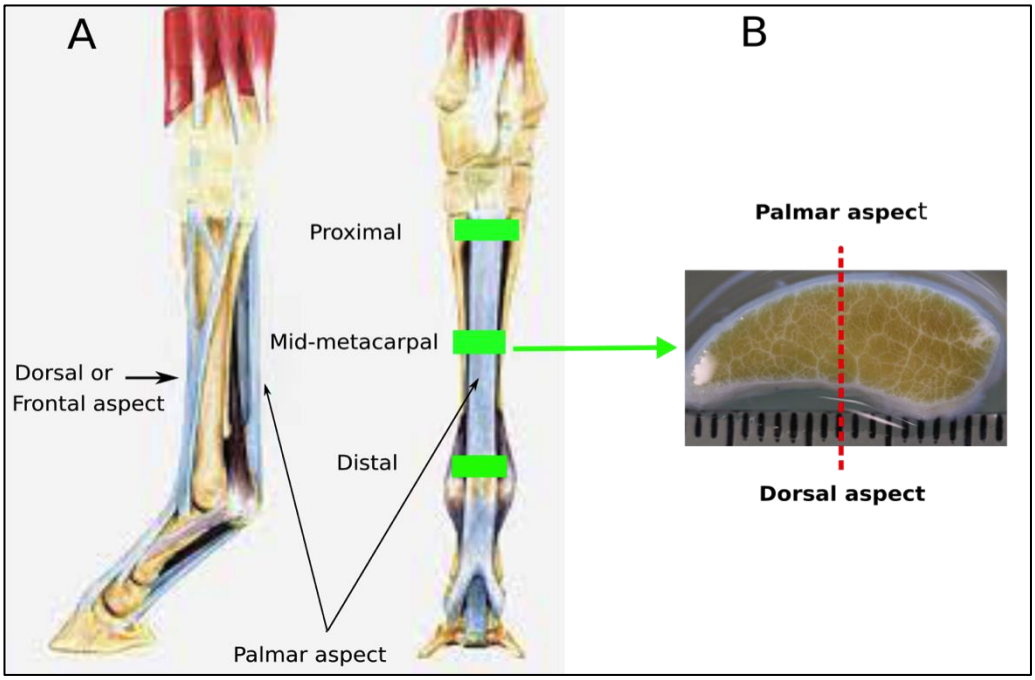

Figure 4.1: A: Normal anatomy of the SDFT from (Ferraro et al., 2009), indicating points of specimen collection from the proximal, mid-metacarpal and distal regions (green). B: SDFT transverse section at the mid-metacarpal region, divided centrally into two halves (red line). The longitudinal cut surface was placed facing towards the microtome knife in order to take a longitudinal section through the widest part of the tendon.

4.2.3 SAMPLE GROUPING

SDFT samples ranged from foetal age to 20-years-old and were arranged into six groups (Table 4.1). This grouping included different stages of development and maturation in order to study the tendon conformation from early life and determine its organisation through life. The horse becomes skeletally mature from approximately two years of age, and whilst in many disciplines horses may not commence fast work until 4-5 years of age, some racing disciplines such as flat racing focus on young (2-3 years-old) horses. The selection of this grouping aimed to document the histological alteration of equine SDFT at intervals of 3-4 years in order encompass all stages of life from foetal to 20-years-old. The rest of other SDFT samples were used for histological description and different ages were selected from foetal to 20 years old.

Table 4.1: Number of SDFT samples from different ages used for general histological description and scoring methods that were grouped according to their regions and ages (P= Proximal, M=Mid-metacarpal, D=Distal, Rt=Right and Lf=Left).

AGE/ YEAR	NUMBER	REGIONS			SIDE	PAIRED LIMB	GROUPS
Foetus	2	P	M	D	Rt	-	Foetus (5-6 month gestation)
1	1	P	M	D	Rt		-
3	3	P	M	D	Rt	-	Group one/ (Very young horses, skeletally immature)
5	1	P	M	D	Both	1 paired	-
7	3	P	M	D	Both	1 paired	Group two (young, skeletally mature horses)
9	5	P	M	D	Rt	-	Group three (mature horses with a complete developed skeleton)
14	4	P	M	D	Lt	-	Group four (mature horses with advanced in ageing)
17	1	P	M	D	Both	1 Paired	Group five (aged horses)
18	2	P	M	D	Both	1 paired	
19	1	P	M	D	Rt	-	
20	1	P	M	D	Rt	-	

The Group were organised into foetal (n=2), Group one (3-years-old, n=3), Group two (7-years-old, n=3), Group three (9-years-old, n=5), Group four (14-years-old, n=4) and Group five (17-20-years-old, n=5),

4.2.4 HISTOLOGICAL SCORING DATA ACQUISITION

To date, histological examination of the tendon architecture of equine SDFT particularly during ageing has not been fully described. Scoring criteria have been established to evaluate histological values of normal and abnormal tendons in human

and equine, based only on visual observation by 2-3 dependent inter-observers (Maffulli et al., 2008, Sodersten et al., 2013). In this study, a new scoring method was developed using ImageJ (Schneider et al., 2012) to evaluate SDFT ultra-structures regionally and during ageing. This new scoring method was based on the following criteria:

1. Normal collagen fibre architecture can be compact, wavy and arranged parallel to the longitudinal axis of the tendon.

2. The crimp pattern is a definitive wavy feature of the collagen fibres and the degree of corrugation varies regionally and with age (Patterson-Kane et al., 1997a, Franchi et al., 2007a).

3. The IFM is an irregular loose fibrous connective tissue running longitudinally and parallel to the collagen bundles. It outlines the individual fascicles and contains vessels, nerves and ECM.

4. Vascularity is demonstrated by the presence of different sizes and numbers of blood vessels that are scattered through the IFM.

5. Tenocytes are normally distributed between the collagen fibres in a uniaxial direction. They range from a round or oval to spindle shape.

6. No inflammatory or necrotic cells are present inside the tendon architecture unless they become injured or inflamed.

An example of the scoring sheet is below (Table 4.2):

Table 4.2: Histological scoring sheet of H&E stained equine SDFT

H&E SCORING METHOD

	Regions		
1- Extracellular Matrix (ECM) organisation Angulation of collagen bundles or fascicles: using ImageJ to measure the degree of fascicular angulation in the proximal, mid-metacarpal and distal regions.	**P**	**M**	**D**
2- Inter-fascicular matrix (IFM) organisation			
A- Angulation: using ImageJ to measure the degree of IFM angulation as with ECM.	**P**	**M**	**D**
B- IFM thickness: using ImageJ to measure the IFM width of the secondary and tertiary fascicles.	**P**	**M**	**D**
3-Cell			
A- Cellular density: Counting number of nuclei lying between the collagen fibres of the fascicles in 10 fields (400X) or (40X objective, 10 X eyepiece), excluding the IFM.	**P**	**M**	**D**
B- Nucleus length: using ImageJ to measure length of the counted nucleus in (A), 450 cells (150 nuclei in each region).	**P**	**M**	**D**
4- Vascularity Counting number of the blood vessels in 10 fields (100X) or (10X objective, 10 X eyepiece), through the IFM.	**P**	**M**	**D**
5- Inflammatory cells or necrosis Recording the presence of any inflammatory or necrotic tissue	**P**	**M**	**D**

(P= proximal, M= Mid-metacarpal and D= Distal)

4.2.4.1 ECM organisation (Angulation of the collagen bundles or fascicles)

To measure the degree of fascicular angulation, the entire SDFT section on the slide was captured under a magnification power of 40X using a Nikon Eclipse 80i

microscope. Using Inkscape (www.inkscape.org), all captured photos were collated and transformed into one image (Figure 4.2). Following this, the collated image was loaded into ImageJ (Schneider et al., 2012) and the fascicular orientations were adjusted to their longitudinal axis. Two longitudinal lines were dragged over the image; the first line was drawn directly over the longitudinal central axis and parallel to the straightest fascicles in the middle of the tendon. The second line was drawn on a transverse level of the lower third of the sections perpendicular to the first line. The second line was used as a guide for measuring the degree of fascicular angulation (Figure 4.2).

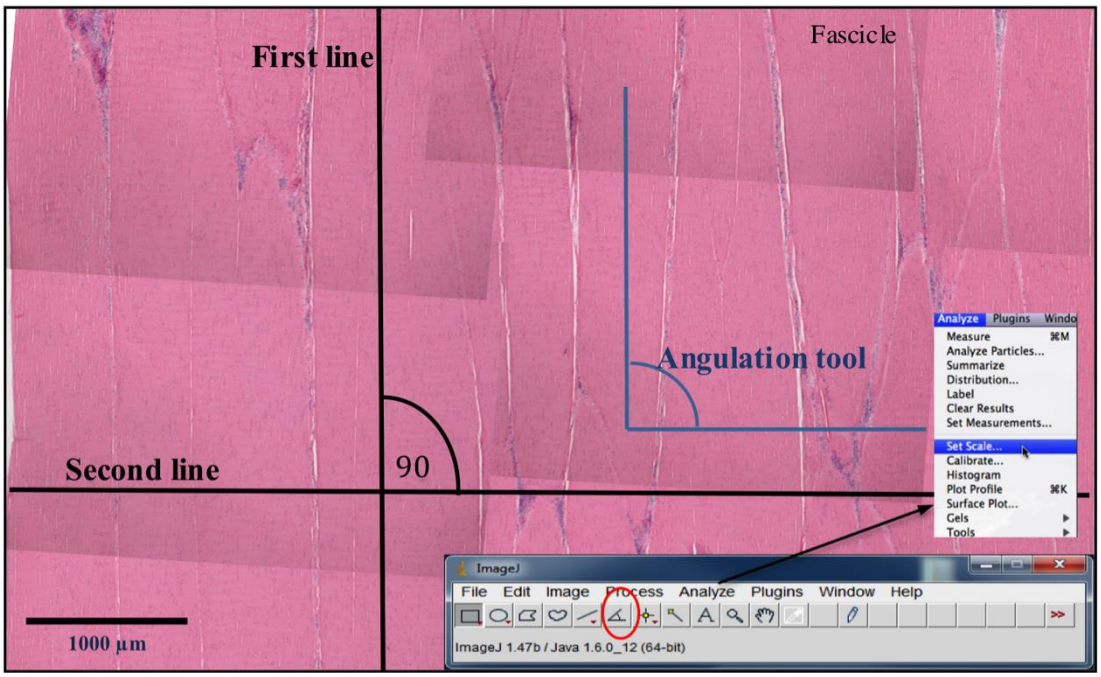

Figure 4.2: Measuring the degree of fascicular angulation individually using ImageJ angulation tool. The two longitudinal lines (first and second lines) are used as the index guides to measure the degree of fascicular angulation. The angle tool (red circle) was then used to measure the degree of fascicular angulation by aligning the horizontal line of the angulation tool parallel to the horizontal guideline (second line) and the vertical line of the angulation tool parallel to the longitudinal axis of each fascicle.

The angulation tool of the ImageJ toolbar (Figure 4.2, red circle) was used to measure the degree of fascicular angulation by aligning the horizontal line of the angle tool parallel to the horizontal guideline and the vertical line parallel to the

longitudinal axis of the fascicle that was extended for up to 3mm. Then the degree of the fascicular angulation was measured individually (Figure 4.2, angulation tool). Finally, from the Analyze tool on ImageJ the measurement option was selected to record the degree of fascicular angulation.

4.2.4.2 IFM organisation

4.2.4.2.1 Angulation of the IFM

The IFM accompanies the fascicles but it is less regular than the fascicles (Figure 4.3). Measurement of the IFM alignment was performed only for a vertically oriented IFM that ran almost parallel to the longitudinal axis of the tendon. To measure the degree of IFM angulation, a modified method of measuring the fascicular angulation was used. The vertical line of the angulation tool was drawn through the longitudinal axis of the IFM instead of the fascicles. The vertical line of the angulation tool was also dragged up to 3 mm length in order to obtain a higher distance of the IFM diversity (Figure 4.3).

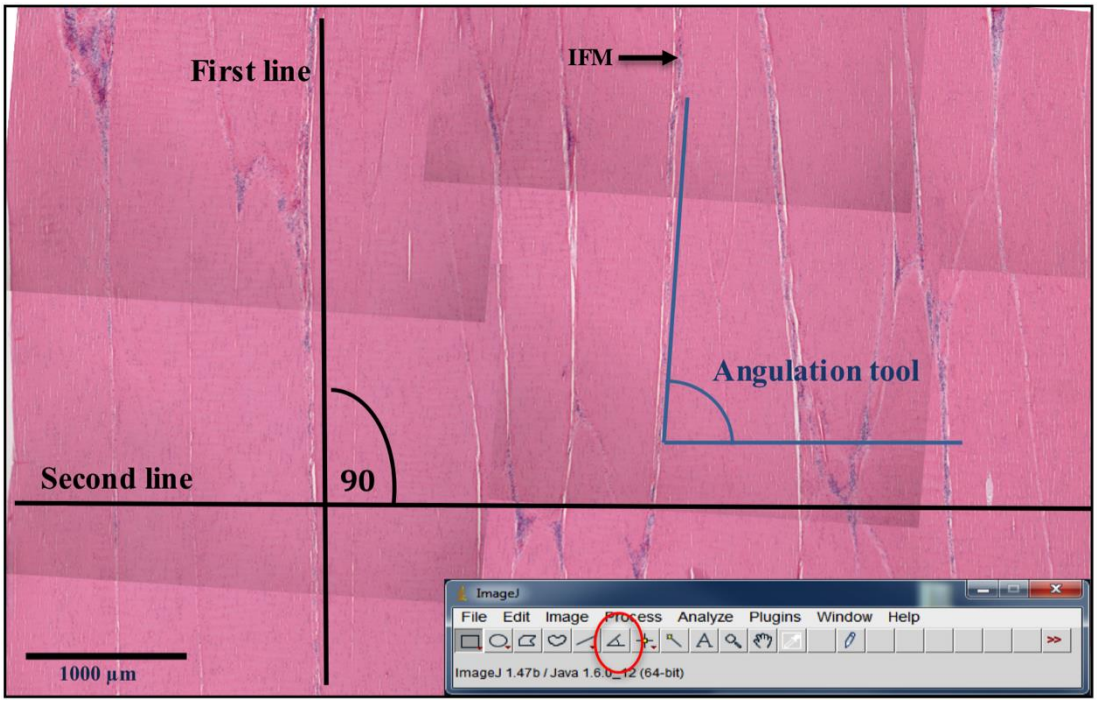

Figure 4.3: Measuring the degree of IFM angulation individually using ImageJ. The two longitudinal (first and second) lines are used as the index guides to measure the degree of IFM angulation. The horizontal line of the angulation tool must be parallel to the horizontal index line (second line) but the vertical line is parallel to the longitudinal axis of the IFM.

4.2.4.2.2 IFM thickness

The entire section surface of the equine SDFT being examined was captured under a magnification power of 40X using a Nikon Eclipse 80i microscope. The IFM thickness was divided into two categories: the IFM thickness between the large (tertiary) fascicles and between the small (secondary) fascicles (Figure 4.4, arrows). For each category, sixty points throughout the IFM were measured at intervals of approximately 200-300µm. ImageJ was used to measure the IFM thickness after setting the scale measurement as described in the next section.

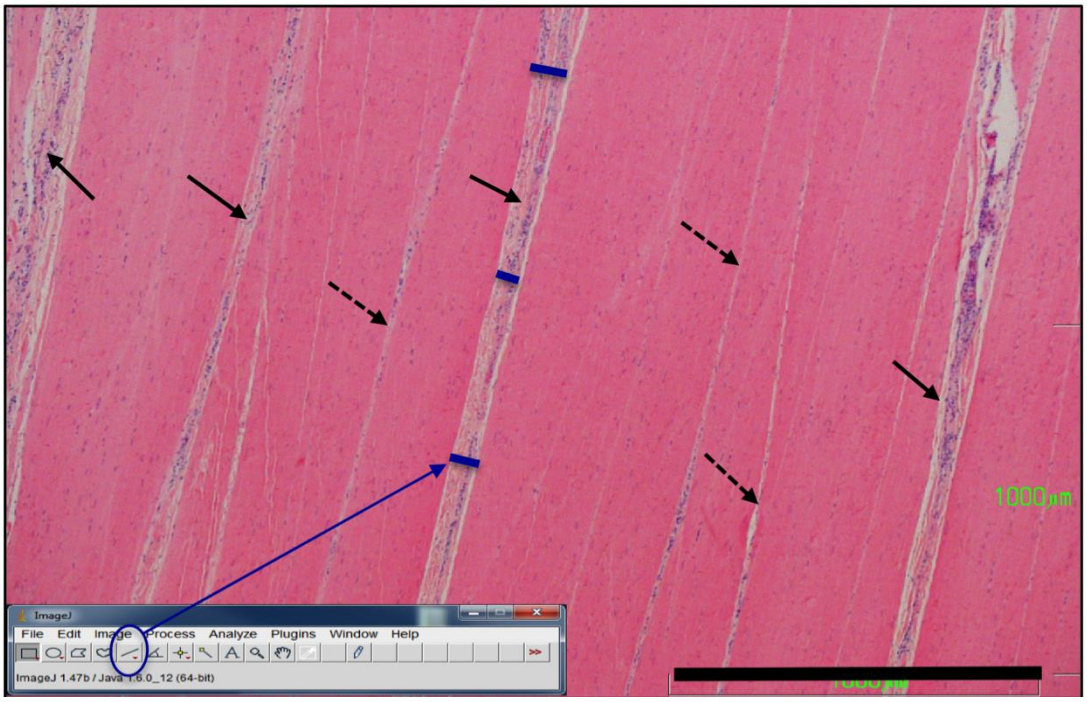

Figure 4.4: Measurement of the IFM thickness in both secondary (dashed arrows) and tertiary fascicles (solid arrows), using ImageJ. Initially the scale measurement was set, then the straight-line tool (blue circle) from the ImageJ toolbar was used to draw a straight line across the IFM thickness (blue lines). Finally, from the Analyze tool the measure option was selected to record the IFM thickness for each point (blue arrow) (Scale bar= 1000 µm).

4.2.4.2.2.1 Setting measurement scale of ImageJ

To determine the IFM thickness, the scale measure of the ImageJ must be set. The image was loaded into the ImageJ program, selecting the straight-line tool (Figure 4.4, blue circle) to draw a straight line across a scale bar of a known distance for instance when the bar is equal to 1000µm. From the Analyse tool, the set scale tool was selected to identify the length of the dragged line over the image scale bar in pixels. Then the known distance (pixels) was converted to a metre measure by typing the scale bar length inside the known distance space in the opened scale window (for instance 1000µm). After setting the scale bar, the setting was confirmed by dragging a new line over the scale bar of the image and measured from the Analyze tool. This should give the same measurement as the scale bar (e.g. 1000µm). Then the IFM thickness was measured by dragging line over all the proposed points, which were then recorded through the Analyze tool (Figure 4.4).

4.2.4.3 Nuclei

4.2.4.3.1 **Nuclear density** (representing cellular density)

This was ascertained by counting the number of cell nuclei (tenocytes) distributed between collagen fibres of the fascicles. In each region 10 fields (400X magnification) over the entire section were selected in a zigzag form. The numbers of cell nuclei were then counted in each field and in three proposed regions (proximal, mid-metacarpal and distal). Nuclei of the IFM were not counted because of the presence of a large numbers of differently shaped nuclei compared to those in the fascicles (Figure 4.5 A).

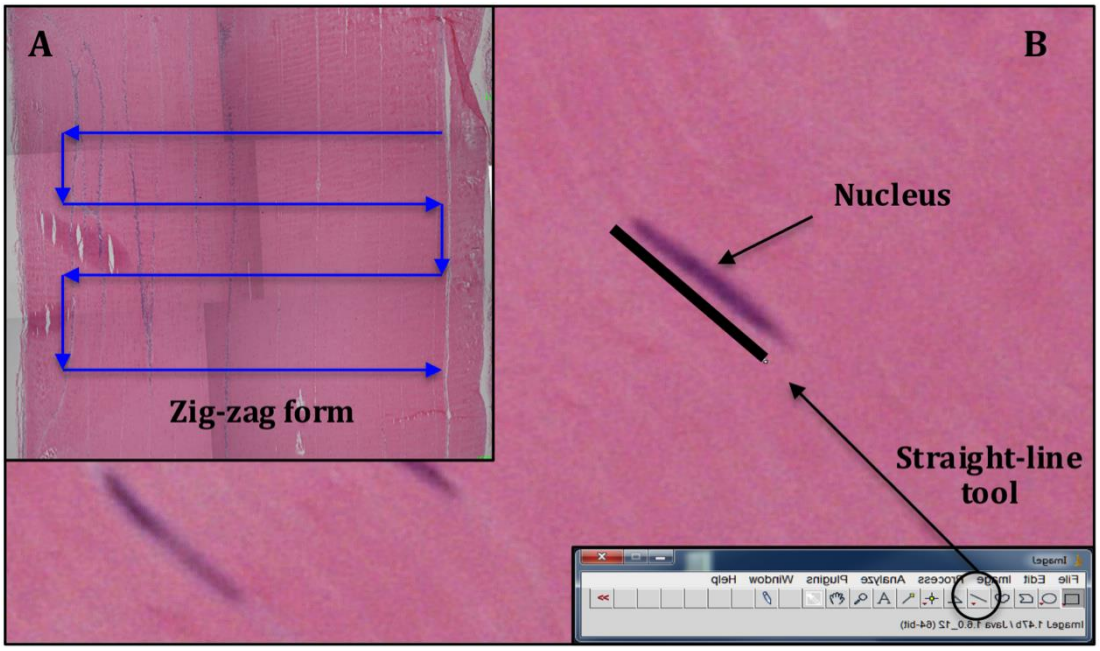

Figure 4.5: A: The intra-fascicular cell nuclei (tenocytes) distributed between collagen fibres were counted in 10 different fields (400X magnification) in a zigzag manner. B: The method of measuring the length of intra-fascicular cell nuclei under a magnification power of 400X, using ImageJ, initially setting the scale measurement (4.2.4.2.2.1), then using the straight-line tool (red circle) to draw a straight line through the length of each nucleus (white line). Finally in the Analyze tool the measurement option was selected to record all nuclear lengths.

4.2.4.3.1 Nuclear length

After counting the number of intra-fascicular cell nuclei, ImageJ was used to measure their lengths in the same fields and regions (10 different fields under 400X magnification) (Figure 4.5). A total number of 450 nuclei were measured in the proximal, mid-metacarpal and distal regions (150 nuclei per each region). The scale measurement tool was set in the same way and then a straight-line tool was used to draw a line along the length of each nucleus from end to end (Figure 4.5 B).

4.2.4.4 Vascularity

Sections of equine SDFT were scanned under a microscope (Nikon Eclipse 80i microscope) in a zig-zag form (100X magnification). The blood vessels were counted in 10 different fields throughout the IFM. The blood vessels distributed throughout the IFM were characterised by having different outlines with a well-

defined lumen surrounded by three layers (tunica intima, media and adventitia) (Figures shown in histology of IFM, 4.3.2) In addition, most of the blood vessels contained precipitated erythrocytes, which appear as a red cluster. It was not feasible to define the very tiny blood vessels because they do not have a definitive identifiable physical characteristic.

4.2.4.5 Inflammatory cells or necrosis

The presence of inflammatory cells or necrosis was recorded as being present or not in each region using low and high magnification power (100-400X).

4.2.5 METHODS OF STAINING

4.2.5.1 Haematoxylin and Eosin (H&E)

Equine SDFT sections were deparaffinised in xylene I and II for 5 minutes each and rehydrated by transferring the slides through graded concentrated ethanol (100%, 96%, 85%, and 70%) down to distilled water. Sections were stained with H&E (TCS Bioscience Ltd) for 5 minutes and then rinsed in tap water for 6 minutes, which was followed by staining with eosin for 2 minutes. They were then directly passed through 3X 96% ethanol, for one minute each, the slides being tapped each time in order to remove the excess stain. Sections were passed through 3X 100% ethanol for 3 minutes each, then cleared in xylene I and II, and finally mounted with Di-n-butyl phthalate in xylene (DPX) (Sigma-Aldrich, UK) and cover slipped (Luna, 1968).

4.2.5.2 Special stains

In addition to H&E staining, sections from different ages were stained with special stains in order to demonstrate some important components of the tendon and particularly to explore components of the IFM such as PG, GAG (Safranin-O and Alcian blue/ PAS) and elastic fibres (Elastin van Gieson).

4.2.5.2.1 Safranin-O

Safranin-O is a cationic dye and reacts with acidic components; it has the affinity to bind to the sulphur units (acidic substrates) of the GAG and gives an orange to red colour. It is usually used to stain cartilage, and similarly in tendon is applied to stain

components such as PG. This stain is used to identify the presence of cartilage, mucin and mast granule cells (Rosenberg, 1971, Schmitz et al., 2010). Sections of SDFT were deparaffinised, rehydrated and stained with Celstine blue for 6 minutes, followed by washing under a running tap water for 6 minutes. The sections were then stained with 0.5 fast green solutions (BDH Chemicals Ltd) for 5 minutes followed by a brief rinse with acetic acid for 10 seconds. Then they were stained with a previously-filtered 1% Safranin-O (TCS Bioscience Ltd) for 2 minutes, blot air dried and quickly dehydrated through absolute alcohols (2X 100% alcohols), cleared in xylenes I and II (2X 5 minutes) and mounted in DPX.

4.2.5.2.2 Alcian blue/ PAS (Periodic Acid Schiffs reagent)

This stain is used to identify and differentiate the amount of acidic and neutral mucins, GAG and mast cell granules (Yamabayashi, 1987, Wulff et al., 2004). Alcian blue is a cationic dye and has an affinity for the anionic and acidic carbohydrate group such as sulphated GAG and glycoproteins. Sections of SDFT were rehydrated and stained with Alcian blue (Sigma-Aldrich, UK) for 30 minutes, washed in running tap water for 2 minutes and then rinsed in distilled water. They were then treated with 0.5% periodic acid (TCS Bioscience Ltd) for 10 minutes, followed by washing in running tap water for 5 minutes and rinsed in DW. They were then treated with Schiff's reagent (TCS Bioscience Ltd) for 20 minutes and washed in running tap water for 5 minutes. After that the nuclei were stained with Mayers Haemalum for 20 seconds followed by washing in running tap water for 5 minutes. Finally the stained sections were dehydrated through graded alcohol, cleared in xylene (2X 5 minutes) and mounted in DPX.

4.2.5.2.3 Elastin Van Gieson (EVG)

This stain was used to determine elastic fibres and differentiate them from the collagen fibres (Wulff et al., 2004). Sections of SDFT were routinely rehydrated and then treated with potassium permanganate for 5 minutes. The sections were then decolourised in 1% oxalic acid for 1 minute, followed by a brief washing under a running tap water and then rinsed in 95% alcohol. The sections were stained with Miller's stain (TCS Bioscience Ltd) for 3 hours, rinsed in 95% alcohol to remove excessive stains and followed by washing in running tap water. Sections were

counter-stained with Van Gieson (TCS Bioscience Ltd) for 4 minutes, dehydrated, cleared and mounted in DPX. The results showed that the elastic fibres were stained blue to black, collagen fibres red and the remaining tissues yellow.

4.2.5 STATISTICAL ANALYSIS

Statistical analysis was carried out using GraphPad Prism Version 6 (California-USA). Initially the data were checked for normality using D'Agostino & Pearson omnibus normality test and they were normalised by using the normalised option tool from the GraphPad Prism. Data were analysed using non-parametric one-way and two-way ANOVA (Kruskal-Wallis and Tukey's multiple comparison tests). Significance was set at a P value of < 0.05.

4.3 RESULTS

4.3.1 GENERAL OBSERVATION OF THE HISTOLOGY OF THE EQUINE SDFT

4.3.1.1 Fascicles

Normal SDFT architecture is comprised of dense regularly organised longitudinal collagen fibres. In this study it was demonstrated that the collagen fibres were packed into different sized bundles (fascicles) arranged parallel to each other and to the longitudinal axis of the tendon. Bundles of collagen fibres formed fascicles, which differed in size and shape (Figure 4.6) coursing through the body of the tendon. During our histological examination, a few small irregularly shaped fascicles were interspersed between the larger fascicles (Figure 4.6 B). Within the fascicles collagen fibres were crimped on their longitudinal axis. The crimp pattern of the collagen fibres demonstrated a wavy pattern for both the individual fibres and a whole tissue surface. This property was not constant during ageing and was typically most prominent in foetal and young horses (Figures 4.6 C and D). Meanwhile, the degree of crimping was not uniform throughout the whole length of the fibres and it varied from region to region (Figures 4.6 C and D).

Fascicles were outlined and separated from each other by the IFM (Figure 4.7). Most of the fascicles continued longitudinally throughout the entire length of tendon sections; however a few fascicles were appeared to be discontinuous and appeared to end both proximally and distally within the section (Figure 4.7 B). The ends of these fascicles were interpolated between larger fascicles and were characterised by having either a flat or an irregular end, or a v-shaped tapered ends (Figure 4.6A). Occasionally a few fascicles were divided transversely into upper and lower portions, which are outlined and separated by a varying amount of IFM (Figure 4.7).

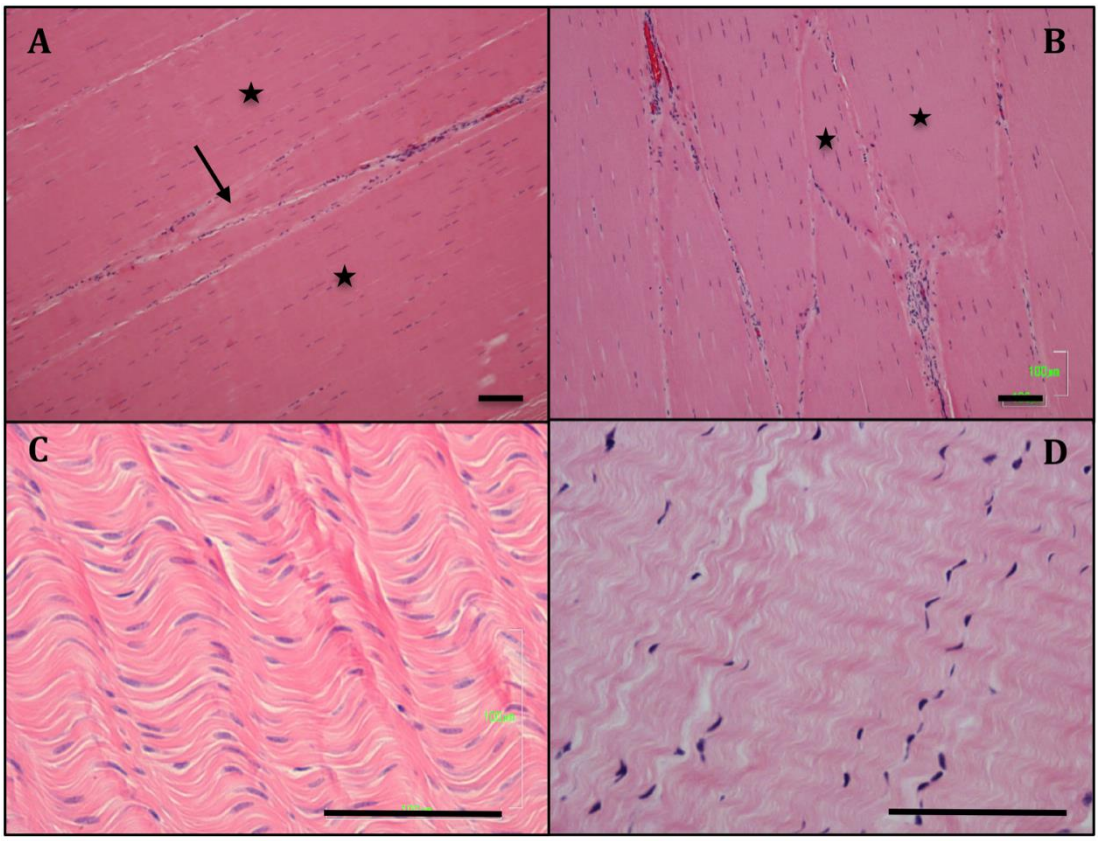

Figure 4.6: Longitudinal sections of the equine SDFT of different ages stained with H&E, A: longitudinal section of one-year-old horse. Note the longitudinally oriented fascicles (asterisk) and the points of apparent ending of a fascicle with a v-shaped tapering conformation (arrow). B: showing differently sized and shaped fascicles on their longitudinal sections of 14-years-old horse. C and D showing the degree of crimp in both the foetal (6 month gestation) and one-year-old horse (Scale bar= 100 μm).

Typically the IFM was composed of an irregular loose fibrous connective tissue network contained various structures such as vessels, nerve fibres, irregular collagen fibres and a large number of non-organised cells (Figures 4.7 C and D). The IFM functions as a reticular tissue that forms divisions between the fascicles but it is less dense than the fascicles. In this study we found that the IFM width varied regionally and did not stay constant when it ran alongside the body of the fascicles (Figure 4.7 A). In some other regions, there were inter-connection between the two vertically oriented IFM regions, which had a clear vascularisation as well as containing a large number of rounds to elliptical fibroblasts (Figure 4.7 B). Fibres within the IFM had a range of different orientations and appear to be more varied in their patterns than

those observed in the collagen fascicles in the main body of the tendon (Figure 4.7 D).

4.3.1.2 Vascularisation

Blood vessels were distributed throughout the IFM, their number, diameters and shapes varying regionally. They varied from being small and round to completely flat vessels. The larger blood vessels were characterised by having defined layers while the smaller ones had only a very thin walls (Figure 4.7 C and D).

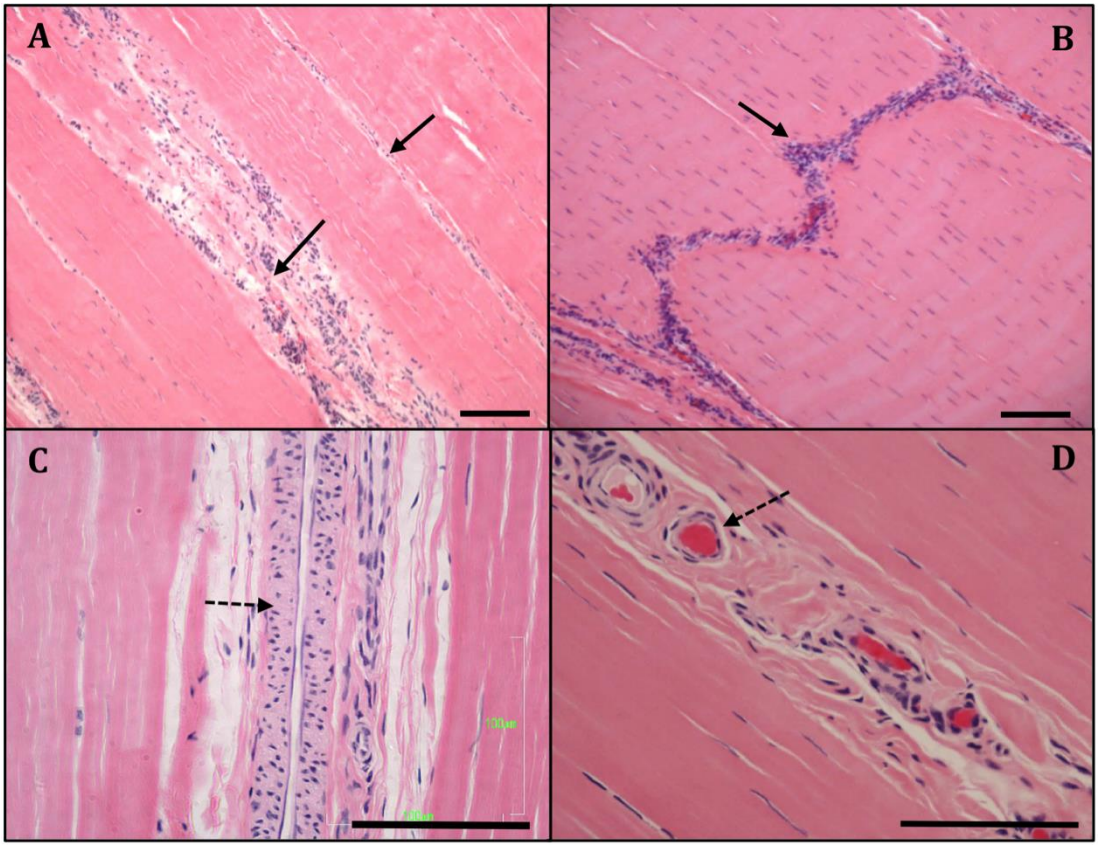

Figure 4.7: Longitudinal sections of equine SDFT of different ages stained with H&E, A: longitudinal section from a one-year-old horse shows various amount of IFM, which aligned with the longitudinal axis of the fascicles (black arrows). B: shows transversely oriented IFM at the mid portion of the fascicle in 14-years-old horse (black arrow). C: the IFM space between fascicles contains various amounts of fibres, cells and large blood vessel (dashed arrow) that have defined layers in a 9-years-old horse. D: numbers of small blood vessels distributed through the IFM (dashed arrow) that contain erythrocytes in a one-year-old horse (Scale bar= 100 μm).

4.3.1.3 Cells

Large numbers of cells of different sizes and shapes were distributed throughout the IFM (Figure 4.7). They ranged from round or oval to fusiform. Some of these cells were embedded into loose connective tissue surrounding the blood vessels, where they appear as a cluster of circular cells around the blood vessels. The intra-fascicular tenocytes were distributed regularly between the collagen fibres and appeared different phenotypically ranging from round to a longitudinal fusiform shape: the greater proportions of cells were fusiform (Figure 4.8).

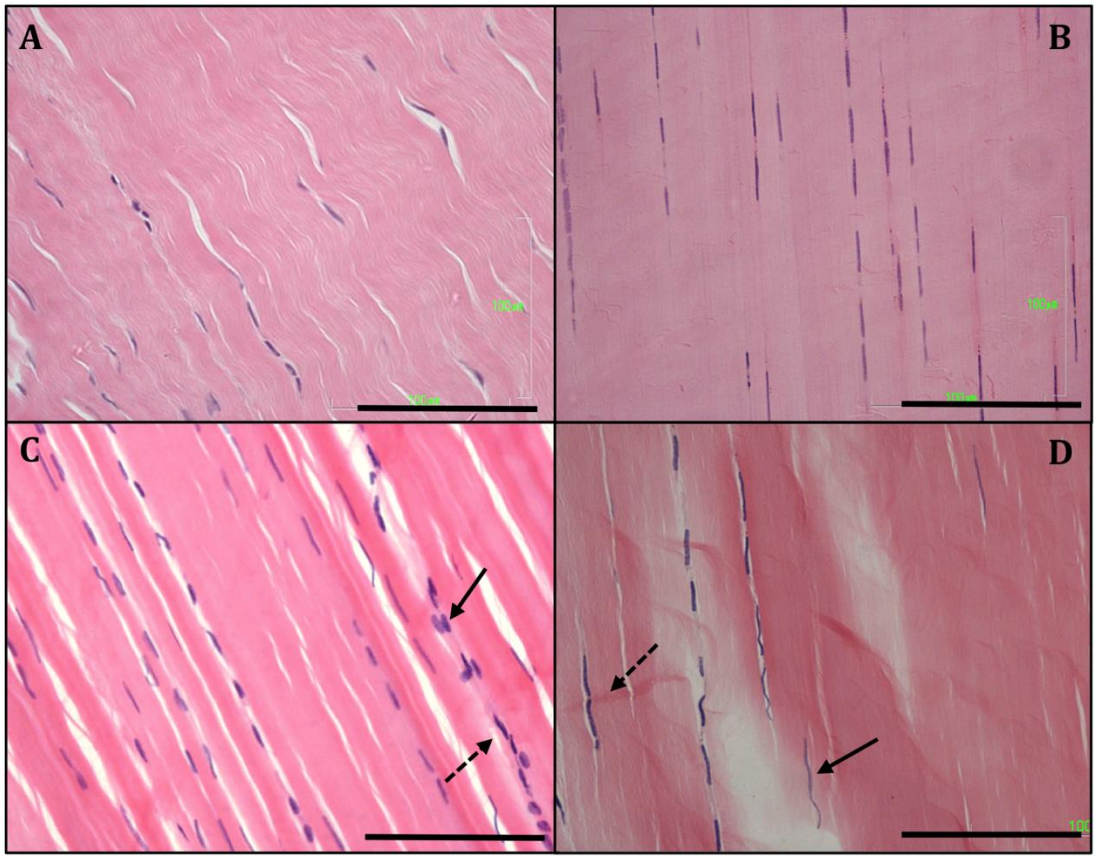

Figure 4.8: Longitudinal sections of equine SDFT of different ages stained with H&E. A: There is some evidence of a crimp pattern of the collagen fibres in a 7-years-old horse. B: Disappearance of the crimp pattern in a 20-years-old horse. C and D: Arrangement of the tenocytes between the collagen, side-to-side (solid arrow) and end-to-end (dashed arrow) communication in a 9-years-old horse (Scale bar= 100 μm).

The intra-fascicular tenocytes were arranged regularly throughout the longitudinal space between collagen fibres (Figure 4.8 A and B). Some of them were considerably elongated and also showed concomitant corrugation with the collagen fibres in the crimp pattern (Figure 4.8 D).

4.3.1.4 Inter-Fascicular Matrix (IFM)

The IFM or endotenon is an irregular fibrous connective tissue, arising from the tendon peritenon (epitenon). It penetrates through the tendon tissue surrounding collagen fibres and clearly organises the tendon into many various sized and shaped bundles of collagen fibres called fascicles. Usually a thick IFM surrounds and defines the big fascicles, then ramifies into smaller branches that penetrate the body of the fascicles and subdivide it into a number of smaller sub-fascicles (Figure 4.9).

When the IFM was stained with H&E the staining was generally homogenous throughout the IFM, but in certain areas the reaction was slightly stronger than in the rest of the IFM. The peripheral aspects of the IFM adjacent to the fascicles retained the eosin stain more than the central part of the IFM. Thus these areas that retained eosin stain indicated the presence of the highest level of nonspecific proteins (Figure 4.9 C and D).

The IFM was organised in different patterns, ranging from longitudinal to a transversely oriented IFM between the fascicles (Figure 4.9 and 4.10). The longitudinally oriented areas of IFM were parallel to the longitudinal axis of the fascicles and occasionally divided into more than one branch, which subsequently subdivided into a number of smaller fascicles. The transversely oriented IFM communicated to two longitudinally oriented IFM and divided a fascicle into upper and lower portions (Figure 4.10 C). The transversely oriented IFM appeared to break the longitudinal continuation of the fascicles, which were apparently a result of fascicular discontinuation.

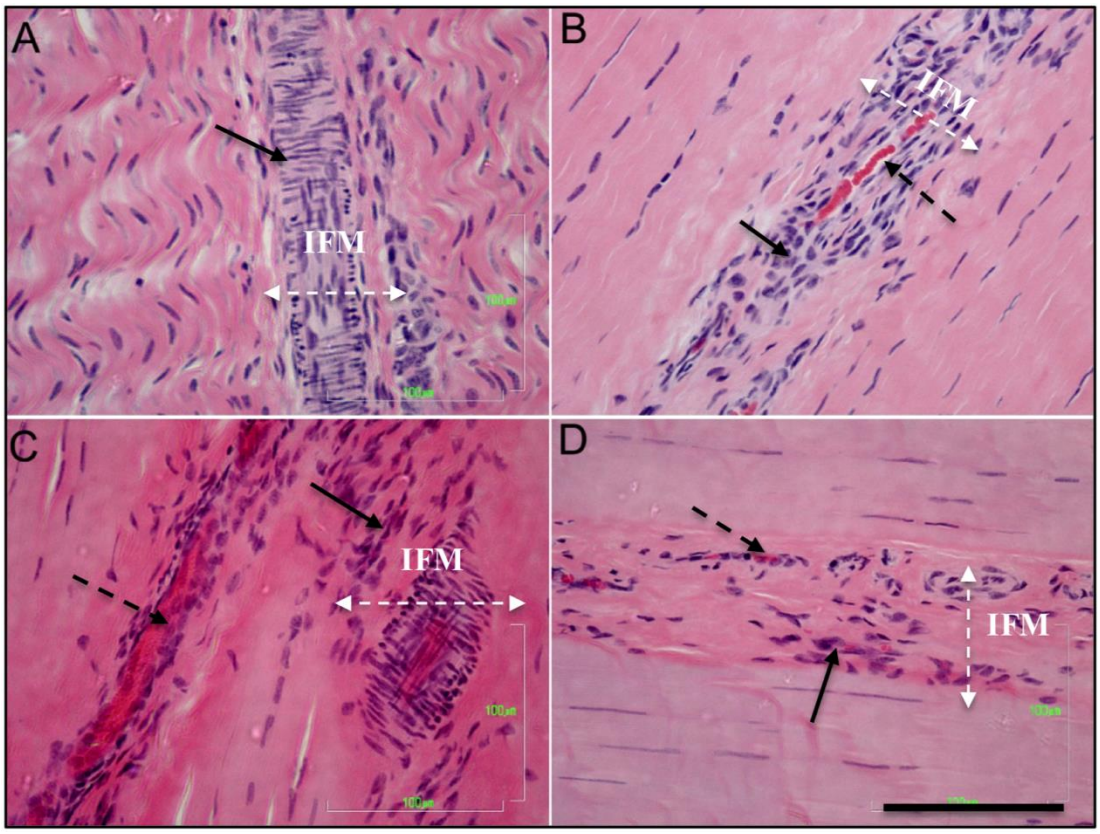

Figure 4.9: H&E staining of the longitudinal sections of the equine SDFT of mid-metacarpal region in different ages. A: IFM in the foetal tendon organised irregularly between the fascicles and containing a large number non-organised cells (arrow). B: IFM of one-year-old horse, stained homogenously, containing blood vessels (and erythrocytes) (dashed arrow) and a large number of irregularly oriented cells (solid arrow). C and D: IFM of a 7 and 20-years-old characterised by non-homogenous staining where the IFM reaction to eosin is stronger than that of the fascicles, and containing vessels (dashed arrows) and a large number of heterogeneous and poorly organised cells (solid arrows), (Scale bar= 100µm).

The IFM contained less dense irregularly oriented fibres. They appeared as fine corrugated fibres running between the fascicular edge and the blood vessels (Figure 4.10, A and B). These fibres appeared to be attached and continuous with the adjacent edges of the fascicles and parts of them surrounded blood vessels. The IFM fibres seemed to arise from the lateral free edge of the fascicles in a form of brush-like filaments (Figure 4.10, C). The crimp outline is apparently higher than that of the collagen fibres of the fascicles and their extent apparently not constant from area to area (Figure 4.10 A and C). Around the blood vessels they form a small bundle of a circular filaments, which contain clusters of cells parallel to the fibre's direction.

These fibres intercommunicate with the tunica adventitia of the blood vessels and appear to continue as a part of the blood vessels (Figure 4.10 B and D).

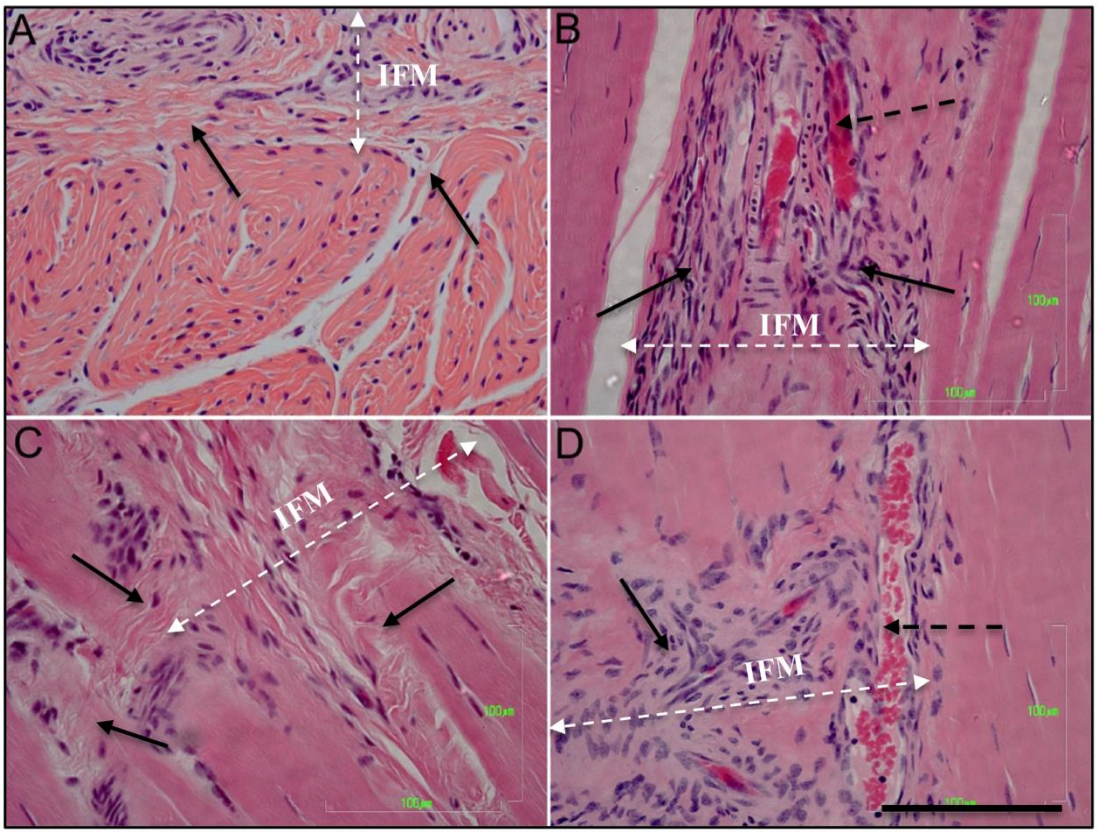

Figure 4.10: H&E staining of the SDFT proximal region at different ages. A: Transverse section of foetal tendon, showing the presence of fine irregular IFM between fascicles and how it is arranged and connected with the lateral boundaries of the fascicles. B: Longitudinal section through the IFM of a one-years-old, note the transversely oriented IFM that contain blood vessels (dashed arrow) and a cluster of cells (solid arrows). C: Longitudinal section from 7-years-old showing the presence of both the longitudinal and transversely oriented IFM where appeared as a brush like filaments (arrows) on the lateral boundary of the fascicles. D: Longitudinal section from 14-years-old, the presence of an irregular outlined IFM that contain large blood (dashed arrow) vessel and clustered cells (arrows), (Scale bar= 100µm).

In the foetal tendon the fibres contents of the IFM appeared to be less dense than the IFM in the SDFT from mature animals (Figure 4.10 A). Fibre orientations were not homogeneous and they varied in density in different sites, for instances in those areas were surrounding the blood vessels appeared to be less dense and had different

orientation (Figure 4.11). In mature SDFT (7-year-old), the IFM appeared denser and less abundant than the foetal tendon (Figure 4.9 and 4.10 A). In the mature SDFT, occasionally the IFM were detached from the fascicles while in other areas were adhered to the free edge of the fascicles and appeared as an extended part of the fascicles (Figure 4.11 A and B). It is likely that this disruption was artefactual due to histological processing.

A large number of disorganised cells of different sizes and shape were distributed between these IFM fibres; their directions were approximately parallel to the longitudinal axis of the fibres (Figures 4.11). These cells ran alongside and surrounded the blood vessels in a variety of directions and occasionally appeared to merge into the vessels' wall (Figures 4.11 B and D). These merged cells organised in two main directions; in the first direction the majority of them were parallel to the walls of the vessels but in the second form they were perpendicularly to the walls of the vessels (Figure 4.11 C and D).

Blood vessels of various sizes were localised within the IFM, ranging from very tiny to large blood vessels (up to 100μm) (Figures 4.9 - 4.11). They were characterised by having distinct layers (tunica interna, media and adventitia), their lumen often containing erythrocytes.

No immediate qualitative differences were identified in the histological architecture of equine SDFT between the three assessed regions (proximal, mid and distal metacarpal region) on those histological sections. In all regions similar structures could be observed within the collagen fascicles and the IFM components. However foetal tendon appeared to characterised by hyper-cellular, more abundant IFM in proportion to their sizes and well-defined crimp pattern to the fascicular matrix (FM). These features progressively declined during ageing; in particular in very old horses (20-years-old) examples the tendon appeared less cellular, had little crimp and less developed IFM. However we planned to semi-objectively quantify changes in regional and age related alteration in tendon ultrastructure with the scoring method described in the histological scoring section (section 4.3.3).

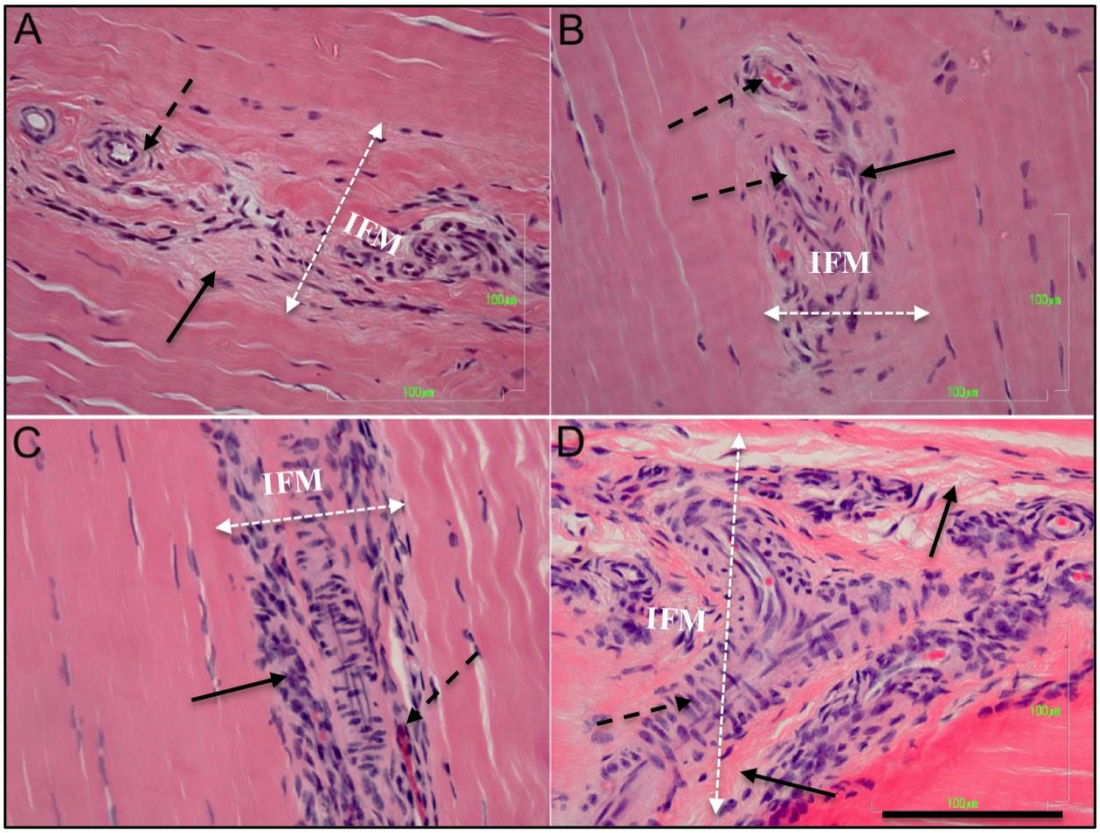

Figure 4.11: H&E staining of the longitudinal sections of the equine SDFT of the distal region at different ages. A: shows fine irregular IFM between the fascicles of one-year-old horse. Note the IFM contains longitudinal (solid arrow) and circularly oriented fibres around the blood vessels (dashed arrow). B: A large portion of an isolated IFM through the body of a fascicle containing blood vessels (dashed arrows) and a number of cells (solid arrow) in a 7-years-old horse. C: IFM of a 9-years-old horse, containing blood vessels (dashed arrow) and a large number of non-organised cells (solid arrow). D: Transversely oriented IFM that continues with the lateral longitudinally oriented IFM in a 14-years-old. Collagen fibres concomitantly oriented with the direction of the IFM (solid arrows), surrounding a blood vessel and accompanied by a large number of poorly organised and various sized cells. Note the cells in the vessels wall arranged in two forms; parallel and the perpendicular forms (dashed arrow), (Scale bar= 100µm).

Moreover, the following specific stains were used to demonstrate more structural components of the IFM, such as non-collagenous protein and elastic fibres;

4.3.1.4.1 Safranin-O

In this study longitudinal equine SDFT sections from different ages were stained with Safranin-O and the result showed that the IFMs were strongly stained with a

dark orange colour, which indicated that this part of the tendon contained the highest amount of non-collagenous protein such as PG and GAG. The positive reaction was seen in all ages (7, 9, 14 and 17-years-old) and it appeared that subjectively in older animals, there was a slightly stronger reaction (Figure 4.12).

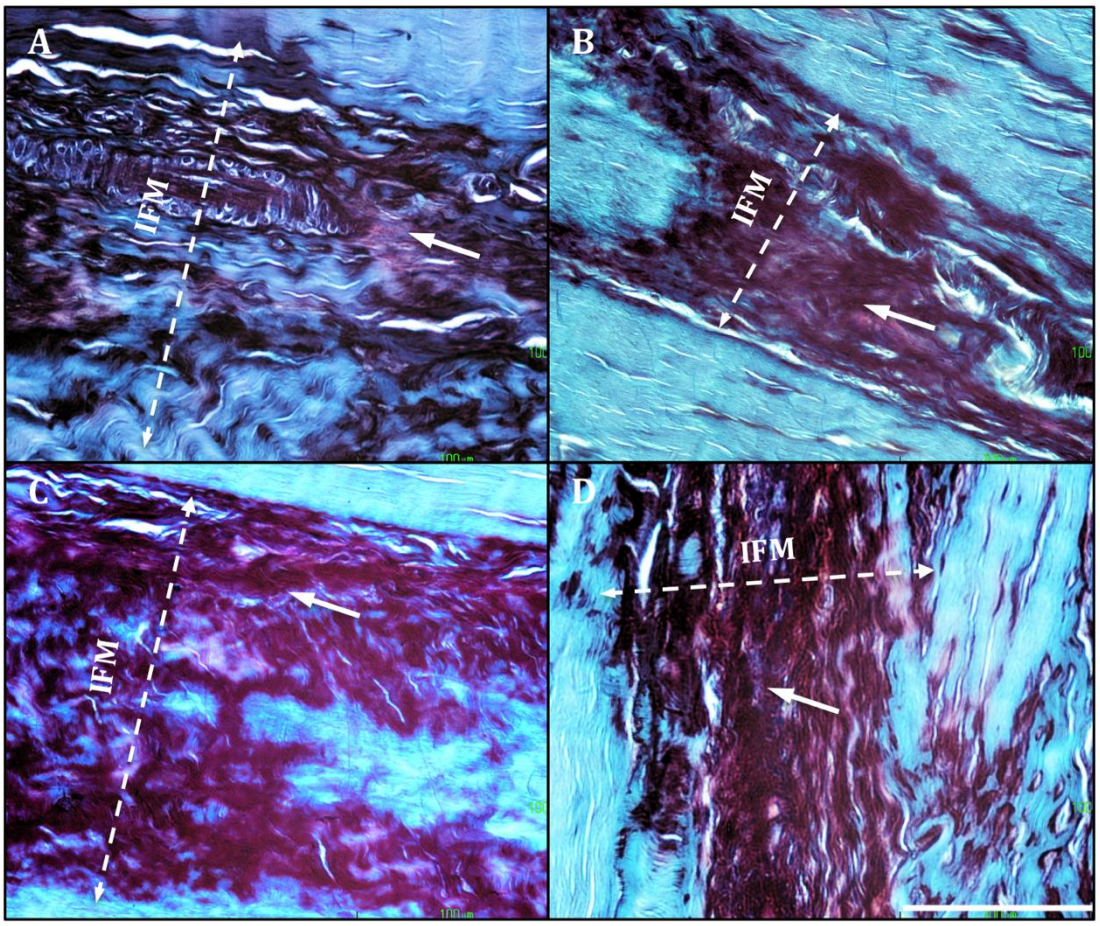

Figure 4.12: Safranin-O staining of the longitudinal sections of the equine SDFT of the mid-metacarpal region in different ages: A and B are sections from a 7 and 9-years-old horse respectively; their IFM has positive Safranin-O staining (white arrows). C and D are sections from a 14 and 17-years-old horse respectively; their IFM has subjectively a greater depth of Safranin-O staining (white arrows) (Scale bar=100µm).

4.3.1.4.2 Alcian blue/PAS

In this study longitudinal sections from equine SDFTs at different ages were stained and it was found that the IFM stained positively with Alcian blue (Figure 4.13). As with Safranin-O staining there was a slight variation in IFM staining to

Alcian blue. In the 7 and 9-years-old horse the Alcian blue staining was moderate (Figure 4.13 A and B) but in the older horses (14 and 17-year-old) the staining appears more intense than the younger horses (Figure 4.13 C and D). Therefore, our findings are suggestive that there are different amounts of PG and GAG present throughout the IFM with ageing (Figure 4.13).

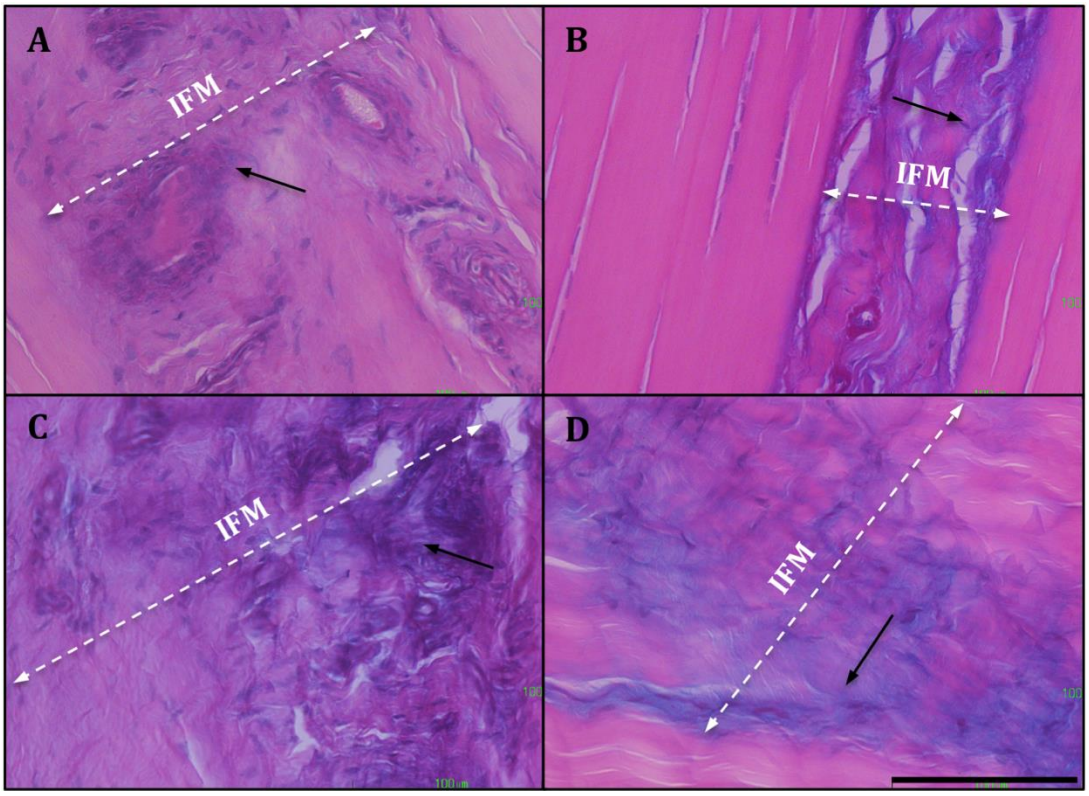

Figure 4.13: Alcian blue-PAS staining of longitudinal sections of equine SDFT of the mid-metacarpal region in different ages: A and B are sections from a 7 and 9-years-old horse respectively and there is mild Alcian blue staining of the IFM (arrow). C and D are sections from 14 and 17-years-old respectively and there is mild Alcian blue-PAS staining of the IFM (arrow). In these sections the stain is distributed around the cells and through the IFM fibres (Scale bar=100µm).

4.3.1.4.3 Elastin Van Gieson stains (EVG)

Typically EVG is used to stain elastic fibres to allow their differentiation from collagen fibres. The elastic fibres and cell nuclei stained black, collagen fibres stained red and the rest of the tissues elements stained yellow. In this study longitudinal sections of equine SDFT of the mid-metacarpal region from different ages were stained and it was found that the IFM contain elastic fibres (Figures 4.14).

The elastic fibres were less dense than the IFM fibres and dispersed through the IFM fibres. The elastic fibres showed a variety of arrangements in the IFM and in some areas the elastic fibres were arranged regularly and transversed from side to side through the IFM (Figures 4.14 A). These elastic fibres were thin and oriented parallel to the collagen fibres of the IFM and appeared to inter-connect with the lateral aspect of the fascicles (Figure 4.14 A). While in other areas a large number of elastic fibres were interwoven through the IFM collagen fibres (Figure 4.14 C) or arranged irregularly in different directions and around the blood vessels (Figure 4.14 B). The elastic fibres often appeared crimped in an approximately similar manner of IFM collagen fibres and were parallel to the adjacent collagen fibres, although in some locations they were curled (Figure 4.14 D) rather than crimped. Elastic fibres were observed in different ages throughout the IFM.

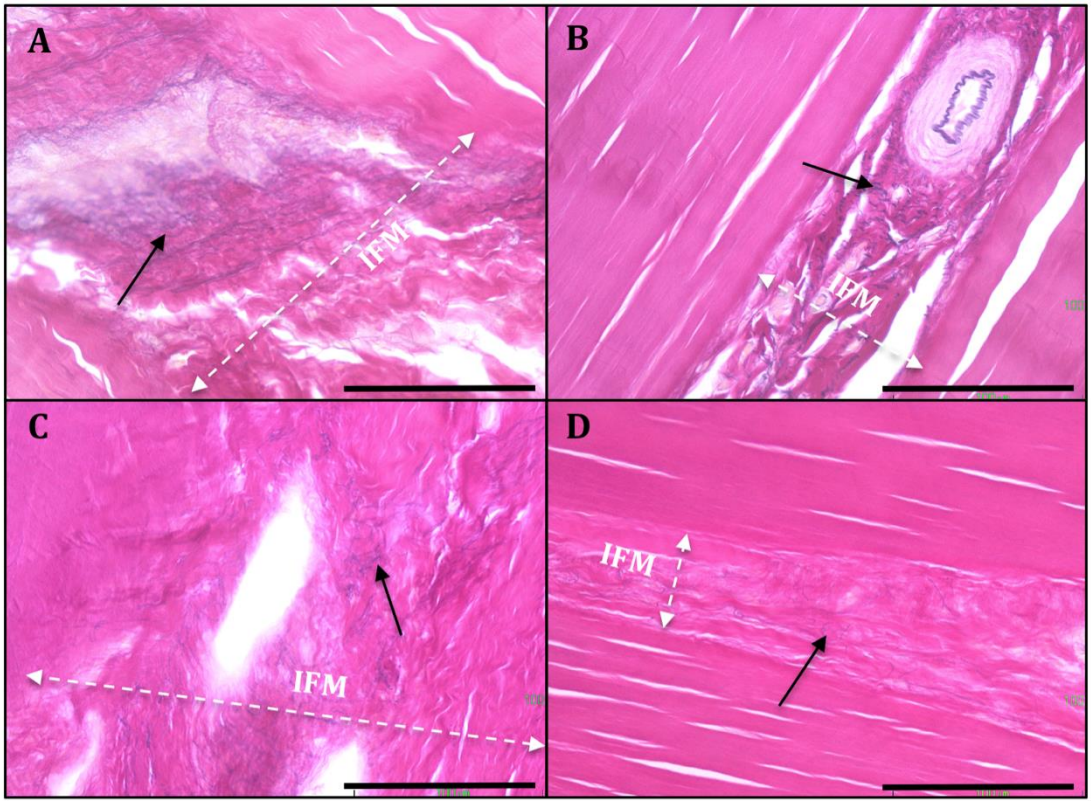

Figure 4.14: Elastin Van Gieson (EVG) stain of longitudinal sections of equine SDFT of the mid-metacarpal region at different ages. A: The IFM contains a large amount of side-to-side parallel-oriented transverse, thin regularly oriented elastic fibres (black fibres) in a 7-years-old horse (arrow). B: The IFM contains irregularly organised elastic fibres particularly around the blood vessel in a 9-years-old horse (arrow). C: The elastic fibres are interwoven through the IFM fibres of a 14-years-old horse (arrow). D: The elastic fibres have a curled form through the IFM of a 20-year-old horse (arrow) (Scale bar=100µm).

4.3.3 HISTOLOGICAL SCORING

4.3.3.1 ECM organisation (Angulation of the collagen bundles)

4.3.3.1.1 Regional differences

In this study it was observed that not all fascicles were parallel to a longitudinal axis and a number of fascicles underwent a minor degree of inclination on their longitudinal axis. Fascicles were angulated either toward the right (abaxial+) or left side (abaxial-) side of the sections. The percentage and degree of angulation varied in different regions (Table 4.3). These values showed that fascicles were angled in all regions and all ages but they were not constant from region to region. Numbers of fascicles, which were angled from the longitudinal axis ranged from 14% to 90%. The degree of angulation (90 ± degree of angulation) were ranged from 0.2° to 22°. The mid-metacarpal region had a lower percentage of angulated fascicles but was not significant statistically in all groups except in Group Four (P value < 0.05) where the mid-metacarpal region showed a significant lower number of angulated fascicles (Figure 4.15). Similarly, the degrees of angulation were insignificantly lower in the mid-metacarpal region than the proximal and the distal regions (Figure 4.16).

Fascicles apparently inclined towards the peripheral border particularly in those regions (proximal and distal) where the tendon slightly increased in size. Generally it was found that the mid-metacarpal region had a higher number of non-angulated fascicles and lower degree of angulation than the proximal and distal regions but this was not statistically significant (Figure 4.15 and 4.16).

4.3.3.1.1 Age related difference

It was found that fascicles were angulated in all ages and regions, but both number and the degree of angulation were not significantly altered during ageing (Figure 4.15- 4.16).

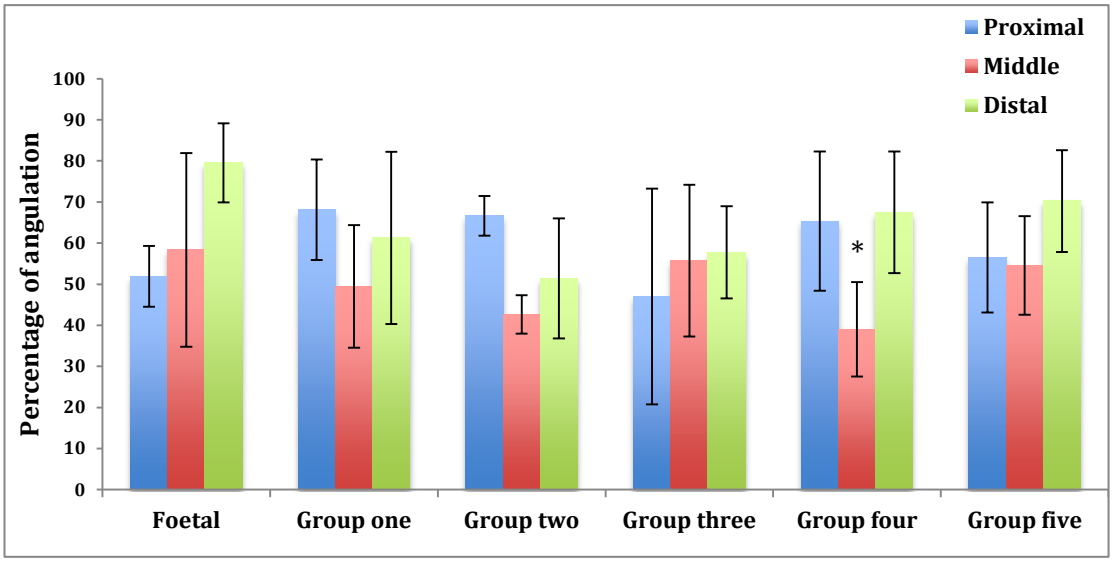

Figure 4.15: The percentage of fascicular angulation in the proximal, mid-metacarpal and the distal region in all groups including foetal age, Group one (3-years-old), Group two (7-years-old), Group three (9-years-old), Group four (14-years-old) and Group five (17-20-years-old). Large numbers of fascicles were angulated in the proximal and distal region but this finding was not statistically significant except in Group four (P value < 0.05) and was not altered with age, Two-way ANOVA (Tukey's multiple comparisons test) (Error bars= standard deviation SD).

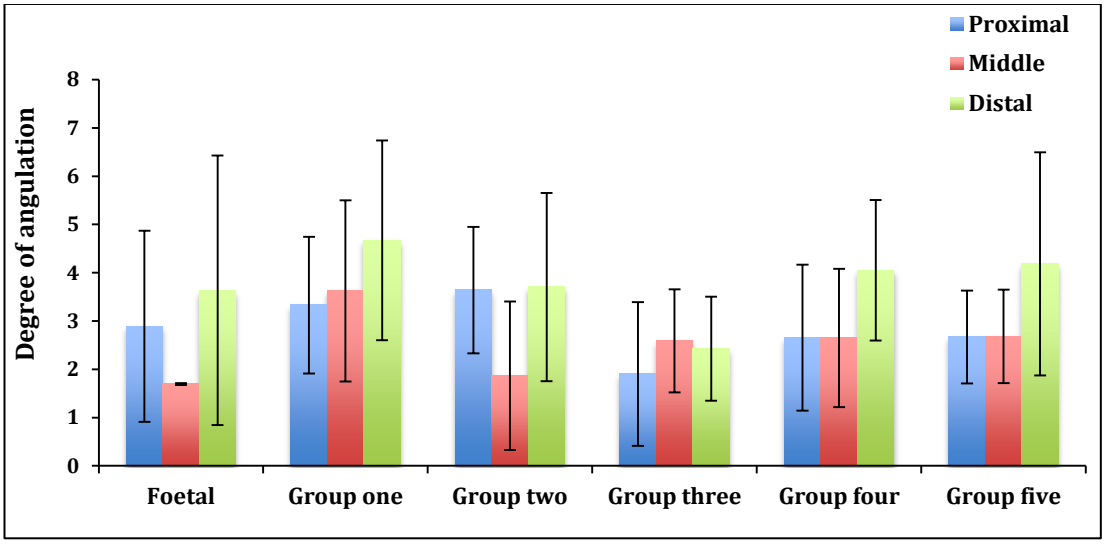

Figure 4.16: The degree of fascicular angulation (90± degree of angulation) in different regions and groups including foetal age, Group one (3-years-old), Group two (7-years-old), Group three (9-years-old), Group four (14-years-old) and Group five (17-20-years-old). Large number of fascicles were angulated in the distal regions but this was not statistically significant and not altered with age (Two-way ANOVA (Tukey's multiple comparisons test) (P value < 0.05) (Error bars= SD).

Table 4.3: The percentage and the degree of fascicular angulation in the proximal, mid-metacarpal and distal regions of the equine SDFT in different age groups. The age groups include foetal, Group one (3-years-old), Group two (7-years-old), Group three (9-years-old), Group four (14-years-old) and Group five (17-20-years-old), (P=proximal, M=mid-metacarpal and D=distal metacarpal regions).

The percentage of fascicular angulation																		
	Foetus %			Group one %			Group two %			Group three %			Group four %			Group five %		
SDFT	P	M	D	P	M	D	P	M	D	P	M	D	P	M	D	P	M	D
1	46.66	75	86.36	80	41.66	85	68.75	46.66	50	53.33	66.66	56.25	73.68	27.27	85.71	58.33	64.28	66.66
2	57.14	41.66	72.72	68.75	66.66	53.33	61.11	43.75	66.66	73.68	35.71	50	75	53.84	64.28	64.28	66.66	80
3				55.55	40	45.45	70	37.5	37.5	66.66	50	71.42	40	41.66	70	60	46.15	66.66
4										31.25	81.81	66.66	72.72	33.33	50	33.33	38.46	53.33
5										10	44.44	44.44				66.66	57.14	84.61
Average	51.9%	58.33%	79.54%	68.1%	49.44%	61.26%	66.62%	42.63%	51.38%	46.98%	55.72%	57.75%	65.35%	39.02%	67.497%	56.52%	54.53%	70.25%
SD	7.41	23.57	9.64	12.23	14.93	20.93	4.812	4.68	14.62	26.24	18.44	11.24	16.925	11.50	14.77	13.380	12.01	12.38
	The degree of fascicular angulation																	
	Foetus			Group one			Group two			Group three			Group four			Group five		
SDFT	P	M	D	P	M	D	P	M	D	P	M	D	P	M	D	P	M	D
1	4.29	1.71	5.61	4.96	5.62	6.81	2.78	0.5	1.69	1.21	2.7	1.78	4.81	1.08	1.95	3.7	1.61	2.43
2	1.49	1.68	1.66	2.63	3.36	2.68	2.99	3.53	3.84	1.25	1.15	2.1	2.2	4.54	4.84	3.27	3.71	5.44
3				2.4	1.89	4.53	5.15	1.57	5.58	3.95	2.14	4.15	2.33	2.3	5.19	1.83	3.25	6.8
4										2.88	4.07	2.7	1.28	2.68	4.22	1.87	2.16	2.06
5										0.22	2.88	1.4						
Average	2.89	1.695	3.635	3.33	3.62	4.67	3.64	1.86	3.70	1.90	2.588	2.426	2.655	2.65	4.05	2.66	2.68	4.18
SD	1.97	0.02	2.79	1.41	1.87	2.06	1.311	1.53	1.94	1.49	1.06	1.07	1.51	1.43	1.45	0.96	0.96	2.31

4.3.3.2 IFM organisation

4.3.3.2.1 IFM angulation

4.3.3.2.1.1 Regional difference

The IFM was arranged longitudinally between the fascicles and angulated concomitantly with the fascicles. The IFM was less regular than the fascicles and they also showed a wide range of angulation in different regions and ages (Table 4.4), their percentage and degree of angulation were higher than the fascicles. The percentage angulation ranged from 20% to 100%, and the degrees of angulation ranged from 0.3° to 40° (90 ± degree of angulation). As found in the FM, these ranges of IFM angulation would also indicate that a greater number of IFM fascicles did not run parallel to the longitudinal axis of the tendon. The percentage and degree of angulation were not constant between different regions and ages. However, the proximal and the distal regions showed a greater number of angulated fascicles than the mid-metacarpal region but it was not statistically significant (P value > 0.05) (Figure 4.17). In the proximal and the distal regions of the SDFTs the degree of fascicular angulation varied markedly between different groups but it was not statistically significant (P value > 0.05) (Figure 4.18).

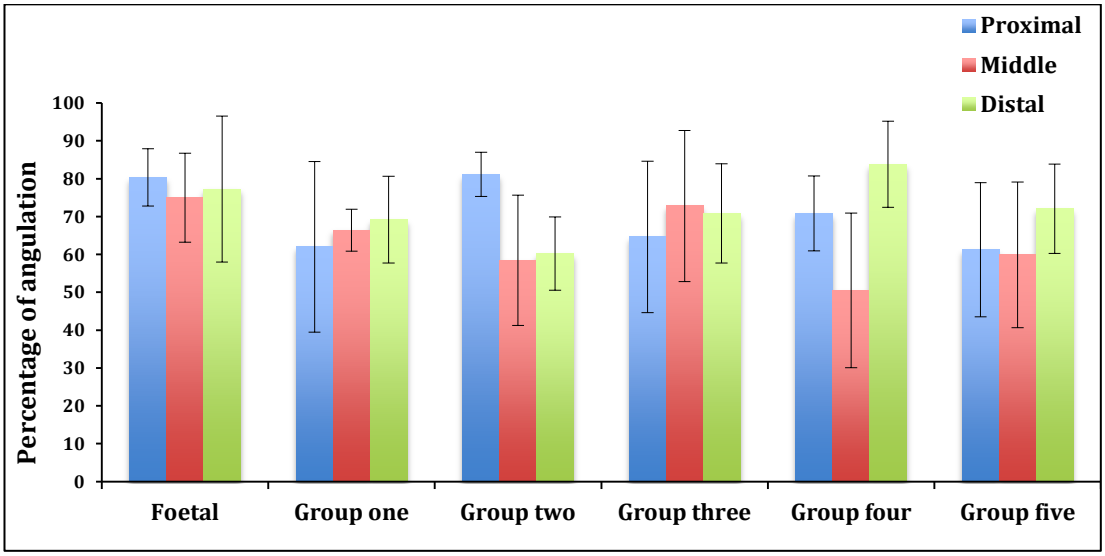

Figure 4.17: The percentage of angulation of IFM fascicles in the proximal, mid-metacarpal and distal parts of the equine SDFT with age. The groups include foetal age, Group one (3-years-old), Group two (7-years-old), Group three (9-years-old), Group four (14-years-old) and Group five (17-20-years-old). There were not any statistically significant differences in the percentage of fascicular angulation between different regions and ages (Error bar= SD).

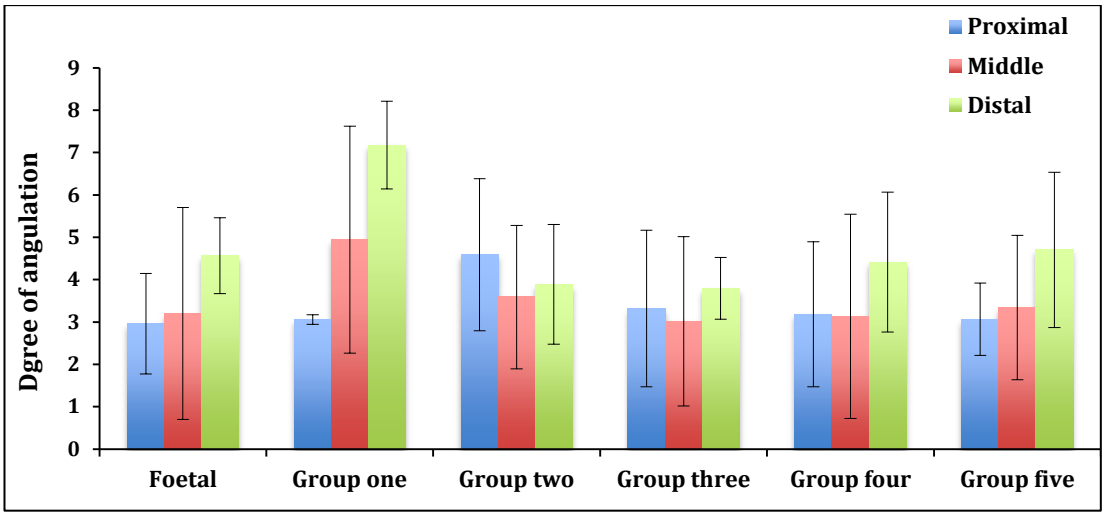

Figure 4.18: This figure illustrates that degree of IFM angulation (90± degree of angulation) is different in regions and groups. The groups include foetal, Group one (3-years-old), Group two (7-years-old), Group three (9-years-old), Group four (14-years-old) and group five (17-20-year-old). The distal-metacarpal region showed a greater degree of angulation but it was not statistically significant compared to the proximal and mid-metacarpal regions and with age (Error bar= SD).

4.3.3.2.1.2 Age related difference

The degree and percentage of IFM angulation were found to be different in all ages but they did not show significant alteration with age (P value > 0.05), (Figures 4.17 and 4.18), (Table 4.4).

Table 4.4: The percentage and the degree of IFM angulation in equine SDFTs in different regions and groups in equine SDFT. They include foetal, Group one (3-years-old), Group two (7-years-old), Group three (9-years-old), Group four (14-years-old) and Group five (17-20-years-old), (P=proximal, M=mid-metacarpal and D=distal metacarpal regions).

	The percentage of fascicular angulation																	
	Foetus %			**Group one %**			**Group two %**			**Group three %**			**Group four %**			**Group five %**		
SDFT	**P**	**M**	**D**	**P**	**M**	**D**	**P**	**M**	**D**	**P**	**M**	**D**	**P**	**M**	**D**	**P**	**M**	**D**
1	85.71	66.66	90.9	81.81	60	82.35	86.66	42.85	61.53	73.33	90.9	76.47	80	60	76.92	83.33	41.66	70
2	75	83.33	63.63	66.66	69.23	61.53	75	76.92	69.23	84.61	72.72	83.33	58.82	58.33	100	60	75	81.81
3				37.5	70	63.63	81.81	55.55	50	78.57	42.85	50	77.77	63.63	83.33	58.82	75	83.33
4										46.66	90.9	77.77	66.66	20	75	34.78	36.36	53.84
5										40	66.66	66.66				69.23	71.42	71.42
Average	80.35 %	74.99%	77.26%	61.99%	66.41%	69.17%	81.1%	58.44%	60.25%	64.63%	72.80%	70.84%	70.81%	50.49%	83.81%	61.23%	59.88%	72.08%
SD	7.57	11.78	19.28	22.52	5.56	11.46	5.857	17.21	9.67	19.99	19.93	13.11	9.89	20.44	11.36	17.74	19.2	11.81
	The degree of fascicular angulation																	
	Foetus			**Group one**			**Group two**			**Group three**			**Group four**			**Group five**		
SDFT	**P**	**M**	**D**	**P**	**M**	**D**	**P**	**M**	**D**	**P**	**M**	**D**	**P**	**M**	**D**	**P**	**M**	**D**
1	3.8	1.43	5.2	2.98	7.59	8.03	3.26	2	5.52	1.99	4.17	2.85	5.75	2.05	4.65	1.9	3.87	4.43
2	2.12	4.97	3.93	3.19	5.01	6.02	3.87	3.4	3.04	0.94	1.38	3.47	2.35	6.53	6.19	3.11	1.22	3.15
3				3.01	2.23	7.48	6.63	5.37	3.11	4.39	1.55	3.67	2.38	2.99	4.63	4.24	5.26	6.09
4										3.72	5.98	4.76	2.25	0.97	2.19	2.74	4.42	7.03
5										5.54	2	4.23				3.33	1.93	2.8
Average	2.96	3.2	4.56	3.06	4.94	7.17	4.58	3.59	3.89	3.31	3.01	3.79	3.18	3.13	4.41	3.06	3.34	4.7
SD	1.18	2.5	0.89	0.11	2.68	1.03	1.79	1.69	1.41	1.84	1.99	0.73	1.71	2.4	1.65	0.85	1.7	1.83

4.3.3.2.2 IFM Thickness

Measurement of the IFM thickness was organised into two categories; the first being the IFM that lies between the tertiary fascicles, which is characterised by being thick and very well defined (see Chapter two- section 2.3.2.3 IFM thickness). The second category is the IFM that divides the tertiary fascicles into the secondary fascicles which is generally thinner in diameter (Figure 4.4). When the IFM thickness was measured, a significant difference was present in between tertiary and secondary IFM thickness in all groups, using Mann Whitney unpaired T-test (Table 4.5). The average IFM thickness of the tertairy fascicles in Groups one, two, three, four and five were 15.48µm (±4.39 SD), 17.89µm (±6.29 SD), 13.65µm (±3.25 SD), 13.44µm (±2.76 SD) and 16.39µm (±3.98 SD) respectively, within a range of of 1.12µm-155µm (Table 4.4). While, the average IFM thickness of the seondary fascicles in Groups one, two, three, four and five were 4.74µm (±1.04 SD), 4.98µm (±0.59 SD), 4.23µm (±0.46 SD), 4.13µm (±0.45 SD) and 3.74µm (±0.35 SD) respectively, with a range of 0.4µm-17µm (Table 4.5) (Figure 4.19). Therefore there is a significant differences in the the average IFM thickness between the tertiary and the secondary fascicles in all groups (P value < 0.05 and 0.01)

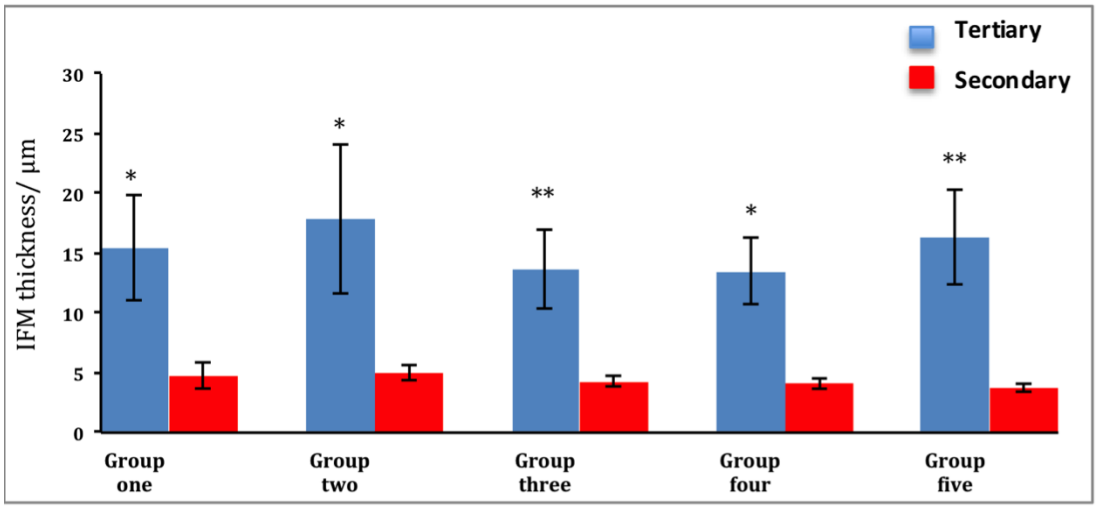

Figure 4.19: This figure illustrates the average IFM thickness between the tertiary and secondary fascicles in all groups, including Group one (3-years-old), Group two (7-years-old), group three (9-years-old), Group four (14-years-old) and Group five (17-20-years-old). The IFM of the tertiary fascicles are significantly thicker than the secondary fascicles, (*P value < 0.05), (**P value < 0.01) (Error bars = SD).

4.3.3.2.2.1 IFM thickness between the tertiary fascicles

4.3.3.2.2.1.1 Regional difference

The IFM lying between the tertiary fascicles altered from the proximal to the distal regions and different area within the same region. In Group one, there was not any significant difference in the IFM thickness between the proximal, mid-metacarpal and distal regions. However, in the other groups there were significant differences between the three regions (p value <0.05), using two-way ANOVA (Kruskal-Wallis test and Dunn's multiple comparisons test). In the second group, the mature group, the mid-metacarpal region showed the lowest level of IFM thickness when compared to the proximal and the distal regions. In Group two the average IFM thickness in the proximal, mid-metacarpal and distal regions were 16.8μm (±6.08 SD), 9.96μm (±3.99 SD) and 17.22μm (±7.15 SD) respectively, where the mid-metacarpal region had the thinnest IFM (P value <0.05). In Group three, their average IFM thicknesses from proximal to distal region were 15.22μm (±3.33 SD), 12.04μm (±3.74 SD) and 13.46μm (±3.76 SD). The proximal region was thicker than the mid-metacarpal and the distal region, while the mid-metacarpal region was significantly smaller than the distal region (P value <0.05). In Group four, the average IFM thicknesses from proximal to distal regions were 15.64μm (±3.86 SD), 10.5μm (±2.74 SD) and 14μm (±4.79 SD). Similarly in this group four the IFM thickness of the mid-metacarpal region was significantly smaller than the proximal and distal regions (P value <0.05). In Group five, the average IFM thickness in the proximal, mid-metacarpal and the distal regions were 21.84μm (±10.78 SD), 13.82μm (±5.83 SD) and 13.41μm (±5.46 SD). The IFM thicknesses in both the mid-metacarpal and the distal regions were significantly decreased in contrast to the proximal region (P value <0.05). In summary the mid-metacarpal regions in all groups had a thinner IFM than the proximal and the distal regions. Similarly, in Groups three and five, the IFM of the distal regions also decreased in comparison to the proximal region, but was not lower than the mid-metacarpal region (Figure 4.20).

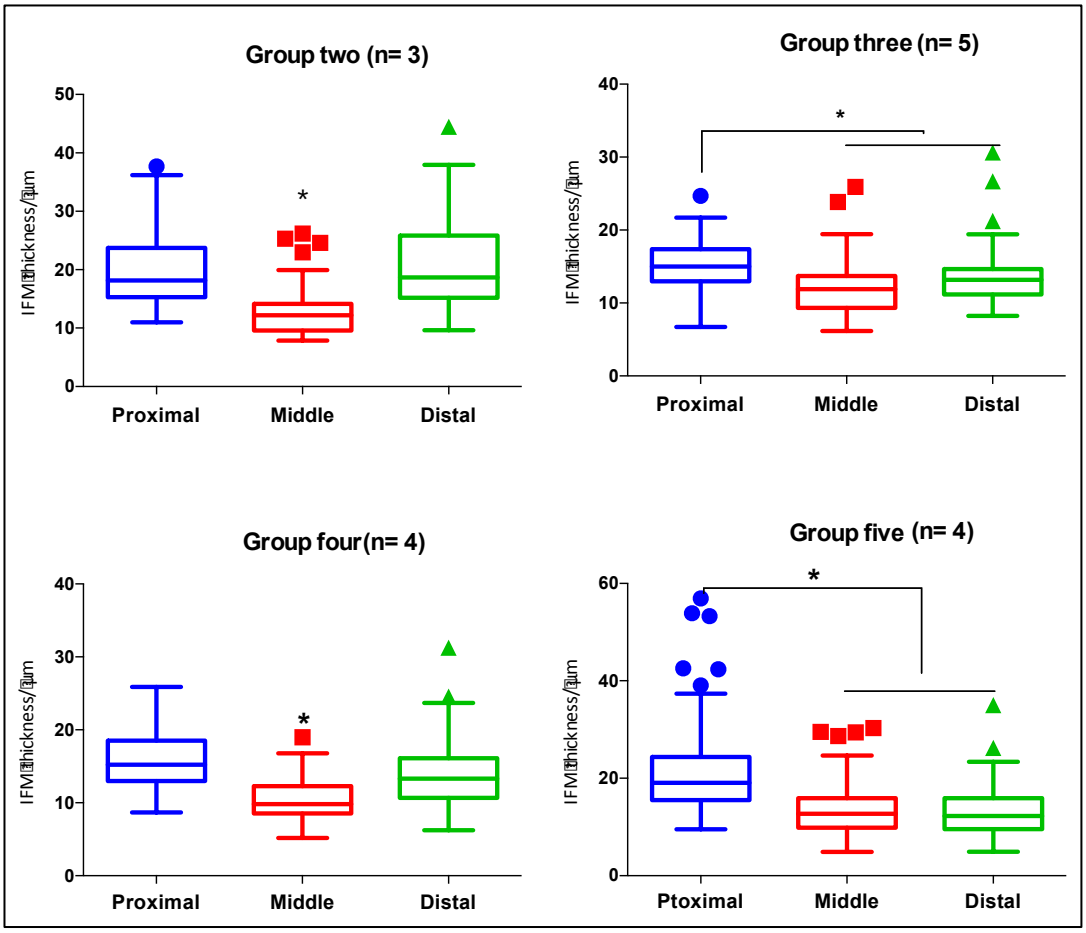

Figure 4.20: The IFM thickness between the tertiary fascicles in the proximal, mid and distal region in Group two (7-years-old), Group three (9-years-old), Group four (14-years-old) and Group five (17-20-years-old). Note the mid-metacarpal region shows the thinnest IFM and differs significantly from the proximal and occasionally distal regions, using Two-way ANOVA (Kruskal-Wallis test and Dunn's multiple comparisons test) (P value <0.05).

4.3.3.2.2.1.2 Age related difference

The IFM thicknesses of the tertiary fascicles were slightly decreased during ageing but this was not statistically significant.

4.3.3.2.2.1.2 IFM thickness between the secondary fascicles

4.3.3.2.2.1.2.1 Regional difference

This IFM was characterised by being thinner and occasionally disappeared at certain points between the secondary fascicles. The IFM of the secondary fascicles varied between regions and different areas within the same region with a range of 0.4μm to 17.5μm. In Group one there was no statistically significant differences between the proximal, mid-metacarpal and the distal regions. The average IFM thickness of group two (proximal, mid-metacarpal and the distal regions) was 4.54μm (±0.77 SD), 4.85μm (±1.14 SD) and 5.22μm (±1.93 SD) respectively. In Group two there was a significant difference between the proximal and the distal region but not with the mid-metacarpal region, in this group the distal region showed a thicker IFM than the proximal region, using Two-way ANOVA (Kruskal-Wallis test and Dunn's multiple comparisons test) (P value <0.05). In Group three, the mid-metacarpal region showed a thinner IFM compared to the proximal and dital regions, the average thickness was 3.47μm (±0.65 SD) in comparison to the proximal 4.59μm (±0.81 SD) and the distal region 4.63μm (±0.93 SD) (p value <0.05). Similarly, in Group four the situation is similar to the third group, where the mid-metacarpal region having the thinnest IFM in contrast to the proximal and the distal region (P value <0.05). Meanwhile, the IFM of the distal region was considerably thicker than the proximal and the mid-metacarpal regions. The average IFM thicknesses in the proximal, mid-metacarpal and the distal region was 4.34μm (±0.66 SD), 2.87μm (±0.45 SD) and 5.18μm (±0.88 SD) respectively. In Group five, the situation was reversed, where the IFM of the proximal region was thicker 4.07μm (±0.76 SD) than mi-metacarpal 3.41μm (±0.61 SD) and the distal region 3.41μm (±0.63 SD) (P value <0.05). Therefore the mid-metacarpal region has the thinnest IFM when compared to the proximal and the distal region, while in the two latter regions, the IFM thickness was not constant and altered between different groups (Figure 4.21).

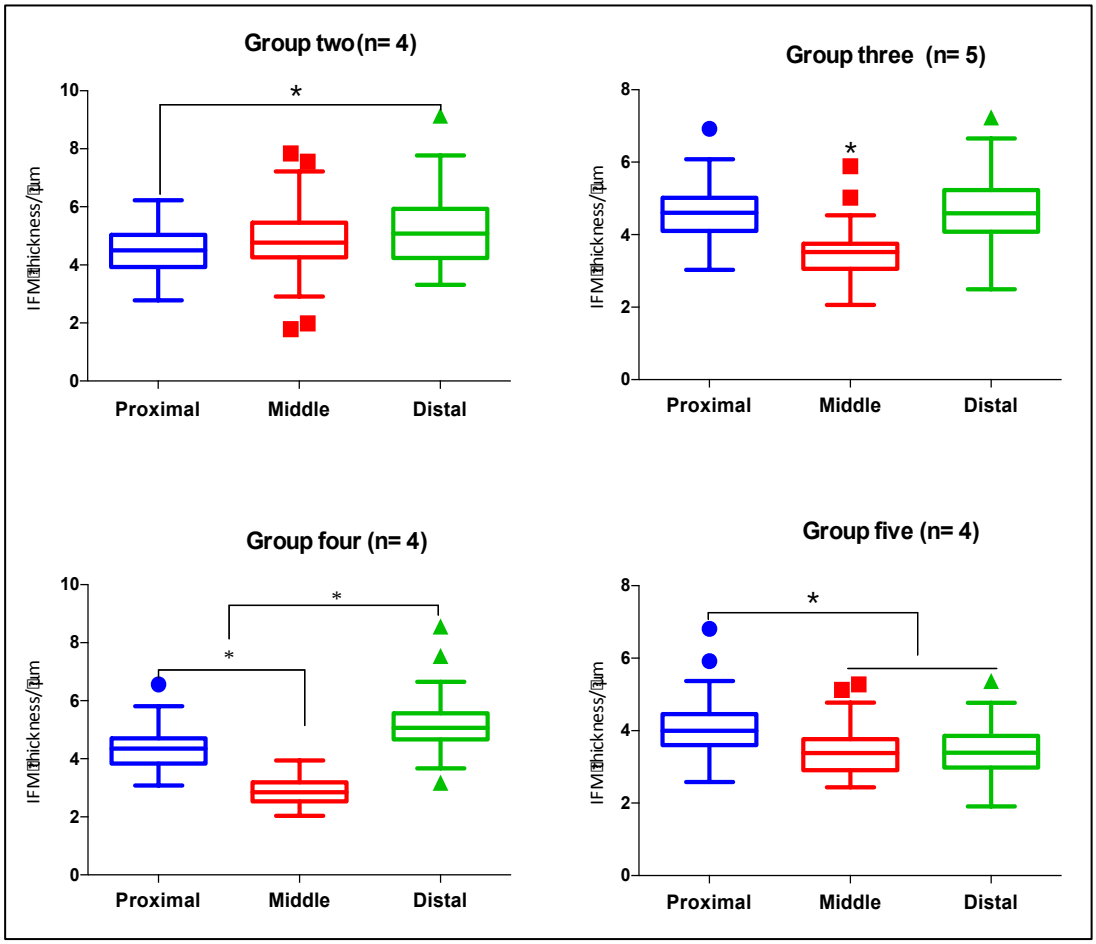

Figure 4.21: The IFM thickness between the secondary fascicles in the proximal, mid and distal region in Group two (7-years-old), Group three (9-years-old), Group four (14-years-old) and Group five (17-20-years-old). Note the IFM alters regionally, the mid-metacarpal region shows the thinner IFM and differs significantly from the proximal and occasionally the distal region (group three and four), using two-way ANOVA (Kruskal-Wallis test and Dunn's multiple comparisons test) (P value < 0.05).

4.3.3.2.2.1.2.2 Age related difference

The IFM of the secondary fascicles underwent further alteration during ageing. Their thicknesses decreased in the proximal, mid-metacarpal and distal regions, but only the mid-metacarpal and the distal regions showed a significant decrease with ageing (P value < 0.05) (Figure 4.22).

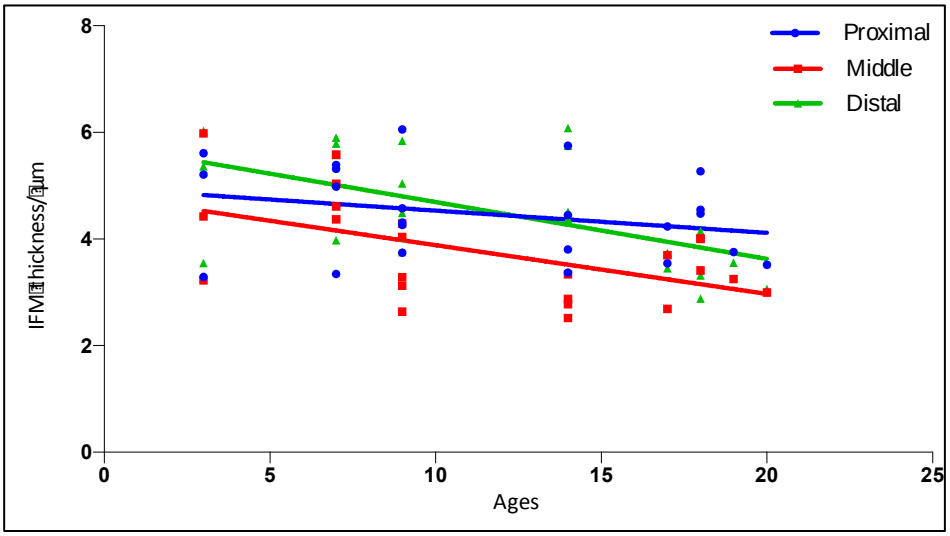

Figure 4.22: The average IFM thicknesses of the secondary fascicles in the proximal, mid-metacarpal and distal regions at different ages. The IFM thicknesses declined during ageing with the mid-metacarpal and the distal regions being significantly reduced using linear regression test (P value < 0.05).

Table 4.5: IFM thicknesses between the tertiary and the secondary fascicles in different regions and ages in equine SDFT. They include Group one (3-years-old), Group two (7-years-old), Group three (9-years-old), Group four (14-years-old) and Group five (17-20-years-old), (P=proximal, M=mid-metacarpal and D=distal metacarpal regions).

	IFM of the tertiary fascicles/µm														
	Group one			**Group two**			**Group three**			**Group four**			**Group five**		
Regions	**P**	**M**	**D**	**P**	**M**	**D**	**P**	**M**	**D**	**P**	**M**	**D**	**P**	**M**	**D**
Maximum	76.32	69.21	82.17	111.99	54.79	95.29	62.3	83.38	60.60	50.12	34.54	83.4	155.13	73.99	68.33
Minimum	3.17	1.33	2.5	2.38	2.38	2.38	2.38	2	1.12	2.38	1.58	2.38	1.19	1.19	1.78
Median	16.88	11.92	12.51	18.09	12.17	18.68	15.01	11.93	13.19	15.19	9.8	13.3	19.06	12.73	12.28
Mean	17.68	14.15	14.28	20.07	12.83	20.51	15.22	12.04	13.46	15.64	10.5	14	21.84	13.82	13.41
STD	6.56	6.70	5.36	6.42	4.218	7.56	3.44	3.74	3.76	3.86	2.74	4.79	10.78	5.83	5.46
STE	0.84	0.86	0.69	0.82	0.54	0.97	0.44	0.48	0.48	0.49	0.35	0.61	1.39	0.75	0.70
IFM of the secondary fascicles/µm															
Maximum	10.15	9.83	11.91	12.71	14.3	14.91	15.1	10.73	11.4	11.14	5.97	17.48	11.94	9.57	9.55
Minimum	0.79	2.38	1.19	0.79	0.79	1.59	0.39	0.79	1.19	0.59	0.79	1.58	1.19	1.59	0.79
Median	4.63	4.50	4.94	4.50	4.771	5.07	4.60	3.52	4.59	4.351	2.85	5.068	3.99	3.38	3.39
Mean	4.70	4.54	4.98	4.54	4.855	5.22	4.59	3.47	4.63	4.34	2.87	5.182	4.07	3.41	3.41
STD	0.85	0.73	1.01	0.77	1.143	1.19	0.81	0.65	0.93	0.66	0.45	0.8833	0.76	0.61	0.63
STE	0.11	0.09	0.13	0.10	0.1476	0.15	0.10	0.08	0.12	0.08	0.05	0.114	0.09	0.07	0.08

4.3.3.3 Cell nucleus

4.3.3.3.1 Cellular density

4.3.3.3.1.1 Regional difference

Numbers of cells in the fascicular matrix (FM) varied regionally and during ageing. Regionally, the mid-metacarpal and the distal regions had an apparent lower cellular density than the proximal but this was not statistically significant.

4.3.3.3.1.2 Age related difference

Interestingly, cellular density declined significantly after birth and then during ageing. Foetal tendon was characterised by a higher cellularity, which was approximately 4-5 times greater than that in the other groups in the proximal, mid-metacarpal and the distal regions (Table 4.6). Nuclei were regularly distributed between the collagen fibres in a uniaxial direction. The presence of this large number of nuclei did not stay constant after the foetal stage and it continued to decline in Group two and then slightly declined further during ageing (Figures 4.23). In the foetal tendons, the average number of nuclei were counted in 10 different fields of view (400X) was 238.2 (±56.33 SD) within a range of 111 to 336 nuclei, which significantly declined to 43.83 (±6.09 SD) (P value <0.0001) in Group one (range of 20 to 97 nuclei (400X)). Subsequently, the average cellular number also continued to decline to 26.33 (±4.79 SD) in Group two with a range of 8 to 57 nuclei. There was further significant decline between the young (Group one) and the mature horses (Group two) (P value < 0.05). In the third, fourth and the fifth groups the average numbers of intra-fascicular cells were 23.17 (±5.2 SD) (range of 3-60 nuclei), 24.86 (±4.62 SD) (range of 6-50 nuclei) and 22.47 (±4.35 SD) (range of 6-50 nuclei) respectively. The cellular density appeared to decline further in the third, fourth and fifth groups but not significantly. Overall there was a definitive correlation between cellular density and age. The cellular density was highest in the foetus and very young horses, and then declined to a definitive number after maturation (Figure 4.23).

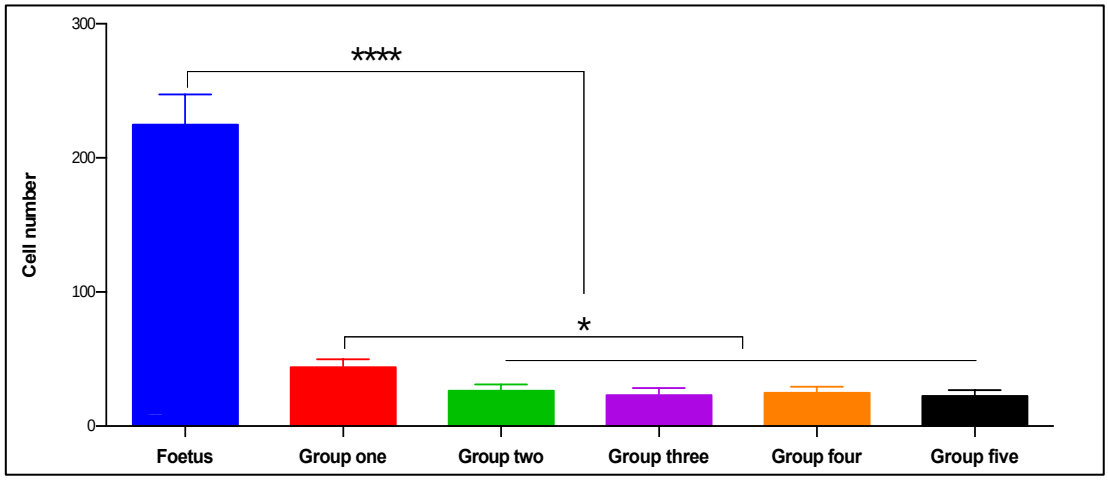

Figure 4.23: Intra-fascicular cellular density at different stages of life including foetal, Group one (3-years-old), Group two (7-years-old), Group three (9-years-old), Group four (14-years-old) and Group five (17-20-years-old). The intra-fascicular cellular density sharply declines after foetal life (P value < 0.0001) and then continues to decline significantly from Group one to Group two (P value < 0.05), (Error bars= SD).

4.3.3.3.2 Nuclear length

4.3.3.3.2.1 Regional difference

Length of the intra-fascicular cell nuclei varied regionally. There was approximately homogeneous intra-fascicular distribution of tenocytes in different regions with the mid-metacarpal region showing longer nuclei than those in the proximal and distal regions but it was not statistically significant (Table 4.6).

4.3.3.3.2.2 Age related difference

Interestingly foetal tendon was characterised by having a large number of small nuclei of oval or elliptical shape, which after birth were reduced in number and became more elongated. The average nuclear length increased significantly following birth and even after maturity (7-years-old) apparently continued to increase in length but this did not achieve statistical significance. In the foetal tendon, the average length of the nucleus in all regions (proximal to distal) was 10.15μm (±0.96 SD), which increased significantly to 15.39μm (±2 SD) in very young horses (Group one) (P value <0.001), then continued to increase until the horse became fully mature (7-years-old) (P value < 0.05), when they reached an

average length of 20.06µm (±1.41 SD). After maturity, the nuclear morphology apparently continued to alter but it was not significant, particularly from age 7 to 20 years old. In Groups three, four and five the average nuclear lengths were 19.09µm (±1.24 SD), 19.29µm (±1.72 SD) and 20.16µm (±1.24 SD), which did not showing significant variation when compared to Group two (Figure 4.24).

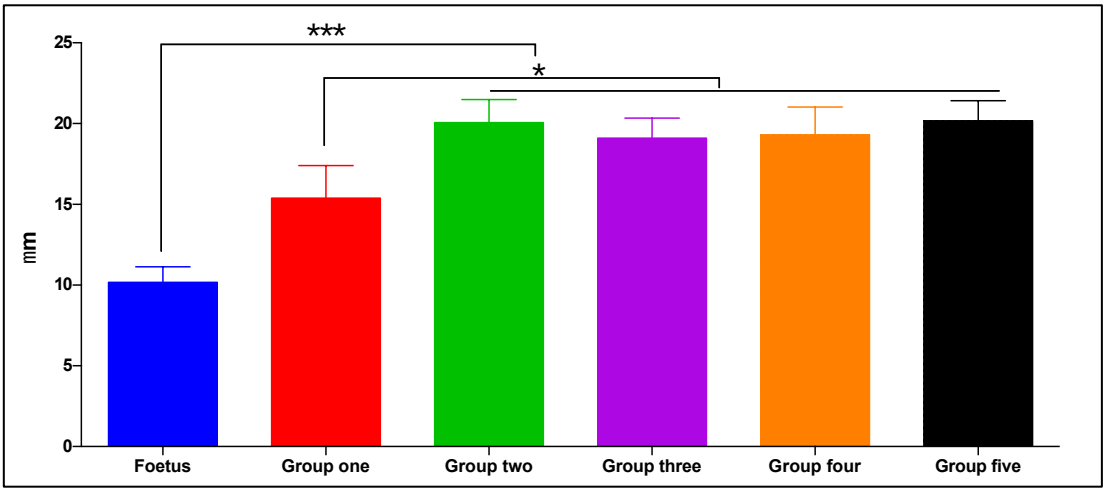

Figure 4.24: The nuclear length in the FM of different aged horses, including foetal, Group one (3-years-old), Group two (7-years-old), Group three (9-years-old), Group four (14-years-old) and Group five (17-20-years-old). The nuclear length significantly altered from foetal to Group one (P value < 0.001) and Group two (P value < 0.05). The nuclear length continued to increase in Groups three, four and five but was not statistically different using a two-way ANOVA (P value < 0.05), (Error bars= SD).

Table 4.6: The nuclear number and length of the fascicular matrix in different regions and ages in the equine SDFT. They include foetal, Group one (3-years-old), Group two (7-years-old), Group three (9-years-old), Group four (14-years-old) and Group five (17-20-years-old), (P=proximal, M=mid-metacarpal and D=distal metacarpal regions).

	Cellular density																	
	Foetus			**Group one**			**Group two**			**Group three**			**Group four**			**Group five**		
	P	**M**	**D**	**P**	**M**	**D**	**P**	**M**	**D**	**P**	**M**	**D**	**P**	**M**	**D**	**P**	**M**	**D**
Maximum	331	268	336	97	68	55	52	48	33	48	60	54	40	47	48	50	42	43
Minimum	111	167	188	23	20	29	8	9	9	11	5	3	6	11	8	8	6	9
Median	244.8	211.3	261.5	46.83	38.67	45	25	31.5	24	26	27.5	26.7	25	26.38	23.5	23.13	21.5	21.75
Mean	244.7	212.7	257.3	46.57	39.27	45.67	24.4	30.43	24.17	26.4	26.46	27.38	25.13	27.85	24.4	23.75	22.2	22.5
STD	16.56	5.94	20.71	6.87	2.56	5.54	3.56	4.92	2.98	4.13	4.88	2.44	3.12	4.77	3.96	3.97	2.73	2.34
STE	5.23	1.88	6.54	2.17	0.81	1.75	1.12	1.55	0.94	1.30	1.54	0.77	0.98	1.51	1.25	1.25	0.86	0.74
Nuclear length/ μm																		
Maximum	24.39	23.17	17.71	40.18	44.2	40.83	50.07	72.48	51.45	46.44	52.07	44.47	48.23	53.92	66.58	52.43	67.05	65.48
Minimum	2.11	3.76	3.53	5.88	3.51	4.7	6.88	7.38	4.57	6.65	5.28	4.92	5.46	4.92	4.22	7.73	7.52	7.38
Median	9.64	10.73	9.72	15.88	15.56	13.8	18.67	23.2	17.02	18.47	20.05	17.78	17.77	21.06	18.5	20.83	22.07	17.4
Mean	9.64	10.9	9.93	16.4	15.6	14.18	19.32	23.54	17.35	18.74	20.45	18.1	17.71	21.28	18.9	20.95	22.54	17.6
STD	2.10	2.39	1.86	3.04	2.94	2.69	4.63	6.17	3.50	2.95	3.33	2.34	2.93	3.79	3.14	3.41	4.09	2.92
STE	0.17	0.19	0.15	0.24	0.24	0.21	0.37	0.50	0.28	0.24	0.27	0.19	0.23	0.30	0.25	0.27	0.33	0.23

4.3.3.4 Vascularity

4.3.3.4.1 Regional difference

In the foetal tendon, the proximal region appeared to be more highly vascularised than the mid-metacarpal or the distal region, but the difference was statistically significant only with the distal region (P value < 0.05). The average numbers of counted blood vessels from the proximal to the distal were 13.1 (±2.99 SD), 8.75 (±2.03 SD) and 2.5 (±0.79 SD) per 10 fields (100X). In Group two the mid-metacarpal region only had a significantly fewer blood vessels compared to the proximal region (p value < 0.05), their numbers from the proximal to the distal were 6.83 (±2.04 SD), 4.66 (±1.35 SD) and 6 (±2.82 SD). Similarly in Group three the mid-metacarpal region had a significantly fewer blood vessels than the proximal and the distal regions (P value <0.05). Their average numbers from proximal to distal were 6.6 (±1.96 SD), 4.6 (±0.97 SD) and 6.72 (±1.62 SD). In Group four, the mid-metacarpal region had a significantly lower level of vascularity (p <0.05) compared to the proximal region. The average numbers from proximal to distal regions was 8.2 (±1.99 SD), 5.32 (±1.58 SD) and 6.32 (±1.96 SD) (Figure 4.25) (Table 4.7). The foetal tendon was characterised by having a well-defined IFM, containing different sized blood vessels that varied regionally. This variation could also be observed after birth, when the mid-metacarpal region in particular manifested a lower level of vascularity. A limitation to this data may be that the observed regional variation in vascularity could due to the orientation and different levels of the tissues during cutting.

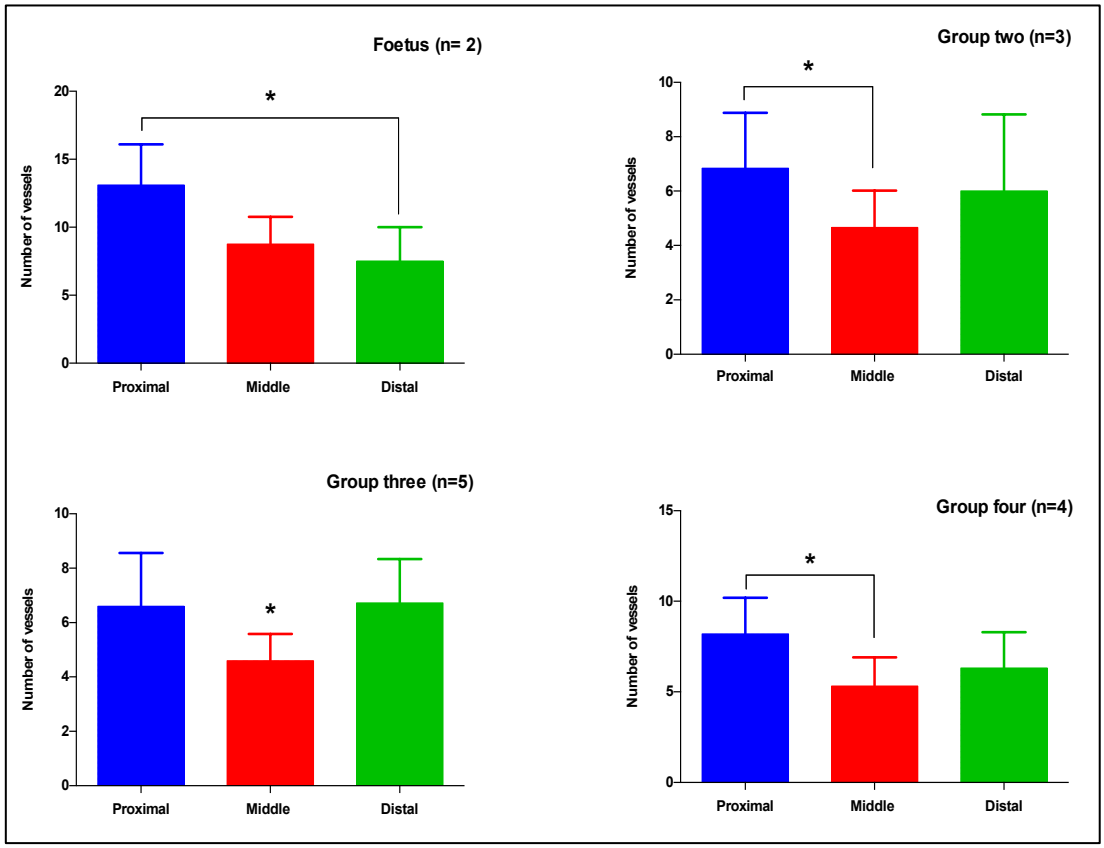

Figure 4.25: Vascularity of the equine SDFT in the proximal, mid-metacarpal and the distal regions of different ages, including foetal, Group two (7-years-old), Group three (9-years-old) and Group four (14-years-old). The proximal region shows the highest level of vascularity while the mid-metacarpal region has a lower level of vascularity than the proximal and the distal regions, using a two-way ANOVA (P value < 0.05), (Error bars= SD).

4.3.3.4.1 Age related difference

It was observed that vascularity slightly decreased during ageing but it was not significant (Table 4.7).

4.3.3.5 Inflammatory cells or necrosis

All SDFT samples were viewed under different magnification powers (40X, 100X and 400X and no inflammatory cells or necrosis were identified.

Table 4.7: The numbers of blood vessels indicative of vascularity in different regions and ages of the equine SDFT. They include foetal, Group one (3-years-old), Group two (7-years-old), Group three (9-years-old), Group four (14-years-old) and Group five (17-20-years-old), (P=proximal, M=mid-metacarpal and D=distal metacarpal regions).

	Vascularity (average number of blood vessels/ 10 fields (100 X magnification)																	
	Foetus			**Group one**			**Group two**			**Group three**			**Group four**			**Group five**		
	P	**M**	**D**	**P**	**M**	**D**	**P**	**M**	**D**	**P**	**M**	**D**	**P**	**M**	**D**	**P**	**M**	**D**
Maximum	19	12	12	7.33	8.66	8	9.66	7	10.67	8.8	6.4	9.6	12.25	8.5	9.25	10.25	9	10.5
Minimum	10	6.5	4	3.33	2.66	4	4	2.33	2.66	3.6	3	4	5.5	2.75	3	2.75	3.5	5.75
Median	12.75	8.5	7.75	4.5	5.16	6.33	7.16	4.66	6.83	7.6	4.5	6.6	8	5.37	6.87	6.37	5.87	7.75
Mean	13.1	8.75	7.5	5	5.56	6.06	6.83	4.66	6	6.6	4.6	6.72	8.2	5.32	6.32	6.6	5.92	7.67
STD	2.99	2.03	2.50	1.44	2.08	1.35	2.04	1.35	2.82	1.96	0.97	1.62	1.99	1.58	1.96	2.43	1.61	1.30
STE	0.94	0.64	0.79	0.45	0.65	0.42	0.64	0.42	0.89	0.62	0.30	0.51	0.63	0.50	0.62	0.77	0.51	0.41

4.4 DISCUSSION

4.4.1 GENERAL OBSERVATION OF SDFT

This study found the histological structures of the equine SDFT to be similar to previous descriptions in the literature. It is composed predominantly of collagen fibres that are outlined by the IFM (Kannus, 2000, Benjamin et al., 2008). Collagen fibres of the fascicles are undulated (crimped) and oriented regularly on the longitudinal axis of the tendon (Patterson-Kane et al., 1997a). We found that the crimp was altered during ageing being clearly defined in the foetal tendon, becoming less distinct in young to mature horse and being mainly absent in aged horses (Figures 4.6 - 4.8). In several studies the degree of crimp angle in equine SDFT has been recorded (Wilmink et al., 1992, Patterson-Kane et al., 1997a). The crimp angle and length at the mid-metacarpal region was reported to decline from 27˚ and 38μm in the foetus, to 19˚-20˚and 17μm-19μm in young horses and to 12˚-17˚ and 11μm-15μm in adults (Wilmink et al., 1992, Patterson-Kane et al., 1997a). In addition studies on the chicken metatarsal and mouse-tail tendons have also found that the crimp angle decreases during ageing (Shah et al., 1982, Legerlotz et al., 2014).

Typically tenocytes are distributed and oriented between the collagen fibres in a uniaxial direction (Kannus, 2000, O'Brien, 2005). In this study it was found that foetal tendons were hyper-cellular having a large number of uniformly shaped nuclei but after birth and particularly around three years old the FM cellular density declined considerably, by as much as 4-5 times (Figure 4.23/ Table 4.6). We also demonstrated that after birth, a heterogeneous nuclear morphology in terms of nuclear shape and length was observed (Figure 4.24). In the foetal SDFT the maximum nuclear length was 24μm whilst after birth it became longer to reach a maximum of 72μm in Group two (Table 4.6). Similarly, a study on ovine calcaneal tendon has also shown that cellular density was significantly decreased with age (Russo et al., 2015). The cellular nuclei aligned themselves with the undulating pattern of the collagen fibres, which apparently undulated with the fibres. Moreover, tenocytes communicated with each other through different gap communication points, through their end-to-end and possibly side-to-side (McNeilly et al., 1996, Clegg et al., 2007).

The IFM separates the fascicles from each other and recently research has described the IFM components in detail and their potential role in the mechanical function of tendon (Thorpe et al., 2013c, Thorpe et al., 2015b). In this study it was found that the IFM is present from the proximal to the distal regions of the tendon, intimately attached to fascicles and outlining them (Figures 49 - 4.11). It is likely that the IFM has the affinity to attract water, possibly due to the presence of a large proportion of negative charge components such as the electrostatic GAG (Adams et al., 2006). This property keeps the ECM and the cells hydrated, possibly protecting the tissue from environmental injury such as dehydration and thermal injury particularly during mechanical movement and assisting sliding of fascicles over reach other (Roughley and Lee, 1994, Iozzo and Murdoch, 1996, Thorpe et al., 2013c). Our future work should concentrate on the role of the IFM, its relationship to attracting water molecules and in aiding prevention and treatment of tendon injury (O'Sullivan, 2007).

The IFM is composed of loose irregular connective tissue that contains blood vessels, nerves, fat droplets, non-collagenous proteins and a huge number of different-shaped and apparently non-organised cells (Kastelic et al., 1978, Kannus, 2000, Benjamin et al., 2008). In this study it has been demonstrated that the collagen fibres through the IFM on their lateral aspect communicated with those fascicles of the FM (Figure 4.9 - 4.11). Therefore, IFM and the fascicles appeared intimately connected to each other in that the IFM appeared to be a part of the fascicles but was less dense and irregular than the fascicular matrix (FM) (Figures 4.9 - 4.11). In addition, staining of the IFM with Safranin-O and Alcian blue stains were more marked than the FM. This would indicate that the IFM contains a larger amount of positively charged proteins such as PGs and GAGs (Bjornsson, 1998, Terry et al., 2000, Yang et al., 2012).

Elastic fibres, approximately up to 2% of dry weight, are reported as being distributed through ECM of human tendon, (Elliott, 1965, Jozsa and Kannus, 1997, Kannus, 2000). In this study elastic fibres in the IFM were arranged in different orientations. The presence of the elastic fibres in the IFM would indicate that the IFM of equine SDFT contributes to the elasticity to the tendon, assisting in mechanical stretching of the tissue during recoiling action (Thorpe et al., 2012,

Thorpe et al., 2016a). In a study of bovine deep digital flexor tendon (DDFT), it has been demonstrated that elastic fibres are deposited primarily around clusters of tenocytes, between the collagen fibres of the FM and IFM playing a role in cellular function and the mechanical deformation of the IFM (Grant et al., 2013).

4.4.2 HISTOLOGICAL SCORING

4.4.2.1 ECM organisation

In this study we aimed to detail the ECM organisation of equine SDFT with histological sections in different regions and ages. The ECM predominantly consisted of the intra-fascicular collagen fibre bundles (the FM) and the IFM. Histological studies have demonstrated that collagen fibres in tendons and ligaments, including the SDFT, are predominantly aligned parallel to each other and to the longitudinal axis of the tendon (Provenzano and Vanderby, 2006, Sodersten et al., 2013). However, electron microscopy studies have reported that not all fibrils are arranged parallel to each other with some of them being interwoven, inter-digitated or oriented transversely forming spiral plaits inside the body of the fascicles (Jozsa et al., 1991, Kannus, 2000). However the degree of angulation or deviation of the fascicles and their IFM are not currently described in the literature and knowledge of their histological arrangement could aid to understanding of how the fascicles in equine SDFT are inter-connected. The degree of FM and IFM angulation could also determine which regions or areas are regularly exposed to heavy load and histological alteration during ageing.

The fascicle is considered as a mechanical unit that transfers the mechanical force within the tendon from the muscles to the bones (Kastelic et al., 1978, Wang, 2006). Fascicles extend longitudinally through the length of the tendon, varying from tendon to tendon and at different levels within the same tendon (Haraldsson et al., 2008, Thorpe et al., 2014b). In an anatomical study of human Achilles tendon it was found that fascicles rotate distally and form a spiral configuration through the distal third (Szaro et al., 2009) of the tendon. The equine SDFT is a long tendon, composed of different sized fascicles which histological features showed variation with age. Moreover, we found that the fascicles and IFM extended longitudinally and parallel to the longitudinal axis of the tendon. However, not all of them were aligned complexly parallel and a significant number were slightly angulated. Both the FM

and IFM in the mid-metacarpal region demonstrated a lower degree and percentage of angulation compared to the proximal and the distal metacarpal regions (Figures 4.15- 4.18). The degree and percentage of angulation were not correlated with age. Un-axial continuity of the fascicles possibly signifies that fascicles might take on a certain form of twisting or spiral configuration (Shearer, 2015b). In a study using polarized light, interference, and phase contrast microscopy on bovine and rat-tail tendons revealed crimped fibres characterised by being intertwined and twisted, further suggesting a spiral organization of fibres when focused on different planes from resin-embedded sections (de Campos Vidal, 2003). Furthermore, Yahia and Drouin found that there are two distinct helical patterns of collagen structures in both canine patellar tendon (PT) and anterior cruciate ligament (ACL), planar and wavy helical patterns, with variation in the degree of collagen waviness in both patterns (Yahia and Drouin, 1989). Different studies have suggested various models of fascicular orientation in human patellar, rat-tail and bovine Achilles tendons. These models demonstrated that crimped and un-crimped collagen fibrils were aligned and parallel with the longitudinal axis of the fascicles or helically arranged on their longitudinal axis or around the longitudinal axis of the fascicles (Grytz and Meschke, 2009, Shearer, 2015b, Shearer, 2015a). In this study it was found that the proximal and distal regions showing higher levels of fascicular angulation (Figures 4.15 and 4.16). These areas also represented the highest proportion of fascicular inclination in the un-axial direction, which might indicate the highest degree of spiral or twisted orientation of the fascicles. Therefore these two regions may have more flexibility than the mid-metacarpal region (Crevier et al., 1996).

4.4.2.2 IFM thickness

The IFM thickness of both secondary and tertiary fascicles was measured in all groups except the foetal tendon, due to its small size, which would not be in proportion with the mature size. A study on ovine calcaneal tendon previously demonstrated that foetal tendons have more developed IFM than in mature (Russo et al., 2015) but did not show its quantification with ages. In our study, different ages of horses were used particularly after the skeleton and the tendon reach their maximum size after two years old (Birch et al., 1999b, Bennet, 2008, Lawrence, 2008). In this study it was found that the mid-metacarpal region in all groups showed the thinnest IFM around both the tertiary and secondary fascicles (Figures 4.20and 4.21). The

proximal metacarpal region showed thicker and well-developed IFMs. In the distal region, the IFM thickness of the tertiary fascicles was approximately similar with those in the mid-metacarpal region.

The IFM is an essential part of the tendon due to the presence of large amount of different components such as PG, GAG, elastic fibres, vessels and cells (Jozsa and Kannus, 1997, Kannus, 2000, Yang et al., 2012). In this study, it was found that the IFM width of tertiary and the secondary fascicles apparently decreased during ageing but only the IFM around secondary fascicles showed a statistical significance. In a study of equine IFM it has been shown that protein abundance is stable with age but the number of neopeptides is decreased in aged IFM. This altered matrix turnover may subsequently contribute in the age-related injury of tendon (Thorpe et al., 2016b). Mechanical testing of the IFM has shown that the sliding capacity decreases with increasing age leading to a decrease of the IFM's ability to withstand repetitive mechanical loads and a potential risk of fatigue injury during ageing. However, the IFM components have not been comprehensively investigated to find an age-related alteration that may affect tendon function (Thorpe et al., 2013c, Thorpe et al., 2013a).

4.4.2.3 Intra-fascicular cellular density and nuclear length

Intra-fascicular cellular density did not significantly vary regionally, but there was a great decline in the cellular number between foetal and mature SDFT. Foetal SDFT was characterised by hyper-cellularity and the average number was 4-5 times greater than in aged horses (Figure 4.23) Different studies on rabbit and equine tendons have reported that tenocytes undergo a series of morphological changes, where the numbers of cells also decrease during ageing; cells become thinner as their cytoplasmic processes becoming longer, denser reducing their inter-cellular gap junction and biosynthetic capacity (Ippolito et al., 1980, Moore and De Beaux, 1987, Goodman et al., 2004, Stanley et al., 2007, Young et al., 2009). In a recent study of cellular maturation in ovine calcaneal tendon, it was found that the foetal tissue is hyper-cellular and its cell density altered during foetal and adult life. It was recorded that cellular density significantly declined from 30% to 14% during the foetal life in a period from the mid to late gestation period and then to 5% in adult tendon (Russo et al., 2015). In this study it was demonstrated that the SDFT intra-fascicular cellular

number alters during ageing. After birth, cellular number rapidly declined by 76.35% (4-5 times) in young horses (Group one) and then continued to decline by 46.77% in the mature horse (Group two), finally declining to 13.4% in aged animals (Group five). A study measuring the DNA content in both SDFT and the CDET, found that the DNA content significantly decreased with ageing only in CDET (Birch et al., 1999a). However, another study showed that DNA content decreased in SDFT during ageing (Batson et al., 2003). These findings suggest that the number of cells possibly decline during ageing. However, these studies have not specified which cells or which parts of the ECM/IFM were measured. In the present study only the FM nuclei were measured. It was found that the number of cells were decreased during ageing, suggesting that the tissue turnover and metabolic process may decline during ageing subsequently leading to an age accumulated injury with the tissue becoming more prone to injuries (Birch et al., 1999b). In a recent study, where the mRNA and protein amounts have measured in cells from SDFTs from horses of different ages (3-30 years old), it was found that mRNA and the protein levels did not decline with ageing (Thorpe et al., 2015c). Whilst the conclusions of the Thorpe and others study support this hypothesis, it is considered by many that the tenocyte ability declines during ageing, resulting in reduced matrix turnover and less ability to repair tissue micro-damage compared to the young tendon. In our study we have shown differences in cell number between foetal and mature horses as well as between young and mature horses, which could lead to an overall failure of synthetic activity (Watts et al., 2011).

The mid-metacarpal region had cells of a slightly longer nucleus than the proximal and the distal regions (Table 4.6). The general average nuclear length in the mid-metacarpal region of all groups was greater by an amount of 9.26% and 18.45% than the proximal and distal regions respectively but statistically it was not significance. This regional variation could indicate that the cellular nuclei of the mid-metacarpal region are more stable and active than either of the other two regions, while it is less vascular and more prone to injury (Patterson-Kane et al., 1998, O'Sullivan, 2007). Another possibility could be related to the collagen fibres arrangement, where the collagen fibres undergo tensional forces, which subsequently make the tenocytes straighter (Murray and Spector, 1999, Legerlotz et al., 2014). A study on cultured

cells taken from three different regions of equine SDFT found that there were little differences in cellular morphology (Hosaka et al., 2010).

In this this study it was found that nuclei of foetal SDFT were small and varied in shape, ranging from round to a cigarette form. In higher magnification they were less dense in staining and contained a number of darkly stained granules (Jozsa and Kannus, 1997). After birth, the nuclei underwent further alterations in terms of size, shape and affinity to stain, which have been also shown by other researchers (Jozsa and Kannus, 1997, Kannus, 2000). In our study it was found that there was a significant alteration of the nuclear morphology during ageing, particularly from foetal to young and then to the adult groups. The nuclear length significantly increased between foetal and young horse (Group one), their average nuclear length increasing by an amount of 51.62%, and then from young to adult their length increased by 30.34%. After maturation (7-years-old), the nuclear length continued to alter, becoming either longer or shorter than the average length of a mature horse's, but this was not statistically significant. In a study on rat-tail tendon, it was found that the foetal tendons are hyper-cellular and two types of cells have identified: the round-shaped (tenoblast) and longer flattened-shapes (mature tenocytes) (Kostrominova et al., 2009). Electron microscopy of these two cell types taken from the musculotendinous junction (MTJ) region *in vivo* showed that foetal tenoblasts did not have a preferential ECM but the adult tenocytes were surrounded by a well-defined ECM (type I collagen) (Kostrominova et al., 2009). These results suggest that tenocytes in mature tendon were more developed and surrounded by abundant ECM than the foetal tendon, which is inversely smaller and surrounded by less dense ECM.

4.4.2.4 Vascularity

SDFT, like other long tendon, is vascularised from different routes; the musculotendinous junction (MTJ), surrounding tissues and the osteotendinous junction (OTJ). The rate of tendon oxygen uptake is 7.5% lower than in the muscles and in aged animals metabolic activity is shifted from aerobic to a slightly anaerobic pathway (Vailas et al., 1978). This anaerobic condition results from declining capillary blood flow and continuous mechanical loading (Astrom, 2000).

In this study it was found that only in four groups (foetal, Groups two, three and four) was there a regional variation in the vascularity of the tendon (Figure 4.25). The mid-metacarpal region showed lower vascularity than proximal and distal regions. A study of human calcaneal tendon found that the middle portion of the tendon was less vascular in amounts of 36.39% and 23.02% than points of calcaneal and area near the MTJ (8 cm far from the calcaneal point) respectively (Carr and Norris, 1989). This could possibly be due to that the primary blood supply of the mid-metacarpal region is intra-tendinous rather than having peripheral supplementation, where the mid-metacarpal region has a continuation of vessels from the proximal region (Kraus-Hansen et al., 1992). By using Doppler ultrasonography, it was found that vascularity in individual tendons varied over time and was affected by exercise (Cook et al., 2005).

4.5 CONCLUSION

This study concluded that the typical histological configuration of equine SDFT was approximately similar in the different regions but varied during development and maturity with the crimp and cellularity declining during ageing. The IFM is a vital part of the tendon, having a positive reaction to histological staining for PG, GAG and elastic fibres. The ECM (FM and IFM) was less regular (angulated) in the non-tensional region and did not alter during ageing. The cellular morphometry was not stable either regionally or during ageing. Foetal tendon was hyper-cellular, and the number of cells sharply declined in number by three years of age and then reaching their lowest number by approximately seven years of age (mature). Moreover, the tensional region (mid-metacarpal) showed more developed nuclei than the non-tensional regions, as well as low vascularity. Understanding tendon histology will facilitate the understanding of age-related predisposition to injury and the evaluation of the extent to which the tendon component is involved in tendinopathy. This will be useful to develop a particular age related programme of exercise induction in order to protect SDFT from injury.

4.6 IMPLICATION

IFM is a complex structure, contains different components and it needs further exploration in order to understand their important value particularly in tendon

development and injury and repair. This scoring method can be applied on other tendons and ligaments such as CDET and DDFT.

CHAPTER FIVE

DEVELOPMENT OF CHONDROID METAPLASIA IN EQUINE SDFT IN ELDERLY HORSES

5.1 INTRODUCTION

The equine SDFT is a highly specialised connective tissue, acting to transfer force from muscle to the bones (Getty, 1975, Pasquini et al., 2003, Durham and Dyson, 2011). The SDFT, like other similar connective tissues, undergoes morphological, mechanical, pathological and biochemical alterations during ageing including changes in both the cellular and extracellular matrix (ECM) (Birch et al., 1999a, Lin et al., 2005b, Thorpe et al., 2015c). The cells can alter their metabolic activity according to the surrounding environment, such as production and/or degradation of the ECM components, which vary regionally in the tendon between tensional and compressive regions (Vogel and Koob, 1989, McNeilly et al., 1996, Tuite et al., 1997). It has been shown in equine SDFT, that when *in vitro* loading causes damage to the ECM, cells became rounded and the inflammatory markers (cyclooxygenase-2 and interleukin-6), metalloproteinase-13 and collagen degradation markers were increased (Thorpe et al., 2015a).

During ageing tendons experience different types of disorders that can be categorised into tendinosis and tendinitis. Tendinitis is an acute inflammatory reaction to sudden injury or infection but tendinosis is a chronic degenerative change of the tissues without notable inflammatory reactions (Paavola et al., 2002). Tendinosis is thought to be a sequel of micro-traumas that occurs as a result of continuous degeneration of the tendon in response to overuse (Bass, 2012). In both instances tenocytes undergo both metabolic and morphometrical alterations (Sharma and Maffulli, 2005). In tendinosis, tenocytes increase in number and become more rounded to form more fibrocartilage-like cells. These fibrocartilage-like cells produce a variety of ECM such as collagens, proteoglycans, and non-collagenous proteins including elastin, which then form localised areas of chondroid metaplasia (Benjamin et al., 1991, Benjamin and Ralphs, 2004).

In equine tendinopathy (tendinitis) there is an increase in the amount of aggrecan, collagen-II, GAG, tenocytes MMP activity, vascularisation, and moderate inflammatory cells (Cadby et al., 2013, Jacobsen et al., 2015). Moreover, it has been demonstrated that in the advanced stage of tendinitis in human Achilles tendon there are areas of hyalinisation and possibly intra-tendinous ossification (Majeed et al., 2015). Researchers documented that the evidence of ossification is considered as

pathological tendinitis in man and horse. Ageing is considered as a contributing factor of microscopic degeneration of the tendon (Birch et al., 1999a). Long term degeneration stimulate tenocytes to produce specific ECM components that develop focal areas of chondroid metaplasia which is possible to be the site for ossification in the future (Lui et al., 2009, Tamam et al., 2011). The hypothesis is that equine SDFT undergo microscopic degeneration during ageing and produce focal areas of chondroid metaplasia. We aim to prove this hypothesis by describing the histological development of chondroid metaplasia in the elderly equine SDFT.

5.2 MATERIALS AND METHODS

5.2.1 SAMPLES

SDFT samples were taken from aged Thoroughbred and Thoroughbred cross horses and younger horses (Chapter four) euthanized for reasons other than orthopaedic disease or injury. Samples were obtained from a commercial abattoir (Potters, Taunton or Wooton Bassett). The study was assessed and approved by the University of Liverpool, Veterinary School Research Ethics Committee (VREC) (study 214). The equine SDFT samples were taken from three different regions (proximal metacarpal, mid-metacarpal and the distal metacarpal). From each region a sample approximately 1cm in length was selected from the central area of the tendon as described in Chapter four (Section 4.3.3, Histological scoring), were further examined in order to identify any chondroid metaplasia addition to the structural data detailed in Chapter four (see 4.2.2, for sample preparation). After staining sections with H&E, the entire surface of the sections was assessed for histological scoring and finding further age related alteration under different magnification powers (100X and 400X). Evidence of chondroid metaplasia was further explored using various histological stains, immunohistochemistry (IHC) and transmission electron microscopy (TEM).

Table 5.1: Number of SDFT samples from different legs and ages that have intra-fascicular chondroid like body (ICB), (P. Proximal, M. Mid-metacarpal, D. Distal, Rt. Right and Lf. Left).

Age/ Years	Number	Regions			Side	Paired limb	Note
17	1	P	M	D	Both	1	These SDFT samples were considered as the aged group
18	2	P	M	D	Both	1	
19	1	P	M	D	Rt	-	
20	1	P	M	D	Rt	-	

5.2.2 SPECIAL STAINS AND IMMUNOHISTOCHEMISTRY (IHC)

In addition to H&E staining and scoring for the ECM organisation in both the fascicular (FM) and inter-fascicular matrices (IFM), sections from the aged group were stained with different special stains (Toluidine blue, Safranin-O, Alcian blue-PAS and Modified Von Kossa's stains) in order to further identify the structural components of these ICBs such as:

1- Proteoglycan (PG) and glycosaminoglycan (GAG) associated with the presence of a cartilaginous tissue. In order to confirm the presence of these component, different special stained were used such as Toluidine blue, Safranin-O, Alcian blue-PAS.

2- Identification the presence of calcium and cartilaginous matrix associated with chondroid tissue.

3- IHC was used to confirm the presence of some specific PGs and collagen type II that associated with chondroid metaplasia.

5.2.2.1 Toluidine blue

Toludine blue is a basic thiazine metachromatic stain, has the affinity to stain acidic components of the tissue such as sulphates, carboxylates, and phosphate radicals. The tendon components such as DNA, RNA and GAG are polyanionic substance whereas most of the proteins are polycationic. Thus, Toluidine blue in the tendon stains DNA, RNA, chromatin and the GAGs, which displayed a purple metachromatic colour (Schmitz et al., 2010). SDFT sections were initially deparaffinised through xylene (2X 5 minutes) and rehydrated through the graded alcohols (100%, 96%, 85% and 70%) to finish with distilled water. Sections were stained with a diluted toluidine blue (1:10) for 30 seconds and then rinsed in water. After that the sections were rinsed in 0.2% acetic acid for 30 seconds and washed under running tap water until the background became almost colourless. Then the sections were blotted with a fibre free paper and dried briefly using a fan-assisted oven with the sections finally being placed into xylene and mounted in Di-N-Butyl Phthalate in Xylene (DPX) (Sigma-Aldrich, UK). The stain presented the nuclei and the background stain shades of pale blue and mast cell granules such as DNA, RNA, Nissl substances and the GAGs as a metachromatic purple colour.

5.2.2.2 Safranin-O and Alcian blue/PAS

This was performed as detailed previously in Chapter Four (Section 4.2.5.2)

5.2.2.3 Modified Von Kossa's stain

This stain was used to identify the presence of calcium deposition through the ECM. The sections were dehydrated through the graded alcohols down to distilled water (as described in the previous sections). Silver nitrate (5%) was filtered onto the sections and then exposed to a strong light (500 watt floodlights about 0.5 meters above the sections) for 15 minutes. Sections were washed in three changes in distilled water, counter stained with 1% neutral red for 1 minute and then washed thoroughly in distilled water. Finally the stained sections were blot air dried and quickly dehydrated through absolute alcohols (2X 100% alcohols), cleared (2X xylene) and mounted in DPX. The results demonstrate that the deposited calcium have black colour and the osteoid material is red in colour.

5.2.2.4 Immunohistochemistry (IHC)

The sections initially were deparaffinised in xylene (2X 10 minutes) and rehydrated through a graded ethanol (100%, 95%, and 70%) to distilled water. Then sections treated with 3% H_20_2 for 10 minutes in order to inhibit endogenous peroxidase activity and then washed in distilled water (2X 10 minutes). Sections were pre-treated with chondroitinase ABC (Sigma-Aldrich, UK) (0.5 U/ml) in 100 mM Tris-HCL pH 7.2-7.4 for 30 for 30 minutes and washed with Tris buffer saline-Tween (0.05%) (TBST) for 5 minutes. Then sections were blocked with 20% goat serum (PCN500, Invitrogen, CA, USA) in TBST for 1 hour at 25°C. After discarding the goat serum, the primary antibodies (mouse monoclonal IgG) were directly applied at the standard concentration diluted in a 5% goat serum of TBST (see Table 4.3). Sections were incubated with primary antibody overnight at 4° C. Two negative controls were included, in the first TBST was applied instead of the primary antibody, whist for the second control the mouse monoclonal IgG isotope was applied instead of the primary antibody. Following washing with TBST for 5 minutes, sections were incubated with peroxidase conjugated secondary antibodies, Goat anti-mouse IgG (Sigma-Aldrich, UK) 1:50 dilution of 20 % goat serum in

TBST for 1 hour in a hybridizer at 25° C. After washing with TBST for 5 minutes, the staining was developed with 3, 3-diaminobenzidine (Sigmafast DAB, Sigma Aldrich, UK) for 1 minute and then washed with distilled water (3X 5 minutes). The nuclei were counterstained with Mayer's haemalum for a few seconds, washed gently with tap water and then dehydrated through graded ethanols, cleaned with xylene and mounted with DPX.

(Note for immunostaining of collagen type II, the sections were not pre-treated with chondroitinase ABC. The primary antibody was the polyclonal rabbit IgG and the secondary antibodies was goat anti-rabbit IgG)

Table 5.2: List of the primary and secondary antibodies used for immunohistochemistry (IHC) on paraffin embedded sections for detection of ECM macromolecules of the ICB.

Primary Antibody	Dilution	Antibody recognition site	Manufactures
Decorin (DECN 70.6) Mouse monoclonal IgG	1/50	Specific for the core protein of decorin	Donated by B. Caterson/ C Hughes (Cardiff University)
Biglycan (PR8A4) Mouse monoclonal IgG	1/50	C-terminal amino acid sequence of human biglycan	Donated by B. Caterson/ C Hughes (Cardiff University)
Aggrecan (7D1) Mouse monoclonal IgG	1/10	G1 and chondroitin sulphate attachment domains	Donated by B. Caterson/ C Hughes (Cardiff University)
Chondroitin-4-sulphate (2B6) Mouse monoclonal IgG	1/100	Chondroitinase ABC-generated-4 sulphated CS stub	Donated by B. Caterson/ C Hughes (Cardiff University)
Chondroitin-6-sulphate (3B3) Mouse monoclonal IgG	1/100	Chondroitinase ABC-generated-6 sulphated CS stub	Donated by B. Caterson/ C Hughes (Cardiff University
Collagen II Rabbit polyclonal anti-collagen type II IgG	1/200	Type II collagens and shows negligible (less than 1%) cross reactivity with Type I, III,IV, V or VI collagens	Abcam Ab34712
Secondary Antibodies			
Goat polyclonal anti-mouse IgG	1/50	Whole molecule–Peroxidase antibody produced in goat	Sigma-Aldrich Company Ltd A4416
Goat polyclonal anti-rabbit IgG	1/50	Whole molecule–Peroxidase antibody produced in goat	Sigma-Aldrich Company Ltd A0545

5.2.3 TRANSMISSION ELECTRON MICROSCOPY

Transmission electron microscopy (TEM) of SDFT contained ICB was performed by Marion Pope in Electron Microscopy Lab, Veterinary Pathology, School of Veterinary Science, University of Liverpool. A large sized ICB on a longitudinal tissue section from one sample (Sample number two, 18-years-old) was localised under a light microscopy (Figure 5.3 D) and prepared for TEM. The process of re-embedding paraffin wax sections into epoxy resin was as follows; the paraffin embedded sections were dewaxed in xylene and rehydrated through a descending series of ethanols to distilled water. The section was then fixed in 2.5% buffered glutaraldehyde, post fixed in 1% osmium tetroxide, 'en bloc' stained with uranyl acetate and dehydrated in an ascending series of ethanols and then transferred into 100% acetone. The slide was then immersed in an ascending series of epoxy resin, acetone solutions and finally to 100% epoxy resin. A BEEM capsule (TAAB Laboratories Equipment Ltd, Unit 3 Minerva House, Calleva Industrial Park, Aldermaston, Reading, Berks, RG7 4QW) containing partially polymerised epoxy resin was inverted over the localised area that contains the ICB on the section. This section was then fully polymerised overnight at 60^{o}C.

The slide with the BEEM capsule was immersed into liquid nitrogen and then the BEEM capsule snapped off containing the area with the ICB present. Ultra-thin sections of the embedded areas that contained ICB were cut on a Reichert-Jung microtome, placed on copper grids, stained with lead citrate (BDH laboratory Supplies, Poole, BH15 1TD) and viewed in a Phillips EM208S transmission electron microscope at 80kv.

5.3 RESULTS

5.3.1 GENERAL OBSERVATION OF THE H&E STAINED ICB

In this study, during microscopic scanning of the SDFT section in aged horses (Seven SDFT from five horses) (17–20 years-old) number of various sized structures were observed. Their number and sizes varied from region to region, even different area within the same region and occasionally disappeared on further sectioning of the tissues. None of these ICBs were identified in horses younger than 17-years-old. In H&E staining, the nucleus stained blue and the surrounding perinuclear area was pale white with a light pinkish colour (Figure 5.1). The structural elements of the individual ICB was not similar to the tissue background particularly the collagen fibres. It contained a rough compact granulated matrix that was arranged in a circular form around the nucleus (Figure 5.1 A). These bodies were dispersed between the collagen fibres of the fascicles and were found at multiple sites within a tendon. They varied from being centred individual cell to large clustered cellular elements that were entrapped between the collagen fibres (Figure 5.1, B-D). The individual cell was characterised by having a rounded nucleus that was surrounded by a round or an oval shaped body, which stained white creamy colour. The individual body appeared as a compact rounded structure separate with no distortion of the surrounding collagen fibres. Their longitudinal axis was parallel to the longitudinal axis of the collagen fibres (Figure 5.1, A-C). The length of the nuclei of an individual body varied from cell to cell, the average length being 5.77μm (± 1.34 SD) (n=5) but the average size of the surrounding bodies was 23.35μm (±7.58 SD) width by 59.06μm (±15.18 SD) length (Figure 5.1A and B).

The larger sized ICB appeared as cluster of aggregated cells and varied in size and shapes (Figure 5.1 B-D). They were arranged from a small (25μm width by 70μm length) to large size (100μm width by 400μm length) being occasionally larger. The numbers of their nuclei within these larger bodies were varied, ranging from a few to up to 100 nuclei (Figure 5.1, B-D). Nuclei in these clustered structures varied from round to an oval shape with the average length of these nuclei being 6.09μm (±1.31 SD). The ECM surrounding the nuclei was mostly rounded but cuboidal shapes were occasionally observed (Figure 5.2 D circle). The large ICB was composed of a number of bodies, which separated from each other, and each body

could be defined as an individual structure (Figure 5.1 B-D). The average size of these individual bodies within the large ICB was 17.81µm (±6.24 SD) width by 22.78µm (±7.29SD) length and almost all of them were spherical and had approximately similar width and structural components of the most outer aspect (periphery) of these bodies became slightly disorganised and inter-connected with each other (Figures 5.2).

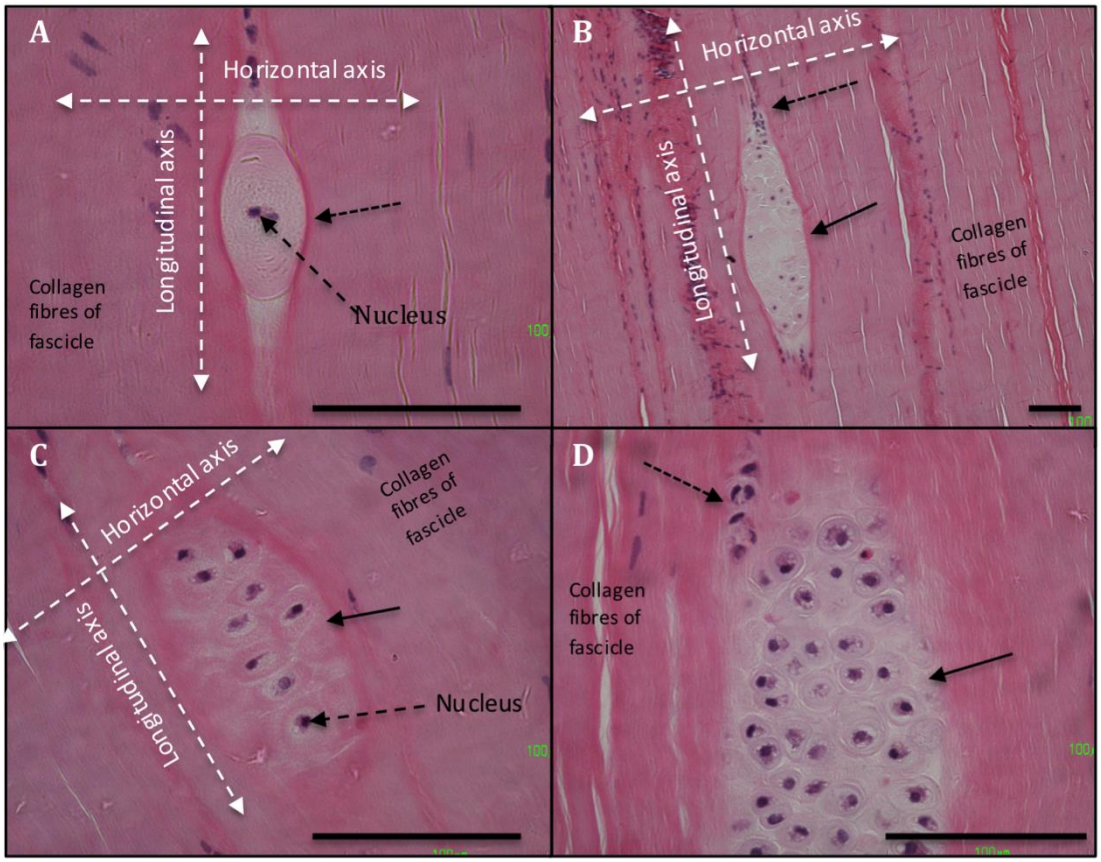

Figure 5.1: H&E staining of longitudinal sections for the equine SDFT taken from a 17-years-old horse. Note the presence of the ICBs between the collagen fibres of the fascicles, their orientation are parallel to the longitudinal axis of the collagen fibres (white dashed arrows), a cluster of a structures vary between a white creamy colour and varying intensity of a pinkish colour (C). A number of different sized irregular nuclei were present on both proximal and distal ends of the large ICBs (B and D, black dashed arrows) (Scale bar=100µm).

If the SDFT sections with ICBs are compared to sections from younger horses the histological architecture of the tendon away from the ICBs is similar; the collagen fibres around the ICBs are arranged longitudinally and parallel to each other (Figure 5.2). However in the areas near to the ICB, the collagen fibres deviated around the

boundaries of the ICB (Figures 5.2A and B) with no apparent disorganisation of the ECM (collagen fibres). The nuclei located in the collagen fascicles away from the ICB were uniform fusiform shape, but those adjacent to the ICB were more rounded. Moreover, a number of cells containing different sized irregular nuclei were present on both proximal and distal ends of the large ICBs, where they were appeared to be confluent, or joining to the ICB. No inflammatory cells or necrotic foci were identified in any sample (Figure 5.2C and D).

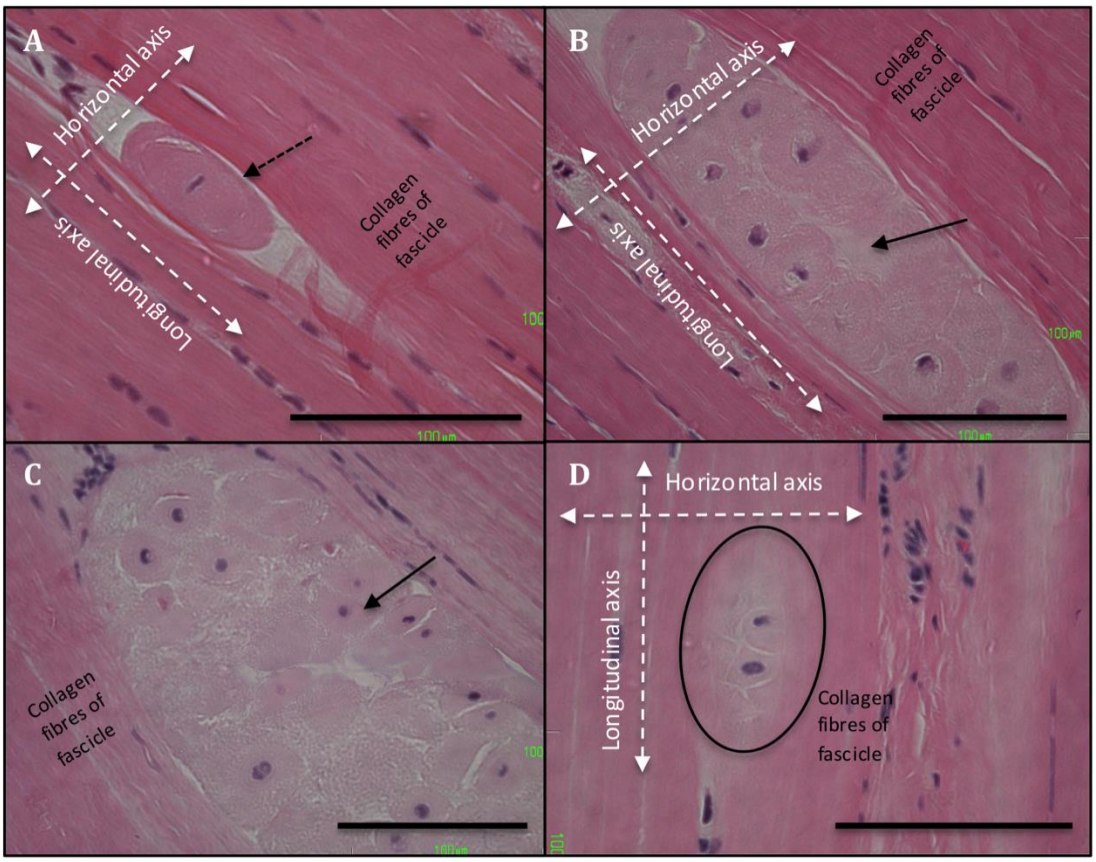

Figure 5.2: H&E staining of the longitudinal sections of equine SDFT, taken from 18-years-old (A and B) and 20-years-old (C and D). Note the presence of the ICBs, lying between the collagen fibres (A and B). The ICBs are arranged as either individual large cells (dashed arrow) (A), or as a cluster of a number of rounded cells (black arrows) or cuboid cells (circle) (D). Their nuclei stained deep blue and the surrounding structures varied between a white creamy colours to different intensities of a pink colour (A-C), (Scale bar=100µm).

The average number and length of nuclei when scored according to our scoring method (Chapter Four) the intra-fascicular were counted in 10 different fields in each

the proximal, mid-metacarpal and the distal metacarpal regions and their average were calculated. Moreover, their length (intra-fascicular nuclei) was also measured and their average was calculated. It was found that the average intra-fascicular nuclear density and length were 22.5 (±4.35 SD) and 20.5µm (±3.6SD) (n=7). Thus the ICBs represented a different cellular conformation, and cellular organisation, which was completely distinct from the tenocytes observed within the normal fascicles.

In addition to the H&E stain, the ICBs were further stained with specific special stains (Toluidine blue, Safranin-O, Alcian blue-PAS, Von Kossa's) in order to define and describe their structural composition. In order to specify and describe the ICB components following special stains were used:

5.3.2.1 Toluidine Blue (TB)

Toluidine blue is usually used to stain the cartilaginous tissue and the ECM proteins such as PG and GAG. In cartilage, components such as cartilage matrix stain deep violet, nuclei blue, the cytoplasm and other tissue elements have various shades of light blue (Schmitz et al., 2010). The outline and morphology of both the individual and large ICBs, when stained with toluidine blue were similar to those with H&E. Nuclei varied from round to an oval shape and stained deep blue in colour. The components surrounding the nuclei stained positively for toluidine blue, demonstrating different intensities of violet and light blue colours (Figure 5.3). The most external aspect of the cells in the ICBs and particularly at both end were stained with a different intensity of violet colour that extended far between the collagen fibres of the fascicles (Figure 5.3A and B). Tenocytes and collagen fibres close to the ICB also stained positively with toluidine blue and this staining intensity was greater around cells than the collagen fibres (Figure 5.3C).

Where there were large ICBs (Figure 5.3D), the nuclei were stained light blue and the surrounding ECM deep violet. The components around the nuclei were organised into two distinctive layers; the first layer directly surrounding the nucleus stained deep violet, while the second outer layer was thicker than the first layer and stained a lighter violet (Figure 5.3D). Each individual ICB was separated from the other and between them there were irregular structures that stained deep violet colour (Figure

5.3D). This acidophilic metachromatic dye (Toluidine blue) is a small weakly hydrophilic cationic dye, has the affinity to stain acidic components of the tissue such as sulphates, carboxylates, and phosphate radicals. The tendon components such as DNA, RNA and GAG are polyanionic substance whereas most of the proteins are polycationic. Thus, Toluidine blue in the tendon stains DNA, RNA, chromatin and the GAGs, which displayed a purple metachromatic colour. Therefore the structural components of the ICB and those close to it are stained deep violet colour (Figure 5.3D), indicating the presence of the GAGs. Other tissue structures such as collagen fibres, IFM and the tenocytes distant to the ICB were normally arranged and apparently unaffected by the ICB, thus the ECM around those bodies had unusual staining for Toluidine blue than the normal tendon ECM.

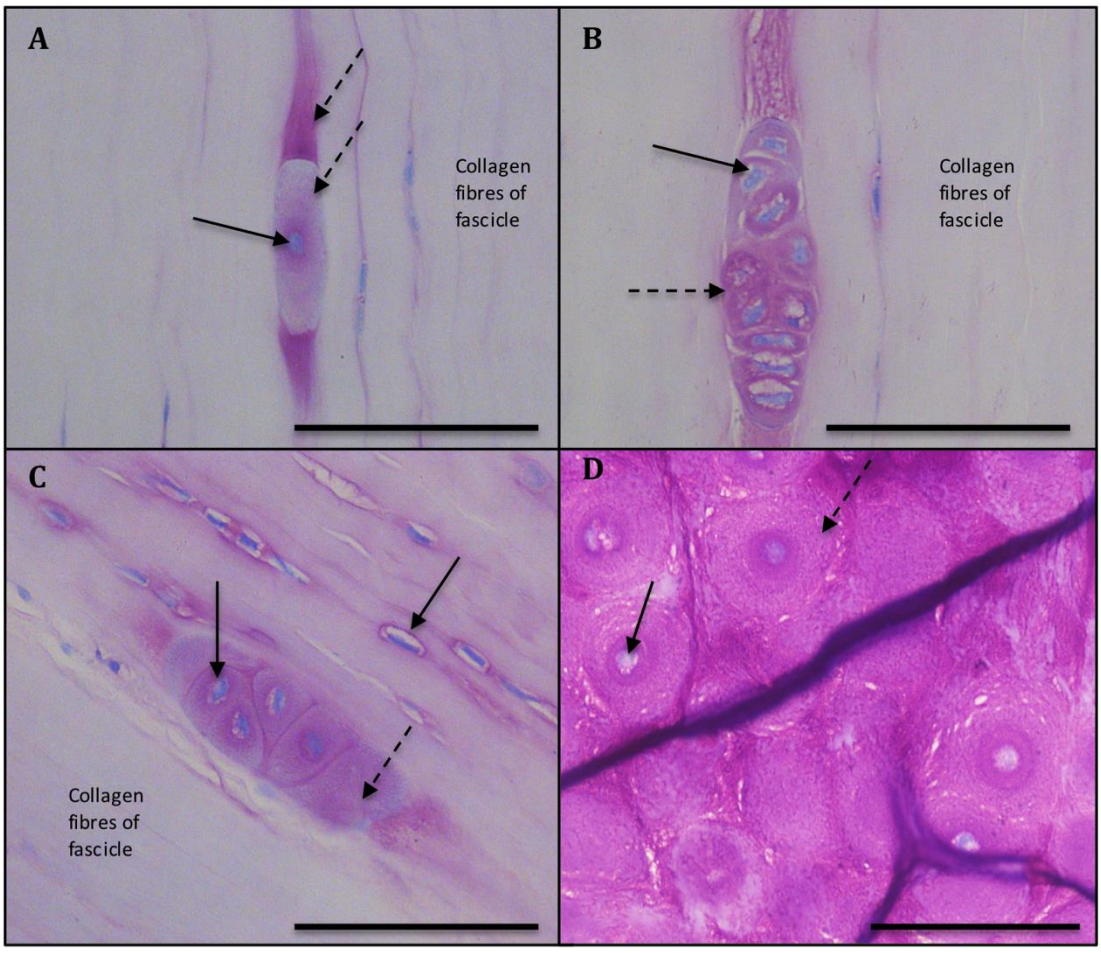

Figure 5.3: Toluidine blue staining of the longitudinal sections of equine SDFT, taken from 20-years-old (A and B) and 18-years-old (C and D) horses. The ICBs are characterised by having a cluster of large rounded structures that stain positively for GAG and proteoglycans (dashed arrows). They are arranged in a form an individual large structure (A) or a cluster of a number of rounded (B and D) and cuboid

structures (C). Their nuclei stained blue (solid arrows) and the surrounding components deep violet (dashed arrows), (Scale bar=100µm).

5.3.2.2 Safranin-O

Safranin-O is a cationic dye and reacts with the acidic components such as acidic PG. It has an affinity to bind to the sulphur units (acidic substrates) of the GAG and where it stains an orange to red colour. It is usually used to stain the proteoglycans of cartilage and we used it here in order to confirm results of the Toluidine blue staining. In tendon, collagen fibres are counter stained with fast green, the nuclei with Mayer's haemalum and the anionic substrates with Safranin-O which display different intensity of orange to red colour (Figure 5.4).

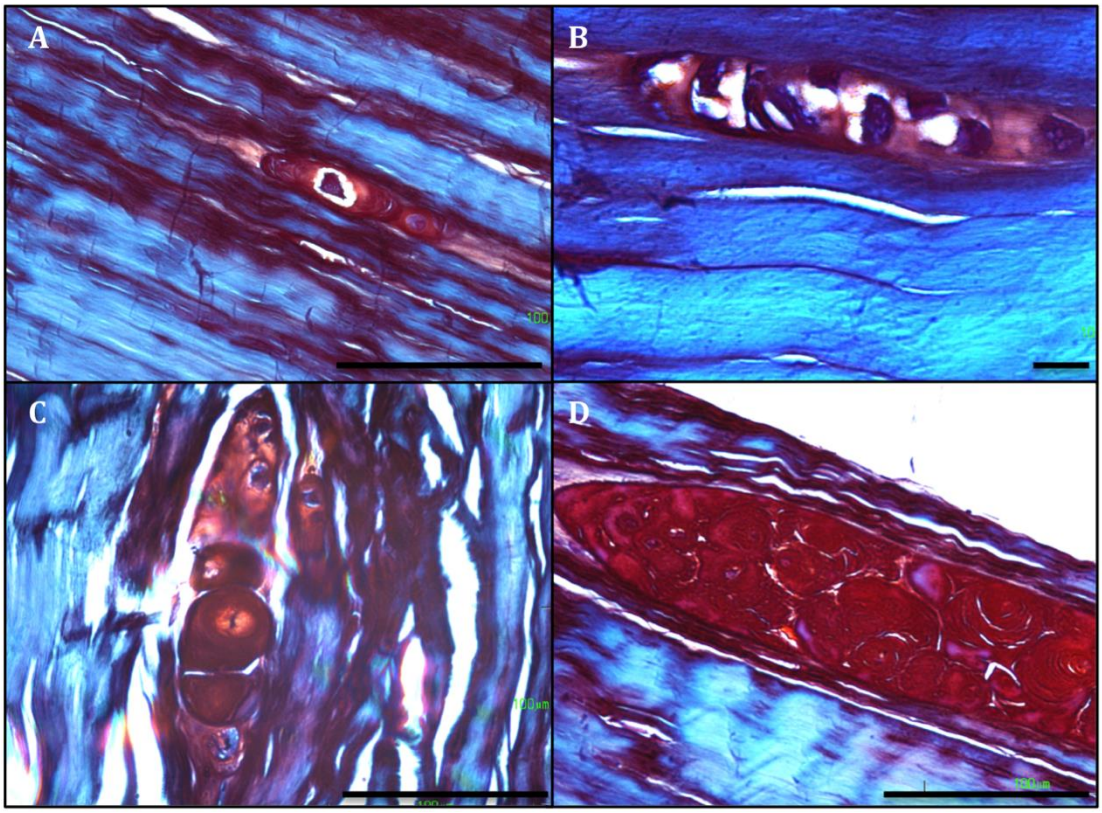

Figure 5.4: Safranin-O staining of the longitudinal sections of the equine SDFT taken from 17-years-old (A and B) and 18-years-old (C and D). The ICBs characterised by clusters of large rounded structures that stained positively with Safranin-O identifying the presence of GAG, proteoglycans. They are arranged either as an individual large structure or as a cluster of a number of rounded structures (C, D). The nuclei stained black and the surrounding components deep orange to red (D) (Small scale bar=10µm and large scale bar=100µm).

The core or the centre of most inclusion bodies contained a small black nucleus, and the pericellular matrix immediately around the nucleus stained light blue. Occasionally around those components number of vacuoles are present which did not have a positive stain with Safranin-O (Figure 5.4A, B). Both the nuclei and vacuoles are surrounded by large circular structures that have a positive reaction to Safranin-O (red colour) (Figure 5.4D). The circular structure arranged regularly in a form of a number of lamellar layers around the cell (Figure 5.4D) similar to that seen with Toluidine blue staining. The components of the IFM or areas close to the ICB also strongly stained with Safranin-O in contrast to those areas that located far from the ICBs (Figure 5.4). The findings overall were similar to that seen with Toluidine blue staining which identified these structures to contain a GAG rich matrix.

5.3.2.3 Alcian blue-PAS

The Alcian blue-PAS stain confirmed that the ECM components of the ICBs stained positively for acidic polysaccharides such as sulphated GAG and glycoproteins of cartilage and connective tissues and the results were therefore similar to that seen with dine blue and Safranin-O staining. The intensity of the stain varied at different points within ICBs (Figure 5.5). Components of the ICBs displayed two different colours; the first being the reaction with the Alcian blue that stained components of the ICB a blue colour and the second being the reaction with PAS that display a magenta colour (Figure 5.5).

Alcian blue is a cationic dye and has the affinity for anionic components and acidic carbohydrates. It is used to stain acidic polysaccharides such as sulphated GAG and glycoproteins of cartilage and connective tissues (Yamabayashi, 1987, Wulff et al., 2004). The ICB stained positively with Alcian blue, the colour intensity was strongest around the ICB for both the individual and the clustered form of ICB. Components at both ends of the ICBs were stained light blue extending proximally and distally between the collagen fibres (Figure 5.5A and B). The larger clustered ICBs were organised in a form of multiple rounded layers similar to that stained with Toluidine blue and Safranin-O (Figure 5.5 C and D). Several larger ICBs were highly organised and appeared as double rings, with an inner ring that stained regularly deep blue with a coarse less regular stained outer ring (Figure 5.5 D, white arrow). The Alcian blue stain has the affinity to stain the sulphated anionic GAG

while PAS stains the glycols and serine-threonine sites of the PG. Therefor both stains confirmed the presence of a large amount of PG and GAG within and around these ICBs (Figure 5.5).

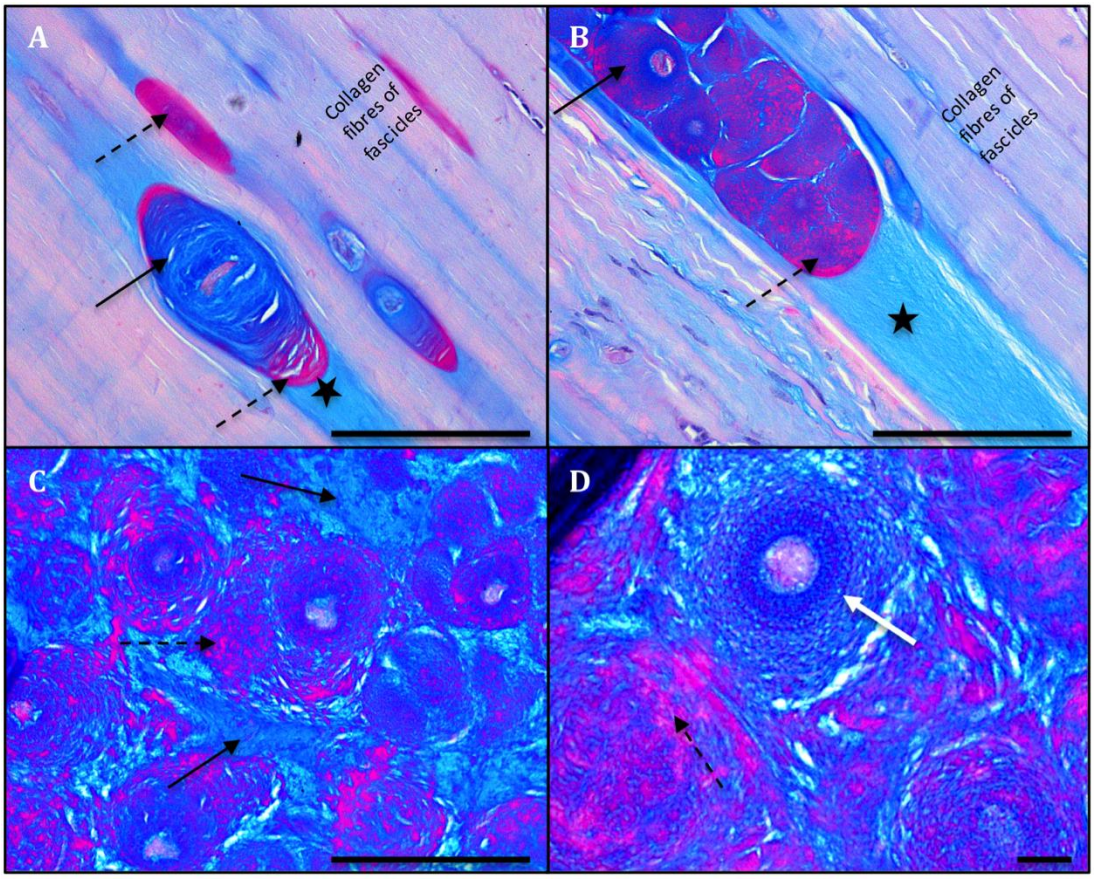

Figure 5.5: Figure 5.5: Alcian blue-PAS staining of the longitudinal sections of equine SDFT from 17-years-old (A and B) and 18-years-old (C and D) horses. The ICBs are arranged as an individual large structure (A) or as a cluster of rounded grape like bodies (B-D) stained positively for Alcian blue (solid black arrow) and PAS (dashed black arrows) indicate the presence of GAGs and proteoglycans. Components at both ends of the ICBs stained light blue extending proximally and distally between the collagen fibres (asterisks). Some pericellular staining appeared as a double ring regularly meshed by a dense multiple threads like fibrils that stained deep blue colour (white arrow), (Large scale bar=100µm (A-C) and small scale bar=10 µm (D)).

5.3.2.4 Modified Von Kossa's

The sections were stained with Von Kossa's stains in order to confirm whether these structures are mineralised and containing calcium. Typically mineralised bone components (calcium) stain black colour and the osteoid components red colour. Von Kossa's stain is based on the precipitation of cationic silver by replacing the calcium being bound to the phosphate or carbonic anion The resulting silver salts are then reduced to metallic silver by light illumination (Suvarna et al., 2012). With Von Kossa's stain the morphological appearances of the ICBs were similar to that observed with other stains as described in the preceding sections. In these sections the ICBs were stained red, which indicates the presence of the basic osteoid or un-mineralised components (Osteoid is a gelatinous substance composed of collagen, fibrous proteins and mucopolysaccharides (PGs and GAGs)) (Figure 5.6 dashed black arrows).

Evidence of calcium deposition is demonstrated by the presence of a small amount of black points inside and around the structures. Calcium was found, distributed around the nuclei and tissue matrices of the ICBs. In the individual ICBs the calcium appeared as a few tiny black points that localised at both the central and peripheral aspects of the ICB (Figure 5.6 solid arrow). Peripherally at both ends of the individual ICB and through their adjacent collagen fibres there was some reaction to calcium ions where it appeared as brown to black colours (Figure 5.6A solid arrow). In the large ICBs there were central and peripheral depositions of calcium (Figure 5.6 C and D solid arrow). In the centre there were many tiny black points of calcium reaction distributed around the cell surface and through the inner ring structure (Figure 5.6 D). The vacuoles around the nucleus and the areas around and close to the inner ring were also free from calcium. The tissue matrices laid between cells of the large ICB demonstrated a weak reaction to calcium (Figure 5.6 D solid arrow). In one of the SDFT samples calcium salts were deposited through the collagen fibres of the fascicles that located close to the ICB (Figure 5.6 B solid arrow).

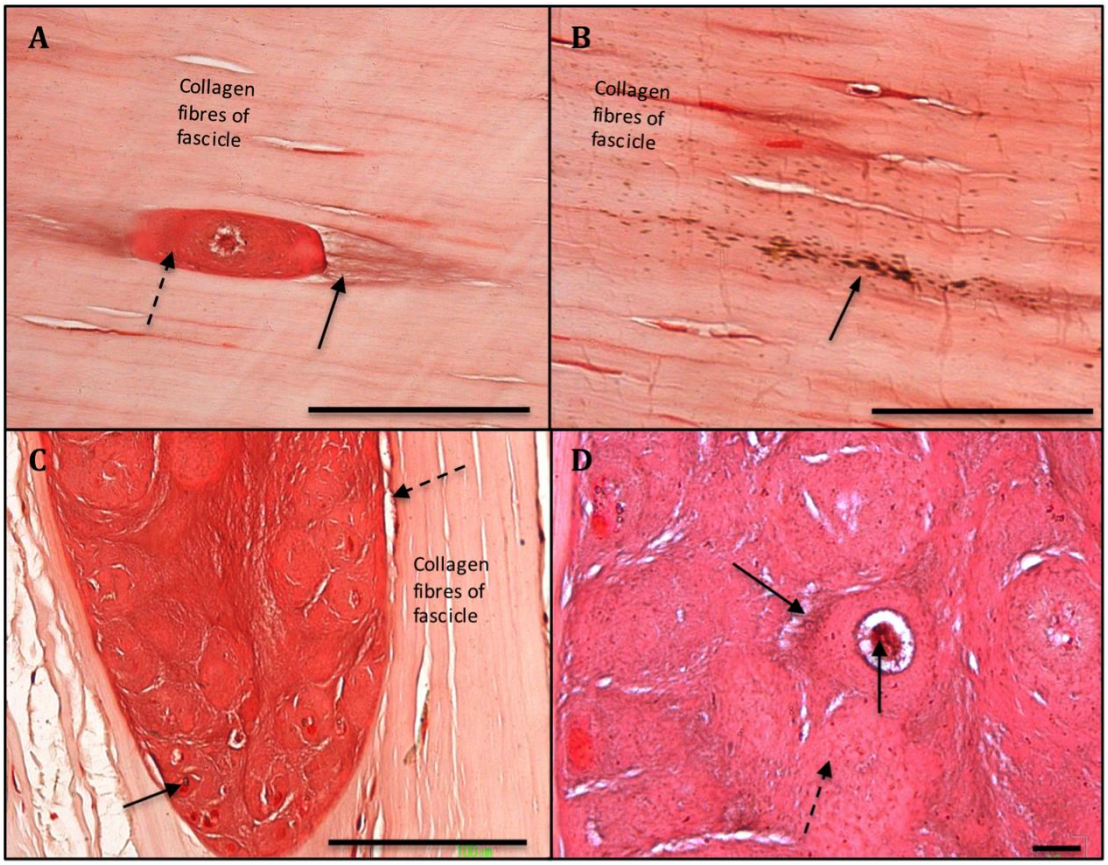

Figure 5.6: A modified Von Kossa staining of the longitudinal sections of equine SDFTs taken from 18-years-old (A and B) and 20-years-old (C and D). The individual and large clustered ICBs had a positive reaction for osteoid structures (red colour, dashed arrows) with different amounts of calcium deposited inside and around these inclusion bodies (solid arrows). Calcium is deposited through the collagen fibres of the fascicles that lie close to the ICB (B, solid arrow), (Large scale bar=100µm (A-C) and small scale bar=10 µm (D)).

5.3.3 MORPHOLOGY OF CELLS WITHIN THE ICBS

Cells within the ICBs were quite varied from the normal tenocytes and were characterised by having more ECM. The nuclei were more rounded and in certain areas their cytoplasm could be outlined (Figure 5.7 dashed arrows). With H&E stain, the cytoplasm ICB cells appeared as a clear boundary around the nucleus with a clear cell membrane around the cytoplasm (Figure 5.7A, dashed arrows). Around the cell membrane there were large amounts of ECM completely surrounding the cells mixed with the ECM of the other adjacent cells (Figures 5.7 ECM). When stained with different special stains, the ICBs were outlined as seen with H&E. For instance, with

Toluidine blue stains, the nuclei were rounded and surrounded by a clear cytoplasm, where the cell membrane was well defined when compared to normal tenocytes that located close to the ICB (Figure 5.7B dashed arrows). The cell membranes were positively stained with Toluidine blue, which was indicative of the presence of GAGs (Figure 5.7 C and D, ECM). The GAGs should be an extracellular rather than the intra-cellular as they are produced in the rough endoplasmic reticulum and secreted to the cell surface. The more prominent ECM around the cells stained with a positive reaction for GAG (Figure 5.7 C and D, ECM). We have described the ICBs as having a new cellular form that varied from the normal tenocytes having the deposition of a large amount of ECM which stains positively for GAGs and that have different outlines completely surrounding the cells.

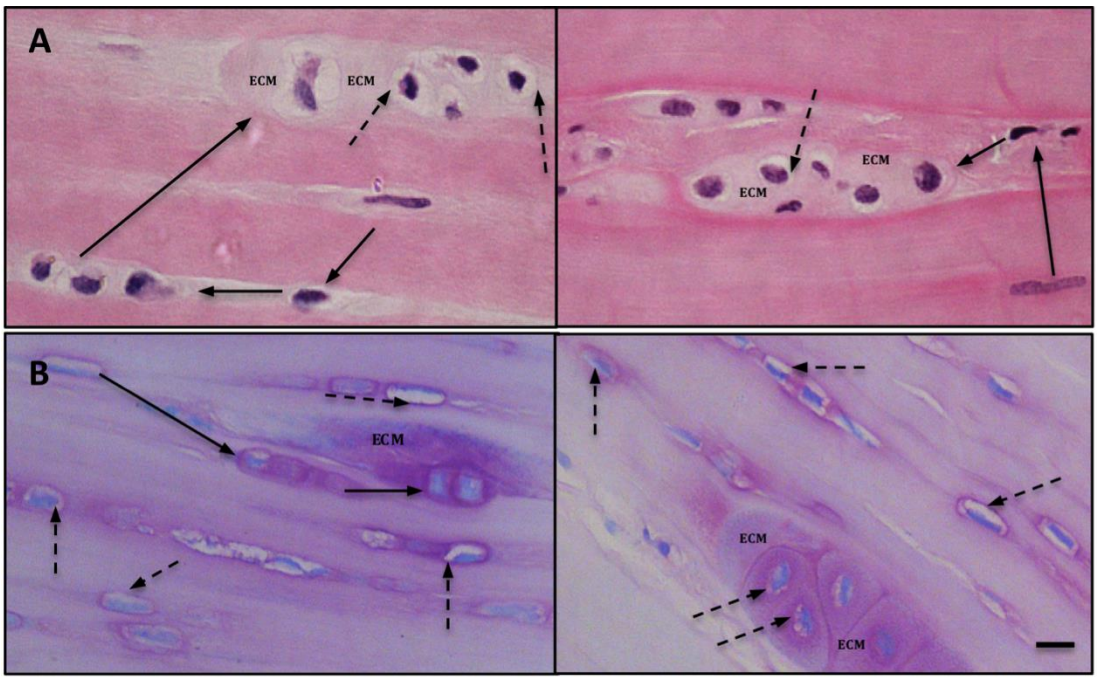

Figure 5.7: A: H&E staining of the ICB in 20-years-old horse; different cells are present that differ from normal tenocytes being cigarette shaped and also rounded surrounded by different amount of ECMs (solid arrows). Note the rounded nuclei of ICBs are surrounded by clear cytoplasm, which were enclosed by cell membrane (dashed arrows). The ECM of almost all the ICBs was communicating with each other. B: Toluidine blue stain of the ICB in 18-years-old horse, different nuclei of the tendon ranged from fusiform to cigarette and rounded forms (solid arrows). Nuclei of ICB were rounded and surrounded by a small cytoplasm, which then enclosed by a cell membrane (dashed arrows), the ECM around the cells had a positive staining for GAG (Scale bar=10 µm).

5.3.4 IMMUNOHISTOCHEMISTRY (IHC)

The equine SDFT sections with these ICBs were further processed for IHC to try and determine which specific ECM proteins were within their structure. The tissues were probed for the presence of aggrecan, biglycan, decorin, chondroitin-4-sulphate (C-4-S) and chondroitin-6-sulphate (C-6-S) and collagen type II as described above (Table 5.2). Meanwhile, two negative controls were included; in the first control where Tris buffer saline-Tween (TBST) buffer was instead of the primary antibody, whilst in the second, mouse IgG (Sigma-Aldrich) was applied instead of the primary antibody.

5.3.4.1 Aggrecan

Aggrecan is known as a cartilage specific proteoglycan protein, it is a member of a family of large aggregating PG and is composed of G1, G2 and G3 domains (Kiani et al., 2002). Immunostaining of the ICBs contained some staining for aggrecan using monoclonal anti-aggrecan mouse IgG (Figure 5.8), which is specific to bind to the G1 domain and chondroitin sulphate attachment domains. The reaction occurred with a different intensity throughout the extracellular (Figure 5.8, solid black arrows) and intracellular components (Figure 5.8 dashed black arrows). The staining of the actual structures was somewhat patchy, but the tendon surrounding the ICBs frequently had more obvious staining (Figure 5.8A). Interestingly, there was a positive intra-cellular immunostaining with aggrecan, which completely surrounded the nuclei and filled a large space inside the cells (Figure 5.8 B and C, dashed black arrows).

The tissue matrices of the large clustered form of the ICB and components lie between the inclusion bodies had a variable positive reaction for aggrecan (Figure 5.8 D, solid black arrows). Moreover, collagen fibres lying close to the large ICBs often had strong immunostaining for aggrecan. There was also a positive reaction in area around the inclusion bodies in the collagen fibres and the IFM (Figure 5.8D, white arrow).

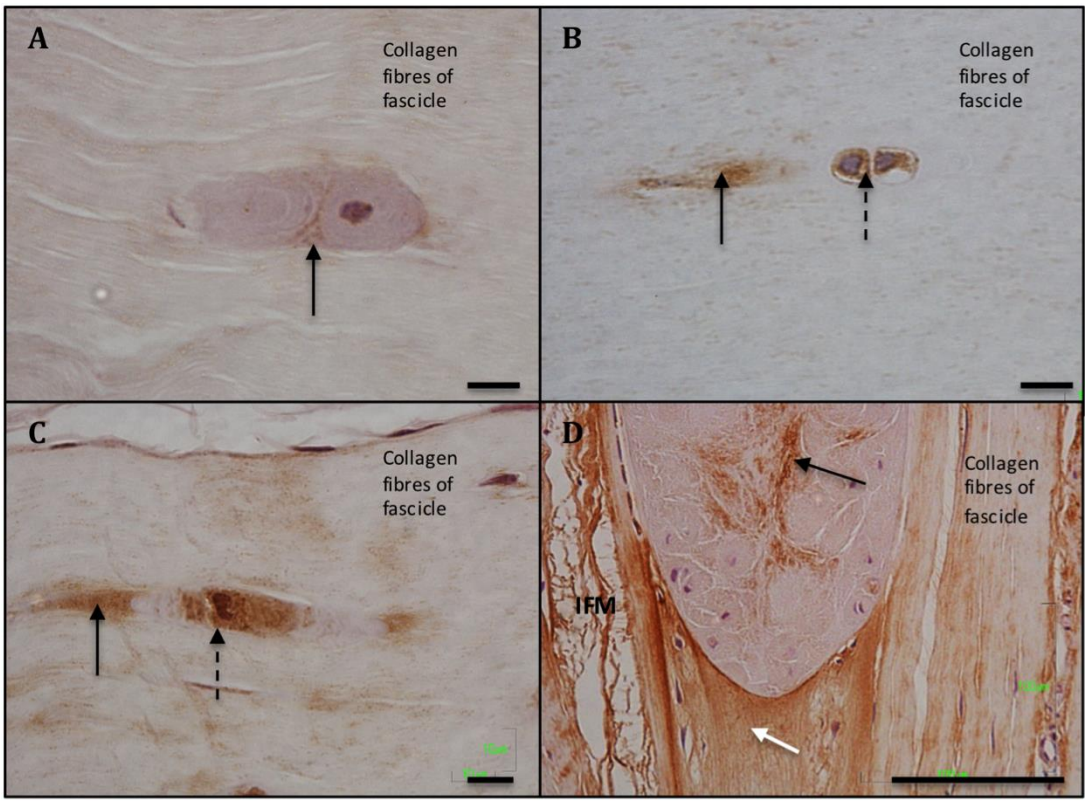

Figure 5.8: This figure shows positive immunostaining with anti-aggrecan mouse monoclonal IgG of the ICBs of equine SDFTs from 17-years-old (A), 18-years-old (B and C) and 20-years-old (D) horses. There is intra (dashed black arrows) and extra (solid arrows) cellular staining of ICBs, note the intracellular reaction is stronger (B and C, black dashed arrows). The large ICB (D) shows a weak immunostaining within the structure of the body (solid black arrow) and strong immunostaining in the surrounding collagenous tissue (white arrow) (Small scale bar=10µm (A-C) and large scale bar=100µm (D)).

5.3.4.2 Biglycan

This antibody binds to the C-terminal amino acid sequence of human biglycan. Biglycan is a small leucin-rich proteogycan SLRP and present in different tissues such as bone, cartilage, tendon and ligament (Iozzo, 1999, Yoon and Halper, 2005). The components of the ICBs did not completely react with this anti-biglycan monoclonal antibody (Figure 5.9). There was some antibody binding intra-cellularly where it reacted with structures around the nuclei of the individual ICBs (Figure 5.9 A and B dashed arrows) while in the large clustered ICB the interior aspect of the

ICBs did not show any reaction to biglycan (Figure 5.9 C and D, asterisks). The collagen fibres and the IFM around the ICBs did have positive immunostaining for biglycan (Figure 5.9 C and D, solid arrows).

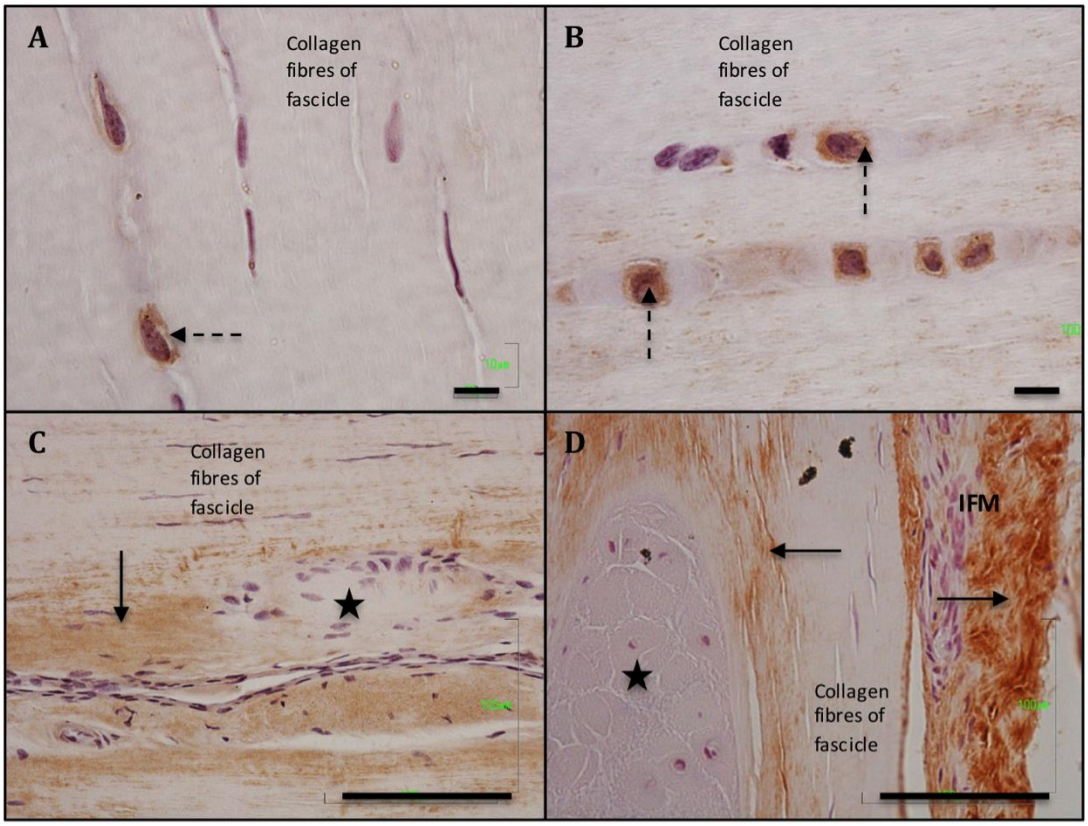

Figure 5.9: This figure shows positive immunostaining for anti-biglycan mouse monoclonal IgG against ICBs in longitudinal sections of the equine SDFTs from 17-years-old (A and B), 18-years-old (C) and 20-years-old (D) horses. There was positive immunostaining around the nuclei to biglycan (intra-cytoplasmic reaction) in the individual ICBs (A and B dashed arrows). Note there is not a positive reaction inside the large clustered ICB (C and D asterisks) but there was positive immunostaining to biglycan in the extracellular matrix close to the inclusion body (C and D, solid arrows), (Small scale bar=10µm (A and B) and large scale bar=100µm (C and D)).

5.3.4.3 Decorin

This antibody is specific for the core protein of decorin, which is a most abundant SLRP and present in different tissues such as bone, cartilage, tendon and ligament

(Iozzo, 1999, Samiric et al., 2004, Vesentini et al., 2005). Immunostaining of the ICBs with anti-decorin monoclonal mouse IgG was negative, however occasionally an intra-cytoplasmic reaction in the nuclei was noted (Figure 5.10 A and C, dashed arrows). The collagen fibres of the equine SDFT demonstrated positive immunostaining to the anti-decorin antibody (Figure 5.10). The ECM of the ICBs did not stain positively for the anti-decorin antibody but the collagen fibres close to the ICB and the fibres of the fascicles and IFM were positive to the antibody (Figure 5.10 solid arrows).

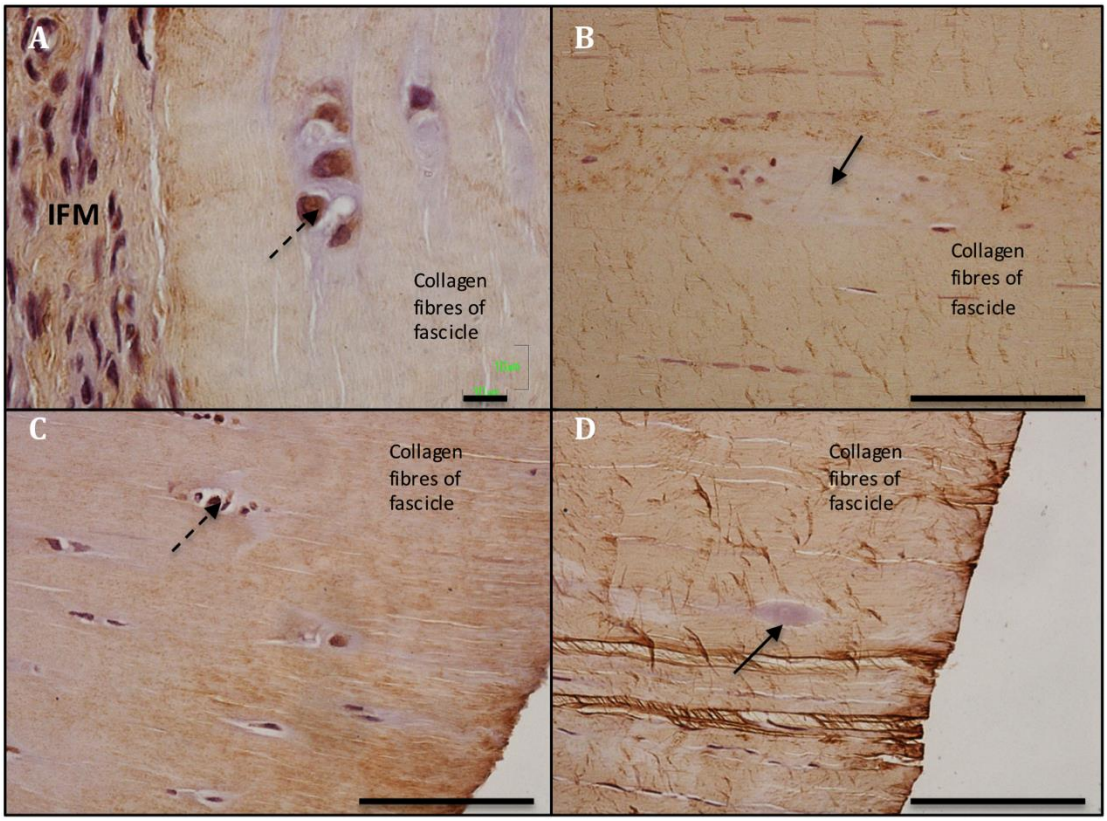

Figure 5.10: Immunostaining of ICBs with anti-decorin mouse monoclonal IgG in the longitudinal sections of the equine SDFTs from 17-years-old (A), 18-years-old (B) and 20-years-old (C and D). There is weak immunostaining around the nuclei (A-C dashed arrows) but the structural components of the ICBs had no immunostaining to decorin (solid arrows) but the collagen fibres and the wider fascicular matrix demonstrated positive immunostaining to decorin (C and D), (Small bar=10µm (A) and large bar=100µm (B-D)).

5.3.4.4 Chondroitin-4-sulphate (2B6)

This monoclonal antibody is specific to chondroitinase ABC-generated-4 sulphated (C-4-S) stub of chondroitin sulphate and dermatan sulphate (DS). Aggrecan is the major PG of cartilage, which has more than 100 GAG chains which are predominantly 4- or 6- sulphated. Generally, C-4-S is associated with large PGs such as aggrecan, versican, brevican and neurocan as well as in small leucine-rich proteoglycans such as decorin and biglycan (Vogel and Heinegard, 1985, Rees et al., 2000, Martinez et al., 2015). In our study, immunolocalisation for C-4-S identified different intensities of pericellular reaction with the tendon as well as around the ICBs (Figure 5.11). The severity of reaction varied from region to region but always there was weak positive staining at both ends of the ICB (Figure 5.11A, solid arrow) whilst other regions had a strong positive immunostaining through the collagen fibres and around the ICB (Figure 5.11B-D, solid arrows). Occasionally the negatively staining cellular outlines appeared as a lacunae that contain two or more than two nuclei (Figure 5.11 C, dashed arrow) but externally there was a positive reaction to C-4-S (Figure 5.11 C, solid arrow). There was no obvious staining of the main body of both individual and large ICBs (Figure 5.11 D, dashed arrow) .

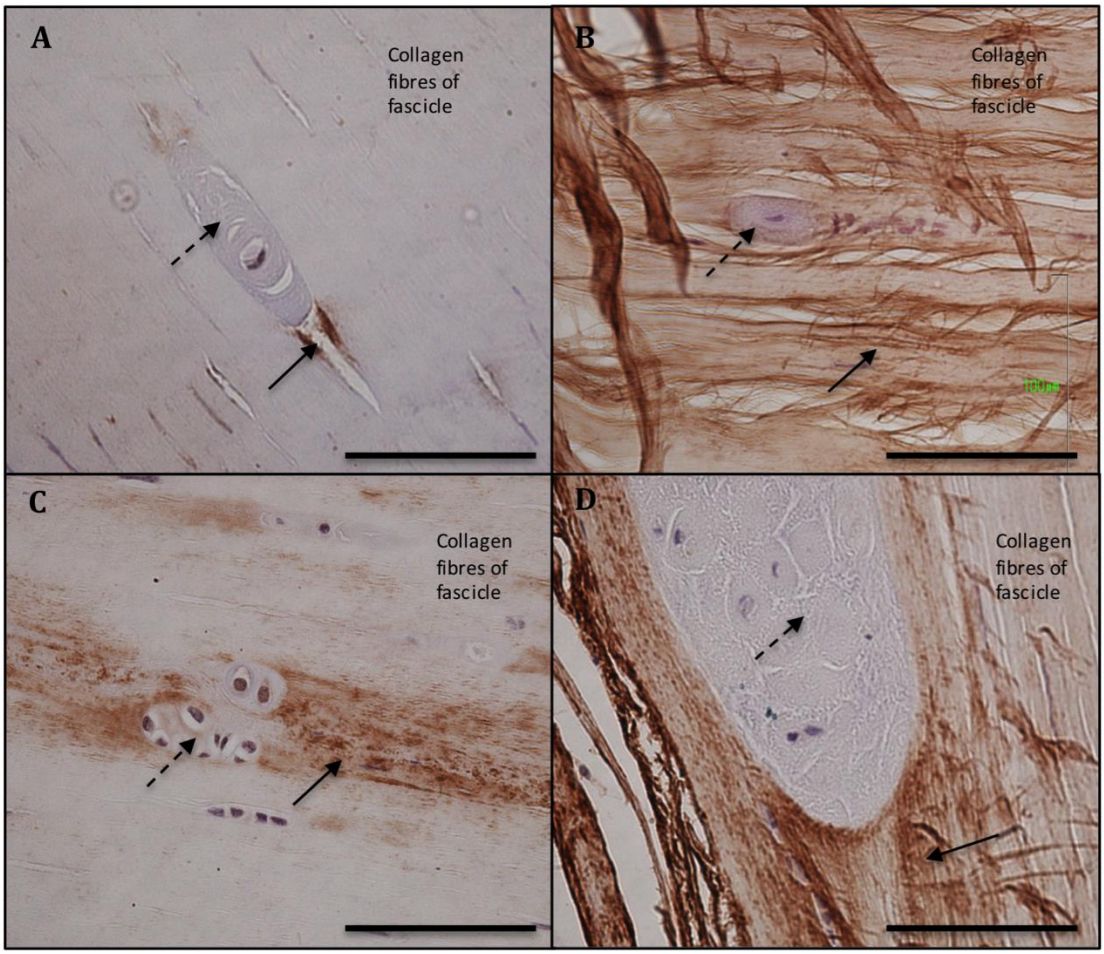

Figure 5.11: Immunostaining of the ICB in the longitudinal sections of equine SDFT with 2B6 monoclonal mouse IgG in 17-years-old (A), 18-years-old (B and C) and 20-years-old (D) horses. There were not positive immunostaining of the structure components of the ICBs with anti-C-4-S (dashed arrows) but collagen fibres around the ICBs had different intensity for immunostaining with anti-C-4-S (solid arrows), (Scale bar =100µm).

5.3.4.4 Chondroitin-6-sulphate (3B3)

This antibody recognises a chondroitinase ABC-6-sulphated disaccharide neoepitopes (C-6-S) that is generated at the non-reducing terminal of CS, which is specific to large aggregated PGs (Caterson et al., 1990, Slater et al., 1995). In our study, individual ICBs had positive immunostaining being mainly intracellular and with the extracellular component of the ICBs (Figure 5.12A and B, dashed arrows), while the surrounding collagen fibres having a weak extracellular reaction and it

varied from different area within a tissue section. The IFM close to the ICBs had a positive reaction to C-6-S with a different staining intensity from different areas (Figure 5.12 B, solid arrow). The large clustered ICBs showed obvious staining to C-6-S with the staining unevenly distributed in both the intracellular (Figure 5.12 C and D, dashed arrows) and extracellular areas (Figure 5.12 C and D, solid arrows). The extracellular components of the large ICBs were strongly immunostained to C-6-S, and the collagen fibres around the large ICBs had a weak reaction.

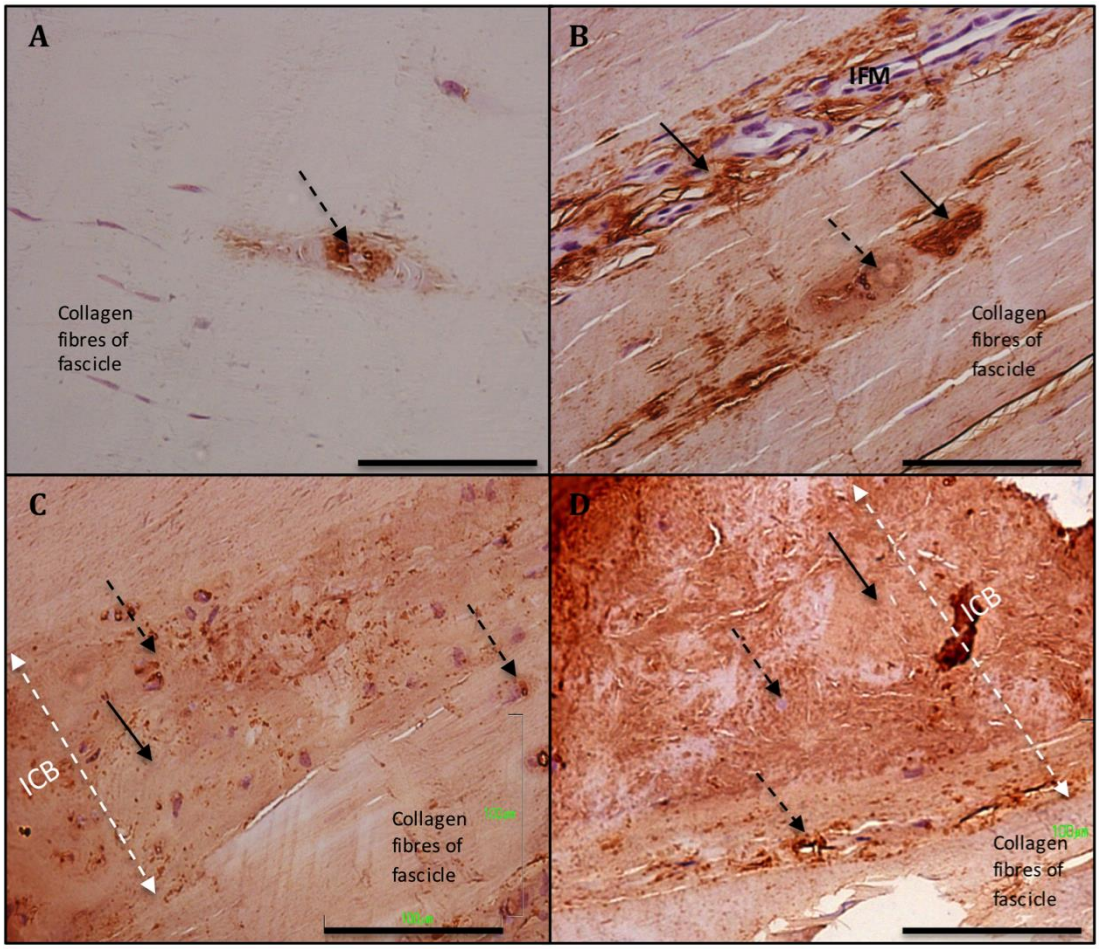

Figure 5.12: This figure shows immunostaining of the ICBs in the longitudinal sections of equine SDFT with C-6-S using 3B3 monoclonal mouse IgG in 17-years-old (A and B) and 18-years-old (C and D) horses. The individual small ICBs react with different intensity to 3B3 with the C-6-S being distributed unevenly in the intracellular (A and B dashed arrows) and pericellular areas (A and B, solid arrows). The large clustered ICBs (dashed white line) have strong positive immunostaining with the C-6-S being unevenly distributed between the intracellular (C and D, dashed arrows) and the extracellular spaces (C and D, solid arrows) (Scale bar=100µm).

5.3.4.5 Collagen type II

This polyclonal antibody (Abcam) reacts with collagen type II and also has a negligible (less than 1%) cross reactivity with type I, III, IV, V or VI collagens (Ab34712 data sheet). Only two of the samples showed positive immunostaining to type II collagen fibres (Figure 5.13). In both samples the tendon ECM (fascicles and IFM) had a different intensity for type II collagen immunostaining with the IFM have a stronger positive immunostaining than the fascicles (Figure 5.13 A and B, arrows). The large clustered ICBs showed weak immunostaining to type II collagen, where it was seen inside and on the periphery of the ICBs (Figure 5.13 C and D, dashed arrows).

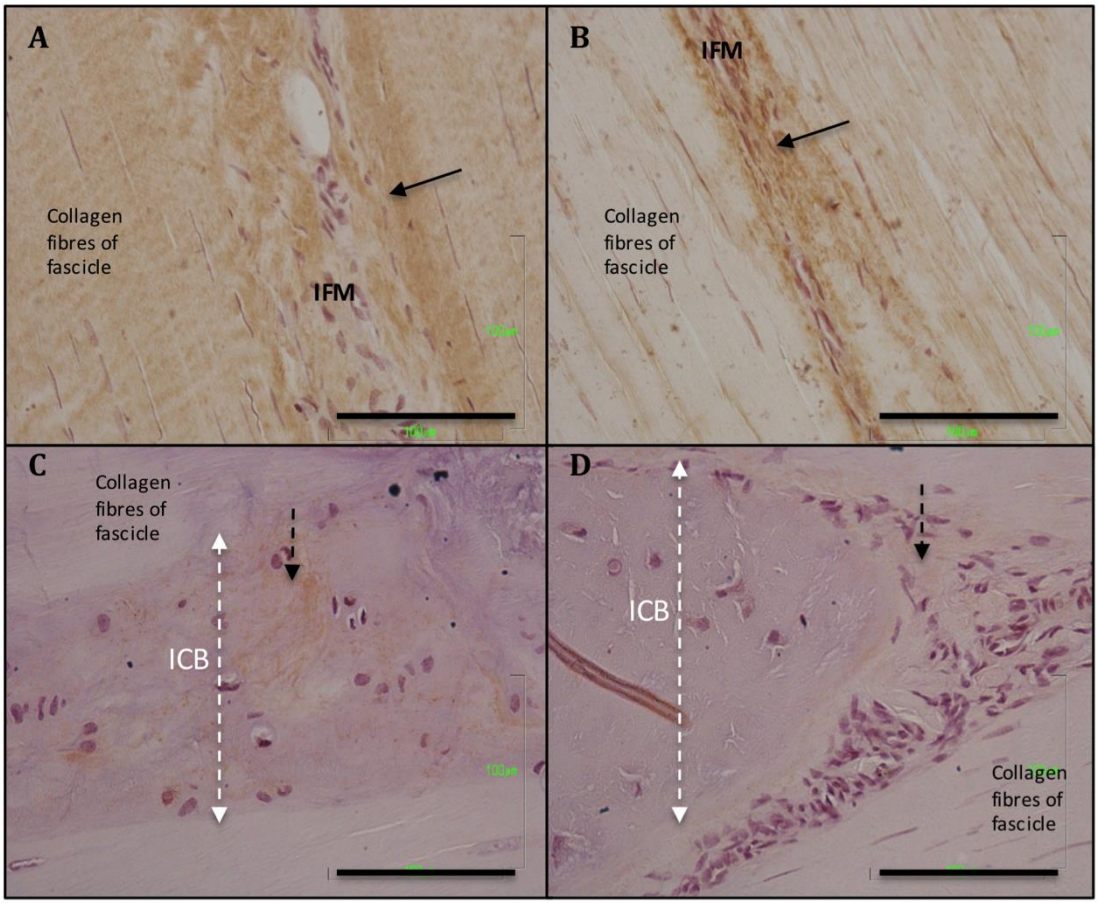

Figure 5.13: Immunostaining of the ICBs in the longitudinal sections of equine SDFTs with collagen type II polyclonal rabbit IgG in 17-years-old (A and B) and 18-years-old (C and D) horses. The fascicles and the IFM display positive reaction to type II collagen (A and B arrows). The structural components of the ICBs have a slight reaction both inside (C dashed arrows) and on the periphery of the ICB (D, dashed arrow) (Scale bar=100µm).

5.3.4.6 Negative controls

Two negative controls were included with all experiments. In the first TBST were applied instead of the primary antibody whilst for the second control the mouse monoclonal IgG isotope for PGs and rabbit IgG (Sigma-Aldrich for collagen type II were applied instead of the primary antibodies (Figures 5.14 and 5.15).

5.3.4.6.1 Proteoglycans (PGs)

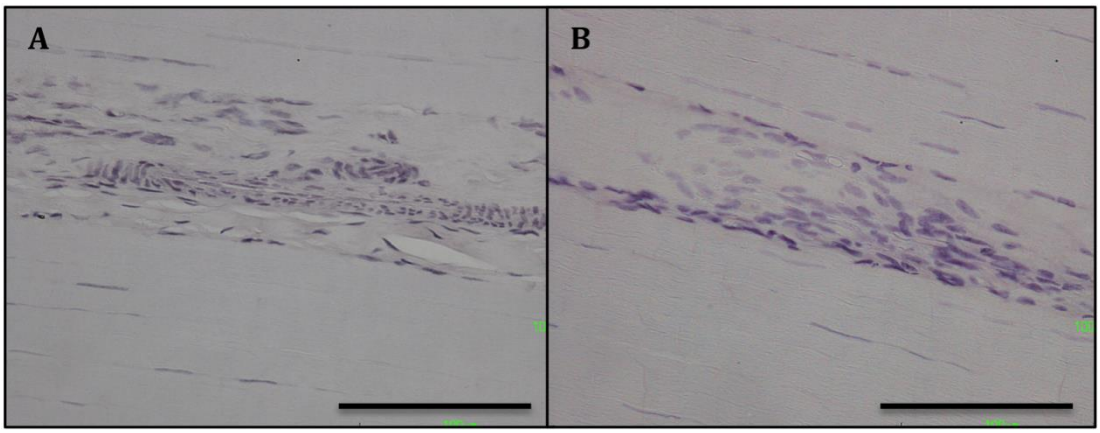

Figure 5.14: This figure represents the negative control for proteoglycans: A. Instead of the primary antibody being applied Tris buffer saline-Tween (TBST) was applied to the section. B. In this section an IgG negative control instead of the primary antibody the mouse monoclonal IgG isotope was applied to the section. Note in both negatives controls there are no immunostaining reactions (Scale bar=100µm).

5.3.4.6.2 Collagen type II

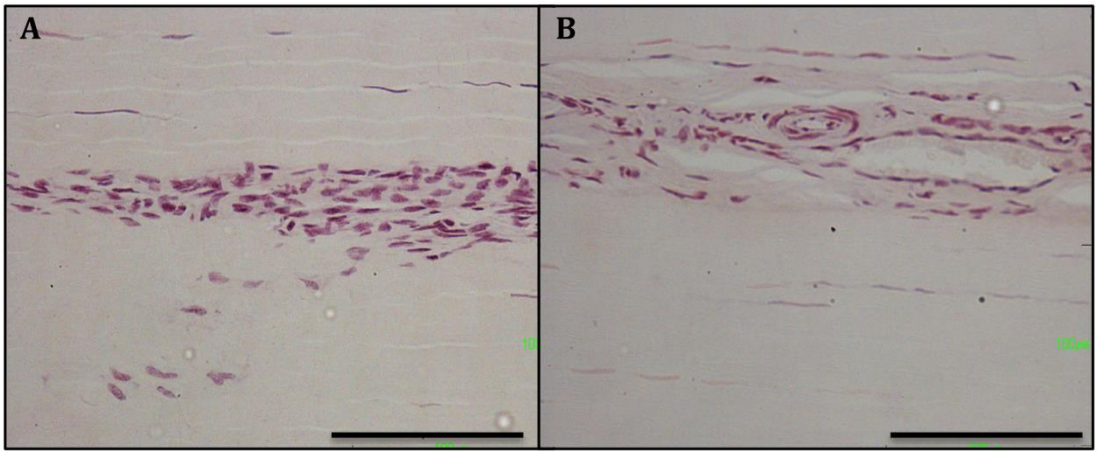

Figure 5.15: This figure represents the negative control for collagen type II: A. Instead of the primary antibody being applied (TBST) was applied to the section. B. In this section an IgG negative control instead of the primary antibody the mouse rabbit monoclonal IgG isotope was applied to the section. Note in both negatives controls there are no immunostaining reactions (Scale bar=100µm).

5.3.5 TRANSMISSION ELECTRON MICROSCOPY

Transmission Electron Microscopy (TEM) was obtained for one ICB sample of an 18-years-old horse that previously stained positively with Toluidine blue and Alcian blue and shown in Figures 5.3D and 5.5D respectively, which then the ICB was localised on the unstained section. With TEM, the ICB demonstrated a number of characteristic features that reflect the cellular elements in the area of ICB, which are nucleus, endoplasmic reticulum and other cellular organelles. The ICB was composed of a number of cells that were outlined and separated from each other (Figure 5.16). Each cell contained a nucleus that contained a small nucleolus and an amount of condensed chromatin. The nucleus was enveloped by a nuclear membrane and separated from the rest of the cytoplasm and their diameters were approximately about 3µm (Figure 5.16 A-C). The material within the cytoplasm was organised into a large amount of alternating layers of dense and translucent lamellar materials (Figure 5.16 A-C, ER). The dense lamellar pattern was indicative of the presence of a highly developed rough endoplasmic reticulum. Moreover there were a number of various sized mitochondria and vesicles between the lamellae of the endoplasmic reticulum inside the cytoplasm. The rough endoplasmic reticulum occupied the whole cytoplasm (Figure 5.16A-D, ER).

The extracellular components of the ICBs around the clustered cells were not homogeneous. Materials around the ICBs that stained positively for GAG that shown in figures 5.3 D and 5.5 D were dense and organized into a circular form around the ICBs and contain few small vacuoles. The free borders of these circular materials were laid beside each other and between them there were large numbers of disorganised fibrils. These fibrils apparently inter-connected the free border of these circular bodies with each other (Figure 5.16, E and F).

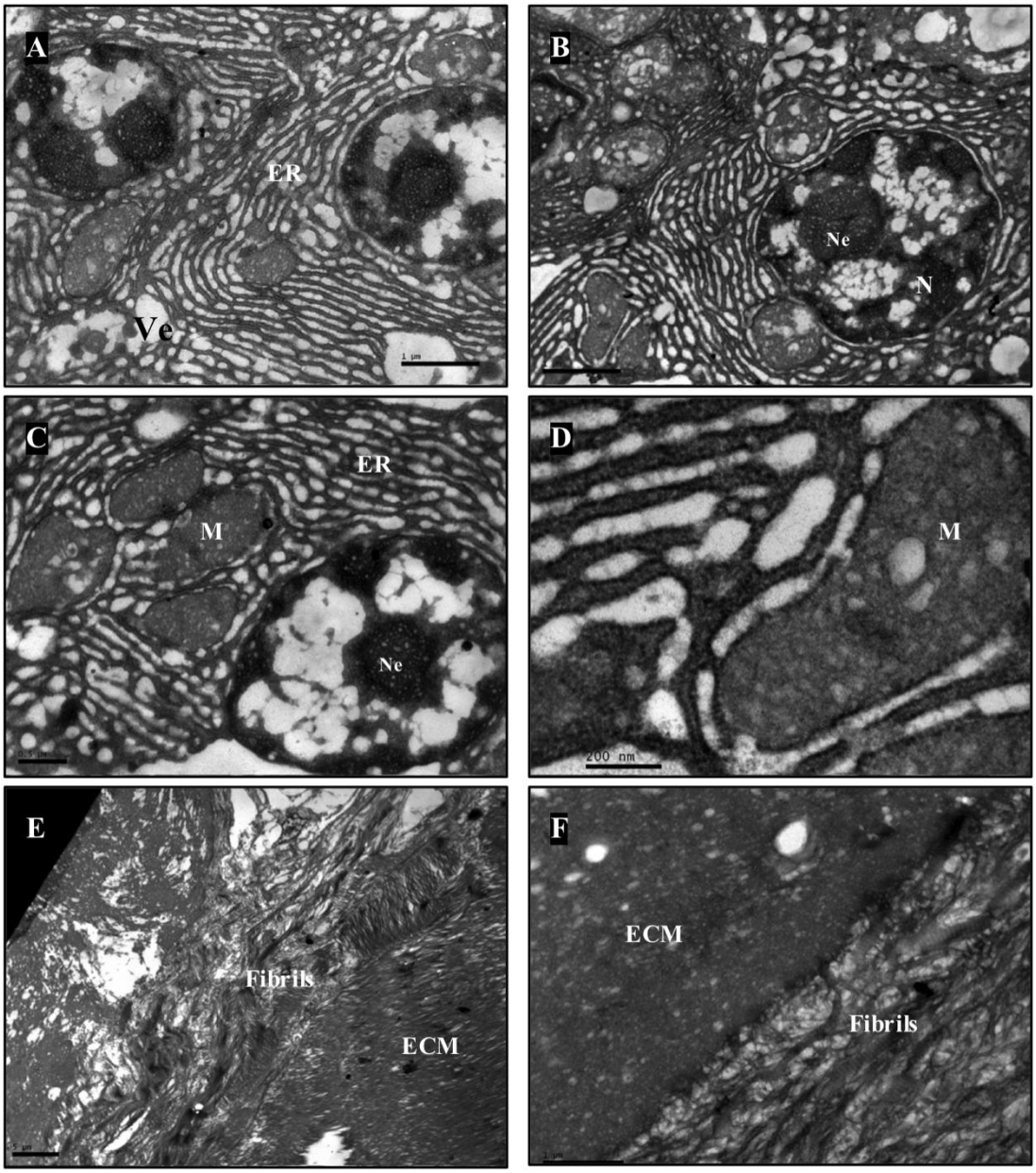

Figure 5.16: Transmission Electron Microscopy (TEM) of the large ICB taken from a sample shown in Figures 5.3 D and 5.5 D from the SDFT of an 18-years-old horse. Panels A-C showing rounded nuclei (N) surrounded by a regularly organised endoplasmic reticulum (ER) that contain different sized mitochondria (M) and vacuoles (Ve). Panel D is the higher magnification of (B) shows one of the mitochondria and portion of ER. Around these cells there is a large amount of deposited ECM (E and F). The ECM is arranged in a circular form around the cells and inter-connects by disorganised micro-fibrils. Scale bars= 1µm (A B and F), 0.5µm (C), 200nm (D), and 5µm (E).

5.4 DISCUSSION

5.4.1 HISTOLOGICAL DESCRIPTION OF THE INTRA-FASCICULAR CHONDROID LIKE BODIES (ICBs)

It has been reported that tendons undergo mechanical, biochemical and cellular alterations during ageing characterised by a decline in homeostasis and an inability to fully tolerate their environmental loading stress (Tuite et al., 1997, Russo et al., 2015). In this study we demonstrated that equine SDFT during ageing undergoes further alterations by developing non-specific intra-fascicular chondroid-like structures (ICBs). These bodies varied in number and size, arranged from an individual cell to a cluster of multiple cells that appeared like a bunch of grapes. Such structures have not been described previously in equine tendons of the SDFT under any classification such as an age related, mechanical or inflammatory. In a study of emu patellar tendons, similar ICBs were described shown as clusters of chondroid-like cells dispersed between the collagen fibres (Regnault et al., 2014). In the young 6 months age emus the tendon is more homogenous with few chondroid cells but in tendons >18 months old the chondroid cells became more prevalent having a strong basophilic reaction with H&E and metachromatic with both Toluidine blue and Safranin-O (Regnault et al., 2014). Different studies have also demonstrated that intra-tendinous ossification normally occurs in birds and dinosaurs (Berge and Storer, 1995, Landis and Silver, 2002, Organ and Adams, 2005).

It has been demonstrated that the fibrocartilaginous, rounded chondroid-like cells are found in the enthesis zone of the tendon and ligaments (Benjamin and McGonagle, 2001). Fibrocartilage is avascular structure and consists of rounded cells within a lacuna or occasionally a number of cells lying within the same lacuna (Benjamin and Evans, 1990, Benjamin and Ralphs, 2004). Similarly, in our study we found both individual and clustered cells, but some ICBs consisted of a large number of cells aggregates, which could contain more than 100 nuclei. The ICBs were isolated from each other and surrounded by larger amount of ECM which demonstrated a positive reaction for stains such as Toluidine blue, Alcian blue, and Safranin-O indicative of proteins such as PGs and GAGs. These special stains have the affinity to bind to the acidic components of the tissue such as sulphates, carboxylates, and phosphate radicals. The tendon components such as DNA, RNA

and GAG are polyanionic substance whereas most of the proteins are polycationic and give the positive reaction (Rosenberg, 1971, Breen et al., 1981, Schmitz et al., 2010, Sridharan and Shankar, 2012). Therefore a great proportion of PG and GAG could be present throughout these ICBs, which may reflect complete tissue alteration from a collagenous connective tissue proper to a chondrogenic tissue.

In a histological study of the canine cranial cruciate ligaments (CCL) in Labrador retriever and the greyhound, it was shown that the formation of fibrocartilaginous cells may not be a pathological degeneration in some dog breeds but may develop as a beneficial physiological adaptation of the cells to load (Comerford et al., 2006). In another study has been identified the presence of abundant fibrocartilaginous proteins in normal canine CCL which likely to be due to physical adaptation of the tissue against compressive or shear forces during knee joint moves through normal range of motion (Kharaz et al., 2016). While in another histological study of the ruptured CCL in canine different breeds (average age 95.11 months ±28.89) found that the ruptured ligaments associated ECM degeneration and chondroid metaplasia compared to the normal healthy ligaments (15.2 months ±4.9) (Ichinohe et al., 2015). Similarly in the distal part of the normal Achilles tendon (compression region) there were fibrocartilage-like cells that positively stained for GAG and PGs (Vidal Bde and Vilarta, 1988, Aparecida de Aro et al., 2012).

In human tendon disease, two main types of tendon disorders have been described: tendonitis and tendinosis (Khan et al., 1999). Tendinitis is an acute inflammatory reaction to sudden injury or infection but tendinosis is characterised by variation in cellular density through the tendon, where the nuclei become rounded and there is a production of PGs (Paavola et al., 2002). The areas of chondroid-like cells are rarely infiltrated by lymphocytes as a part from a healing process as tendinosis is not accompanied by an inflammatory reaction (Jarvinen et al., 1997, Khan et al., 1999). In the present study there was normal alignment of the collagen fibres, no inflammatory response and the density of the intra-fascicular tenocytes (Chapter four, section 4.3.3 histological scoring) did not significantly vary from the mature horse (7, 9 and 14-years-olds). For instance, the average number of intra-fascicular tenocytes in ten different fields (400X magnification) was in SDFT with chondroid metaplasia (n=5) was (22.5 ±4.35 SD), which did not significantly varied

from other mature ages such as approximately similar in 9-years-old horses was 23.17 (±5.2 SD). This could indicate that SDFTs with the ICBs were free from tendonitis and the presence of the ICB is an age related alteration, which was possibly accompanied by a variable amount of accumulative micro-trauma. In an experimental study of an induced overused supraspinatus tendinosis in a rat model, it was found that tendinosis was associated with local stimulation rather than the extrinsic inflammation, where the tenocytes increased and became rounded being also was accompanied by an increase of GAG and collagen fragmentation (Scott et al., 2007). In equine SDFT, three types of phenotypic cells has been recognised, ranging from normal fusi to chondroid-like cells, the latter typically found in compressed region regions of tendons where the matrix is fibrocartilaginous as possibly resulting from micro-damage of the ECM (Patterson-Kane et al., 2012). It has been reported that the histological structure of SDFT alters during injury and tendinopathy, positively staining with Toluidine blue and Alcian blue, which is manifested by an increase in the amounts of aggrecan, collagen type II, GAG, tenocytes, MMP activity, vascularisation and inflammatory cells (Cadby et al., 2013, Jacobsen et al., 2015). In a few ICBs, the ECM around few individual cells contained an organised mesh of micro-fibrils of what collagen (Figure 5.5 D). This finding has also been reported in the pericellular ECM around the normal and osteoarthritic chondrocytes where collagen type VI and II form a network in addition to the other pericellular matrices (Soder et al., 2002).

However, chondroid metaplasia and calcium deposition in the human rotator cuff tendon has been described as a pathological alteration of the tissue preceded by degenerative changes caused by micro-trauma (Hashimoto et al., 2003, Benjamin et al., 2008). A histological study of ruptured human Achilles and quadriceps tendons in more mature people (average of 45 and 69 years old), found that ruptured tendons were characterised by loss of fibre alignment, marked hyalinisation and round nuclei, with increased vascularity and staining for GAG indicative of marked chondroid metaplasia particularly at the superficial layers of the tendon (Maffulli et al., 2000, Maffulli et al., 2012). In other clinical studies of human Achilles tendinopathy and ruptured tendon have demonstrated that the intra-tendinous ossification found in aged patients with a history of previous injury, in histological examination have shown the presence of intramembranous ossification, lamellar bone formation and

dystrophic calcifications with variable inflammatory reaction (Aksoy and Surat, 1998, Richards et al., 2008, Tamam et al., 2011). In our study we found in certain cases calcium salt was deposited within and areas close to the ICB. There was also strong positive immunostaining for type II collagen around the ICB and occasionally within the ICB as has been described in collagenous-induced tendon degeneration in rat model (Lui et al., 2009). Therefore the ICBs contain a large amount of mucopolysaccharides, which could indicate an early stage of the tissue to undergo chondroid or osteoid metaplasia that is likely could be due to adaptation of the tissue against repetitive shear force during ageing.

Cells derived from ageing (12-17 years-old) hamstring tendon explants cultured in different media for 21 days, demonstrated that in chondrogenic media there was cells positively stained for collagen II but when in osteogenic media they had a positive staining for calcium deposition possibly indicative of early chondroid metaplasia (de Mos et al., 2007). Recently, *in vitro* induction of the tendon stem/progenitor cells (TSPC) populations of equine SDFT with osteogenic and chondrogenic media, found that the TSPCs when plated with a medium pre-coated with fibronectin promote both osteogenic and chondrogenic differentiation (Williamson et al., 2015). This provides evidence that the equine SDFT is prone to undergo chondroid metaplasia as we observed that in ICBs cells underwent their morphological differentiation compared to the intra-fascicular tenocyrtes. The conformation and structure outlines of these ICB are similar to those of cartilage possibly due to the fact that the ECM of the tendon may have a different intensity to turn into the cartilaginous tissue with excessive load (chondroid metaplasia). In a mechanical study of equine SDFT it has been shown that fascicles from aged horses were less resistant to cyclical load failure and failed at a lower cycle than in younger horses (Thorpe et al., 2014b). During ageing horses are exposed to cumulative exercise regimens and this possibly leads to an accumulation of the micro-damage (Lam et al., 2007b, Reardon, 2013) and the risk of SDFT injury is increased in aged horses (Perkins et al., 2005, Avella et al., 2009). Similarly, it has been observed in human tendon that repetitive and continuous micro-structural damage occurs within the physiological limits which leads to an accumulative micro-trauma (Arndt et al., 1998). This kind of ICBs could be due to an age related mechanical influence on the tendon microstructures, which affect cellular ability to produce an abundant ECM.

However, this kind of chondroid metaplasia could not be exactly identical to the cartilaginous or bone such as in bird's tendon (Berge and Storer, 1995, Landis and Silver, 2002, Organ and Adams, 2005) because of the nature of the tissue and the early stage of the process of metaplasia within a narrow range of ages (17-20 years-old).

5.4.2 IMMUNOHISTOCHEMISTRY (IHC)

The ICBs found in the aged equine SDFTs, in this study were probed for different PGs and GAGs that have been reported in tendon (Vogel and Trotter, 1987, Iozzo and Murdoch, 1996, Yoon and Halper, 2005). These PGs and GAGs include aggrecan, biglycan, decorin and chondroitin sulphate. Aggrecan immunostaining was positive intra-cellularly, through the ICBs and around the ICBs, while biglycan had a similar distribution but did not react through the ICB (Figures 5.8 and 5.9). It has been shown that different PGs and GAG are present intra-cellularly, on cell surfaces and more frequently in the connective tissues (Silbert, 1982, Caterson et al., 1990). Different amounts of aggrecan can manifest in different stages of ICBs developments, which could be from early development to a complete altered ECM into ICBs (Smith et al., 2009). Immunostaining for decorin was positive around the ICB and within the collagen fibres of the tendon but not through the ICB (Figure 5.10). This was found in cartilaginous tissue where the area where surrounding the nucleus was free from decorin but the inter-territorial matrix reacted with decorin antibody (Hagg et al., 1998). Therefore the material deposited around these inclusion bodies is likely to be a cartilaginous matrix, where their organisation completely differs from cellular structure and the ECM of the normal tendon.

Immunostaining for both epitopes C-4-S and C-6-S varied in its localisation. Chondroitin-6-sulphate- (C-6-S) strongly reacted with the ECM proteins inside the ICB and the area around them but the C-4-S epitope only had a positive reaction around the ICBs (Figures 5.11 and 5.12). Chondroitin and dermatan sulphate are composed of N-acetyl galactosamine that linked to either glucuronic or iduronic acid respectively. N-acetyl galactosamine can be non-sulphated or sulphated at position 4 and 6 (Hileman et al., 1998). The 3B3 (C-6-S) monoclonal antibody recognises carbohydrate epitopes of the terminal unsaturated uronic acid that is linked to 6-sulfated galactosamine produced after enzymatic digestion by chondroitinase ABC

(Bautch et al., 2000, Caterson, 2012). These reactions, particularly with the C-6-S epitopes, indicate that the components within and around the ICBs are a cartilaginous matrix as C-6-S usually occurs with development of the cartilage (Caterson et al., 1990, Slater et al., 1995). It has been reported in a study on rat periodontal ligaments that both the C-4-S and C-6-S epitopes associated with hyalinisation are present in the osteoid, precementum, lacunae and canaliculi of osteocytes (Kagayama et al., 1996). They also found that C-6-S was related to the compressive loads in both hyalinised and non-hyalinised periodontal ligaments, where it was influenced by mechanical stress (Kagayama et al., 1996). It has been shown that the presence of C-6-S and increased levels of C-4-S were found in the development of cartilage (foetal and growth plate cartilage) and osteoarthritis (Caterson et al., 1990, Byers et al., 1992). In the early stages of osteoarthritis of knee joints, there was loss and reduction in the sizes of PG (aggrecan) as a result of proteolytic cleavage (metalloproteinase and aggrecanase) of the core protein within the interglobular domain and associated GAGs (Caterson et al., 1990). This then resulted in an increase in the level of both C-4-S and C-6-S epitopes in both human and animal models, which may be used as a specific anabolic marker of the early degenerative joint disease (Caterson et al., 1990, Ratcliffe et al., 1993, Visco et al., 1993, Lin et al., 2004).

In bovine tendon, it has been shown that regions that subjected to compressed load demonstrated three times higher amounts of a large chondroitin sulphate rich-proteoglycan compared to the tensile regions (Vogel and Heinegard, 1985, Robbins et al., 1997). In the deep digital flexor tendon (DDFT) it has been shown in the compressed region C-6-S is associated with the high molecular-mass of aggrecan (Rees et al., 2000). In the human extensor tendon at the level of metacarpophalangeal region (compressed region) similar findings have been reported, where aggrecan is the predominant PG associated with C-6-S (Milz et al., 1999), however 3b3 could recognise C-6-S epitopes of versican PG (Wu et al., 2005). Versican is a Modular (Lectican) with a high molecular weight but fewer side chains of chondroitin sulphate (10-30 CS) than the aggrecan, and is present in the tensional region of tendon (Samiric et al., 2004, Yoon and Halper, 2005) and its expression is increased during tendinopathy (Ireland et al., 2001). In this study, it was shown that there was a strong positive reaction for 3B3 (C-6-S) through the entire ICBs and moderate reaction to 2B6 (C-4-S) only around the ICBs in addition to very weak

immunostaining for aggrecan. Meanwhile, the decreased level of aggrecan might be due to enzymatic degradation (Caterson et al., 1990). Therefore the positive staining of the presented ICB with those antibodies would indicate that the SDFT was differentiating into cartilaginous matrix during ageing, however, other reasons such as stress, accumulative micro-trauma, or cellular metabolism should not be excluded (Benjamin et al., 1991, Hashimoto et al., 2003, Smith et al., 2009). Therefore, with age, if the ECM equine SDFT is exposed to various repetitive loads, hypoxic and micro-trauma, this may be followed by an accumulation of damaged ECM that is accompanied by alteration of certain components (PGs and GAGs) and deposition of cartilaginous tissue matrices (Patterson-Kane et al., 2012).

5.4.1 TRANSMISSION ELECTROM MICROSCOPY

Transmission electron microscopy (TEM) illustrated that the ICB contained a number of rounded nuclei were surrounded by lamella arranged endoplasmic reticulum (ER) (Figure 5.16 A-C). This lamellar form of ER allowing abnormal-inclusions-protein to be transformed or self-assembled to ultra-structurally evident forms, which suggests that the cells were more actively producing ECM components. In a study of calcification in the leg's tendon turkey, it has been shown that in areas near the site of mineralization cells appear to have increased amounts of endoplasmic reticulum and Golgi apparatus, which require for active protein synthesis (Landis, 1986). This is similar to the situation observed in chondrocytes from pseudoachondroplastic patients (Shapiro et al., 2006, Merritt et al., 2007). Other intracellular components such mitochondria and vacuoles were also seen. The lamellar shaped ER has been previously documented in chondrocytes-like cells in the degenerative zone of bone epiphyseal plate and the fibrocartilage cells of tendon and ligaments at the insertion zone in pseudoachondroplastic dwarf patients (Cooper et al., 1973, Maddox et al., 1997). In these individuals the cartilage cells became large and contained curvi-lammellar bodies within a distended rough ER where there were small lipid droplets. The pseudoachondroplasia is caused by a genetic mutation of the cartilage oligomeric proteins (COMP) that leads to cartilage matrix deficiencies and incomplete growth of the cartilage (Hecht et al., 1995, Thur et al., 2001, Hecht et al., 2005). It has been found that in pseudoachondroplastic mice normal tenocytes did not display these properties ER of abnormal chondrocytes but it was observed

that collagen fibres were disorganised and the tendons became more loose in cyclic strain tests (Pirog et al., 2010). Thus the highly development of the rER would indicate that the cells were became more active and secret a large amount of ECM and this was obvious where the area surrounding those cells rich in a specialised ECM which is very different from normal tendon. The ECM of the ICBs in our study was apparently a dense ECM and arranged in a circular form around the cells and inter-connected by various amount of disorganised fibrils. Exposure to a heavy mechanical or progressive load of the cellular elements or micro-trauma of the ECM may lead to metabolic alteration of the cells, resulting in them becoming rounded and chondroid-like cells in response to abnormal loads (Benjamin and Ralphs, 2004).

5.5 CONCLUSION

In this study we concluded that equine SDFTs during ageing undergo micro-structural alteration, where a number of localised ICBs were developed and accompanied by a positive reaction to proteoglycans and GAG. Their reaction to different monoclonal antibodies, in particular 3B3 would indicate that these structures contained cartilaginous matrices. With the cellular alteration the rER was more abundant than in the normal tendon and secreted a large amount ECM. These findings confirmed that the equine SDFT could undergo chondroid metaplasia during ageing which might be secondary to previous long-term accumulative micro-trauma and/or focal-hypoxia of the tissue. Finally we can support the hypothesis that equine SDFTs undergo substantial focal alteration that are accompanied by localised aggregation of chondroid-like cells surrounded large amount of specific ECM.

2.6 LIMITATION

There were only a limited number of samples with narrow range of ages and no data was available on the work history of the horses. The study was entirely cross-sectional in nature so it is not possible to infer anything relating to onset or progression of these features.

5.7 FUTURE WORK

Further work with larger numbers of horse with a more advanced age is needed in order to explore in detail the aetiology of this alteration. Exploring how these

chondroid-like structures affects the mechanical propertied of the collagen fibres within the fascicles. Determination of the expression of specific genes such as COMP, aggrecan in order to find the specific genes that is responsible such alterations may also be useful.

CHAPTER SIX

SUPERFICIAL DIGITAL FLEXOR TENDON (SDFT) TENDINOPATHY

6.1 INTRODUCTION

Injury is common in horses of all disciplines, especially racehorses, where different studies have reported different types of injuries particularly involving the superficial digital flexor tendon (SDFT) and suspensory ligament (Williams et al., 2001, Ely et al., 2004). It has been shown that SDFT injury accounted for 75-93% of injuries and commonly involved the forelimb (95%) (Ely et al., 2004, Kasashima et al., 2004, Lam et al., 2007a). Injuries were frequently localised within the central core of the tendon and extended longitudinally down through the tendon (Meghoufel et al., 2010, Thorpe et al., 2010a). Post-mortem examination of injured SDFT, which presented with swelling and pain; there was discolouration and degenerative changes of the central core of the tendon and swelling of both paratenon and epitenon (Webbon, 1977, Birch et al., 1998, Cadby et al., 2013). It has been shown, using B-scan ultrasonography, that the injured SDFT manifests with destruction of the extracellular matrix (ECM), in particular the inter-fascicular matrix (IFM), which has subsequently decrease the number of fascicular bundles by approximately 20% (Meghoufel et al., 2010, Cadby et al., 2013). During injury the conformation of the ECM including fascicles and the IFM are distorted, which not displayed as the uniform structure seen in normal tendon (Birch et al., 1998, Sharma and Maffulli, 2005, Lacerda Neto et al., 2013).

Microscopically both ECM and the tenocytes undergo variable degenerative change following tendon injury. In a descriptive study of the SDFT pathology, it was shown that the injured tendon displayed areas of necrosis, haemorrhage, pyknotic nuclei, disintegrated fibrils and presence of organised and disorganised fibroblast and up-regulation of PG and the proteolytic enzymes (Clegg et al., 2007, Sodersten et al., 2013). Similarly, in experimentally induced injuries of equine SDFT, it was shown that the injured tendons were softer, showed pink discolouration and contained red tinged fibrous lesions. Histologically there was an alteration in the collagen fibre alignment, an increased number of both intra-fascicular and inter-fascicular cells, which had altered morphology, and the ECM stained positively for PG and GAG (Parkinson et al., 2011, Cadby et al., 2013, Jacobsen et al., 2015).

In human tendinopathy, the injured tendon demonstrates similar clinical, gross and histological alterations to that seen in the horse, but in rare cases the injured

tendon undergoes further alteration (Birch et al., 1998, Sodersten et al., 2013). It is characterised by deposition of various amount of calcium that subsequently develops in areas of hyalinisation, which then is followed by intra-tendinous ossification (Aksoy and Surat, 1998, Richards et al., 2008, Tamam et al., 2011).

Equine SDFT is a long tendon and frequently becomes injured (Ely et al., 2004, Thorpe et al., 2010a); the gross, three-dimensional and histological configurations of injury are still unclear, particularly the location of the injury and how the injury distributes longitudinally through the length of the tendon. Though using three-dimensional reconstruction (Chapter two) and the histological scoring (Chapter four) I explored the abnormal anatomical and histological alterations of injured tendon. Thus, the aim of this study is to explore the gross, three-dimensional and histological configuration of the injured SDFT and further to compare with the normal tendons and/ or normal regions of the same tendon.

6.2 MATERIALS AND METHODS

6.2.1 SAMPLES

SDFT samples were obtained either from a commercial abattoir (Potters, Taunton or Wootton Bassett) or from Thoroughbred or Thoroughbred cross horses euthanased at the University of Liverpool Equine Hospital with the owners' informed consent. The study was assessed and approved by the University of Liverpool, Veterinary School Research Ethics Committee (VREC, study 214).

6.2.2 SAMPLE PREPARATION

Six samples were collected from the forelimbs of different aged horses and prepared for gross three-dimensional (3D), histological scoring, special stains and immunohistochemistry (IHC) (Table 6.1). For 3D study samples were dissected from surrounding tissues, wrapping in foil and storing at -20ºC. The dissected SDFT represented the whole metacarpal length, extending from the carpometacarpal to the metacarpophalangeal joints.

Table 6.1: Shows numbers of the injured SDFT collected from the forelimbs of different ages (Mean= 7.8 ±5.2 years), one SDFT was taken from each horse.

No	Age/ Years	Number of SDFT	Side
1	2	1	Left limb
2	3	1	Left limb
3	6	1	Right limb
4	9	1	Left limb
5	11	1	Left limb
6	16	1	Left limb

In order to describe the how the injury appears in a 3D form, and it varied histologically from normal tendon, the SDFT samples designed as follow:

1- General gross view of injured SDFT on transverse sections: The frozen SDFT samples were sectioned into a series transverse sections (2-3mm thick) (Chapter two, section 2.2.2.), then hydrated (Chapter two, section 2.2.3) and photographed sequentially using a Canon camera (Canon EOS 5D Mark III, 1000 IOS-speed, 100 mm focal length) (Chapter two, section 2.2.4). The cross sectional areas (CSA) of the injured tendons approximately at the mid-metacarpal region were measured, using the free hand tool in ImageJ (Chapter two, section2.2.5.1).

2- IMOD 3D modelling: IMOD programmes were used to outline and reconstruct the three-dimensional anatomy of the injured SDFT (Chapter two, section 2.2.5.2).

3- Histological scoring, especial stains and IHC: Small pieces (about 20mm^2) were collected from the transverse sections of the mid-metacarpal region and fixed in 4% phosphate-buffered formaldehyde solution, pH 7.4, at room temperature for histological analysis. The tissue blocks were then cut into 5-µm-thick sections, collected on polylysine slides for:

A- Haematoxylin & Eosin (H&E): (Chapter four, section 4.2.5.1), then H&E stained sections were scored according to our scoring method as described in Chapter four (section 4.2.4).

B- Alcian blue stain: (Chapter four, section 4.2.5.2.2).

C- Immunohistochemistry: immunostained for decorin, aggrecan and chondroitin-4-sulpahte (Chapter five section 5.2.2.4).

6.2.3 STATISTICAL ANALYSIS

Statistical analysis was carried out using GraphPad Prism Version 6 (California-USA). Initially the data were checked for normality using D'Agostino & Pearson omnibus normality test. Data were analysed using Mann-Whitney unpaired T-test, significance was set at a p value of < 0.05.

6.3 RESULTS

6.3.1 GENERAL GROSS OBSERVATION OF THE INJURED SDFT

In the injured SDFT section, it was shown that the injuries were most frequently present in the mid-metacarpal region and ran distally toward the metacarpophalangeal joint. In injured SDFTs the size of the tendon cross sectional area (CSA) was increased and there was deformation of the normal conformational outline of the tendons. Furthermore the injured areas were discoloured, the intensity of discolouration were varied from region to region and from tendon to tendon. The injured tendon demonstrated patchy heterogeneous discolouration. Generally, it included a mixture of white-pinkish discolouration that occasionally accompanied by the presence of many dark points of red or black (Figure 6.1 A-D).

The ECM of the injured area appeared as a heterogeneous structure that characterised by slimy shiny white creamy colour (Figure 6.1 A, C). The ECM including fascicles and the IFM were often completely destroyed and no fascicular structure could be determined. In particular the IFM was absent when compared with the normal transverse section (Figure 6.1 B and D). The IFM in the peripheral aspect of the sections often remained apparent but became thin toward the centre of the lesions where it frequently was absent. Destruction of the IFMs led to apparent merging of a number of fascicles in the injured area. Fascicles in these injured areas were not clearly demarcated, and frequently partially or completely inter-connected with each other. Nevertheless, traces of IFMs were apparent inside some core lesions that were surrounded by areas of pink to red discolouration that could possibly indicate haemorrhage. In severe injuries (Figure 6.1 B, C) a large area of the SDFT CSA was involved, both IFM and the fascicles outlines were completely destructed and appeared as a mixture of heterogeneous white to pink components.

On closer examination, a number of dilated blood vessels were seen dispersed throughout the tendons, which were not visible in normal tendon. The epitenon was frequently swollen and the severity of swelling varied from tendon to tendon and between different levels within the same tendon. In severe cases the epitenon lost its demarcated outline and merged with the tendon parenchyma throughout the peripheral aspect of the injured tendon (Figure 6.1 C). In certain cases, particularly in

the core of the tendon the injured area developed number of tinged black-discoloured patchy areas (Figure 6.1 D, dashed arrows).

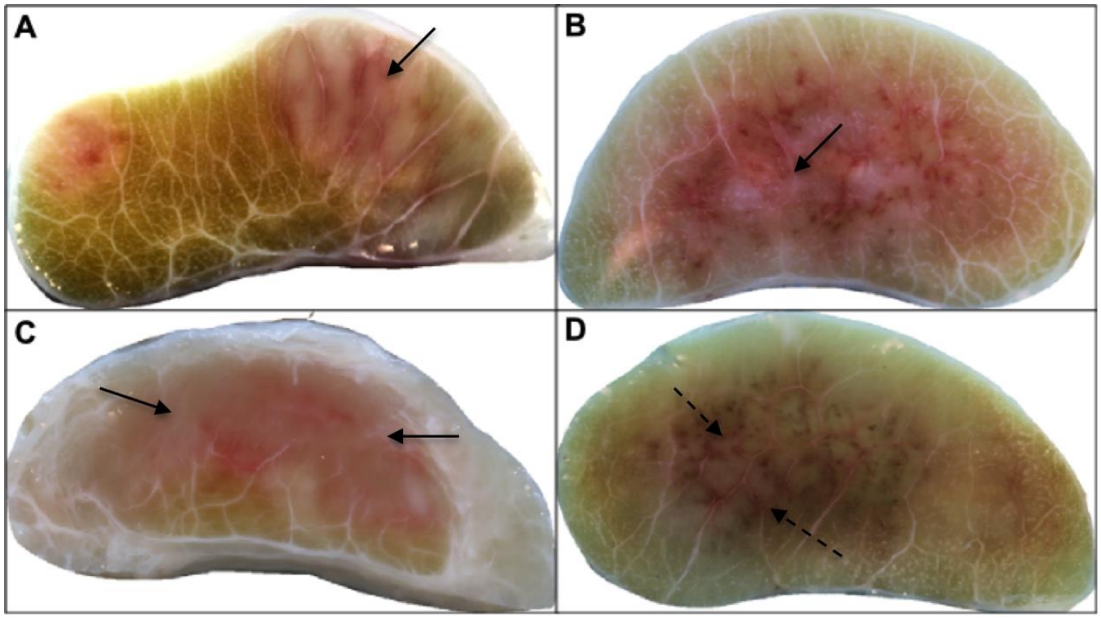

Figure 6.1: Transverse SDFT sections through the mid-metacarpal region from different horses. A: An injured SDFT from 11-years-old horse; the injured areas are localised on both the medial-palmar and lateral-palmar aspect of the tendon, characterised by swelling and discolouration of the injured areas (solid arrow). B: Injured SDFT from 6-years-old horse, the injured area localised within the core of the tendon, where the area is discoloured and the ECM particularly the IFM is disrupted (solid arrow). C: Injured SDFT from 2-years-old, note the injured area extended approximately through the much of the surface of the sections, the surrounding soft tissues (epitenon and paratenon) are swollen and both IFM and the epitenon have lost their structural demarcation (solid arrow). D: An injured SDFT from 9-years-old, the core lesion contains a number of black-discoloured points (dashed arrow).

The CSA of the injured tendons approximately at the mid-metacarpal region were compared to the most normal proximal part of the same tendon. It was found that the CSA was increased at the injured mid-metacarpal region and the volume of swelling varied from tendon to tendon, ranging from minor to a severe swelling. Two of these injured SDFTs showed large increase in their size, their CSA increased in an amount by 81% and 66% than their proximal regions. Both these tendons showed severe

destruction of their parenchyma and the epitenon. Whilst in the other injured SDFT the CSA were increased but to a more minor or moderate degree, ranging from 10% to 37% (Table 6.2).

Table 6.2: the cross sectional area CSA/mm^2 of the most non injured proximal region at the level of carpometacarpal joint and their injured area at the mid-metacarpal region, note an increase in the CSA at the injured regions.

No	Age/ Years	CSA/mm^2 of the non-injured proximal region	CSA/mm^2 of the injured mid-metacarpal region	Difference in CSA/ mm^2	% Difference
1	11	206	227.19	21.19	10.28
2	16	97.58	133.79	36.21	37.10
3	9	143.67	287.61	13.94	9.70
4	6	128.68	233.11	104.23	80.99
5	3	112.09	132.02	19.93	17.78
6	2	122.72	204.08	81.36	66.29

6.3.2 THREE-DIMENSIONAL RECONSTRUCTION OF INJURED SDFT

For 3D reconstruction of the injured tendons IMOD free software (Version 4.7) was used to process a series of TIFF images (Kremer J.R., 1996). A series of transverse sections were Z-stacked and processed for 3D reconstruction according to the protocols outlined in Chapter two.

6.3.2.1 The XYZ planes of the injured SDFT

In the 3D reconstruction of the sample number 4 (6-years-old horse), it was found that the ECM was very abnormal (Figure 6.2). The injured area was localised within the core of tendon substantially increasing the CSA of the tendon. When viewed on XYZ planes both the fascicles and the IFM did not show a normal regular longitudinal outline compared to normal tendon (see Chapter two). The Z-plane demonstrating the transverse section of the SDFT showed the largest area of injury in the mid-metacarpal region (Figure 6.2, arrow indicating destroyed IFM). The SDFT was especially enlarged in dorso-palmar direction. Fascicles and the IFM outlines through the injured areas varied from region to region but those on the peripheral aspect of the tendon frequently, remained intact. In the core of the lesion the IFM was completely disrupted while those in the periphery remained intact and clearly outlined fascicles. Disruptions of the IFM allowed the fascicles to merge with each other and subsequently led to formation of a large centrally localised area of scar tissue. However, IFM at the distant region from the mid-metacarpal region such as those in the upper third of the metacarpal region were not disrupted and clearly outlined the fascicles (Figure 6.2).

In the X and Y planes fascicles extended longitudinally and were outlined by a non-organised IFM. The IFM extended irregularly from the proximal to the distal aspects of the tendon. In different regions of the tendon the IFM was interrupted and were not continuous through the tendon. Both the IFM and the fascicles demonstrated an irregular outlined structure, which at certain levels merged with each other (Figure 6.2). At the site of the greatest injury, fascicles appeared darker and increased in size and contain small amount of intermittent IFM. When moving the XY planes across the tendon it showed frequent fascicular and IFM deformity (Figure 6.2, Y plane).

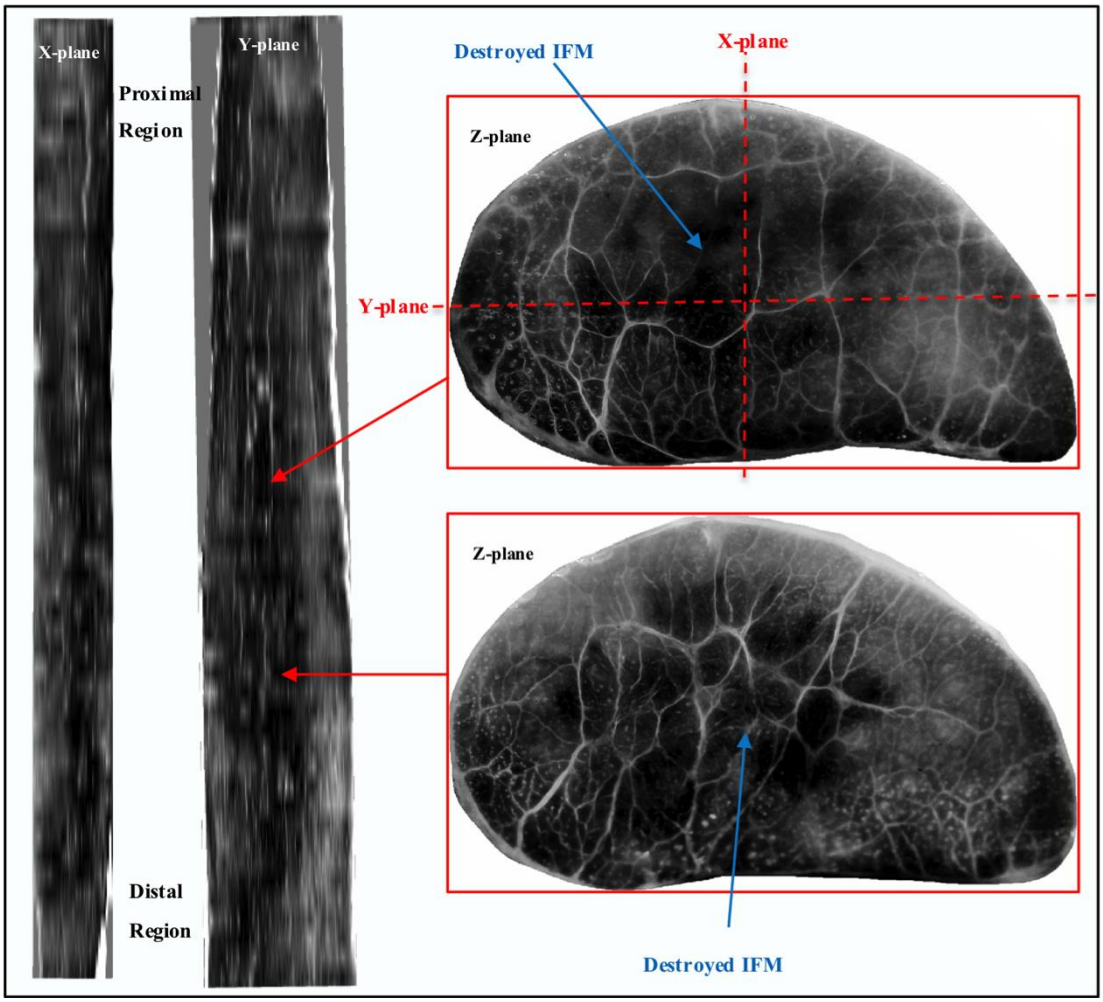

Figure 6.2: The XYZ planes of the injured SDFT through the length of the metacarpal bone in a 6-years-old horse. Note the IFM between the fascicles was destroyed and leading to fascicles merging with each other to form a central region of scar tissue (arrows). In the X and Y planes both fascicles and the IFM are disorganised on their longitudinal axis and their conformation was altered at different levels through the injured area from proximal to distal.

6.3.2.2 3D reconstruction of the injured SDFT using IMOD drawing tool

The injured SDFT (6, 9 and 11 years-old) along the length of the metacarpal bone was reconstructed to see how the injury was distributed throughout the SDFT. The injured areas were distributed longitudinally throughout the SDFT length. In most of the cases the injury was localised within the core of the tendon (Figure 6.3 A and associated video 6.1) but in certain instances the injury was localised at the periphery

of the tendon (Figure 6.3 B and associated video 6.2). The extension of injury also varied from point to point and it appeared that it extended toward the metacarpo-phalangeal joint (Figure 6.3 A, B). In all cases the proximal metacarpal region showed little or no injury. Occasionally two separate injured areas were present in the body of the tendon, although these two separate injury sites were distinct with relation to their size and presence within the tendon (Figure 6.3 B and associated video 6.2).

Fascicles in the non-injured areas were reconstructed and the injured/scarred area was considered as a single fascicle due to disruption of the IFM that allow fascicles to merge with each other (Figure 6.3C IV and associated video 6.3). The size of this single fascicle/scar tissue varied at different levels through the tendon. Proximally it started as a small point and progressively increased toward the mid and distal portion of the tendon. The injured area was characterised by having a large dimension and communicated with the collateral fascicles either through a partial or complete loss of the IFM between them (Figure 6.3C IV and associated video 6.3). Within the injured zone a central areas were severely affected and extended longitudinally through the core of the tendon with various conformation pattern at different levels (Figure 6.3C V and associated video 6.3). Fascicles in the intact uninjured peripheral area were continuous through the tendon and demonstrated divergence, convergence and interconnection with each other (Figure 6.3C III and associated video 6.3). On closer examination blood vessels were obvious through the Z-stack. A large number of blood vessels were observed that dispersed intermittently through the Z-stack and extended along the longitudinal axis of the tendon (Figure 6.3C VI and associated video 6.3).

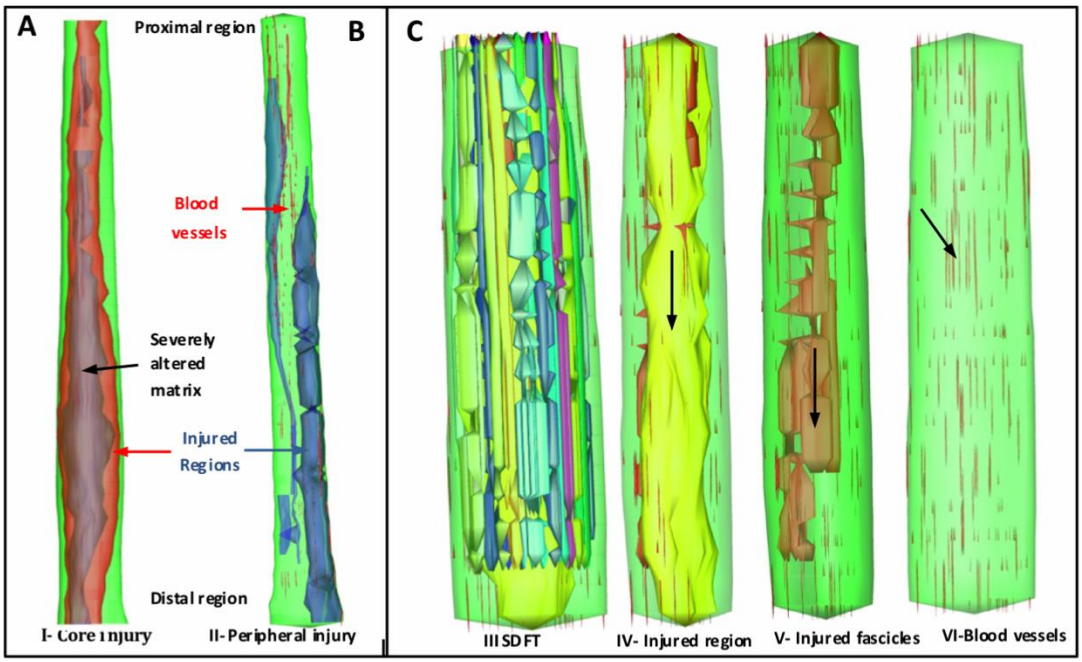

Figure 6.3: Three-dimensional reconstruction of the injured SDFT. A: A 3D reconstruction of the whole SDFT from the carpal to the metacarpo-phalangeal joint in 9-years-old horse. Note the injured area is localised within the central core of the tendon, extend throughout the whole length of the tendon. The size of the injured area is varied from region to region and within the inured zone there is a dark central area that shows a severely altered matrix, where the ECM was completely disrupted (arrow). B: A 3D reconstruction of the whole SDFT from the carpal to the metacarpo-phalangeal joint level in an 11-years-old horse. The injured areas are extended throughout the peripheral regions of the tendon. The size of the injured area are varied from region to region and accompanied by an increase in the size of blood vessels (arrows). C: Shows a fully reconstructed metacarpal region (6 cm long) of injured SDFT from a 9-years-old. III: Fascicles on the peripheral aspect were not affected. IV: The injured area extended longitudinally through the core of the tendon, where the IFM was disrupted and the fascicles fused with each other to form an irregular structure (yellow coloured, arrow). V: At the injured zone, a central irregular area of severely destroyed area is present (red coloured, arrow). VI: In the injured SDFT the blood vessels are clearly visible on close inspection (arrow). Supplementary videos are provided in the links below:

PhD thesis- Othman, Ali- Three-dimensional supplementary videos/6.1.wmv

PhD thesis- Othman, Ali- Three-dimensional supplementary videos/6.2.wmv

PhD thesis- Othman, Ali- Three-dimensional supplementary videos/6.3.wmv

6.3.3 HISTOLOGY OF THE INJURED SDFT

6.3.3.1 General histological observation

6.3.3.1.1 Haematoxylin and Eosin stain (H&E)

The cross section of the injured areas, when stained with H&E, found that the ECM were disorganised and the IFMs were not present at different sites. The IFM in the core of the lesion was completely absent (Figure 6.4 A-C, solid arrows) but in the other areas, especially at the periphery it was still intact (Figure 6.4 B, D, dashed arrows). This histological configuration would support the gross observation that mentioned in Section 6.3.1, where the IFM was clearly disrupted in all sections. Disruption of the IFM led to merging of adjacent fascicles with each other, resulting in the injured area appearing to be made from one fascicle.

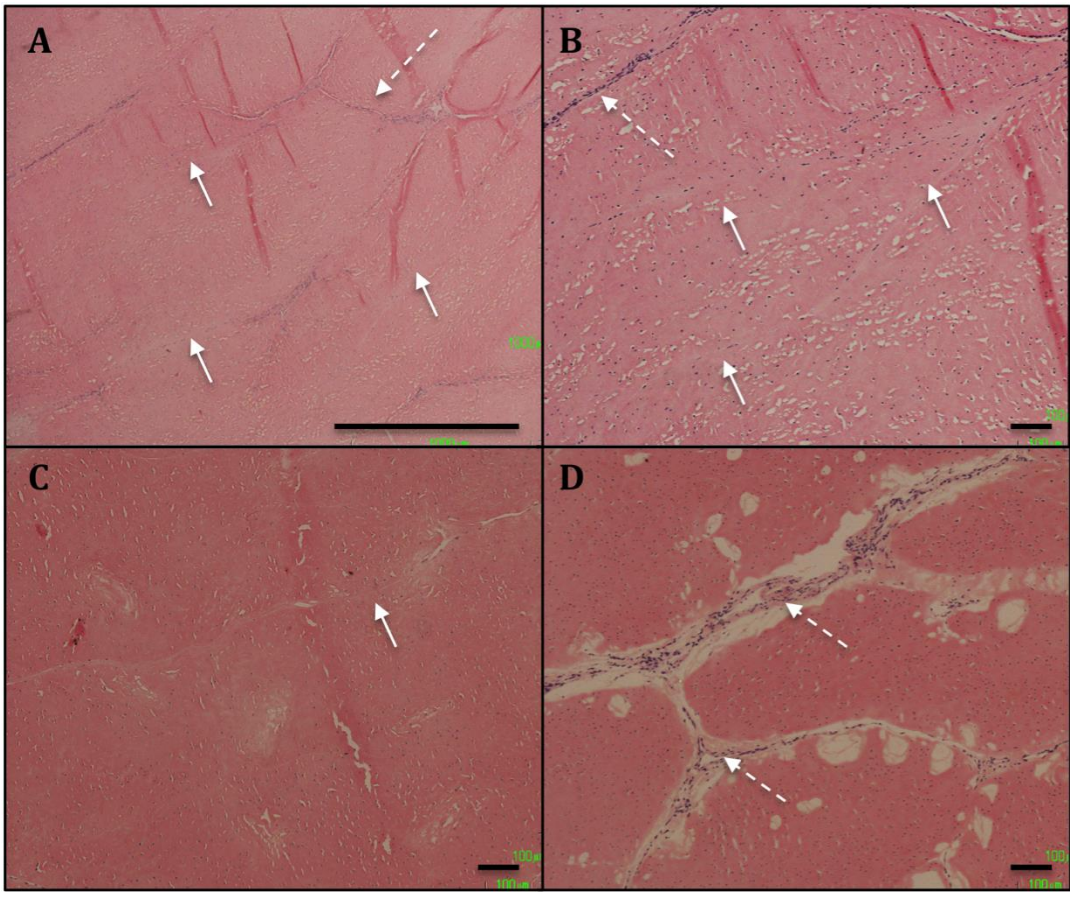

Figure 6.4: The cross section of the injured SDFT stained with H&E. Note the IFM in the injured area was indistinct or absent (solid arrows), but areas around the injured site have approximately an intact IFM (dashed arrows), (Large scale bar= 1000µm (A) and small scale bar=100 µm (B-D)).

Moreover, on transverse and longitudinal sections of the injured SDFT, the tissue architecture demonstrated various amounts of disorganisation (Figure 6.5 B, C). A number of different sized spaces were appeared within the injured area and particularly around the IFM. The content of these spaces did not stain with H&E but a few thin fibrils like structures were found, where arranged in an irregular shaped structures and occasionally a multiple meshed like fibrils (Figure 6.5 A and B). In severe injury the tendon ECM were severely disrupted; the collagen fibres of the fascicles were disrupted, disorganised and there was a lack of definition between the IFM and their adjacent fascicles. Moreover a number of different shaped spaces were also present throughout the tissue (Figure 6.5 C). The cellular content of both the IFM and the fascicles was apparently increased; the tendon became hypercellular when compared to the normal SDFT (Chapter four-scoring methods, section 4.2.4). Different sized and shaped intra-fascicular tenocytes-nuclei were observed, arranged along the longitudinal axis of the collagen fibres (Figure 6.5 D). The nuclear shape arranged from oval to an elongated fusi form. Occasionally a few apparently apoptotic cells were appeared between the collagen fibres. Apoptotic nuclei were characterised by condensation their chromatin, blebbing and fragmentation (Figure 6.5 D, dashed arrows).

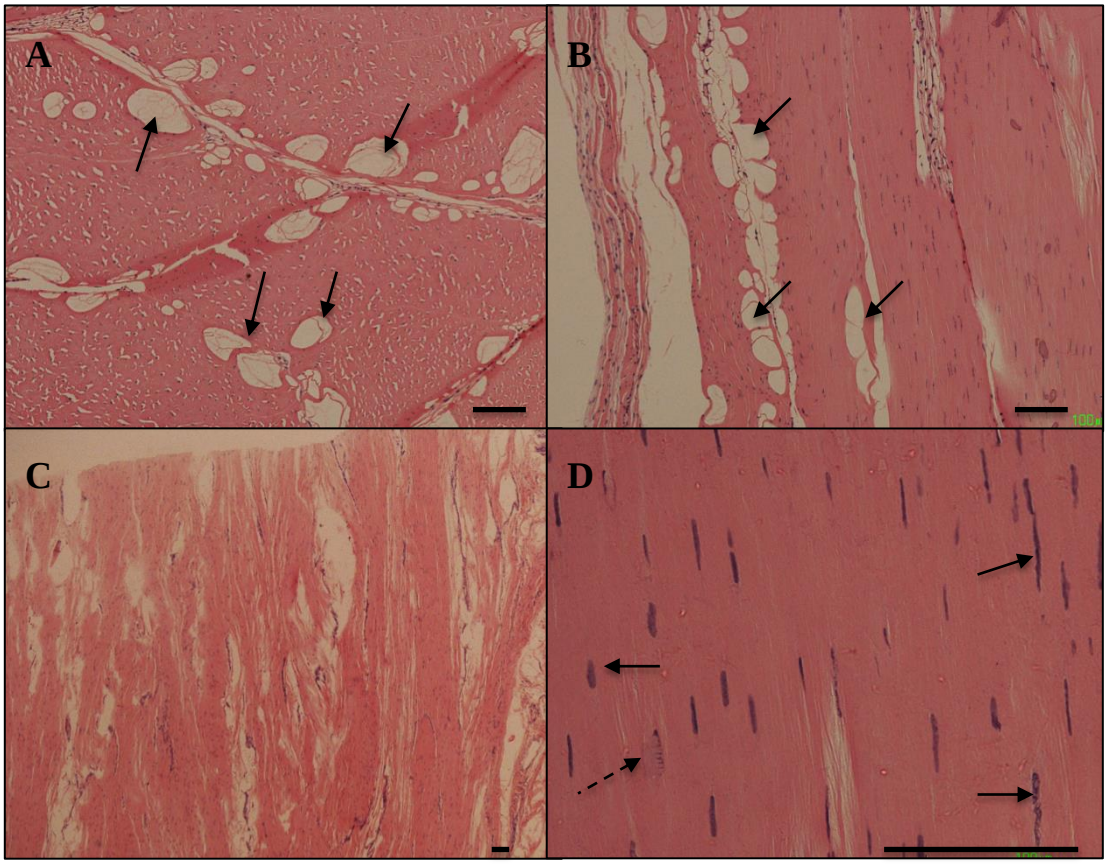

Figure 6.5: H&E staining of the injured SDFT. A: This section represents a transverse section from the injured area, 6-years-old horse, where a number of different sized spaces present inside the fascicles and close to the IFM (arrows). B: This section shows the longitudinal section of the injured SDFT, 6-years-old horse, where the tissue architectures are damaged and contain a number of different sized spaces (arrows). C: This section shows the longitudinal section of the injured SDFT, 3-years-old, there is severe disruption of fascicles and the IFM. D: This section demonstrates that different shaped intra-fascicular nuclei are present between the collagen fibres, arranged from an oval to a long fusiform (arrows), note the presence of apparently apoptotic nuclei that have condensed chromatin, bulged and fragmentation, 3-year-old horse (dashed arrows), (Scale bar =100 µm).

6.3.3.1.2 Alcian blue-PAS staining

The injured SDFTs were further stained with Alcian blue/ PAS in order to show the whether the observed pathology was associated with PG and GAG accumulation. It was found that all injured SDFTs had a positive reaction but this staining varied in intensity. The intensity of reaction to Alcian blue staining varied from region to region and was seen both intra-fascicularly, in the IFM, and pericellularly (Figure 6.6). Moreover, areas around the injured areas and resultant spaces as well as their boundaries showed a positive reaction for Alcian blue staining. The mesh like

content of the spaces was also had a positive reaction to Alcian blue-PAS (Figure 6.6 A and B). The areas inside the spaces appeared as granulated structures around the longitudinal cord like structures. In few regions there were strong intra-fascicular, pericellular and intra-space staining (Figure 6.6 C). In other area tenocytes were aggregated and the cells appeared rounded, which likely indicate fibrocartilaginous cells (Figure 6.6 D). Positive staining of all injured SDFT with Alcian blue-PAS indicates that certain component such as PG and GAG were expressed in different intensities in different tendons and various regions within the same tendon.

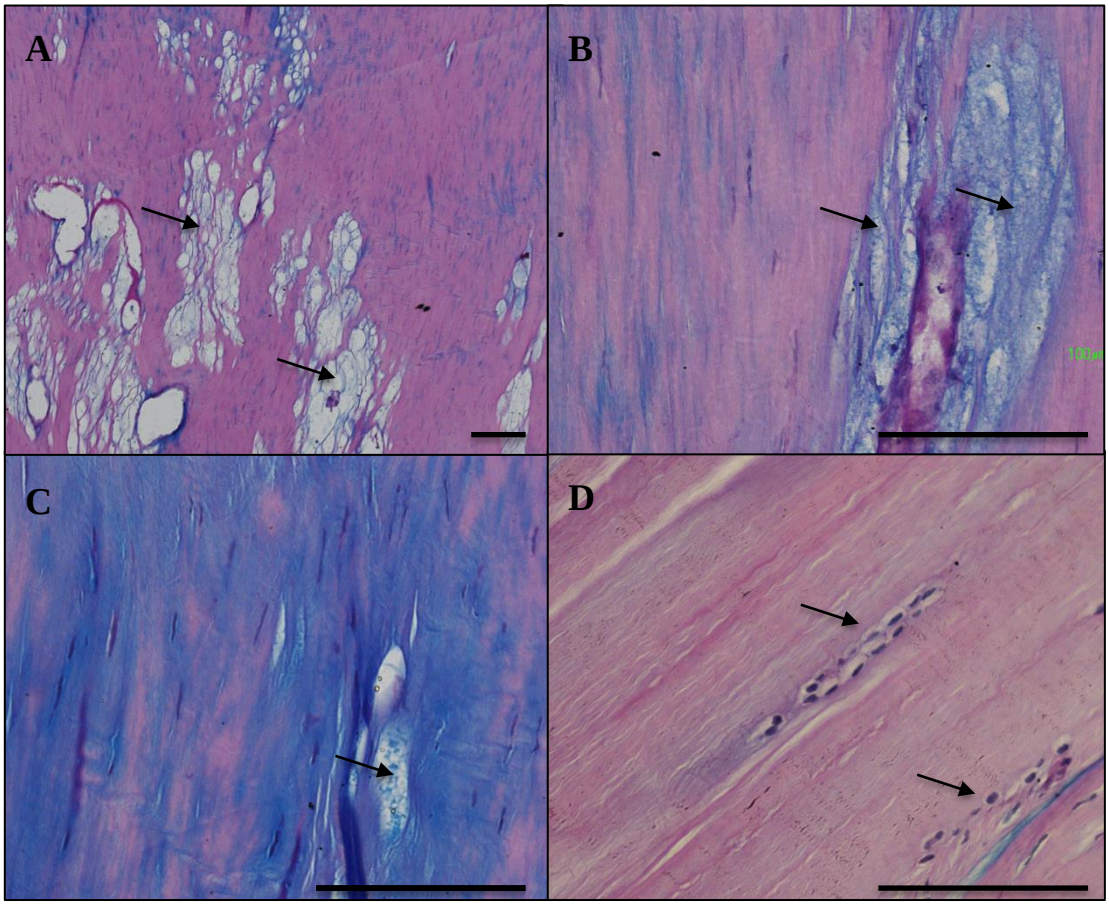

Figure 6.6: Alcian blue-PAS staining of different injured SDFTs. A: Represents the longitudinal sections of injured area, 9-years-old horse, positive staining of the ECM with Alcian blue, the intra-fascicular spaces have no content but the surrounding borders are positive for Alcian blue (arrows). B: Represents the longitudinal sections of injured area, 9-years-old horse, the content of the intra-fascicular spaces are positive for Alcian blue staining (arrows). C: Represents the longitudinal sections of injured area, 6-year-old horse; collagen fibres around the small spaces have a strong positive reaction (arrows). D: Represents the longitudinal sections of injured area, 3-years-old horse, shows a number of aggregated intra-fascicular tenocytes that are rounded possibly indicating fibrocartilaginous differentiation (arrows), (Scale bar=100 µm).

6.3.3.2 Histological scoring

6.3.3.2.1 Fascicles and IFM angulation

The percentage and degree of both fascicles and the IFM alignment was scored according to the scoring methods described in Chapter four (section 4.2.4.1). It was found that there was an alteration of these anatomical parameters when compared to the normal tendon. The percentage of angulation of the fascicular and the IFMs were apparently increased in injured tendon. The degrees of fascicular and IFM angulation were measured in all injured SDFT, using ImageJ. It was found that the average number of angulated fascicles was increased from approximately 55% (±16.9 SD) (normal mature horses) to 59% (±18 SD) in injured SDFT. As well as the IFM angulation increased from approximately 68% (± 21 SD) (normal mature horses) to 75% (±6 SD) in injured SDFT (Figure 6.7). However, there was not an increase in the average degree of both fascicular and IFM angulation in injured SDFT (Table 6.3). Therefore, there was a slight increase in the average number of angulated fascicles in the injured SDFT an amount of 4.14% and the IFM were increased in an amount of 7.42%, thus the IFM was the most part of the ECM were deformed during injury (Figure 6.7). This apparent alteration in angulation did not reach statistical significance.

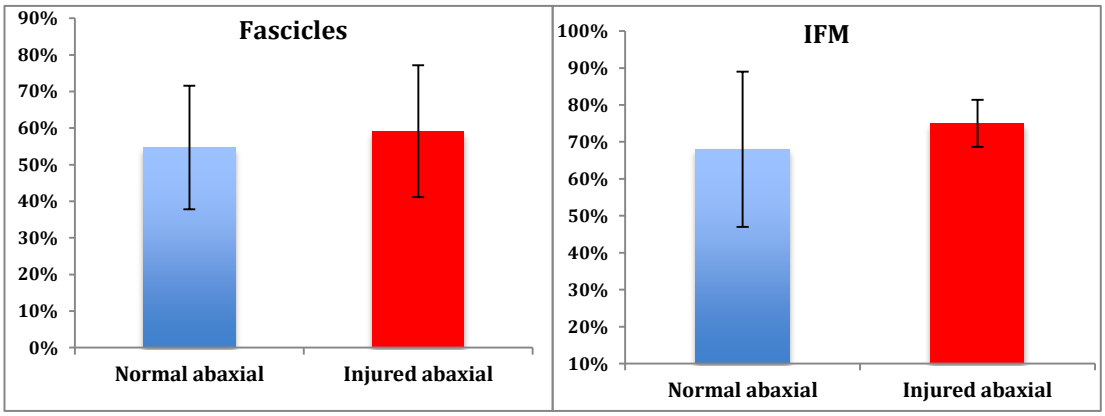

Figure 6.7: The percentage of both the fascicular and the IFM angulation in injured (n=6) and non-injured SDFT (n=6). Note that whilst there is an apparent increase in the number of angulated fascicles and IFMs in injured tendon, this did not achieve statistical significance, unpaired T-test (P> 0.05), (Error bars= SD).

6.3.3.2.2 IFM thickness

Moreover, the IFM thickness of the tertiary fascicles close to the the injured areas of all injured SDFT were measured. For each injured SDFT 60 points of the non disrupted IFM were measured, their average was calculated and then compared to the IFM thickness of the normal mature horses. It was found that there was a profound alteration in the amount of IFM between the teritary fascicles. The average IFM thickness of the injured SDFT was 27.73µm (±11.55 SD, n=6), which was significantly greater ($P < 0.05$) than the tertiary IFM of the normal mature horses (12.34µm ± 3.07 SD, n=6) (Figure 6.8). Therefore, there was an increase in the amount of IFM in injured SDFT but the amount of IFM alteration varied from tendon to tendon and different region within the same tendon (Table 6.3).

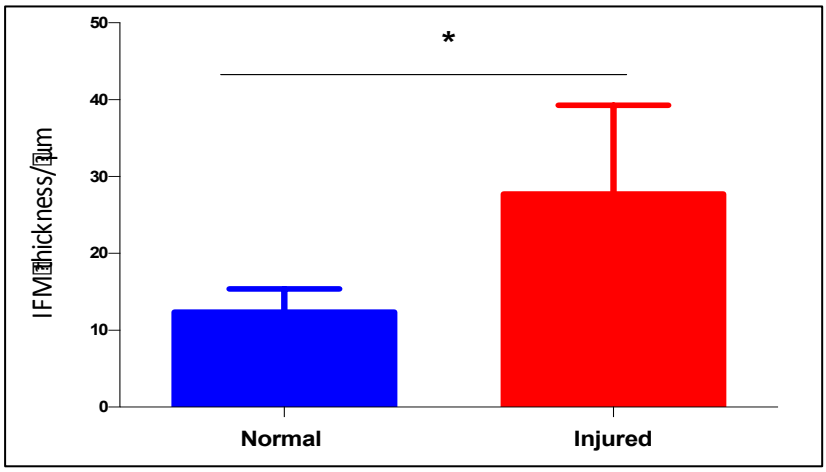

Figure 6.8: The IFM thickness between the injured and the normal SDFT, note there is significant increase in IFM thickness in the injured SDFT (n=6), using Mann-Whitney unpaired T-test ($P < 0.05$), (Error bar= SD).

6.3.3.2.3 Cellular alteration

Numbers and length of nuclei were scored in all injured tendon (scoring method in Chapter four, section 4.2.4.3) and then compared to mature normal tendons (9-years-old horse). Then their average number (average in 10 different fields/400X magnification) were calculated and compared to the normal mature horses. In the injured tendons, it was found that there was a significant increase in the number of intra-fascicular tenocytes. The average number of intra-fascicular tenocytes in 10

fields (400X magnification) was 45.67 (±12.69 SD) in injured tendons (n=6) and 26.86 (± 8.22 SD) in normal mature (n=6) tendons, which was significantly hgher in the injured SDFT than the normal mature horses (P <0.01) (Figure 6.8 A). Therefore, the number of the intra-fascicular tenocytes approximately increased by 70% in injured SDFTs, although the the cellular density were varied from tendon to tendon (Table 6.3, Intra-fascicular cell density).

Moreover, in each injured SDFT, the average nuclear length were also measured (150 nuclei in 10 different fields, 400X magnification) and compared to the normal tendon (9-years-old horse). It was found that there were a marked alteration of the intra-fascicular nuclear length in the injured SDFT (Table 6.3, nuclear length/µm). The injured SDFTs were characterised by the presence of different shaped and sized nuclei. In all injured SDFTs there was a significant reduction in the length of intra-fascicular nuclei. The average length of intar-fascicular nuclei of injured SDFT (n=6) was 14.43µm (±1.86 SD). When compared to the normal SDFT (n=6) it was 20.96µm (±2.42 SD), (P< 0.01) (Figure 6.8 B). There was a significant decrease in nuclear length in injured SDFT, where the the average length of nuclei was decreased in an amount of 31.15% in contrast to the normal tendon (Table 6.3).

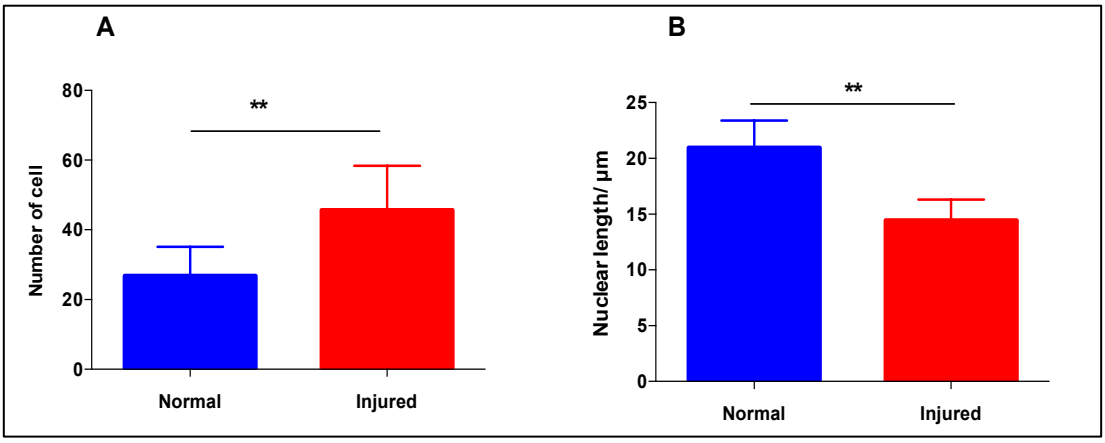

Figure 6.8: A: The average number of intra-fascicular tenocytes in 10 different fields (400X) measured and compared to the non-injured SDFT of mature horses (n=6), there was a significant increase in the number of intra-fascicular tenocytes in injured SDFT, using Mann-Whitney unpaired T-test (P<0.01). B: The average length of the intra-fascicular nuclei were measured in 10 different fields of view (400X) of all injured SDFT (n=6), there was a significant decrease in the length of the intra-fascicular nuclear length in injured SDFT than the non-injured SDFT (n=6), using Mann-Whitney unpaired T-test (P< 0.01), (Error bars= SD).

Table 6.3: Different histological parameters of the injured SDFT, including age, ECM angulations, IFM thickness and cellular parameter (SD= standard deviation).

No	Age	Fascicle angulation/ degree	IFM angulation/ degree	IFM thickness	Intra-fascicular cell density	Nuclear length/µm
1	11	2.28	3.28	46.77	51.5	12.13
2	16	2.63	2.83	21.99	38	14.16
3	9	2.01	2.54	29.76	69	12.31
4	6	4.75	5.77	12.82	37.7	16.05
5	3	1.07	1.89	22.79	41.4	15.9
6	2	2.94	3.6	32.20	36.4	16.05
Mean	**8.8**	**2.61**	**3.31**	**27.73**	**45.66**	**14.43**
SD	**5.26**	**1.22**	**1.34**	**11.55**	**12.69**	**1.86**
The normal values were obtained from normal mature horses are shown below with their SD						
Mean	**9**	**2.41**	**3.48**	**12.34**	**26.86**	**20.96**
SD	**-**	**0.79**	**1.40**	**3.07**	**8.22**	**2.42**

6.3.4 IMMUNOHISTOCHEMISTRY OF INJURED SDFT

The antibodies used in this section are described in detail in Chapter five (Section 5.2.2.4)

6.3.2.1 Decorin

Immunostaining with anti-decorin monoclonal mouse-IgG showed positive staining in all injured SDFTs. The intensity of the reaction varied between tendons and from region to region, and there were intra-fascicular, IFM and pericellular reactions (Figure 6.7). The areas around the spaces and their boundaries showed positive reaction for decorin. Within these spaces there was positive immunostaining for decorin (Figure 6.7 B). In few regions there were strong intra-fascicular, IFM and the pericellular positive immunostaining for decorin (Figure 6.6 C and D). In other

areas, there was also positive immunostaining around the tenocytes (Figure 6.7 D). Positive immunostaining of all injured SDFTs with decorin would support greater amounts of decorin being present in injured tendons and different regions within the same tendon.

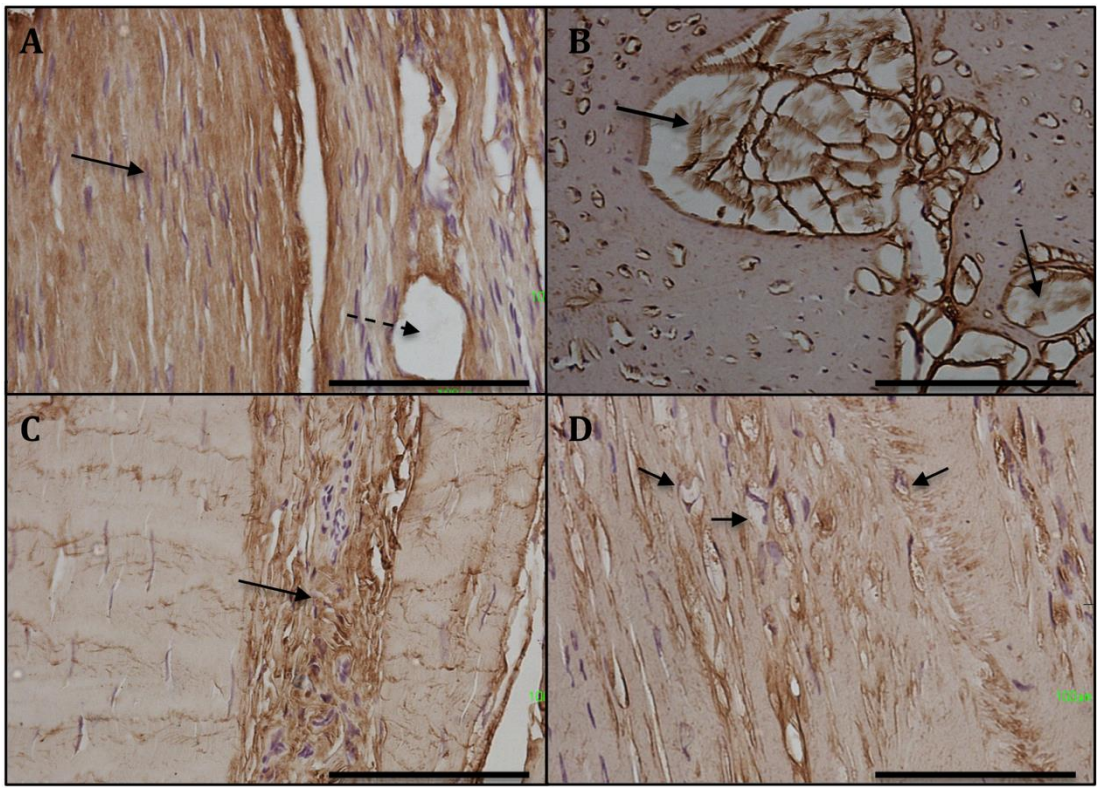

Figure 6.7: Immunostaining of the injured SDFT with mouse monoclonal anti-decorin-IgG. A: This section represent a longitudinal section of injured area, 3-years-old horse, the collagen fibres of the fascicles have a strong positive immunostaining with anti-decorin in a (solid arrow), with few spaces (dashed arrow). B: Transverse section of injured SDFT from a 6-years-old horse, shows the spaces and its contents have a positive reaction for anti-decorin-IgG (arrows). C: Represent a longitudinal section of injured area, 16-years-old horse, both collagen fibres of the fascicles and the IFMs (arrows) are positive with different intensities to the anti-decorin antibody, where the IFM shows stronger positive staining for decorin. D: Represent a longitudinal section of injured area, 6-years-old horse, shows the intra-fascicular pericellular reaction for anti-decorin (arrows), (Scale bar=100µm).

6.3.2.2 Aggrecan

Immunostaining with anti-aggrecan monoclonal mouse-IgG was positive in all injured SDFTs but the intensity of reaction was weaker than seen with decorin. The intra-fascicular reactions were not uniform, and were frequently patchy (Figure 6.8,

A and B). The IFMs were positive for aggrecan and they appeared to stain with slightly stronger intensity than that seen in the fascicles (Figure 6.8 B dashed arrow). Moreover the free borders around the spaces had a small amount of aggrecan staining. In certain areas there were positive pericellular immunostaining for aggrecan (Figure 6.8 C black arrows).

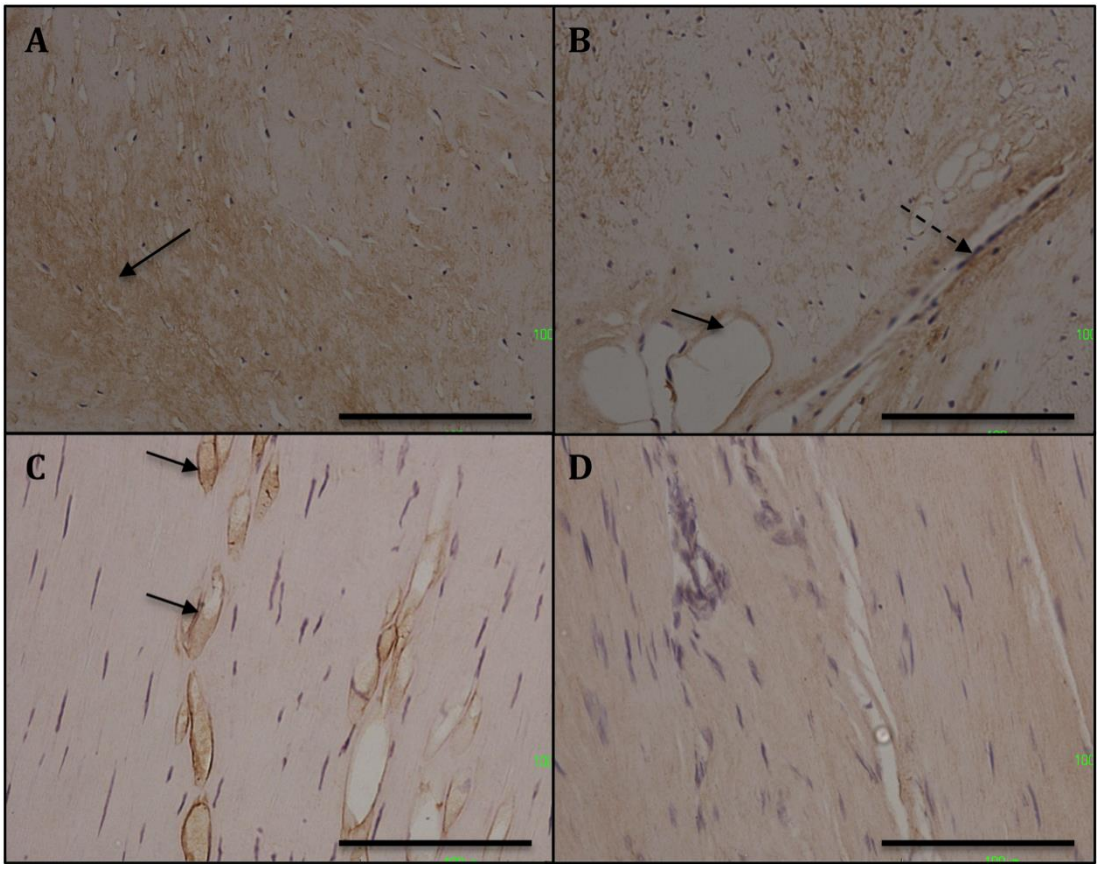

Figure 6.8: Immunostaining of the injured SDFT with monoclonal anti-aggrecan mouse-IgG. A: Represent a transverse section of injured area, 9-years-old, shows a patchy positive reaction for aggrecan (solid arrow). B: Represent a transverse section of injured area, 9-years-old, there is immunostaining of the IFM (dashed arrow) and free border of the small spaces (solid arrow). C: A longitudinal section of injured area, 11-years-old, shows the intra-fascicular pericellular reaction (solid arrows). D: A longitudinal section of injured area, 3-years-old, demonstrates a weak immunostaining of the intra-fascicular collagen fibres, (Scale bar=100 µm).

6.3.2.2 Chondroitin-4-sulphate-4 (C-4-S)

This monoclonal antibody is specific to chondroitinase ABC-generated chondroitin-4-sulphated (C-4-S) stub of chondroitin sulphate and dermatin sulphate

(DS). In all injured SDFTs there was strong positive immunostaining for C-4-S. There were positive reactions throughout the intra-fascicular, IFM and structures of the injured areas/ spaces (Figure 6.9 A and B) in the tendons. In areas where the the collagen fibres were deformed and contained different sized spaces there was a strong positive reaction to C-4-S. Inside the spaces there was a mesh structure of thin fibrils that also had a strong positive immunostaining for C-4-S (Figure 6.9 B and D). Therefore, during injury it appears that a large amount of C-4-S is produced and distributed throughout the tendon indicating that there was the possibility of an increase in the amount of both CS and DS during injury.

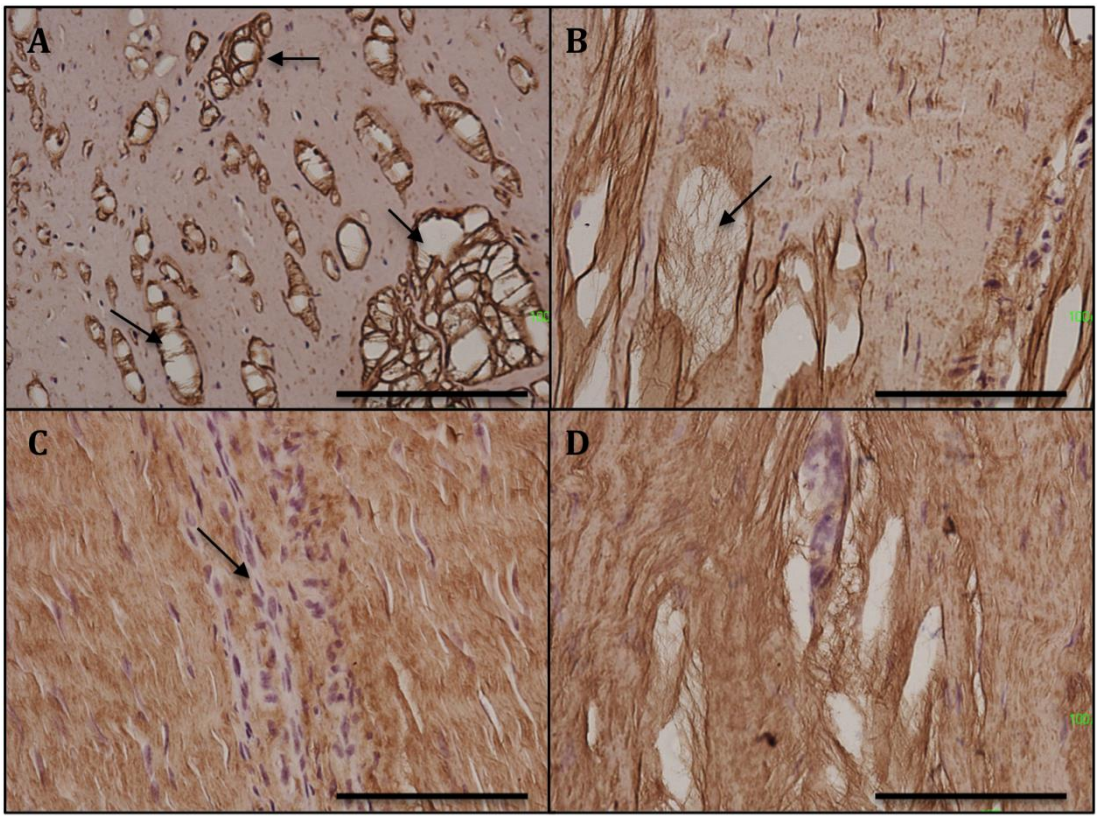

Figure 6.9: Immunostaining of different injured SDFT with anti-C-4-S monoclonal mouse-IgG. A: This section represents a transverse section of injured area, 11-years-old, shows strong positive reaction to C-4-S through the ECM and the hole like spaces (arrows). B: Represent a longitudinal section of injured area, 11-years-old, shows reaction of the ECM and the spaces to C-4-S (arrow). C: Represent a longitudinal section of injured area, 9-years-old, there is a very strong positive reaction of the fascicular ECM and the IFM (arrow) to C-4-S. D: Represent a longitudinal section of injured area, 3-years-old, there is a strong affinity of C-4-S to the meshwork present within the spaces (Scale bar=100 µm).

5.3.3.6 Negative control

Two negative controls were included, in the first Tris Buffer Saline-Tween TBST was applied instead of the primary antibody, while for the second control the mouse monoclonal IgG isotope was applied instead of the primary antibodies (Figure 6.10).

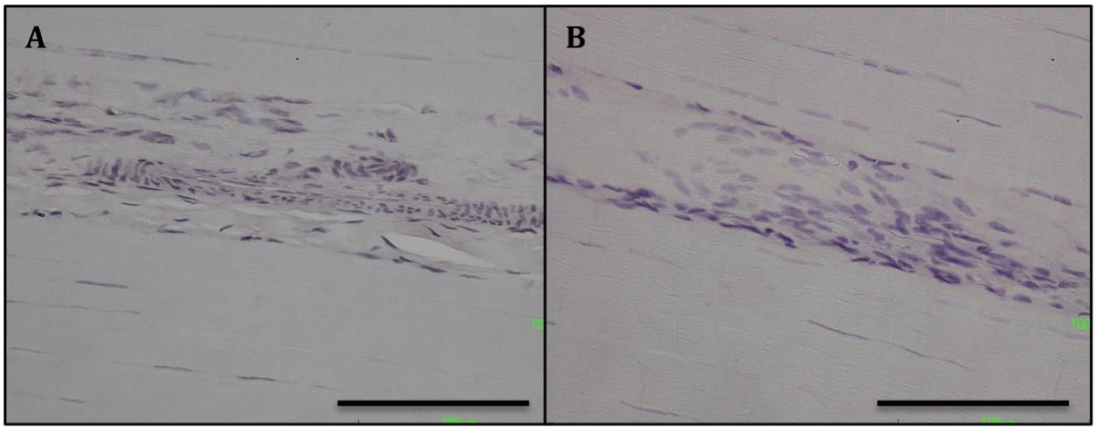

Figure 6.10: This section represents a negative control for proteoglycans. A: In this section negative buffer control instead of the primary antibody the TBST was applied. B: In this section IgG negative control instead of the primary antibody the mouse monoclonal IgG isotope was applied. Note in both controls there are no immunostaining reactions.

6.4 DISCUSSION

6.4.1 MACROSCOPIC OBSERVATION OF INUJURED SDFT

In this study, it was shown that injuries to the SDFT were varied from tendon to tendon and within different areas of the same tendon (Figure 6.1 A-D). The severity of the injury depends on different factors including both an intrinsic and extrinsic factors (Williams, 1986, Kobayashi et al., 1999). The prevalence of SDFT tendinopathy has been shown to be higher in old horses than in younger animals (Avella et al., 2009). In a study it was demonstrated that SDFT overloading may occur due to fatigue of the deep digital flexor muscle which then renders the tendon to being more susceptible to fatigue injury (Butcher et al., 2007). The aetiology of tendon injury is multifactorial, tendon ECM could undergo age and cyclical degeneration, that frequently affecting the central core of tendon and it has been found in both equine (Meghoufel et al., 2010) and human athletes (Aksoy and Surat, 1998, Richards et al., 2008, Tamam et al., 2011).

The injured SDFT was characterised by swelling, discolouration of the injured region, dilation of the blood vessels. Similar gross morphological features have been described in different studies, which demonstrated that the lesion was predominantly localised within the central core of SDFT (Webbon, 1977, Birch et al., 1998, Cadby et al., 2013). The degree of swelling was varied from tendon to tendon. Typically, it has been shown that the cross sectional areas (CSA) of the normal SDFT is smaller in the mid metacarpal region than in the proximal and the distal regions (Smith et al., 1994, Agut et al., 2009). In this study, it was shown that the injured mid-metacarpal region has a markedly increased CSA when compared to the apparently normal proximal-metacarpal region. Moreover, the injured area was not always localised within the core of the tendon and that the lesion could localised in both in the central core or the peripheral aspect of the tendon (Birch et al., 1998, Meghoufel et al., 2010). In the latter form the injury was involved the most palmar aspect of the tendon which may be due to the position of the limb, where the palmar surface of SDFT is less protected (Baxter, 2011). However, most tendon injuries are due to extrinsic strain injuries rather than a consequence of external impact (Sharma and Maffulli, 2005, Butcher et al., 2007). In a clinical and ultrasonographic examination of SDFT tendinitis, which involved the proximal metacarpal region of injured SDFT,

it was found that cases that were accompanied by lameness a large area from the SDFT CSA was injured (50-100%) and their prognosis were poor (Chesen et al., 2009). Similarly, in the present study it was found that the CSA enlargement varied from tendon-to-tendon (9% to 80%) and the maximum swelling varied regionally between tendons. The injured SDFTs also showed various intensities of tissue discolouration; in certain region the discoloured area appeared to form a mixture of white to pinkish materials. Where both the fascicles and the IFM were completely affected and distorted, it was not possible to discern any FM/IFM organisation. Moreover, in certain case a number of small black spots were apparent, which felt hard on palpation (Webbon, 1977, Birch et al., 1998). In a post-mortem study of injured equine SDFT, it has been shown in an area of chondroid metaplasia macroscopically, a hard body was surrounded by a thin capsule embedded into the anterior surface and the tendon sheath of SDFT (Webbon, 1977). In this study these black hard points on the transverse SDFT section could possibly indicate developments of hard fibrous tissue or may be an early fibrochondrogenic change or mineralisation of the injured tissue in response to chronic tendon injuries, however these change were not identified histologically. The gross pathological alteration of the tendon was clearly outlined and could be processed into the following stages of models or conformational studies.

6.4.2 THREE-DIMENSIONAL RECONSTRUCTION OF INURED SDFT

In this study, we described the distribution and extent of the injured area within the body of SDFT. In both, central and the peripheral localisation of the injured SDFT, it was demonstrated that the injuries extended longitudinally quite some considerable distance from proximal to distal. The CSA of the injuries also varied at different level. In both instances the injury CSA was highest at the mid-metacarpal region extending down to the metacarpo-phalangeal joint, with little extension of the injuries proximally. In the XYZ planes views, it was observed that the tendon ECM was severely affected; in particular the IFM was intermittently lost and disrupted (Figure 6.2). In a study, using B-scanning ultrasonography, it was shown approximately similar features, where the injury, localised within the core of the tendon and accompanied by destruction of the thinnest IFM (van Schie et al., 2003, Meghoufel et al., 2010). Destruction of the IFM makes the fascicles to merge and

form a large mass of scar tissue within the core of the tendon, which possibly do not allow fascicles to slide smoothly over each other, that subsequently affect their mechanobiology (Thorpe et al., 2012). This could lead to a stiffer tendon matrix which is both at higher risk of future injury, as well as being less appropriate for locomotory efficiency

Using the IMOD tool to reconstruct component of the injured SDFTs, here it was also found that the injured lesions were distributed from the proximal to the distal region. They involved both the peripheral and the central core of the tendon in different horses (Figure 6.3). The CSA of the lesion varied regionally from proximal to distal. In an experimentally induced partial resection of the SDFT, it was observed that the lesion rapidly developed and extended through the entire length of the tendon (Jacobsen et al., 2015). Thus, when the mid-metacarpal region becomes injured the injury may rapidly extend proximally and distally. In this study, it was found that the injuries frequently extend from the proximal to the distal but the lower 2/3 of the tendon had the most extended lesion within the body of the tendon. The severely extended area showed a great distortion of the ECM that could be more sensitive to mechanical rupture than the other region. In an ultrasonography and mechanical testing study of both normal and injured SDFTs, it was found that the injured SDFT showed greater CSA, lower echogenicity (low fibre alignment), decreased elastic modulus and a decrease in stress at tendon rupture. Thus the injured site could be fragile and more predisposes to re-injury or rupture (Crevier-Denoix et al., 1997, Crevier-Denoix et al., 2005). In this study, it was found that the injured tendon extended as an irregular deformed mass with variable CSA as it ran proximal to distal. In the adjacent non-injured regions of the tendon, the FM/IFM anatomy could appear normal and longitudinally aligned. A number of small blood vessels were apparent in injured tendons, particularly associated with the IFM, particularly at the IFM junction sites. Increasing tendon vasculature during injuries have also been shown in canine flexor tendons and its sheaths (Potenza, 1962, Gelberman et al., 1981), human flexor tendons (Richards, 1980) and equine SDFT (Schultz, 2004, Werpy and Barrett, 2012). In equine SDFT, using colour Doppler ultrasonography to monitor the blood flow in tendinopathy, it has been shown that in the acute phase, tendon is rich in blood vessels but fewer in remodelling phase and the number of blood vessels decreased at the injury areas, where filled with scar tissue (Murata et

al., 2012, Hatazoe, 2015). Similarly, in our 3D reconstruction, the blood vessels were most frequently observed in the peripheral parts of the tendon surrounding the injured lesion, and coursed longitudinally through the tendon. 3D reconstruction of the injured tendon accurately described the extent of the injured tendon, and the resulting scar tissue within the tendon and vasculature.

6.4.3 MICROSCOPIC ALTERATION OF INURED SDFT

In this study we demonstrated considerable histological alterations in the injured SDFT. Histologically, it was confirmed that the IFM between the fascicles at the site of injury was frequently disrupted or had even disappeared, (Figure 6.4) which led to fascicles losing their distinct conformational pattern. However, in the peripheral aspect of the injured region the IFM was frequently enlarged/thickened. In an ultrasonographic study of injured equine SDFT, it has been shown that there is disruption of intra-tendinous IFM by necrotic tissue leading to merging of fascicles, moderate entropy, and high waviness ratios but in late granulation tissues it was characterised by swollen IFM and incomplete organisation of the ECM (van Schie et al., 2003).

Previous researchers have demonstrated that histological scoring parameters, relating to fascicles, IFM, and the cellular morphometry are altered in contrast to the normal tendon in horses (Sodersten et al., 2013). Similarly in an experimentally partial transection through creation of a V-shaped area, which subsequently filled with red-tinged fibrous tissue. This study also demonstrated that the injured area of the SDFT demonstrated a pink-discolouration with apparent areas of softness. Histological scoring, including intra-fascicular cellularity, cell morphology, collagen fibres alignments and vascularity were significantly greater in injured than in the normal tendons (Jacobsen et al., 2015). In this study, a number of different sized and shaped spaces were found in all injured SDFT, where their content more or less contained un-identified structures that had positive reaction for PG and GAG. It is possibly that these spaces could be a cutting artefact, but they were observed in all the samples, and contained some structural elements, which stained positively for ECM molecules, and were observed on both longitudinal and transverse sections. It is likely that *in-vivo* these spaces could contain extracellular fluid. Similarly, in human Achilles tendinopathy areas of the injured tendon showed large mucoid

patches and vacuoles between fibres as well as lipoid degeneration (Burry and Pool, 1971, Burry and Pool, 1973, Sharma and Maffulli, 2005). Furthermore, in a case report of an injured 6-year-old male Thoroughbred horse, it was characterised by swelling around the SDFT of the right forelimb. On histological examination it was observed that the injured SDFT exhibited exuberant granulation, large number of activated tenocytes, hemorrhage, and a small number of inflammatory cells when compared to the normal SDFT (Kobayashi et al., 1999). In our study, it was found that both fascicles and the IFM were less regular on their longitudinal axis, that represent disruption and slight local displacement of these structures. Moreover, the IFM surrounding the injured area were significantly enlarged/thickened, fascicles became hypercellular (70% increase in cells) and nuclei length was smaller (approximately 31% smaller). In a surgically created incision in the SDFT, it was found that microscopic and biochemical assessments all indicated that tendons 6 weeks post-surgery very closely resembled naturally occurring tendinopathy (Cadby et al., 2013). In other tendons such as CDET, similar histological alteration has been found (Beck et al., 2011). In human tendinopathy similar microscopic characteristic features have been demonstrated, and occasionally it's accompanied by intra-tendinous ossification and subsequent rupture of the tendon (Aksoy and Surat, 1998, Maffulli and Kader, 2002). Meanwhile, it has been established that SDFT injury in equine athletes is one of the most well accepted scientifically supported companion animal models of human disease (Patterson-Kane et al., 2012, Patterson-Kane and Rich, 2014)

We demonstrated that the injured SDFT demonstrated areas that contained fibro-cartilaginous or chondroid-like cells, where the cells had more rounded form rather than the spindle shapes, which has been previously reported in a pathogenesis of SDFT micro-damages (Patterson-Kane et al., 2012) and is also a common feature of human tendinopathy (Maffulli et al., 2008). Moreover a number potentially apoptotic nuclei appeared in the injured tendon as also described in the human disease (Yuan et al., 2003). The injured areas showed variable staining intensity for Alcian blue, which could indicate that the cells have differentiated and are producing greater amounts of GAG and PG. In a surgically created incision of the SDFT it was found that the GAG content was increased and was accompanied by plump nuclei and a scarcity of inflammatory cells (Cadby et al., 2013, Jacobsen et al., 2015).

Histological examination of the DDFT from horses with chronic foot pain demonstrated that the injured area manifested zones of fibrocartilaginous metaplasia, contained chondrocyte clusters that had a strong positive staining with Safranin-O, which indicated the presence of PGs in the injured zones (Beck et al., 2011).

In a recent immunohistochemical study, different SLRP have been shown in equine SDFT and found that decorin is one of the most abundant PG that distributed through the IFM and the fascicles (Thorpe et al., 2016a). In this study, different monoclonal antibodies were used in order to specify that the presence of specific ECM molecules. It was found that the injured SDFT stained variously positive for a variety of PGs. interestingly injured SDFTs had positive reaction for both decorin (mouse monoclonal anti-decorin-IgG) and C-4-S (anti-C-4-S monoclonal mouse-IgG). It has previously been shown in different injured SDFT have a positive reaction for decorin, and C-4-S (Kobayashi et al., 1999, Watanabe et al., 2005). Similarly, in an experimentally induced tendinopathy it was found that the amount of decorin, chondroitin sulphate and dermatan sulphate increase in an injured tendon (Smith et al., 2008, Cadby et al., 2013). The C-4-S reacts with both chondroitin sulphate as well as dermatan sulphate. In this study we found that there was a strong positive reaction for both antibodies. This would indicate that these components are significant components of injured tendon that possibly play role in healing or formation of deleterious fibrochondrogenic scar tissue. It has been shown in normal tendon collagen fibres are organised by decorin through preventing a lateral fusion of the collagen fibres (Watanabe et al., 2005). Others have shown in injured SDFT, that hyaluronic acid (HA), dermatan sulphate (DS), and chondroitin sulphate (CS) are the significant components of the injured tendon (Kobayashi et al., 1999, Cadby et al., 2013). These finding suggest that the decorin and the chondroitin sulphate expressed highly in injured tendon, which possibly influence tissue strength, fibrillogenesis, cell differentiation and tissue repair (Iozzo and Murdoch, 1996, Jarvelainen et al., 2006). Moreover, chondroitin sulphate provides tissue strength, through binding of water to form hydrated matrices, provide tissue lubrication and promoting fibrillogenesis (Vogel and Heinegard, 1985, Rees et al., 2000, Martinez et al., 2015). Thus, it is important to consider that PG and the GAG could modulate tendon components during injury through their role in making the tissue to counter act against further destruction of the tissue and enhance to remodel the decayed tissue.

6.5 CONCLUSION

In this study, we have demonstrated the typical macro and microscopic appearance of injured tendon, defining the ECM disruption occurring in injury and how injuries extend in different planes from proximal to the distal region of the tendon. The injured area affected the normal anatomical microscopic architecture of the tendon. 3D reconstruction will further displayed how the injured lesion appeared through the tendon in relation to the normal surrounding architectures. Microscopically the injured tendon displayed up-regulation of all scoring parameters as well as they had a strong positive correlation with decorin and chondroitin sulphate, which could have a role in protecting the tissue from further damage tendon.

6.7 LIMITATION

Small number of SDFT samples with no exercise history or duration of injury.

6.8 RECOMMENDATION

A greater number of SDFT samples need to be collected from different racing disciplines and ages in order to understand how the occurs in relation to exercise and ages. Furthermore to explore the effect of injury on the mechanical function of equine SDFT and further dedicating a specific exercise protocol in order to protect tendon from injury.

CHAPTER SEVEN

GENERAL DISCUSSION AND FUTURE WORK

7.1 DISCUSSION

In this thesis, we aimed to define normal anatomical arrangements of the hierarchical units in equine SDFT and further more we wished to document heterogeneity of such units (fascicles) in different regions and during tendinopathy. Previously, it has been demonstrated that the hierarchical organisation of the tendon is comprised of different sized fascicles or collagen bundles (Kastelic et al., 1978, Kannus, 2000). The fascicle is considered as an important mechanical unit of the tendon (Haraldsson et al., 2008), whilst additionally the inter-fascicular connecting matrices (IFM) were also thought to contribute to the mechanobiology of the tendon (Thorpe et al., 2012). To date, the normal anatomical arrangements of the equine SDFT subunits have not been fully described. In particular, how these units contribute to tendon hierarchical structure and they can vary regionally, between individual limbs or tendinopathy. It was our hypothesis that in equine SDFT there is a variable anatomical arrangement to tendon fascicles longitudinally and fascicles are split, merge or intermittently inter-connect with each other and not always continuous through the length of the equine SDFT. Histologically, cellular and the ECM of these structural subunits vary regionally and will altered particularly in tendinopathy. Therefore the aim of this thesis was to describe the gross and microscopic three-dimensional (3D) anatomy of equine SDFT, to document the organisation of the individual sub-units (fascicles) and how this organisation may vary regionally and between individuals. Furthermore we wished to explore the histological scoring of the SDFT and document how its histological structures vary regionally and during ageing and tendinopathy.

7.1.1 THREE-DIMENSIONAL STUDY OF EQUINE SDFT

7.1.1.1 Macroscopic 3D reconstruction

In this study we developed a new anatomical sectioning method, image analysis and 3D reconstruction of the tendon fascicles on gross images, using computational tools (ImageJ and IMOD) in equine SDFT. Initially, it was found that when sections of the SDFT were immersed in water (hydration) for short periods (15 minutes) the tendon appearance was altered; in particular the IFM became more distinct between the fascicles, appearing as a shiny white structure. This is probably due to the presence of GAG, which has a negative charge attracting water molecules (Jozsa and

Kannus, 1997, Kannus, 2000, Yang et al., 2012). After absorbing of water, the IFM bulges and becomes more prominent, protruding above the cut edge of the tendon. Using this new sectioning method, the IFM and the fascicles were discriminated from each other and furthermore the dimensions of these structures could be measured accurately like other advanced methods such as ultrasonography or micro CT scan (Meghoufel et al., 2010, Shearer et al., 2014). Although, ultrasonographic examination of equine SDFT has shown that the IFM of the tertiary fascicles are thicker than the secondary fascicles, it has not shown a range or an average IFM thickness of each tertiary and secondary (Meghoufel et al., 2010). Importantly, in this study, defining the anatomy at a hierarchical macroscopic level, it was shown that the shapes and number of the fascicles varied from tendon to tendon and region-to-region within the same tendon. Their orientations were as to be expected, predominantly parallel to the longitudinal axis of the tendon. Previously it has been shown that the hierarchical organisation of the tendon is built up according to the size and overall structural organisation of the tendon subunits comprising of tertiary, secondary and primary fascicles (Kastelic et al., 1978, Kannus, 2000). Nevertheless, no accurate criteria have been developed to recognise these fascicular units other than their sizes (Kastelic et al., 1978, Kannus, 2000). Interestingly, in our study, it was demonstrated how to discriminate tertiary and secondary fascicles on a transverse tendon section on the basis of image optimisation, size of fascicles and the IFM thickness (Chapter two, section 2.2.5.1). The largest units called tertiary fascicles that outlined by a well-defined IFM; tertiary fascicles are further subdivided into smaller secondary fascicles that outlined by a thinner IFM. Interestingly, it was found that number, shape and sizes of the tertiary and secondary fascicles varied from region to region and different area within the same region of SDFT and were heterogeneous between different legs particularly between forelimb and hind limb (Szaro et al., 2009). IFM quantification and fascicular discrimination could help to understand at what level the IFM undergoes alteration during injury.

In this study, it was found that the reconstructed fascicles underwent specific alterations when coursing through the tendon body such as divergence, convergence and inter-connection. In a study using polarised light microscopy, it has been shown that fascicles of the porcine deep digital flexor tendon can converge (Kondratko-Mittnacht et al., 2015). Similarly, in an anatomical study of human supraspinatus

tendon it has been shown that an average of 18% of the supraspinatus tendon fascicles converged into larger fascicles from the proximal to the distal end (Fallon et al., 2002). Therefore, our findings indicated that SDFT fascicles did not have a constant morphology and varied from proximal to distal within the tendon. Whilst it is at a very different scale, another hierarchical level using the Transmission Election Microscopy (TEM) demonstrated that most of the individual fibril and fibril bundles run longitudinally and parallel to the longitudinal axis of the tendon, however some bundles oriented transversely, cross each other and form a spiral plait (Jozsa et al., 1991). Collectively, these alterations would support our hypothesis that there was a variable anatomical arrangement to tendon fascicles longitudinally through the tendon and fascicles may split, merge or intermittently inter-connect with each other. Although, to date, it is not clear which level of the tendon hierarchical structures have the most influential effect on the mechanobiology of the tendon (Shearer, 2015a). Therefore an in-depth understanding of the 3D structural organisation of SDFT will facilitate understanding of the role of both fascicles and IFM in mechanobiology of the tendon and how they are affected by ages and tendinopathy, while 3D findings could help to define different hierarchical level in the next step using light microscopy or TEM in the future (Chapter two).

7.1.1.2 Microscopic 3D reconstruction

In this study, microscopic 3D reconstruction of the SDFT fascicles was carried out on serial histological sections (approximately 1cm long). Similarly it was found that all fascicles were parallel to the longitudinal axis of the tendon. Shapes of the fascicles were not constant at different levels and transverse regions of the tendon. It was confirmed that fascicles in the equine SDFT in different regions inter-connected with each other as well as dividing and converging. Points of inter-connection were manifested by a linear transfer of collagen fibres between fascicles that has been previously shown in rat-tail tendon (Kastelic et al., 1978) and chick embryo tendon (Birk et al., 1989). Here, the presence of inter-connection points between fascicles will raise questions of the importance of these features in tendon function and mechanobiology. These inter-connection points lead to the fascicles being attached to each other and would allow mechanical force to be transferred between fascicles (Thorpe et al., 2012). Interestingly, there was a partial break or discontinuity within

the body of number of fascicles, which contained varying amounts of IFM. Histologically, it has been shown that IFM space contains blood vessels, and varying amounts of irregular fibres, PG, GAG and elastic fibres (Kastelic et al., 1978, Jozsa and Kannus, 1997, Kannus, 2000, Yang et al., 2012), which play role in SDFT mechanobiology (Thorpe et al., 2012, Thorpe et al., 2015b).

In complete 3D reconstruction of a portion (1cm long) from the mid-metacarpal region (500 slides), fascicles apparently had twisted configurations on their longitudinal axis. Similarly, different twisted or spiral configuration have also been shown and described in human tendon and ligament using computed X-ray tomography (Kalson et al., 2012, Shearer et al., 2014, Balint et al., 2016). In a study at a different hierarchical level using a mechanobiology approach in equine SDFT, has shown helically arranged sub-structures within the fascicles (Thorpe et al., 2013b). In a review article, the same authors present a TEM reconstruction of a fascicle demonstrating a helical arrangement within the fascicle (Thorpe et al., 2015d). Therefore, our data does support the presence of helical fascicles within the SDFT. The presence of the twisted structures will support fascicles to resist stretching and extensible forces in both human and equine models (Kalson et al., 2012, Thorpe et al., 2013b). These anatomical arrangements of fascicles and IFM would suggest that equine SDFT is a much more complex and sophisticated structure than previously demonstrated by current anatomical models (Kastelic et al., 1978, Kannus, 2000). Although not all fascicles were twisted and this could contribute to early mechanical damages of the tendon, further investigation particularly at the TEM level will reveal which parts of the tendon hierarchy are arranged helically and contribute to mechanobiology whilst other parts are damaged (Chapter three).

7.1.2 HISTOLOGICAL OBSERVATION AND SCORING

In our histological sections, a new scoring method was developed to describe histological structures of the equine SDFT and how the structure may vary regionally and during ageing. This histological scoring will help us to understand the structural developments during ageing and maturation, which will be useful to develop a particular age related programme of exercise induction in order to protect SDFT from injury. Typically, tendon is composed of a parallel and regularly oriented ECM (collagen bundles and IFM) that contains different types of collagen fibres and cells.

It has been shown that fascicles in different tendons including SDFT are angulated, which could be because of the presence of the spiral helical configuration (Yahia and Drouin, 1989, Vidal, 2003, Kalson et al., 2012, Thorpe et al., 2013b). Similarly it was demonstrated that the cellular morphology undergoes age-related alteration in different various animal species including horses (Floridi et al., 1981, Batson et al., 2003, Legerlotz et al., 2014).

IFM is composed of loose irregular connective tissue that contains that contains different structures such as blood vessels, nerves, non-collagenous protein and non-organised cells (Kastelic et al., 1978, Kannus, 2000, Benjamin et al., 2008). My data demonstrates additionally the presence of elastic fibres through the IFM, which show distinct patterns including straight, interwoven, irregular and curled configurations (Chapter four, section 4.3.1.4.3). The presence of elastic fibres through the IFM and in different configuration are likely to play a role in IFM mechanobiology but their contribution may vary from region to region, tendon status and during ageing, which would require further studies to quantify the 3D arrangement of elastic fibres and how they may contribute to tendon mechanobiology (Thorpe et al., 2016c).

In this study, it was found that a considerable proportion of the ECM units (fascicles and IFM) were angulated. Not all fascicles and IFM were perpendicular (90°) with the longitudinal axis of the tendon. Fascicles and IFM were slightly inclined from their longitudinal axis within a range of 0.2° to 22° and 0.3° to 40° respectively. Similarly, in the human extensor carpi ulnaris tendon a range of 5-22° of fascicular angulation over 4.5 mm length has been recorded (Kalson et al., 2012). Importantly, the width of secondary IFM in the mid-metacarpal and the distal region was significantly thinner in ageing. Mechanically, it has been shown that IFM sliding capacity decreases during ageing, which subsequently renders it incapable to withstand repetitive mechanical loads and a potential risk of fatigue injury during ageing (Thorpe et al., 2013c, Thorpe et al., 2013a). Moreover, in a proteomic study it has been shown that IFM protein abundance is generally constant with ageing but the number of cleaved matrix peptides (neopeptides) was decreased during ageing as a result of decreased matrix turnover, which could lead to accumulation of micro-damage with ageing (Thorpe et al., 2016b). To date the IFM matrix components have not been comprehensively investigated, in particular to find an age-related alteration

of IFM constituents because it is only recently been considered an important structure of the tendon. Although in this study a gross and histological 2D structure of the IFM was demonstrated, whilst, in the future next step it is important to explore structural 3D model of the IFM at the TEM level and quantify it during ageing.

The intra-fascicular cellular morphology varied from region to region and between ages. The average number nuclei present in the fascicles were variable between individual tendons. In different animal models including horses, it has been shown that tenocytes undergo a series of morphometric changes during ageing (Ippolito et al., 1980, Moore and De Beaux, 1987, Goodman et al., 2004, Stanley et al., 2007, Young et al., 2009). Similarly we found that the intra-fascicular nuclear morphology and density were reciprocally altered during ageing, particularly from foetal life to seven-years-old. These histological alterations during ageing indicate that the integrity of the tissue declines, which likely makes the tendon to be prone to age-related accumulated damage (Peffers et al., 2015) (Chapter four).

Interestingly, a number of chondroid-like bodies were identified in elderly horses (17-20 years-old). These bodies appeared as form of an individual cell to a cluster of multiple cells that appeared like a bunch of grapes (Chapter five). Such structures have not been described previously in normal equine SDFT, but it has been described in tendinopathy (Webbon, 1977, Jacobsen et al., 2015). In mammalian tendon, calcification is rare but is considered pathological when it occurs (Khan et al., 1999, Benjamin et al., 2008). The nuclei of these bodies had a small rounded cytoplasm that surrounded by a large amount of ECM that had a strong staining reaction for PG and GAGs. This indicates that the SDFT cell phenotype was altered and became more active, as shown by these chondroid cells which contained an intensive lamellar arranged endoplasmic reticulum (ER), that are likely to have produced large amounts of ECM. This lamellar development of the ER it has been shown in chondrocytic-like cells of the degenerative zone in the epiphyseal region of bones and the fibrocartilage cells of tendon in pseudoachondroplastic dwarf patient (Cooper et al., 1973, Maddox et al., 1997), and cells in the mineralised zone of turkey's tendon, this alteration in endoplasmic reticulum is required for active protein synthesis (Landis, 1986). Our findings were further confirmed by immunohistochemistry (IHC), where there was a reaction to specific PGs and GAGs

such as decorin, aggrecan, biglycan and chondroitin -4- and -6-sulphate. Meanwhile, positive immunostaining for C-6-S antibody in both human and animal models are used as specific anabolic marker of the early degenerative joint disease (Caterson et al., 1990, Byers et al., 1992, Ratcliffe et al., 1993, Visco et al., 1993, Lin et al., 2004). The presence of these different phenotypic cells in equine SDFT could result from either ageing of the ECM or continuous cyclical loading of the tendon inducing local micro-damage of the ECM that followed by alteration of the cells that turned into the chondroid-like cells in response to mechanical stimuli (Benjamin and Ralphs, 2004). The biomechanical consequences of these features are unclear, but it is plausible that their presence could lead to increased risk of tendon injury at these sites because of altered biomechanics between these chondroid material and the surrounding fascicles. Furthermore it is possible that these structures could be the site for ossification in the future (Lui et al., 2009, Tamam et al., 2011) as it has been shown that intra-tendinous ossification occurs normally in birds (Berge and Storer, 1995, Landis and Silver, 2002, Organ and Adams, 2005). These chondroid-like cells need to be further investigated and analysed in older ages in order to understand how they develop, contribute in tendon function and prognosis during life (Chapter five).

During tendinopathy both ECM and the tenocytes were involved, the injured tissue demonstrated typical macro- and microscopic areas of injury. The injured areas manifested variable extents of ECM disruption in particular to the IFM (van Schie et al., 2003, Meghoufel et al., 2010). In our study, it was shown how the injured lesion extended through the tendon in relation to the surrounding normal tendon tissue. Moreover, a strong positive staining with decorin and chondroitin sulphate, indicative of chondrogenic differentiation, which could have a role in protecting the tissue from further damage tendon. This needs further investigation in order to understand the critical role of decorin during injury (Kobayashi et al., 1999, Watanabe et al., 2005). Injuries of the SDFT are common causes of equine wastage and different studies have recorded that age is considered as an important factor of musculoskeletal injury (Williams et al., 2001, Perkins et al., 2005) commonly affecting the forelimb (Kasashima et al., 2004). It has been found that tendon injury is a gradual process from wear and tear as a result of an overuse, ageing and exercise (Smith et al., 2002, Patterson-Kane et al., 2012). However in the horse, tendon injury occurs as a result of hyperextension of the limb during racing or vigorous exercise

that push the tendon beyond their capacity, which frequently affects the forelimb and the injury involves the central part of the tendon, where the tissue is damaged and undergo further degeneration (Birch et al., 1998, Meghoufel et al., 2010). Moreover, predisposing factors such as hyperthermia, ischaemia, irregular or insufficient exercise, ageing, reduction of crimp pattern type of ground floor and early fatigue of the deep digital flexor muscle are contributed to tendon injury (Tidball, 1991, Birch et al., 1997, Butcher et al., 2007). Both cellular and ECM are damaged and it has been shown that the IFM between the fascicles is severely destroyed and partially disappeared that make the fascicles merge to each other (Meghoufel et al., 2010). In an experimentally induced partial resection of the SDFT, it was observed that the lesion rapidly developed and extended through the entire length of the tendon (Jacobsen et al., 2015). Further investigation of the relationship between the predisposing factors and the tendon injury would help to determine the weakest points of the hierarchical structures that undergo early degenerative changes during injury. In our study, it was shown that various forms of SDFT injuries of the fore limbs, where the lesion was commonly affecting the central region of the tendon, may be due to variation in conformational pattern of the collagen fibres and fascicles of the central region from the periphery (Parry et al., 1978, Patterson-Kane et al., 1997a). Importantly, this new method of sectioning and 3D reconstruction of the injured SDFT could explain how the injury extend and progressed through the tendon and which part of the ECM is more vulnerable to disruption (IFM) (Chapter six).

7.2 FUTURE DIRECTION

1- Techniques to allow more accurate method of exploring the normal anatomical architecture at different hierarchical level, 3D electron microscopy will allow structural data to be obtained at the level of the collagen fibre (Canty and Kadler, 2005, Kadler et al., 2007), in particular during ageing and tendinopathy in order to understand which part of the hierarchical level are undergo early degenerative change.

2- Experimental mechanical study of the individual fascicles during SDFT extension and rupture at different loads followed by rapid freezing for a long time, then using anatomical dissection and 3D reconstruction.

3- Exploration of the structural properties of the IFM will aid understanding of structure/function relationships in the tendon hierarchy and ultimately how such variations affect the mechanobiology of the tendon. Using new imaging techniques, such as 3D electron microscopy, will develop an understanding its structural organisation such as vessels, cells and fibers in relation with regions, ages and tendinopathy.

4- IHC study of equine SDFT in more advanced aged (20-30) in order to find that this type of chondroid metaplasia and how it may progress in aged horses, or show expression of chondrogenic markers.

5- Mechanical testing of aged SDFT that show by such chondroid metaplasia in order to quantify the percentage of mechanical loss during ageing and to determine the early rupture of the fascicular structures in the chondroid areas.

6- Anatomical 3D reconstruction of SDFT will direct our attention to be applied to other structures such as CDET, DDFT and suspensory ligaments in order to describe their 3D anatomical and how vary during ageing and pathology.

7- Further investigation is needed to define and understand the fascicular organisation using another advanced technique such as computed tomography (Micro CT) scanning or MRI after finding and developing a new method of tissue staining with different contrast media such as sodium tungstate.

8- The new histological scoring method can be applied on other tendons such as CDET or DDFT and comparing them with SDFT.

APPENDIX

PhD thesis/Othman, Ali/ Three-dimensional supplementary videos

REFERENCES

ADAMS, M. A., BURTON, K. & BOGDUK, N. 2006. *The Biomechanics of Back Pain*, Churchill Livingstone Elsevier.

AGUT, A., MARTINEZ, M. L., SANCHEZ-VALVERDE, M. A., SOLER, M. & RODRIGUEZ, M. J. 2009. Ultrasonographic characteristics (cross-sectional area and relative echogenicity) of the digital flexor tendons and ligaments of the metacarpal region in Purebred Spanish horses. *Vet J,* 180**,** 377-83.

AKSOY, M. C. & SURAT, A. 1998. Fracture of the ossified Achilles tendon. *Acta Orthop Belg,* 64**,** 418-21.

APARECIDA DE ARO, A., VIDAL BDE, C. & PIMENTEL, E. R. 2012. Biochemical and anisotropical properties of tendons. *Micron,* 43**,** 205-14.

ARNDT, A. N., KOMI, P. V., BRUGGEMANN, G. P. & LUKKARINIEMI, J. 1998. Individual muscle contributions to the in vivo achilles tendon force. *Clin Biomech (Bristol, Avon),* 13**,** 532-541.

ASTROM, M. 2000. Laser Doppler flowmetry in the assessment of tendon blood flow. *Scand J Med Sci Sports,* 10**,** 365-7.

AVELLA, C. S., ELY, E. R., VERHEYEN, K. L. P., PRICE, J. S., WOOD, J. L. N. & SMITH, R. K. W. 2009. Ultrasonographic assessment of the superficial digital flexor tendons of National Hunt racehorses in training over two racing seasons. *Equine Veterinary Journal,* 41**,** 449-454.

BAER, E., HILTNER, A. & FRIEDMAN, B. 1976. Structural hierarchies and interactions in the tendon composite. *Polymer Mechanics,* 12**,** 619-629.

BALINT, R., LOWE, T. & SHEARER, T. 2016. Optimal Contrast Agent Staining of Ligaments and Tendons for X-Ray Computed Tomography. *PLoS One,* 11**,** e0153552.

BASS, E. 2012. Tendinopathy: Why the Difference Between Tendinitis and Tendinosis Matters. *Int J Ther Massage Bodywork,* 5**,** 14-7.

BATSON, E. L., PARAMOUR, R. J., SMITH, T. J., BIRCH, H. L., PATTERSON-KANE, J. C. & GOODSHIP, A. E. 2003. Are the material properties and matrix composition of equine flexor and extensor tendons determined by their functions? *Equine Veterinary Journal,* 35**,** 314-318.

BAUTCH, J. C., CLAYTON, M. K., CHU, Q. & JOHNSON, K. A. 2000. Synovial fluid chondroitin sulphate epitopes 3B3 and 7D4, and glycosaminoglycan in human knee osteoarthritis after exercise. *Ann Rheum Dis,* 59**,** 887-91.

BAXTER, G. M. 2011. *Manual of Equine Lameness*, Wiley.

BECK, S., BLUNDEN, T., DYSON, S. & MURRAY, R. 2011. Are matrix and vascular changes involved in the pathogenesis of deep digital flexor tendon injury in the horse? *Veterinary Journal,* 189**,** 289-295.

BENJAMIN, M. & EVANS, E. J. 1990. Fibrocartilage. *J Anat,* 171**,** 1-15.

BENJAMIN, M., KAISER, E. & MILZ, S. 2008. Structure-function relationships in tendons: a review. *J Anat,* 212**,** 211-28.

BENJAMIN, M. & MCGONAGLE, D. 2001. The anatomical basis for disease localisation in seronegative spondyloarthropathy at entheses and related sites. *J Anat,* 199**,** 503-26.

BENJAMIN, M. & RALPHS, J. R. 2004. Biology of fibrocartilage cells. *Int Rev Cytol,* 233**,** 1-45.

BENJAMIN, M., TYERS, R. N. & RALPHS, J. R. 1991. Age-related changes in tendon fibrocartilage. *J Anat,* 179**,** 127-36.

BENNET, D. 2008. Timing and rate of skeletal maturation in horses. http://www.equinestudies.org/ranger_2008/ranger_piece_2008_pdf1.pdf.

BERGE, J. C. V. & STORER, R. W. 1995. Intratendinous ossification in birds: A review. *Journal of Morphology,* 226**,** 47-77.

BIANCALANA, A., VELLOSO, L. A., TABOGA, S. R. & GOMES, L. 2012. Implications of obesity for tendon structure, ultrastructure and biochemistry: a study on Zucker rats. *Micron,* 43**,** 463-9.

BIRCH, H. L. 2007. Tendon matrix composition and turnover in relation to functional requirements. *Int J Exp Pathol,* 88**,** 241-8.

BIRCH, H. L., BAILEY, A. J. & GOODSHIP, A. E. 1998. Macroscopic 'degeneration' of equine superficial digital flexor tendon is accompanied by a change in extracellular matrix composition. *Equine Vet J,* 30**,** 534-9.

BIRCH, H. L., BAILEY, J. V., BAILEY, A. J. & GOODSHIP, A. E. 1999a. Age-related changes to the molecular and cellular components of equine flexor tendons. *Equine Vet J,* 31**,** 391-6.

BIRCH, H. L., MCLAUGHLIN, L., SMITH, R. K. & GOODSHIP, A. E. 1999b. Treadmill exercise-induced tendon hypertrophy: assessment of tendons with different mechanical functions. *Equine Vet J Suppl***,** 222-6.

BIRCH, H. L., RUTTER, G. A. & GOODSHIP, A. E. 1997. Oxidative energy metabolism in equine tendon cells. *Res Vet Sci,* 62**,** 93-7.

BIRCH, H. L., WILSON, A. M. & GOODSHIP, A. E. 2008. Physical activity: does long-term, high-intensity exercise in horses result in tendon degeneration? *J Appl Physiol (1985),* 105**,** 1927-33.

BIRK, D. E., HAHN, R. A., LINSENMAYER, C. Y. & ZYCBAND, E. I. 1996. Characterization of collagen fibril segments from chicken embryo cornea, dermis and tendon. *Matrix Biol,* 15**,** 111-8.

BIRK, D. E., NURMINSKAYA, M. V. & ZYCBAND, E. I. 1995. Collagen fibrillogenesis in situ: fibril segments undergo post-depositional modifications resulting in linear and lateral growth during matrix development. *Dev Dyn,* 202**,** 229-43.

BIRK, D. E., SOUTHERN, J. F., ZYCBAND, E. I., FALLON, J. T. & TRELSTAD, R. L. 1989. Collagen fibril bundles: a branching assembly unit in tendon morphogenesis. *Development,* 107**,** 437-43.

BIRK, D. E., ZYCBAND, E. I., WOODRUFF, S., WINKELMANN, D. A. & TRELSTAD, R. L. 1997. Collagen fibrillogenesis in situ: Fibril segments become long fibrils as the developing tendon matures. *Developmental Dynamics,* 208**,** 291-298.

BJORNSSON, S. 1998. Quantitation of proteoglycans as glycosaminoglycans in biological fluids using an alcian blue dot blot analysis. *Anal Biochem,* 256**,** 229-37.

BREEN, M., KNEPPER, P. A., WEINSTEIN, H. G., BLACIK, L. J., LEWANDOWSKI, D. G. & BALTRUS, B. M. 1981. Microanalysis of glycosaminoglycans. *Anal Biochem,* 113**,** 416-22.

BRUNS, J., KAMPEN, J., KAHRS, J. & PLITZ, W. 2000. Achilles tendon rupture: experimental results on spontaneous repair in a sheep-model. *Knee Surg Sports Traumatol Arthrosc,* 8**,** 364-9.

BURRY, H. C. & POOL, C. J. 1971. The pathology of the painful heel. Br J Sports Med

;6:9-12.

BURRY, H. C. & POOL, C. J. 1973. Central degeneration of the achilles tendon. Rheumatology

Rehabilitation ;12:177-81.

BUTCHER, M. T., HERMANSON, J. W., DUCHARME, N. G., MITCHELL, L. M., SODERHOLM, L. V. & BERTRAM, J. E. 2007. Superficial digital flexor tendon lesions in racehorses as a sequela to muscle fatigue: a preliminary study. *Equine Vet J,* 39**,** 540-5.

BYERS, S., CATERSON, B., HOPWOOD, J. J. & FOSTER, B. K. 1992. Immunolocation analysis of glycosaminoglycans in the human growth plate. *J Histochem Cytochem,* 40**,** 275-82.

CADBY, J. A., DAVID, F., VAN DE LEST, C., BOSCH, G., VAN WEEREN, P. R., SNEDEKER, J. G. & VAN SCHIE, H. T. 2013. Further characterisation of an experimental model of tendinopathy in the horse. *Equine Vet J,* 45**,** 642-8.

CANTY, E. G. & KADLER, K. E. 2005. Procollagen trafficking, processing and fibrillogenesis. *J Cell Sci,* 118**,** 1341-53.

CARR, A. J. & NORRIS, S. H. 1989. The blood supply of the calcaneal tendon. *J Bone Joint Surg Br,* 71**,** 100-1.

CATERSON, B. 2012. Fell-Muir Lecture: Chondroitin sulphate glycosaminoglycans: fun for some and confusion for others. *International Journal of Experimental Pathology,* 93**,** 1-10.

CATERSON, B., MAHMOODIAN, F., SORRELL, J. M., HARDINGHAM, T. E., BAYLISS, M. T., CARNEY, S. L., RATCLIFFE, A. & MUIR, H. 1990. Modulation of native chondroitin sulphate structure in tissue development and in disease. *J Cell Sci,* 97 (Pt 3)**,** 411-7.

CHEN, L., WANG, G. D., LIU, J. P., WANG, H. S., LIU, X. M., WANG, Q. & CAI, X. H. 2015. miR-135a modulates tendon stem/progenitor cell senescence via suppressing ROCK1. *Bone,* 71**,** 210-6.

CHESEN, A. B., DABAREINER, R. M., CHAFFIN, M. K. & CARTER, G. K. 2009. Tendinitis of the proximal aspect of the superficial digital flexor tendon in horses: 12 cases (2000-2006). *J Am Vet Med Assoc,* 234**,** 1432-6.

CLEGG, P. D., STRASSBURG, S. & SMITH, R. K. 2007. Cell phenotypic variation in normal and damaged tendons. *Int J Exp Pathol,* 88**,** 227-35.

COMERFORD, E. J., TARLTON, J. F., WALES, A., BAILEY, A. J. & INNES, J. F. 2006. Ultrastructural differences in cranial cruciate ligaments from dogs of two breeds with a differing predisposition to ligament degeneration and rupture. *J Comp Pathol,* 134**,** 8-16.

COOK, J. L., KISS, Z. S., PTASZNIK, R. & MALLIARAS, P. 2005. Is vascularity more evident after exercise? Implications for tendon imaging. *AJR Am J Roentgenol,* 185**,** 1138-40.

COOPER, R. R., PONSETI, I. V. & MAYNARD, J. A. 1973. Pseudoachondroplastic Dwarfism. *A ROUGH-SURFACED ENDOPLASMIC RETICULUM STORAGE DISORDER,* 55**,** 475-484.

CORPS, A. N., ROBINSON, A. H., MOVIN, T., COSTA, M. L., IRELAND, D. C., HAZLEMAN, B. L. & RILEY, G. P. 2004. Versican splice variant messenger RNA expression in normal human Achilles tendon and tendinopathies. *Rheumatology (Oxford),* 43**,** 969-72.

CREVIER, N., POURCELOT, P., DENOIX, J. M., GEIGER, D., BORTOLUSSI, C., RIBOT, X. & SANAA, M. 1996. Segmental variations of in vitro mechanical properties in equine superficial digital flexor tendons. *Am J Vet Res,* 57**,** 1111-7.

CREVIER-DENOIX, N., COLLOBERT, C., POURCELOT, P., DENOIX, J. M., SANAA, M., GEIGER, D., BERNARD, N., RIBOT, X., BORTOLUSSI, C. & BOUSSEAU, B. 1997. Mechanical properties of pathological equine superficial digital flexor tendons. *Equine Vet J Suppl***,** 23-6.

CREVIER-DENOIX, N. & POURCELOT, P. 1997. Additional research on tendon strains and stresses. *Am J Vet Res,* 58**,** 569-70.

CREVIER-DENOIX, N., RUEL, Y., DARDILLAT, C., JERBI, H., SANAA, M., COLLOBERT-LAUGIER, C., RIBOT, X., DENOIX, J. M. & POURCELOT, P. 2005. Correlations between mean echogenicity and material properties of normal and diseased equine superficial digital flexor tendons: an in vitro segmental approach. *J Biomech,* 38**,** 2212-20.

DAHLGREN, L. A., MOHAMMED, H. O. & NIXON, A. J. 2005. Temporal expression of growth factors and matrix molecules in healing tendon lesions. *J Orthop Res,* 23**,** 84-92.

DAKIN, S. G., WERLING, D., HIBBERT, A., ABAYASEKARA, D. R., YOUNG, N. J., SMITH, R. K. & DUDHIA, J. 2012. Macrophage sub-populations and the lipoxin A4 receptor implicate active inflammation during equine tendon repair. *PLoS One,* 7**,** e32333.

DE CAMPOS VIDAL, B. 2003. Image analysis of tendon helical superstructure using interference and polarized light microscopy. *Micron,* 34**,** 423-32.

DE MOS, M. 2009. *Tendon Cell Behavior and Matrix Remodeling in Degenerative Tendinopathy.* Ph.D. thesis, Erasmus University Rotterdam.

DE MOS, M., KOEVOET, W. J., JAHR, H., VERSTEGEN, M. M., HEIJBOER, M. P., KOPS, N., VAN LEEUWEN, J. P., WEINANS, H., VERHAAR, J. A. & VAN OSCH, G. J. 2007. Intrinsic differentiation potential of adolescent human tendon tissue: an in-vitro cell differentiation study. *BMC Musculoskeletal Disorders,* 8**,** 1-12.

DOWLING, B. A. & DART, A. J. 2005. Mechanical and functional properties of the equine superficial digital flexor tendon. *The Veterinary Journal,* 170**,** 184-192.

DOWLING, B. A., DART, A. J., HODGSON, D. R., ROSE, R. J. & WALSH, W. R. 2002. Recombinant equine growth hormone does not affect the in vitro biomechanical properties of equine superficial digital flexor tendon. *Vet Surg,* 31**,** 325-30.

DURHAM, M. & DYSON, S. J. 2011. Chapter 9 - Applied Anatomy of the Musculoskeletal System. *In:* DYSON, M. W. R. J. (ed.) *Diagnosis and Management of Lameness in the Horse (Second Edition).* Saint Louis: W.B. Saunders.

DYSON, S. J. 2004. Medical management of superficial digital flexor tendonitis: a comparative study in 219 horses (1992-2000). *Equine Vet J,* 36**,** 415-9.

EDWARDS, D. A. W. 1946. The blood supply and lymphatic drainage of tendons. *Journal of Anatomy,* 80**,** 147-152.2.

ELLIOTT, D. H. 1965. Structure and Function of Mammalian Tendon. *Biol Rev Camb Philos Soc,* 40**,** 392-421.

ELY, E. R., VERHEYEN, K. L. P. & WOOD, J. L. N. 2004. Fractures and tendon injuries in National Hunt horses in training in the UK: a pilot study. *Equine Vet J,* 36**,** 365-367.

ESKO JD, K. K., LINDAHL U 2009. Chapter 16 Proteoglycans and Sulfated Glycosaminoglycans. *In:* VARKI, A., CUMMINGS, R. D., ESKO, J. D., FREEZE, H. H., STANLEY, P., BERTOZZI, C. R., HART, G. W. & ETZLER, M. E. (eds.) *Essentials of Glycobiology.* Cold Spring Harbor (NY): Cold Spring Harbor Laboratory Press.

EVANKO, S. P. & VOGEL, K. G. 1990. Ultrastructure and proteoglycan composition in the developing fibrocartilaginous region of bovine tendon. *Matrix,* 10**,** 420-36.

EYRE, D. R., WEIS, M. A. & WU, J. J. 2008. Advances in collagen cross-link analysis. *Methods,* 45**,** 65-74.

FALLON, J., BLEVINS, F. T., VOGEL, K. & TROTTER, J. 2002. Functional morphology of the supraspinatus tendon. *J Orthop Res,* 20**,** 920-6.

FAN, L., SARKAR, K., FRANKS, D. J. & UHTHOFF, H. K. 1997. Estimation of total collagen and types I and III collagen in canine rotator cuff tendons. *Calcified Tissue International,* 61**,** 223-229.

FEITOSA, V. L., REIS, F. P., ESQUISATTO, M. A., JOAZEIRO, P. P., VIDAL, B. C. & PIMENTEL, E. R. 2006. Comparative ultrastructural analysis of different regions of two digital flexor tendons of pigs. *Micron,* 37**,** 518-25.

FERRARO, G. L., STOVER, S. M. & WHITCOMB, M. B. 2009. Suspensory Ligament Injuries in Horses. Center for Equine Health, School of Veterinary Medicine, University of California, Davis http://www.missourifoxtrottersatoz.com.

FESSEL, G., GERBER, C. & SNEDEKER, J. G. 2012. Potential of collagen cross-linking therapies to mediate tendon mechanical properties. *J Shoulder Elbow Surg,* 21**,** 209-17.

FLORIDI, A., IPPOLITO, E. & POSTACCHINI, F. 1981. Age-related changes in the metabolism of tendon cells. *Connect Tissue Res,* 9**,** 95-7.

FRANCHI, M., DE PASQUALE, V., MARTINI, D., QUARANTA, M., MACCIOCCA, M., DIONISI, A. & OTTANI, V. 2010. Contribution of glycosaminoglycans to the microstructural integrity of fibrillar and fiber crimps in tendons and ligaments. *ScientificWorldJournal,* 10**,** 1932-40.

FRANCHI, M., FINI, M., QUARANTA, M., DE PASQUALE, V., RASPANTI, M., GIAVARESI, G., OTTANI, V. & RUGGERI, A. 2007a. Crimp morphology in relaxed and stretched rat Achilles tendon. *J Anat,* 210**,** 1-7.

FRANCHI, M., TRIRE, A., QUARANTA, M., ORSINI, E. & OTTANI, V. 2007b. Collagen structure of tendon relates to function. *ScientificWorldJournal,* 7**,** 404-20.

FU, S. C., CHAN, K. M. & ROLF, C. G. 2007. Increased deposition of sulfated glycosaminoglycans in human patellar tendinopathy. *Clin J Sport Med,* 17**,** 129-34.

FUKUTA, S., OYAMA, M., KAVALKOVICH, K., FU, F. H. & NIYIBIZI, C. 1998. Identification of types II, IX and X collagens at the insertion site of the bovine achilles tendon. *Matrix Biol,* 17**,** 65-73.

GATHERCOLE, L. J. & KELLER, A. 1978. Early development of crimping in rat tail tendon collagen: A polarizing optical and SEM study. *Micron (1969),* 9**,** 83-89.

GATHERCOLE, L. J. & KELLER, A. 1991. Crimp morphology in the fibre-forming collagens. *Matrix,* 11**,** 214-34.

GELBERMAN, R. H., AMIFL, D., GONSALVES, M., WOO, S. & AKESON, W. H. 1981. The influence of protected passive mobilization on the healing of flexor tendons: a biochemical and microangiographic study. *Hand,* 13**,** 120-8.

GETTY, R. 1975. *The anatomy of the domestic animals,* Philadelphia : Saunders, .

GIGANTE, A., SPECCHIA, N., RAPALI, S., VENTURA, A. & DE PALMA, L. 1996. Fibrillogenesis in tendon healing: an experimental study. *Boll Soc Ital Biol Sper,* 72**,** 203-10.

GILLIS, C., MEAGHER, D. M., CLONINGER, A., LOCATELLI, L. & WILLITS, N. 1995a. Ultrasonographic cross-sectional area and mean echogenicity of the superficial and deep digital flexor tendons in 50 trained thoroughbred racehorses. *Am J Vet Res,* 56**,** 1265-9.

GILLIS, C., SHARKEY, N., STOVER, S. M., POOL, R. R., MEAGHER, D. M. & WILLITS, N. 1995b. Effect of maturation and aging on material and ultrasonographic properties of equine superficial digital flexor tendon. *Am J Vet Res,* 56**,** 1345-50.

GILLIS, C., SHARKEY, N., STOVER, S. M., POOL, R. R., MEAGHER, D. M. & WILLITS, N. 1995c. Ultrasonography as a method to determine tendon cross-sectional area. *Am J Vet Res,* 56**,** 1270-4.

GOODMAN, S. A., MAY, S. A., HEINEGARD, D. & SMITH, R. K. 2004. Tenocyte response to cyclical strain and transforming growth factor beta is dependent upon age and site of origin. *Biorheology,* 41**,** 613-28.

GRANT, T. M., THOMPSON, M. S., URBAN, J. & YU, J. 2013. Elastic fibres are broadly distributed in tendon and highly localized around tenocytes. *J Anat,* 222**,** 573-9.

GREENLEE, T. K., JR. & ROSS, R. 1967. The development of the rat flexor digital tendon, a fine structure study. *J Ultrastruct Res,* 18**,** 354-76.

GRYTZ, R. & MESCHKE, G. 2009. Constitutive modeling of crimped collagen fibrils in soft tissues. *J Mech Behav Biomed Mater,* 2**,** 522-33.

HAGG, R., BRUCKNER, P. & HEDBOM, E. 1998. Cartilage fibrils of mammals are biochemically heterogeneous: differential distribution of decorin and collagen IX. *J Cell Biol,* 142**,** 285-94.

HANSON, A. N. & BENTLEY, J. P. 1983. Quantitation of Type I to type III collagen ratios in small samples of human tendon, blood vessels, and atherosclerotic plaque. *Analytical Biochemistry,* 130**,** 32-40.

HARALDSSON, B. T., AAGAARD, P., QVORTRUP, K., BOJSEN-MOLLER, J., KROGSGAARD, M., KOSKINEN, S., KJAER, M. & MAGNUSSON, S. P. 2008. Lateral force transmission between human tendon fascicles. *Matrix Biology,* 27**,** 86-95.

HASHIMOTO, T., NOBUHARA, K. & HAMADA, T. 2003. Pathologic evidence of degeneration as a primary cause of rotator cuff tear. *Clin Orthop Relat Res***,** 111-20.

HATAZOE, T. 2015. A study of the distribution of color Doppler flows in the superficial digital flexor tendon of. 26**,** 99-104.

HAYEM, G. 2001. Tenology: a new frontier. *Joint Bone Spine,* 68**,** 19-25.

HAZELEGER, E. 2013. The biochemical differences of the superficial digital flexor tendon and the common digital extensor tendon between Warmbloods, Friesians and Thoroughbreds. *Master thesis, Utrecht University*.

HECHT, J. T., HAYES, E., HAYNES, R. & COLE, W. G. 2005. COMP mutations, chondrocyte function and cartilage matrix. *Matrix Biol,* 23**,** 525-33.

HECHT, J. T., NELSON, L. D., CROWDER, E., WANG, Y., ELDER, F. F., HARRISON, W. R., FRANCOMANO, C. A., PRANGE, C. K., LENNON, G. G., DEERE, M. & ET AL. 1995. Mutations in exon 17B of cartilage oligomeric matrix protein (COMP) cause pseudoachondroplasia. *Nat Genet,* 10**,** 325-9.

HEDBOM, E. & HEINEGARD, D. 1989. Interaction of a 59-kDa connective tissue matrix protein with collagen I and collagen II. *J Biol Chem,* 264**,** 6898-905.

HEINEMEIER, K., LANGBERG, H., OLESEN, J. L. & KJAER, M. 2003. Role of TGF-beta1 in relation to exercise-induced type I collagen synthesis in human tendinous tissue. *J Appl Physiol (1985),* 95**,** 2390-7.

HILEMAN, R. E., FROMM, J. R., WEILER, J. M. & LINHARDT, R. J. 1998. Glycosaminoglycan-protein interactions: definition of consensus sites in glycosaminoglycan binding proteins. *Bioessays,* 20**,** 156-67.

HOSAKA, Y., KIRISAWA, R., YAMAMOTO, E., UEDA, H., IWAI, H. & TAKEHANA, K. 2002. Localization of cytokines in tendinocytes of the superficial digital flexor tendon in the horse. *J Vet Med Sci,* 64**,** 945-7.

HOSAKA, Y. Z., URATSUJI, T., UEDA, H., UEHARA, M. & TAKEHANA, K. 2010. Comparative study of the properties of tendinocytes derived from three different sites in the equine superficial digital flexor tendon. *Biomed Res,* 31**,** 35-44.

ICHINOHE, T., KANNO, N., HARADA, Y., YOGO, T., TAGAWA, M., SOETA, S., AMASAKI, H. & HARA, Y. 2015. Degenerative changes of the cranial cruciate ligament harvested from dogs with cranial cruciate ligament rupture. *J Vet Med Sci,* 77**,** 761-70.

IOZZO, R. V. 1999. The biology of the small leucine-rich proteoglycans. Functional network of interactive proteins. *J Biol Chem,* 274**,** 18843-6.

IOZZO, R. V. & MURDOCH, A. D. 1996. Proteoglycans of the extracellular environment: clues from the gene and protein side offer novel perspectives in molecular diversity and function. *Faseb j,* 10**,** 598-614.

IPPOLITO, E., NATALI, P. G., POSTACCHINI, F., ACCINNI, L. & DE MARTINO, C. 1980. Morphological, immunochemical, and biochemical study of rabbit achilles tendon at various ages. *J Bone Joint Surg Am,* 62**,** 583-98.

IRELAND, D., HARRALL, R., CURRY, V., HOLLOWAY, G., HACKNEY, R., HAZLEMAN, B. & RILEY, G. 2001. Multiple changes in gene expression in chronic human Achilles tendinopathy. *Matrix Biol,* 20**,** 159-69.

JACOBSEN, E., DART, A. J., MONDORI, T., HORADOGODA, N., JEFFCOTT, L. B., LITTLE, C. B. & SMITH, M. M. 2015. Focal experimental injury leads to widespread gene expression and histologic changes in equine flexor tendons. *PLoS One,* 10**,** e0122220.

JARVELAINEN, H., PUOLAKKAINEN, P., PAKKANEN, S., BROWN, E. L., HOOK, M., IOZZO, R. V., SAGE, E. H. & WIGHT, T. N. 2006. A role for decorin in cutaneous wound healing and angiogenesis. *Wound Repair Regen,* 14**,** 443-52.

JARVINEN, M., JOZSA, L., KANNUS, P., JARVINEN, T. L., KVIST, M. & LEADBETTER, W. 1997. Histopathological findings in chronic tendon disorders. *Scand J Med Sci Sports,* 7**,** 86-95.

JOZSA, L., KANNUS, P., BALINT, J. B. & REFFY, A. 1991. Three-dimensional ultrastructure of human tendons. *Acta Anat (Basel),* 142**,** 306-12.

JÓZSA, L., RÉFFY, A. & BÁLINT, J. B. 1984. Polarization and electron microscopic studies on the collagen of intact and ruptured human tendons. *Acta Histochemica,* 74**,** 209-215.

JOZSA, L. G. & KANNUS, P. 1997. *Human Tendons: Anatomy, Physiology, and Pathology*, Human Kinetics.

KADLER, K. E., BALDOCK, C., BELLA, J. & BOOT-HANDFORD, R. P. 2007. Collagens at a glance. *J Cell Sci,* 120**,** 1955-8.

KAGAYAMA, M., SASANO, Y., MIZOGUCHI, I., KAMO, N., TAKAHASHI, I. & MITANI, H. 1996. Localization of glycosaminoglycans in periodontal ligament during physiological and experimental tooth movement. *J Periodontal Res,* 31**,** 229-34.

KALISIAK, O. 2012. Parameters influencing prevalence and outcome of tendonitis in Thoroughbred and Arabian racehorses. *Pol J Vet Sci,* 15**,** 111-8.

KALSON, N. S., MALONE, P. S., BRADLEY, R. S., WITHERS, P. J. & LEES, V. C. 2012. Fibre bundles in the human extensor carpi ulnaris tendon are arranged in a spiral. *J Hand Surg Eur Vol,* 37**,** 550-4.

KANNUS, P. 2000. Structure of the tendon connective tissue. *Scand J Med Sci Sports,* 10**,** 312-20.

KANNUS, P., NIITTYMAKI, S., JARVINEN, M. & LEHTO, M. 1989. Sports injuries in elderly athletes: a three-year prospective, controlled study. *Age Ageing,* 18**,** 263-70.

KASASHIMA, Y., KUWANO, A., KATAYAMA, Y., TAURA, Y. & YOSHIHARA, T. 2002. Magnetic resonance imaging application to live horse for diagnosis of tendinitis. *J Vet Med Sci,* 64**,** 577-82.

KASASHIMA, Y., TAKAHASHI, T., SMITH, R. K., GOODSHIP, A. E., KUWANO, A., UENO, T. & HIRANO, S. 2004. Prevalence of superficial digital flexor tendonitis and suspensory desmitis in Japanese Thoroughbred flat racehorses in 1999. *Equine Vet J,* 36**,** 346-50.

KASTELIC, J., GALESKI, A. & BAER, E. 1978. The multicomposite structure of tendon. *Connect Tissue Res,* 6**,** 11-23.

KASTELIC, J., PALLEY, I. & BAER, E. 1980. A structural mechanical model for tendon crimping. *J Biomech,* 13**,** 887-93.

KER, R. F., ALEXANDER, R. M. & BENNETT, M. B. 1988. Why are mammalian tendons so thick? *Journal of Zoology,* 216**,** 309-324.

KHAN, K. M., COOK, J. L., BONAR, F., HARCOURT, P. & ASTROM, M. 1999. Histopathology of common tendinopathies. Update and implications for clinical management. *Sports Med,* 27**,** 393-408.

KHARAZ, Y. A., TEW, S. R., PEFFERS, M., CANTY-LAIRD, E. G. & COMERFORD, E. 2016. Proteomic differences between native and tissue-engineered tendon and ligament. *Proteomics,* 16**,** 1547-56.

KIANI, C., CHEN, L., WU, Y. J., YEE, A. J. & YANG, B. B. 2002. Structure and function of aggrecan. *Cell Res,* 12**,** 19-32.

KIHARA, R., KASASHIMA, Y., ARAI, K. & MIYAMOTO, Y. 2011. Injury Induces a Change in the Functional Characteristics of Cells Recovered from Equine Tendon. *Journal of equine science,* 22**,** 57-60.

KIM, B., YOON, J. H., ZHANG, J., ERIC MUELLER, P. O. & HALPER, J. 2010. Glycan profiling of a defect in decorin glycosylation in equine systemic proteoglycan accumulation, a potential model of progeroid form of Ehlers-Danlos syndrome. *Arch Biochem Biophys,* 501**,** 221-31.

KIRKENDALL, D. T. & GARRETT, W. E. 1997. Function and biomechanics of tendons. *Scand J Med Sci Sports,* 7**,** 62-6.

KJAER, M. 2004. Role of extracellular matrix in adaptation of tendon and skeletal muscle to mechanical loading. *Physiol Rev,* 84**,** 649-98.

KJAER, M., MAGNUSSON, P., KROGSGAARD, M., BOYSEN MOLLER, J., OLESEN, J., HEINEMEIER, K., HANSEN, M., HARALDSSON, B., KOSKINEN, S., ESMARCK, B. & LANGBERG, H. 2006. Extracellular matrix adaptation of tendon and skeletal muscle to exercise. *J Anat,* 208**,** 445-50.

KOBAYASHI, A., SUGISAKA, M., TAKEHANA, K., YAMAGUCHI, M., EERDUNCHAOLU, IWASA, E. K. & ABE, M. 1999. Morphological and histochemical analysis of a case of superficial digital flexor tendon injury in the horse. *J Comp Pathol,* 120**,** 403-14.

KONDRATKO-MITTNACHT, J., DUENWALD-KUEHL, S., LAKES, R. & VANDERBY, R., JR. 2015. Shear load transfer in high and low stress tendons. *J Mech Behav Biomed Mater,* 45**,** 109-20.

KOROL, R. M., FINLAY, H. M., JOSSEAU, M. J., LUCAS, A. R. & CANHAM, P. B. 2007. Fluorescence spectroscopy and birefringence of molecular changes in maturing rat tail tendon. *J Biomed Opt,* 12**,** 024011.

KOSTROMINOVA, T. Y., CALVE, S., ARRUDA, E. M. & LARKIN, L. M. 2009. Ultrastructure of myotendinous junctions in tendon-skeletal muscle constructs engineered in vitro. *Histol Histopathol,* 24**,** 541-50.

KRAUS-HANSEN, A. E., FACKELMAN, G. E., BECKER, C., WILLIAMS, R. M. & PIPERS, F. S. 1992. Preliminary studies on the vascular anatomy of the equine superficial digital flexor tendon. *Equine Vet J,* 24**,** 46-51.

KREMER J.R., D. N. M. A. J. R. M. 1996. Computer visualization of three-dimensional image data using IMOD. *J. Struct. Biol.,* 116**,** 71-76.

LACERDA NETO, J. C. D., FREITAS, J. M. R. D., POGGIANI, F. M., DIAS, D. P. M., GRAVENA, K., BERNARDI, N. S., RIBEIRO, G. & PALMEIRA-BORGES, V. 2013. Serial superficial digital flexor tendon biopsies for diagnosing and monitoring collagenase-induced tendonitis in horses. *Pesquisa Veterinária Brasileira,* 33**,** 710-718.

LAKEMEIER, S., BRAUN, J., EFE, T., FOELSCH, C., ARCHONTIDOU-APRIN, E., FUCHS-WINKELMANN, S., PALETTA, J. R. & SCHOFER, M. D. 2011. Expression of matrix metalloproteinases 1, 3, and 9 in differing extents of tendon retraction in the torn rotator cuff. *Knee Surg Sports Traumatol Arthrosc,* 19**,** 1760-5.

LAM, K. H., PARKIN, T. D., RIGGS, C. M. & MORGAN, K. L. 2007a. Descriptive analysis of retirement of Thoroughbred racehorses due to tendon injuries at the Hong Kong Jockey Club (1992-2004). *Equine Vet J,* 39**,** 143-8.

LAM, K. K., PARKIN, T. D., RIGGS, C. M. & MORGAN, K. L. 2007b. Evaluation of detailed training data to identify risk factors for retirement because of tendon injuries in Thoroughbred racehorses. *Am J Vet Res,* 68**,** 1188-97.

LANDIS, W. J. 1986. A study of calcification in the leg tendons from the domestic turkey. *J Ultrastruct Mol Struct Res,* 94**,** 217-38.

LANDIS, W. J. & SILVER, F. H. 2002. The structure and function of normally mineralizing avian tendons. *Comp Biochem Physiol A Mol Integr Physiol,* 133**,** 1135-57.

LANGBERG, H., OLESEN, J. L., GEMMER, C. & KJAER, M. 2002. Substantial elevation of interleukin-6 concentration in peritendinous tissue, in contrast to muscle, following prolonged exercise in humans. *J Physiol,* 542**,** 985-90.

LAWRENCE, L. A. 2008. Principle of bone development in horses. *Kentucky Equine Research, Versailles, Kentucky, USA.*

LEGERLOTZ, K., DORN, J., RICHTER, J., RAUSCH, M. & LEUPIN, O. 2014. Age-dependent regulation of tendon crimp structure, cell length and gap width with strain. *Acta Biomater,* 10**,** 4447-55.

LIN, P. M., CHEN, C. T. & TORZILLI, P. A. 2004. Increased stromelysin-1 (MMP-3), proteoglycan degradation (3B3- and 7D4) and collagen damage in

cyclically load-injured articular cartilage. *Osteoarthritis Cartilage,* 12**,** 485-96.

LIN, Y. L., BRAMA, P. A., KIERS, G. H., DEGROOT, J. & VAN WEEREN, P. R. 2005a. Functional adaptation through changes in regional biochemical characteristics during maturation of equine superficial digital flexor tendons. *Am J Vet Res,* 66**,** 1623-9.

LIN, Y. L., BRAMA, P. A. J., KIERS, G. H., VAN WEEREN, P. R. & DEGROOT, J. 2005b. Extracellular Matrix Compositon of the Equine Superficial Digital Flexor Tendon: Relationship with Age and Anatomical Site. *Journal of Veterinary Medicine Series A,* 52**,** 333-338.

LUI, P. P.-Y., FU, S.-C., CHAN, L.-S., HUNG, L.-K. & CHAN, K.-M. 2009. Chondrocyte Phenotype and Ectopic Ossification in Collagenase-induced Tendon Degeneration. *Journal of Histochemistry and Cytochemistry,* 57**,** 91-100.

LUNA, L. G. 1968. Manual of Histochemical Staining Methods of Armed Forces Institute of Pathology. *Aktuelle Gerontol,* 3rd edn**,** 32.

LUNDBORG, G., MYRHAGE, R. & RYDEVIK, B. 1977. The vascularization of human flexor tendons within the digital synovial sheath region--structureal and functional aspects. *J Hand Surg Am,* 2**,** 417-27.

MADDOX, B. K., KEENE, D. R., SAKAI, L. Y., CHARBONNEAU, N. L., MORRIS, N. P., RIDGWAY, C. C., BOSWELL, B. A., SUSSMAN, M. D., HORTON, W. A., BACHINGER, H. P. & HECHT, J. T. 1997. The fate of cartilage oligomeric matrix protein is determined by the cell type in the case of a novel mutation in pseudoachondroplasia. *J Biol Chem,* 272**,** 30993-7.

MAEDA, E., NOGUCHI, H., TOHYAMA, H., YASUDA, K. & HAYASHI, K. 2013. Biomechanical study of healing of patellar tendon after resection of the central one-third in an adult-mature rabbit model. *Biomed Mater Eng,* 23**,** 173-81.

MAFFULLI, N., BARRASS, V. & EWEN, S. W. 2000. Light microscopic histology of achilles tendon ruptures. A comparison with unruptured tendons. *Am J Sports Med,* 28**,** 857-63.

MAFFULLI, N., DEL BUONO, A., SPIEZIA, F., LONGO, U. G. & DENARO, V. 2012. Light microscopic histology of quadriceps tendon ruptures. *Int Orthop,* 36**,** 2367-71.

MAFFULLI, N. & KADER, D. 2002. Tendinopathy of tendo achillis. *J Bone Joint Surg Br,* 84.

MAFFULLI, N., LONGO, U. G., FRANCESCHI, F., RABITTI, C. & DENARO, V. 2008. Movin and Bonar Scores Assess the Same Characteristics of Tendon Histology. *Clin Orthop Relat Res,* 466**,** 1605-11.

MAFFULLI, N., MOLLER, H. D. & EVANS, C. H. 2002. Tendon healing: can it be optimised? *Br J Sports Med,* 36**,** 315-6.

MAGNUSSON, S. P., BEYER, N., ABRAHAMSEN, H., AAGAARD, P., NEERGAARD, K. & KJAER, M. 2003a. Increased cross-sectional area and reduced tensile stress of the Achilles tendon in elderly compared with young women. *J Gerontol A Biol Sci Med Sci,* 58**,** 123-7.

MAGNUSSON, S. P., HANSEN, P. & KJAER, M. 2003b. Tendon properties in relation to muscular activity and physical training. *Scand J Med Sci Sports,* 13**,** 211-23.

MAJEED, H., DEALL, C., MANN, A. & MCBRIDE, D. J. 2015. Multiple intratendinous ossified deposits of the Achilles tendon: Case report of an unusual pattern of ossification. *Foot Ankle Surg,* 21**,** e33-5.

MARTINEZ, P., DENYS, A., DELOS, M., SIKORA, A. S., CARPENTIER, M., JULIEN, S., PESTEL, J. & ALLAIN, F. 2015. Macrophage polarization alters the expression and sulfation pattern of glycosaminoglycans. *Glycobiology,* 25**,** 502-13.

MCLATCHIE, G. R. & LENNOX, C. M. E. 1993. *The Soft Tissues: Trauma and Sports Injuries*, Butterworth-Heinemann.

MCNEILLY, C. M., BANES, A. J., BENJAMIN, M. & RALPHS, J. R. 1996. Tendon cells in vivo form a three dimensional network of cell processes linked by gap junctions. *J Anat,* 189 (Pt 3)**,** 593-600.

MEGHOUFEL, A., CLOUTIER, G., CREVIER-DENOIX, N. & DE GUISE, J. A. 2010. Ultrasound B-scan image simulation, segmentation, and analysis of the equine tendon. *Med Phys,* 37**,** 1038-46.

MEGHOUFEL, A., CLOUTIER, G., CREVIER-DENOIX, N. & DE GUISE, J. A. 2011. Tissue Characterization of Equine Tendons With Clinical B-Scan Images Using a Shock Filter Thinning Algorithm. *Ieee Transactions on Medical Imaging,* 30**,** 597-605.

MENARD, D. & STANISH, W. D. 1989. The aging athlete. *Am J Sports Med,* 17**,** 187-96.

MERRITT, T. M., BICK, R., POINDEXTER, B. J., ALCORN, J. L. & HECHT, J. T. 2007. Unique Matrix Structure in the Rough Endoplasmic Reticulum

Cisternae of Pseudoachondroplasia Chondrocytes. *The American Journal of Pathology,* 170**,** 293-300.

MILZ, S., PUTZ, R., RALPHS, J. R. & BENJAMIN, M. 1999. Fibrocartilage in the extensor tendons of the human metacarpophalangeal joints. *The Anatomical Record,* 256**,** 139-145.

MOFFAT, P. A., FIRTH, E. C., ROGERS, C. W., SMITH, R. K., BARNEVELD, A., GOODSHIP, A. E., KAWCAK, C. E., MCILWRAITH, C. W. & VAN WEEREN, P. R. 2008. The influence of exercise during growth on ultrasonographic parameters of the superficial digital flexor tendon of young Thoroughbred horses. *Equine Vet J,* 40**,** 136-40.

MOORE, M. J. & DE BEAUX, A. 1987. A quantitative ultrastructural study of rat tendon from birth to maturity. *J Anat,* 153**,** 163-9.

MORAWETZ, H. 1958. Recent advances in gelatin and glue research. Edited by G. STAINSBY. Pergamon Press, New York-London-Los Angeles-Paris, 1958. 277 pp. $12.00. *Journal of Polymer Science,* 31**,** 34-34.

MORI, Y. 1991. Inflammation and proteoglycans. In: New Experimental Biochemistry,Vol. 3, 1st Edit., M. Muramatsu and K. Nagai, Eds, Tokyo Kagaku Dohjin, Tokyo, pp. 442–448. .

MULLER, G., MICHEL, A. & ALTENBURG, E. 1998. COMP (cartilage oligomeric matrix protein) is synthesized in ligament, tendon, meniscus, and articular cartilage. *Connect Tissue Res,* 39**,** 233-44.

MURATA, D., MISUMI, K. & FUJIKI, M. 2012. A preliminary study of diagnostic color Doppler ultrasonography in equine superficial digital flexor tendonitis. *J Vet Med Sci,* 74**,** 1639-42.

MURRAY, M. M. & SPECTOR, M. 1999. Fibroblast distribution in the anteromedial bundle of the human anterior cruciate ligament: the presence of alpha-smooth muscle actin-positive cells. *J Orthop Res,* 17**,** 18-27.

NAGASE, H., VISSE, R. & MURPHY, G. 2006. Structure and function of matrix metalloproteinases and TIMPs. *Cardiovasc Res,* 69**,** 562-73.

NAGASE, H. & WOESSNER, J. F., JR. 1999. Matrix metalloproteinases. *J Biol Chem,* 274**,** 21491-4.

NAKAGAWA, Y., HAYASHI, K., YAMAMOTO, N. & NAGASHIMA, K. 1996. Age-related changes in biomechanical properties of the Achilles tendon in rabbits. *Eur J Appl Physiol Occup Physiol,* 73**,** 7-10.

NAKAGAWA, Y., MAJIMA, T. & NAGASHIMA, K. 1994. Effect of ageing on ultrastructure of slow and fast skeletal muscle tendon in rabbit Achilles tendons. *Acta Physiol Scand,* 152**,** 307-13.

NARICI, M. V. & MAGANARIS, C. N. 2006. Adaptability of elderly human muscles and tendons to increased loading. *J Anat,* 208**,** 433-43.

O'BRIEN, M. 1992. Functional anatomy and physiology of tendons. *Clin Sports Med,* 11**,** 505-20.

O'CONNOR, W. N. & VALLE, S. 1982. A combination Verhoeff's elastic and Masson's trichrome stain for routine histology. *Stain Technol,* 57**,** 207-10.

O'BRIEN, M. 1997. Structure and metabolism of tendons. *Scand J Med Sci Sports,* 7**,** 55-61.

O'BRIEN, M. 2005. Anatomy of Tendons. *In:* MAFFULLI, N., RENSTRÖM, P. & LEADBETTER, W. (eds.) *Tendon Injuries.* Springer London.

O'SULLIVAN, C. B. 2007. Injuries of the Flexor Tendons: Focus on the Superficial Digital Flexor Tendon. *Clinical Techniques in Equine Practice,* 6**,** 189-197.

OCHIAI, N., MATSUI, T., MIYAJI, N., MERKLIN, R. J. & HUNTER, J. M. 1979. Vascular anatomy of flexor tendons. I. Vincular system and blood supply of the profundus tendon in the digital sheath. *J Hand Surg Am,* 4**,** 321-30.

ORGAN, C. L. & ADAMS, J. 2005. The histology of ossified tendon in dinosaurs. *Journal of Vertebrate Paleontology,* 25**,** 602-613.

PAAVOLA, M., KANNUS, P., JARVINEN, T. A., KHAN, K., JOZSA, L. & JARVINEN, M. 2002. Achilles tendinopathy. *J Bone Joint Surg Am,* 84-A.

PARKIN, T. D., CLEGG, P. D., FRENCH, N. P., PROUDMAN, C. J., RIGGS, C. M., SINGER, E. R., WEBBON, P. M. & MORGAN, K. L. 2005. Risk factors for fatal lateral condylar fracture of the third metacarpus/metatarsus in UK racing. *Equine Vet J,* 37**,** 192-9.

PARKINSON, J., SAMIRIC, T., ILIC, M. Z., COOK, J. & HANDLEY, C. J. 2011. Involvement of proteoglycans in tendinopathy. *J Musculoskelet Neuronal Interact,* 11**,** 86-93.

PARRY, D. & CRAIG, A. 1984. Growth and development of collagen fibrils in connective tissue. In: Ruggeri A. and Motta PM. eds. 'Ultrastructure of the Connective Tissue Matrix'.Martinus Nijhoff, Boston

PARRY, D. A., BARNES, G. R. & CRAIG, A. S. 1978. A comparison of the size distribution of collagen fibrils in connective tissues as a function of age and a possible relation between fibril size distribution and mechanical properties. *Proc R Soc Lond B Biol Sci,* 203**,** 305-21.

PASQUINI, C., SPURGEON, T. L. & PASQUINI, S. 2003. *Anatomy of Domestic Animals: Systemic and Regional Approach,* Sudz Pub.

PATTERSON-KANE, J. C., BECKER, D. L. & RICH, T. 2012. The pathogenesis of tendon microdamage in athletes: the horse as a natural model for basic cellular research. *J Comp Pathol,* 147**,** 227-47.

PATTERSON-KANE, J. C., FIRTH, E. C., GOODSHIP, A. E. & PARRY, D. A. D. 1997a. Age-related differences in collagen crimp patterns in the superficial digital flexor tendon core region of untrained horses. *Australian Veterinary Journal,* 75**,** 39-44.

PATTERSON-KANE, J. C., PARRY, D. A. D., BIRCH, H. L., GOODSHIP, A. E. & FIRTH, E. C. 1997b. An age-related study of morphology and cross-link composition of collagen fibrils in the digital flexor tendons of young thoroughbred horses. *Connective Tissue Research,* 36**,** 253-260.

PATTERSON-KANE, J. C. & RICH, T. 2014. Achilles tendon injuries in elite athletes: lessons in pathophysiology from their equine counterparts. *Ilar j,* 55**,** 86-99.

PATTERSON-KANE, J. C., WILSON, A. M., FIRTH, E. C., PARRY, D. A. & GOODSHIP, A. E. 1998. Exercise-related alterations in crimp morphology in the central regions of superficial digital flexor tendons from young thoroughbreds: a controlled study. *Equine Vet J,* 30**,** 61-4.

PEFFERS, M. J., FANG, Y., CHEUNG, K., WEI, T. K., CLEGG, P. D. & BIRCH, H. L. 2015. Transcriptome analysis of ageing in uninjured human Achilles tendon. *Arthritis Res Ther,* 17**,** 33.

PERKINS, N. R., REID, S. W. & MORRIS, R. S. 2005. Risk factors for injury to the superficial digital flexor tendon and suspensory apparatus in Thoroughbred racehorses in New Zealand. *N Z Vet J,* 53**,** 184-92.

PIEZ, K. A. 1984. Molecular and aggregate structures of the collagens. Elsevier New York.

PINCHBECK, G. L., CLEGG, P. D., PROUDMAN, C. J., STIRK, A., MORGAN, K. L. & FRENCH, N. P. 2004. Horse injuries and racing practices in National Hunt racehorses in the UK: the results of a prospective cohort study. *Vet J,* 167**,** 45-52.

PINS, G. D., CHRISTIANSEN, D. L., PATEL, R. & SILVER, F. H. 1997. Self-assembly of collagen fibers. Influence of fibrillar alignment and decorin on mechanical properties. *Biophys J,* 73**,** 2164-72.

PIROG, K. A., JAKA, O., KATAKURA, Y., MEADOWS, R. S., KADLER, K. E., BOOT-HANDFORD, R. P. & BRIGGS, M. D. 2010. A mouse model offers novel insights into the myopathy and tendinopathy often associated with pseudoachondroplasia and multiple epiphyseal dysplasia. *Human Molecular Genetics,* 19**,** 52-64.

PONT, M., PROBST, A., BOCK, P., HINTERHOFER, C., SORA, M. C. & KONIG, H. E. 2004. Sectional anatomy of the equine digit - fine structure of the elastic layer between deep digital flexor tendon and middle phalanx. *Pferdeheilkunde,* 20**,** 415-+.

POTENZA, A. D. 1962. Tendon healing within the flexor digital sheath in the dog. *J Bone Joint Surg Am,* 44-a**,** 49-64.

PROVENZANO, P. P. & VANDERBY, R., JR. 2006. Collagen fibril morphology and organization: implications for force transmission in ligament and tendon. *Matrix Biol,* 25**,** 71-84.

RAMACHANDRAN, G. N. & CHANDRASEKHARAN, R. 1968. Interchain hydrogen bonds via bound water molecules in the collagen triple helix. *Biopolymers,* 6**,** 1649-58.

RATCLIFFE, A., SHURETY, W. & CATERSON, B. 1993. The quantitation of a native chondroitin sulfate epitope in synovial fluid lavages and articular cartilage from canine experimental osteoarthritis and disuse atrophy. *Arthritis & Rheumatism,* 36**,** 543-551.

REARDON, R. J., BODEN, L. A., MELLOR, D. J., LOVE, S., NEWTON, J. R., STIRK, A. J. & PARKIN, T. D. 2012. Risk factors for superficial digital flexor tendinopathy in Thoroughbred racehorses in hurdle starts in the UK (2001-2009). *Equine Vet J,* 44**,** 564-9.

REARDON, R. J., BODEN, L. A., MELLOR, D. J., LOVE, S., NEWTON, J. R., STIRK, A. J. & PARKIN, T. D. 2013. Risk factors for superficial digital flexor tendinopathy in Thoroughbred racehorses in steeplechase starts in the United Kingdom (2001-2009). *Vet J,* 195**,** 325-30.

REARDON, R. J. M. 2013. An investigation of risk factors associated with injuries to horses undertaking jump racing in Great Britain. PhD thesis, University of Glasgow.

REDDY, G. K., STEHNO-BITTEL, L. & ENWEMEKA, C. S. 1999. Matrix remodeling in healing rabbit Achilles tendon. *Wound Repair and Regeneration,* 7**,** 518-527.

REES, S. G., DENT, C. M. & CATERSON, B. 2009. Metabolism of proteoglycans in tendon. *Scand J Med Sci Sports,* 19**,** 470-8.

REES, S. G., FLANNERY, C. R., LITTLE, C. B., HUGHES, C. E., CATERSON, B. & DENT, C. M. 2000. Catabolism of aggrecan, decorin and biglycan in tendon. *Biochem J,* 350 Pt 1**,** 181-8.

REES, S. G., WAGGETT, A. D., DENT, C. M. & CATERSON, B. 2007. Inhibition of aggrecan turnover in short-term explant cultures of bovine tendon. *Matrix Biol,* 26**,** 280-90.

REESE, S. P. & WEISS, J. A. 2013. Tendon Fascicles Exhibit a Linear Correlation Between Poisson's Ratio and Force During Uniaxial Stress Relaxation. *Journal of Biomechanical Engineering-Transactions of the Asme,* 135.

REGNAULT, S., PITSILLIDES, A. A. & HUTCHINSON, J. R. 2014. Structure, ontogeny and evolution of the patellar tendon in emus (Dromaius novaehollandiae) and other palaeognath birds. *PeerJ,* 2**,** e711.

RICHARDS, H. J. 1980. Repair and healing of the divided digital flexor tendon. *Injury,* 12**,** 1-12.

RICHARDS, P. J., BRAID, J. C., CARMONT, M. R. & MAFFULLI, N. 2008. Achilles tendon ossification: pathology, imaging and aetiology. *Disabil Rehabil,* 30**,** 1651-65.

RICHARDSON, L. E., DUDHIA, J., CLEGG, P. D. & SMITH, R. 2007. Stem cells in veterinary medicine – attempts at regenerating equine tendon after injury. *Trends in Biotechnology,* 25**,** 409-416.

RIEMERSMA, D. J. & DEBRUYN, P. 1986. Variations in Cross-Sectional Area and Composition of Equine Tendons with Regard to Their Mechanical Function. *Research in Veterinary Science,* 41**,** 7-13.

RIEMERSMA, D. J. & SCHAMHARDT, H. C. 1985. In vitro mechanical properties of equine tendons in relation to cross-sectional area and collagen content. *Res Vet Sci,* 39**,** 263-70.

RIGOZZI, S., MULLER, R. & SNEDEKER, J. G. 2010. Collagen fibril morphology and mechanical properties of the Achilles tendon in two inbred mouse strains. *J Anat,* 216**,** 724-31.

RILEY, G. P., HARRALL, R. L., CONSTANT, C. R., CHARD, M. D., CAWSTON, T. E. & HAZLEMAN, B. L. 1994. Tendon degeneration and chronic shoulder pain: changes in the collagen composition of the human rotator cuff tendons in rotator cuff tendinitis. *Annals of the Rheumatic Diseases,* 53**,** 359-366.

ROBBINS, J. R., EVANKO, S. P. & VOGEL, K. G. 1997. Mechanical loading and TGF-beta regulate proteoglycan synthesis in tendon. *Arch Biochem Biophys,* 342**,** 203-11.

ROBBINS, J. R. & VOGEL, K. G. 1994. Regional expression of mRNA for proteoglycans and collagen in tendon. *Eur J Cell Biol,* 64**,** 264-70.

ROSENBERG, L. 1971. Chemical basis for the histological use of safranin O in the study of articular cartilage. *J Bone Joint Surg Am,* 53**,** 69-82.

ROSS, M. W. & DYSON, S. J. 2010. *Diagnosis and Management of Lameness in the Horse*, Elsevier Health Sciences.

ROUGHLEY, P. J. & LEE, E. R. 1994. Cartilage proteoglycans: structure and potential functions. *Microsc Res Tech,* 28**,** 385-97.

ROWE, R. W. D. 1985. The Structure of Rat Tail Tendon Fascicles. *Connective Tissue Research,* 14**,** 21-30.

RUSSO, V., MAURO, A., MARTELLI, A., DI GIACINTO, O., DI MARCANTONIO, L., NARDINOCCHI, D., BERARDINELLI, P. & BARBONI, B. 2015. Cellular and molecular maturation in fetal and adult ovine calcaneal tendons. *J Anat,* 226**,** 126-42.

SAMIRIC, T., ILIC, M. Z. & HANDLEY, C. J. 2004. Large aggregating and small leucine-rich proteoglycans are degraded by different pathways and at different rates in tendon. *Eur J Biochem,* 271**,** 3612-20.

SCHMITZ, N., LAVERTY, S., KRAUS, V. B. & AIGNER, T. 2010. Basic methods in histopathology of joint tissues. *Osteoarthritis Cartilage,* 18 Suppl 3**,** S113-6.

SCHNEIDER, C. A., RASBAND, W. S. & ELICEIRI, K. W. 2012. "NIH Image to ImageJ: 25 years of image analysis", Nature methods 9(7): 671-675,. http://imagej.nih.gov/ij/**,** 1997-2015.

SCHULTZ, L. B. 2004. *Howell Equine Handbook of Tendon and Ligament Injuries*, Hoboken, NJ: Howell Book House.

SCOTT, A., COOK, J. L., HART, D. A., WALKER, D. C., DURONIO, V. & KHAN, K. M. 2007. Tenocyte responses to mechanical loading in vivo: a

role for local insulin-like growth factor 1 signaling in early tendinosis in rats. *Arthritis Rheum,* 56**,** 871-81.

SCREEN, H. R. 2009. Hierarchical approaches to understanding tendon mechanics. *Journal of Biomechanical Science and Engineering,* 4**,** 481-499.

SESE, M., UEDA, H., WATANABE, T., YAMAMOTO, E., HOSAKA, Y., TANGKAWATTANA, P. & TAKEHANA, K. 2007. Characteristics of collagen fibrils in the entire equine superficial digital flexor tendon. *Okajimas Folia Anat Jpn,* 84**,** 111-4.

SHADWICK, R. E. 1990. Elastic energy storage in tendons: mechanical differences related to function and age. *J Appl Physiol (1985),* 68**,** 1033-40.

SHAH, J. S., PALACIOS, E. & PALACIOS, L. 1982. Development of crimp morphology and cellular changes in chick tendons. *Dev Biol,* 94**,** 499-504.

SHAPIRO, F., MULHERN, H., WEIS, M. A. & EYRE, D. 2006. Rough endoplasmic reticulum abnormalities in a patient with spondyloepimetaphyseal dysplasia with scoliosis, joint laxity, and finger deformities. *Ultrastruct Pathol,* 30**,** 393-400.

SHARMA, P. & MAFFULLI, N. 2005. Tendon injury and tendinopathy: healing and repair. *J Bone Joint Surg Am,* 87**,** 187-202.

SHEARER, T. 2015a. A new strain energy function for modelling ligaments and tendons whose fascicles have a helical arrangement of fibrils. *J Biomech,* 48**,** 3017-25.

SHEARER, T. 2015b. A new strain energy function for the hyperelastic modelling of ligaments and tendons based on fascicle microstructure. *J Biomech,* 48**,** 290-7.

SHEARER, T., RAWSON, S., CASTRO, S. J., BALINT, R., BRADLEY, R. S., LOWE, T., VILA-COMAMALA, J., LEE, P. D. & CARTMELL, S. H. 2014. X-ray computed tomography of the anterior cruciate ligament and patellar tendon. *Muscles Ligaments Tendons J,* 4**,** 238-44.

SHOULDERS, M. D. & RAINES, R. T. 2009. COLLAGEN STRUCTURE AND STABILITY. *Annu Rev Biochem,* 78**,** 929-58.

SILBERT, J. E. 1982. Structure and metabolism of proteoglycans and glycosaminoglycans. *J Invest Dermatol,* 79 Suppl 1**,** 31s-37s.

SILVA, M. E. & DIETRICH, C. P. 1975. Structure of heparin. Characterization of the products formed from heparin by the action of a heparinase and a heparitinase from Flavobacterium heparinum. *J Biol Chem,* 250**,** 6841-6.

SILVER, F. H. & BIRK, D. E. 1984. Molecular structure of collagen in solution: comparison of types I, II, III and V. *International Journal of Biological Macromolecules,* 6**,** 125-132.

SILVER, F. H., EBRAHIMI, A. & SNOWHILL, P. B. 2002. Viscoelastic properties of self-assembled type I collagen fibers: molecular basis of elastic and viscous behaviors. *Connect Tissue Res,* 43**,** 569-80.

SILVER, F. H., FREEMAN, J. W. & SEEHRA, G. P. 2003. Collagen self-assembly and the development of tendon mechanical properties. *J Biomech,* 36**,** 1529-53.

SLATER, R. R., JR., BAYLISS, M. T., LACHIEWICZ, P. F., VISCO, D. M. & CATERSON, B. 1995. Monoclonal antibodies that detect biochemical markers of arthritis in humans. *Arthritis Rheum,* 38**,** 655-9.

SMITH, J. W. 1965. Blood supply of tendons. *The American Journal of Surgery,* 109**,** 272-276.

SMITH, M. M., SAKURAI, G., SMITH, S. M., YOUNG, A. A., MELROSE, J., STEWART, C. M., APPLEYARD, R. C., PETERSON, J. L., GILLIES, R. M., DART, A. J., SONNABEND, D. H. & LITTLE, C. B. 2008. Modulation of aggrecan and ADAMTS expression in ovine tendinopathy induced by altered strain. *Arthritis Rheum,* 58**,** 1055-66.

SMITH, M. M., SMITH, S. M., YAMAGUCHI, H., KIKUKAWA, K., MONDORI, T., SUENAGA, N., GOODEN, B., YOUNG, A. A., SONNABEND, D. H. & LITTLE, C. B. 2009. Chondroid metaplasia is a long-term consequence of tendinopathy induced by both stress-deprivation and over-stress: temporal differences in molecular pathology. *55th Annual Meeting of the Orthopaedic Research Society***,** http://www.ors.org/Transactions/55/0029.pdf.

SMITH, R. K., BIRCH, H. L., GOODMAN, S., HEINEGARD, D. & GOODSHIP, A. E. 2002. The influence of ageing and exercise on tendon growth and degeneration--hypotheses for the initiation and prevention of strain-induced tendinopathies. *Comp Biochem Physiol A Mol Integr Physiol,* 133**,** 1039-50.

SMITH, R. K., JONES, R. & WEBBON, P. M. 1994. The cross-sectional areas of normal equine digital flexor tendons determined ultrasonographically. *Equine Vet J,* 26**,** 460-5.

SMITH, R. K., ZUNINO, L., WEBBON, P. M. & HEINEGARD, D. 1997. The distribution of cartilage oligomeric matrix protein (COMP) in tendon and its variation with tendon site, age and load. *Matrix Biol,* 16**,** 255-71.

SODER, S., HAMBACH, L., LISSNER, R., KIRCHNER, T. & AIGNER, T. 2002. Ultrastructural localization of type VI collagen in normal adult and osteoarthritic human articular cartilage. *Osteoarthritis Cartilage,* 10**,** 464-70.

SODERSTEN, F., EKMAN, S., ELORANTA, M. L., HEINEGARD, D., DUDHIA, J. & HULTENBY, K. 2005. Ultrastructural immunolocalization of cartilage oligomeric matrix protein (COMP) in relation to collagen fibrils in the equine tendon. *Matrix Biol,* 24**,** 376-85.

SODERSTEN, F., HULTENBY, K., HEINEGARD, D., JOHNSTON, C. & EKMAN, S. 2013. Immunolocalization of collagens (I and III) and cartilage oligomeric matrix protein in the normal and injured equine superficial digital flexor tendon. *Connect Tissue Res,* 54**,** 62-9.

SQUIER, C. A. & MAGNES, C. 1983. Spatial relationships between fibroblasts during the growth of rat-tail tendon. *Cell Tissue Res,* 234**,** 17-29.

SRIDHARAN, G. & SHANKAR, A. A. 2012. Toluidine blue: A review of its chemistry and clinical utility. *J Oral Maxillofac Pathol,* 16**,** 251-5.

STANLEY, R. L., FLECK, R. A., BECKER, D. L., GOODSHIP, A. E., RALPHS, J. R. & PATTERSON-KANE, J. C. 2007. Gap junction protein expression and cellularity: comparison of immature and adult equine digital tendons. *J Anat,* 211**,** 325-34.

STARBORG, T., LU, Y., HUFFMAN, A., HOLMES, D. F. & KADLER, K. E. 2009. Electron microscope 3D reconstruction of branched collagen fibrils in vivo. *Scand J Med Sci Sports,* 19**,** 547-52.

STEPHENS, P. R., NUNAMAKER, D. M. & BUTTERWECK, D. M. 1989. Application of a Hall-effect transducer for measurement of tendon strains in horses. *Am J Vet Res,* 50**,** 1089-95.

STREETER, I. 2011. A molecular dynamics study of the interprotein interactions in collagen fibrils. 7**,** 3373-82.

SUVARNA, K. S., LAYTON, C. & BANCROFT, J. D. 2012. *Bancroft's Theory and Practice of Histological Techniques,* Elsevier Health Sciences UK.

SZARO, P., WITKOWSKI, G., SMIGIELSKI, R., KRAJEWSKI, P. & CISZEK, B. 2009. Fascicles of the adult human Achilles tendon - an anatomical study. *Ann Anat,* 191**,** 586-93.

TAMAM, C., YILDIRIM, D., TAMAM, M., MULAZIMOGLU, M. & OZPACACI, T. 2011. Bilateral Achilles tendon ossification: diagnosis with ultrasonography and Single Photon Emission Computed Tomography/Computed Tomography. Case report. *Med Ultrason,* 13**,** 320-2.

TAYLOR, D. C., DALTON, J. D., JR., SEABER, A. V. & GARRETT, W. E., JR. 1990. Viscoelastic properties of muscle-tendon units. The biomechanical effects of stretching. *Am J Sports Med,* 18**,** 300-9.

TERRY, D. E., CHOPRA, R. K., OVENDEN, J. & ANASTASSIADES, T. P. 2000. Differential use of Alcian blue and toluidine blue dyes for the quantification and isolation of anionic glycoconjugates from cell cultures: application to proteoglycans and a high-molecular-weight glycoprotein synthesized by articular chondrocytes. *Anal Biochem,* 285**,** 211-9.

THORPE, C. T., BIRCH, H. L., CLEGG, P. D. & SCREEN, H. R. 2013a. The role of the non-collagenous matrix in tendon function. *Int J Exp Pathol,* 94**,** 248-59.

THORPE, C. T., CHAUDHRY, S., LEI, II, VARONE, A., RILEY, G. P., BIRCH, H. L., CLEGG, P. D. & SCREEN, H. R. 2015a. Tendon overload results in alterations in cell shape and increased markers of inflammation and matrix degradation. *Scand J Med Sci Sports,* 25**,** e381-91.

THORPE, C. T., CLEGG, P. D. & BIRCH, H. L. 2010a. A review of tendon injury: Why is the equine superficial digital flexor tendon most at risk? *Equine Vet J,* 42**,** 174-180.

THORPE, C. T., GODINHO, M. S., RILEY, G. P., BIRCH, H. L., CLEGG, P. D. & SCREEN, H. R. 2015b. The interfascicular matrix enables fascicle sliding and recovery in tendon, and behaves more elastically in energy storing tendons. *J Mech Behav Biomed Mater*.

THORPE, C. T., KARUNASEELAN, K. J., NG CHIENG HIN, J., RILEY, G. P., BIRCH, H. L., CLEGG, P. D. & SCREEN, H. R. 2016a. Distribution of proteins within different compartments of tendon varies according to tendon type. *J Anat*.

THORPE, C. T., KLEMT, C., RILEY, G. P., BIRCH, H. L., CLEGG, P. D. & SCREEN, H. R. 2013b. Helical sub-structures in energy-storing tendons provide a possible mechanism for efficient energy storage and return. *Acta Biomater,* 9**,** 7948-56.

THORPE, C. T., MCDERMOTT, B. T., GOODSHIP, A. E., CLEGG, P. D. & BIRCH, H. L. 2015c. Ageing does not result in a decline in cell synthetic activity in an injury prone tendon. *Scand J Med Sci Sports*.

THORPE, C. T., PEFFERS, M. J., SIMPSON, D., HALLIWELL, E., SCREEN, H. R. & CLEGG, P. D. 2016b. Anatomical heterogeneity of tendon: Fascicular and interfascicular tendon compartments have distinct proteomic composition. *Sci Rep,* 6**,** 20455.

THORPE, C. T., RILEY, G. P., BIRCH, H. L., CLEGG, P. D. & SCREEN, H. R. 2014a. Effect of fatigue loading on structure and functional behaviour of fascicles from energy-storing tendons. *Acta Biomater,* 10**,** 3217-24.

THORPE, C. T., RILEY, G. P., BIRCH, H. L., CLEGG, P. D. & SCREEN, H. R. 2014b. Fascicles from energy-storing tendons show an age-specific response to cyclic fatigue loading. *J R Soc Interface,* 11**,** 20131058.

THORPE, C. T., RILEY, G. P., BIRCH, H. L., CLEGG, P. D. & SCREEN, H. R. 2016c. Fascicles and the interfascicular matrix show adaptation for fatigue resistance in energy storing tendons. *Acta Biomater*.

THORPE, C. T., SPIESZ, E. M., CHAUDHRY, S., SCREEN, H. R. & CLEGG, P. D. 2015d. Science in brief: recent advances into understanding tendon function and injury risk. *Equine Vet J,* 47**,** 137-40.

THORPE, C. T., STARK, R. J., GOODSHIP, A. E. & BIRCH, H. L. 2010b. Mechanical properties of the equine superficial digital flexor tendon relate to specific collagen cross-link levels. *Equine Vet J Suppl***,** 538-43.

THORPE, C. T., STREETER, I., PINCHBECK, G. L., GOODSHIP, A. E., CLEGG, P. D. & BIRCH, H. L. 2010c. Aspartic acid racemization and collagen degradation markers reveal an accumulation of damage in tendon collagen that is enhanced with aging. *J Biol Chem,* 285**,** 15674-81.

THORPE, C. T., UDEZE, C. P., BIRCH, H. L., CLEGG, P. D. & SCREEN, H. R. 2013c. Capacity for sliding between tendon fascicles decreases with ageing in injury prone equine tendons: a possible mechanism for age-related tendinopathy? *Eur Cell Mater,* 25**,** 48-60.

THORPE, C. T., UDEZE, C. P., BIRCH, H. L., CLEGG, P. D. & SCREEN, H. R. C. 2012. Specialization of tendon mechanical properties results from interfascicular differences. *J R Soc Interface,* 9**,** 3108-17.

THUR, J., ROSENBERG, K., NITSCHE, D. P., PIHLAJAMAA, T., ALA-KOKKO, L., HEINEGARD, D., PAULSSON, M. & MAURER, P. 2001. Mutations in cartilage oligomeric matrix protein causing pseudoachondroplasia and multiple epiphyseal dysplasia affect binding of calcium and collagen I, II, and IX. *J Biol Chem,* 276**,** 6083-92.

TIDBALL, J. G. 1991. Myotendinous junction injury in relation to junction structure and molecular composition. *Exerc Sport Sci Rev,* 19**,** 419-45.

TRESOLDI, I., OLIVA, F., BENVENUTO, M., FANTINI, M., MASUELLI, L., BEI, R. & MODESTI, A. 2013. Tendon's ultrastructure. *Muscles Ligaments Tendons J,* 3**,** 2-6.

TUITE, D. J., RENSTRÖM, P. A. F. H. & O'BRIEN, M. 1997. The aging tendon. *Scandinavian Journal of Medicine & Science in Sports,* 7**,** 72-77.

UHTHOFF, H. K., SARKAR, K. & MAYNARD, J. A. 1976. Calcifying tendinitis: a new concept of its pathogenesis. *Clin Orthop Relat Res***,** 164-8.

VAILAS, A. C., TIPTON, C. M., LAUGHLIN, H. L., TCHENG, T. K. & MATTHES, R. D. 1978. *Physical activity and hypophysectomy on the aerobic capacity of ligaments and tendons*.

VAN SCHIE, H. T., BAKKER, E. M., JONKER, A. M. & VAN WEEREN, P. R. 2003. Computerized ultrasonographic tissue characterization of equine superficial digital flexor tendons by means of stability quantification of echo patterns in contiguous transverse ultrasonographic images. *Am J Vet Res,* 64**,** 366-75.

VANDERBY JR, R. & PROVENZANO, P. P. 2003. Collagen in connective tissue: from tendon to bone. *Journal of Biomechanics,* 36**,** 1523-1527.

VESENTINI, S., REDAELLI, A. & MONTEVECCHI, F. M. 2005. Estimation of the binding force of the collagen molecule-decorin core protein complex in collagen fibril. *J Biomech,* 38**,** 433-43.

VIDAL, B. D. C. 2003. Image analysis of tendon helical superstructure using interference and polarized light microscopy. *Micron,* 34**,** 423-432.

VIDAL BDE, C. & VILARTA, R. 1988. Articular cartilage: collagen II-proteoglycans interactions. Availability of reactive groups. Variation in birefringence and differences as compared to collagen I. *Acta Histochem,* 83**,** 189-205.

VILAR, J. M., SANTANA, A., ESPINOSA, J. & SPINELLA, G. 2011. Cross-sectional area of the tendons of the tarsal region in Standardbred trotter horses. *Equine Vet J,* 43**,** 235-9.

VISCO, D. M., JOHNSTONE, B., HILL, M. A., JOLLY, G. A. & CATERSON, B. 1993. Immunohistochemical analysis of 3-b-3(–) and 7-d-4 epitope expression in canine osteoarthritis. *Arthritis & Rheumatism,* 36**,** 1718-1725.

VOGEL, H. G. 1980. Influence of maturation and aging on mechanical and biochemical properties of connective tissue in rats. *Mech Ageing Dev,* 14**,** 283-92.

VOGEL, K. G. & HEINEGARD, D. 1985. Characterization of proteoglycans from adult bovine tendon. *J Biol Chem,* 260**,** 9298-306.

VOGEL, K. G. & KOOB, T. J. 1989. Structural specialization in tendons under compression. *Int Rev Cytol,* 115**,** 267-93.

VOGEL, K. G. & PETERS, J. A. 2005. Histochemistry defines a proteoglycan-rich layer in bovine flexor tendon subjected to bending. *J Musculoskelet Neuronal Interact,* 5**,** 64-9.

VOGEL, K. G., SANDY, J. D., POGANY, G. & ROBBINS, J. R. 1994. Aggrecan in bovine tendon. *Matrix Biol,* 14**,** 171-9.

VOGEL, K. G. & TROTTER, J. A. 1987. The effect of proteoglycans on the morphology of collagen fibrils formed in vitro. *Coll Relat Res,* 7**,** 105-14.

WAGGETT, A. D., RALPHS, J. R., KWAN, A. P., WOODNUTT, D. & BENJAMIN, M. 1998. Characterization of collagens and proteoglycans at the insertion of the human Achilles tendon. *Matrix Biol,* 16**,** 457-70.

WANG, J. H. 2006. Mechanobiology of tendon. *J Biomech,* 39**,** 1563-82.

WATANABE, T., HOSAKA, Y., YAMAMOTO, E., UEDA, H., SUGAWARA, K., TAKAHASHI, H. & TAKEHANA, K. 2005. Control of the collagen fibril diameter in the equine superficial digital flexor tendon in horses by decorin. *Journal of Veterinary Medical Science,* 67**,** 855-860.

WATANABE, T., IMAMURA, Y., HOSAKA, Y., UEDA, H. & TAKEHANA, K. 2007. Graded arrangement of collagen fibrils in the equine superficial digital flexor tendon. *Connective Tissue Research,* 48**,** 332-337.

WATKINS, J. P., AUER, J. A., MORGAN, S. J. & GAY, S. 1985. Healing of surgically created defects in the equine superficial digital flexor tendon: effects of pulsing electromagnetic field therapy on collagen-type transformation and tissue morphologic reorganization. *Am J Vet Res,* 46**,** 2097-103.

WATTS, A. E., YEAGER, A. E., KOPYOV, O. V. & NIXON, A. J. 2011. Fetal derived embryonic-like stem cells improve healing in a large animal flexor tendonitis model. *Stem Cell Research & Therapy,* 2.

WEBBON, P. M. 1977. A post mortem study of equine digital flexor tendons. *Equine Vet J,* 9**,** 61-7.

WEINTRAUB, W. 2003. *Tendon and Ligament Healing: A New Approach to Sports and Overuse Injury*, Paradigm Publications.

WERPY, N. M. & BARRETT, M. F. 2012. *Advances in Equine Imaging, An Issue of Veterinary Clinics: Equine Practice*, Elsevier Health Sciences.

WIGHT, T. N. & MECHAM, R. P. 2013. *Biology of Proteoglycans*, Elsevier Science.

WILLIAMS, I. F., CRAIG, A. S., PARRY, D. A. D., GOODSHIP, A. E., SHAH, J. & SILVER, I. A. 1985. Development of collagen fibril organization and collagen crimp patterns during tendon healing. *International Journal of Biological Macromolecules,* 7**,** 275-282.

WILLIAMS, J. G. 1986. Achilles tendon lesions in sport. *Sports Med,* 3**,** 114-35.

WILLIAMS, R. B., HARKINS, L. S., HAMMOND, C. J. & WOOD, J. L. N. 2001. Racehorse injuries, clinical problems and fatalities recorded on British racecourses from flat racing and National Hunt racing during 1996, 1997 and 1998. *Equine Veterinary Journal,* 33**,** 478-486.

WILLIAMSON, K. A., LEE, K. J., HUMPHREYS, W. J., COMERFORD, E. J., CLEGG, P. D. & CANTY-LAIRD, E. G. 2015. Restricted differentiation potential of progenitor cell populations obtained from the equine superficial digital flexor tendon (SDFT). *J Orthop Res,* 33**,** 849-58.

WILMINK, J., WILSON, A. M. & GOODSHIP, A. E. 1992. Functional significance of the morphology and micromechanics of collagen fibres in relation to partial rupture of the superficial digital flexor tendon in racehorses. *Res Vet Sci,* 53**,** 354-9.

WU, H., ZHAO, G., ZU, H., WANG, J. H. C. & WANG, Q.-M. 2015. Aging-related viscoelasticity variation of tendon stem cells (TSCs) characterized by quartz thickness shear mode (TSM) resonators. *Sensors and Actuators B: Chemical,* 210**,** 369-380.

WU, Y. J., PIERRE, D. P. L. A., WU, J., YEE, A. J. & YANG, B. B. 2005. The interaction of versican with its binding partners. *Cell Res,* 15**,** 483-494.

WULFF, S., HAFER, L., CHELES, M., HTL, D. A. & STANFORTH, D. A. 2004. Guide to special stains.

YAHIA, L. H. & DROUIN, G. 1989. Microscopical investigation of canine anterior cruciate ligament and patellar tendon: collagen fascicle morphology and architecture. *J Orthop Res,* 7**,** 243-51.

YAMABAYASHI, S. 1987. Periodic acid — Schiff — Alcian Blue: A method for the differential staining of glycoproteins. *The Histochemical Journal,* 19**,** 565-571.

YANG, Y., RUPANI, A., BAGNANINCHI, P., WIMPENNY, I. & WEIGHTMAN, A. 2012. Study of optical properties and proteoglycan content of tendons by

polarization sensitive optical coherence tomography. *J Biomed Opt,* 17**,** 081417.

YONATH, A. & TRAUB, W. 1969. Polymers of tripeptides as collagen models: IV. Structure analysis of poly(l-prolyl-glycyl-l-proline). *Journal of Molecular Biology,* 43**,** 461-477.

YOON, J. H. & HALPER, J. 2005. Tendon proteoglycans: biochemistry and function. *J Musculoskelet Neuronal Interact,* 5**,** 22-34.

YOUNG, N. J., BECKER, D. L., FLECK, R. A., GOODSHIP, A. E. & PATTERSON-KANE, J. C. 2009. Maturational alterations in gap junction expression and associated collagen synthesis in response to tendon function. *Matrix Biol,* 28**,** 311-23.

YUAN, J., WANG, M. X. & MURRELL, G. A. 2003. Cell death and tendinopathy. *Clin Sports Med,* 22**,** 693-701.

ZHANG, J. & WANG, J. H. C. 2015. Moderate Exercise Mitigates the Detrimental Effects of Aging on Tendon Stem Cells. *PLoS ONE,* 10**,** e0130454.